UPDATE OF THE BM18 ESRF BEAMLINE DEVELOPMENT: PRESENTATION OF SELECTED EQUIPMENT AND THEIR COMMISSIONING

F. Cianciosi†, A.-L. Buisson, P. Carceller, P. Tafforeau, P. Van Vaerenbergh, ESRF, Grenoble, France

Abstract

This article highlights specific equipment that have not yet been described in previous publications, notably the in-vacuum cooled fast shutter for high-energy, the wide aluminium window and tailored high-precision slits (400 × 200 mm opening). 2022 and 2023 have seen the installation and commissioning of these new equipment. The ID18 beamline opened for user applications in September 2022 with limited capabilities and has been increasing its possibilities since then. It is expected to be fully equipped by the end of 2024.

INTRODUCTION AND BEAMLINE PERFORMANCES

The ESRF-EBS beamline BM18 has been tailored for hierarchical propagation phase-contrast tomography. The 220 m long beamline benefits from a high-coherence at high-energy beam from a 1.56 T triple short wiggler of the new 4th generation storage ring. The beamline combines a resolution range from 120 µm down to 0.65 µm with the possibility to scan samples up to 2.5 m high and 1.2 m in diameter. With a beam width up to 35 cm and energies ranging from 40 to 280 keV (polychromatic), the main applications are material sciences, cultural heritage, geology, biomedical imaging and industrial applications.

Due to the delays in the development and installation of the large sample stage previously described in [1], the beamline started user operation in September 2022 using a new version of a smaller sample stage initially developed by *LAB Motion Systems* in 2012 for palaeontology on the ID19 (2 stages) and ID17 (1 stage) beamlines and of which two more copies were installed later on BM05. The maximum dimensions of samples are therefore limited to 30cm in diameter, 30 kg in weight, and 50 cm vertically. Once the large sample stage is operational, the maximum dimensions will be 1.2 m diameter, 300 kg and 2.5 m vertically.

IN-VACUUM COOLED FAST SHUTTER

During the commissioning and the initial operation of the BM18 beamline, the quick obturation of the photon beam was made using the photon absorber placed at the end of the Optical Hutch. However, this instrument is not optimal for this purpose, because it is relatively slow (about 1s/cycle), it has a relatively short life (about 100k cycles) and it is part of the safety equipment of the beamline, therefore its use should be reserved to this function only.

For an impinging power of 300 W, and a beam size of 100 × 5 mm, it was decided to develop a specific beam shutter with the aim of shutting off the beam quickly (maximum opening/closing time: 0.1 s), the possibility of continuous operation (i.e. frequency: 1 Hz) and for a long-life (several millions of cycles).

The shutter itself is constituted by a tungsten blade, which rotates by 30° to either intercept the beam or let it pass. It is actioned by a cooled stepper motor. All the components are in vacuum. The blade is isolated from the shaft by a PEEK spacer. When the blade is in the upper position, it remains in contact with a water-cooled copper block which cools the tungsten blade. This block is mounted on springs to ensure good contact pressure with the blade and a perfect alignment between the contact surfaces. Figure 1 shows the blade in the open position (the blade in closed position is superimposed in transparency).
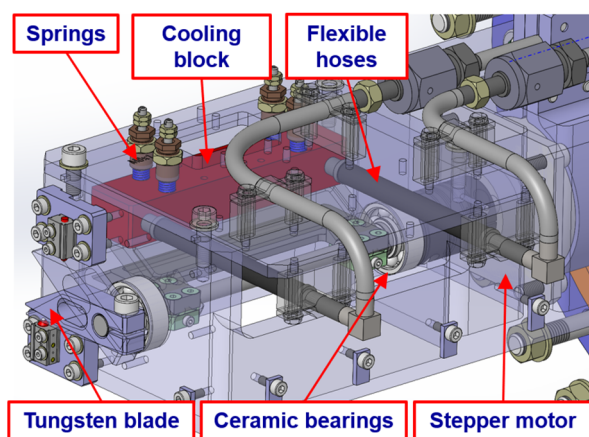
Figure 1: Design of the in-vacuum cooled fast shutter.

Calculated pressure contact between the blade and the cooling block is 0.85 bar. FEA calculations (Fig. 2) demonstrate that, for a thermal contact exchange coefficient of 800W/m²K [2], the blade would not exceed 214 degrees more than that of the cooling water temperature (20 ºC).

The control of the motor is done with an IcePAP controller [3] and the software is under development.

The foreseen closing movement will be done in two phases: a quick rotation to intercept the beam in the required time, followed by a slower movement to ensure contact with the cooling block.

The manufacturing drawings have been completed and the parts have been ordered. The assembly will be done at ESRF and the first test is scheduled before the end of 2023.

---

† cianciosi@esrf.fr

NEW DEVELOPMENTS AND STATUS OF XAIRA, THE NEW MICROFOCUS MX BEAMLINE AT THE ALBA SYNCHROTRON

N. González[†], J. Juanhuix, J. Nicolás, D. Garriga, M. Quispe, A. Crisol, I. Sics, C. Colldelram

ALBA Synchrotron Light Source, Cerdanyola del Vallés, Spain

Abstract

The new BL06-XAIRA microfocus macromolecular crystallography beamline at ALBA synchrotron is currently under commissioning and foreseen to enter into user operation in 2024. The aim of XAIRA is to provide a $4 - 14$ keV, stable, high flux beam, focused to 3×1 μm² FWHM. The beamline includes a novel monochromator design combining a cryocooled Si(111) channel-cut and a double multilayer diffracting optics for high stability and high flux; and new mirror benders with dynamical thermal bump and figure error correctors. In order to reduce X-ray parasitic scattering with air and maximize the photon flux, the entire end station, including sample environment, cryostream and detector, is enclosed in a helium chamber. The sub-100 nm SoC diffractometer, based on a unique helium bearing goniometer also compatible with air, is designed to support fast oscillation experiments, raster scans and helical scans while allowing a tight sample to detector distance. The beamline is also equipped with a double on-axis visualization system for sample imaging at sub-micron resolutions. The general status of the beamline is presented here with particular detail on the in-house fully developed end station design.

INTRODUCTION

ALBA is a synchrotron light source located in the Barcelona area hosting ten operating beamlines, with four more beamlines in design or construction phases. Long-term plans include the upgrade of the facility to a 4th generation source together with major upgrades of the existing beamlines.

BL06-XAIRA is a new microfocus macromolecular crystallography (MX) beamline currently in commissioning, expecting first users along 2024. The beamline is designed to deliver high quality data from micron-sized and/or poorly diffracting crystals from oscillation and fixed-target MX experiments, as well as from experiments at low photon energies exploiting the anomalous signal of the metals naturally occurring in proteins (native phasing), which is enhanced in the case of small crystals. To this aim XAIRA is foreseen to provide a $\sim 4 - 14$ keV, 3×1 μm² FWHM (h × v), which can be slit down to 1×1 μm², with a flux of $>10^{13}$ ph/s/250 mA at 1 Å wavelength (12.4 keV).

The entire end station, that is detector, cryostream, diffractometer and sample conditioning elements, is enclosed in a helium chamber to provide optimal conditions for experiments at low energies as low as 3 keV. The system allows the recovery of the helium and is compatible with standard operation in air.

† ngonzalez@cells.es

BEAMLINE DESCRIPTION

The optical design of the beamline was first described in the SRI2018 conference in Taiwan [1]. The beamline is fed by a permanent magnet in-vacuum undulator, IVU19, with a magnetic period of 19.9 mm and a minimum gap of 5.2 mm [2]. The high power produced by the undulator, up to 4.3 kW at 250 mA, and the absence of vacuum windows to maximize the flux at low photon energies impose severe constraints on the cooling systems of the optical elements up to the monochromator. To mitigate this, the aperture of the front-end moveable masks is set to limit the power delivered to the beamline optics to 1.3 kW.

The complete beamline layout is shown in Figure 1. The beam is focused by two horizontal focusing mirrors, the horizontally prefocusing (HPM) and focusing (HFM) mirrors, and a vertically focusing mirror (VFM), the two latter mounted as a KB mirror pair. The mirrors are elliptically bent in the meridional direction by ALBA mirror benders, which provide sub-nanometric resolution and stability and allow correcting the wavefront deformations caused by static or dynamic effects such as long-period figure errors and thermal bumps [3]. High-precision slits (HSS) are placed at the focal position of the HPM to reduce the horizontal beam size, so that it can be further focused by the HFM to 1 μm FWHM at the sample position.

The energy is selected using a cryogenically cooled monochromator that combines a narrow gap, 4.5 mm, channel-cut monochromator (CCM) and a double multi-layer monochromator (DMM) mounted on the same Bragg axis. The geometry has been optimized to switch from one to another without the need of any translations. The beam diagnostics include one cooled and 4 non-cooled fluorescence screens (FS) [4] to monitor the beam profile and shape, and two 20 μm thickness CVD diamond XBPMs from Cividec to position and measure the incoming beam flux and two sets of slits to reduce the beam divergence.

The sample is located just 1 m downstream the last KB mirror, the HFM, in a vertically oriented goniometer. The entire end station, which includes the diffractometer, the detector, the cryostream and the sample visualization system, among others, is enclosed in a helium chamber, which can also be opened to air. In between the KB chamber and the helium chamber, the Beam Conditioning Elements (BCEM) enclose a fast shutter, a 4-blade slits set, an XBPM and a beam diagnostic unit with a YAG:Ce screen and a phodiode. The vacuum-helium or air interface between the BCEM chamber and the end station is maintained with a 10 μm thickness and 2 mm diameter diamond window. Besides, so as to monitor the beam stability at sample position, the two XBPMs include Q-Tools

THERMAL-DEFORMATION-BASED X-RAY ACTIVE OPTICS DEVELOPMENT IN IHEP*

Dezhi Diao[1], Han Dong[1], Jun Han[1], Shaofeng Wang, Fugui Yang[†1], Ming Li[1], Weifan Sheng[1],
Xiaowei Zhang, Institute of High Energy Physics, Beijing, China
Le Kang, Spallation Neutron Source Science Center, Dongguan, China
[1]also at University of Chinese Academy of Sciences, Beijing, China

Abstract

Active optics is a key technology for maintaining wavefront preservation during X-ray beam transport in fourth-generation light sources. In this paper, we propose a concept for surface thermal-driven active optics. In this scheme, the overlap between the position of driving source and the x-ray footprint can give strong modulation performance, including spatial resolution and modulation efficiency. Finite element analysis has experimentally verified the high modulation performance of this approach. To give the feedback of the modulation, we have established a vacuum in-situ surface profile measurement system. Preliminary experiments show that the measurement accuracy of the system's flat mirror can reach 80 nrad rms. The development of these technologies will provide new, low-cost solutions for fully exploiting the performance of fourth-generation light sources.

INTRODUCTION

The High Energy Photon Source (HEPS) currently under construction will be China's first fourth-generation X-ray light source with high energy and high brightness. Like other similar facilities, the quality of various optical instruments and equipment on the beamline seriously affects the X-ray beam transport performance of the beamline. On the one hand, it is important to choose high-quality optical components, such as ultra-precision X-ray mirrors and crystals. On the other hand, it is also necessary to consider the deformation errors of optical optics caused by clamping and thermal loads in the working environment. To solve these problems, the synchrotron radiation field has developed various active optics technologies over the past few decades, including bimorph mirrors [1, 2], bent mirrors [3, 4], phase plates [5-7], and REAL [8, 9] technology. To reduce the engineering risk of HEPS and the difficulties of budgeting, we propose and study a low-cost, low-technical-difficulty active optics technology scheme. By integrating the mirror surface with the driving element, the overlap between the footprint of x-ray beam and the driving modulation unit can be achieved, which is also conducive to improving the spatial frequency and driving efficiency of modulation. In conjunction with the surface shape modulation device, high-precision surface shape detection equipment is an important link in achieving feedback adjustment. To achieve in-situ measurement, extensive research has been done on various light sources,

including measurement schemes using interferometers [10, 11] and long trace profilers [12-15]. However, due to the influence of scanning window errors, the measurement error of the system is relatively large. In this project, we have developed a vacuum-based surface profiler metrology system. Finally, a closed-loop active optics modulation system is formed.

DEFORMABLE MIRROR AND PERFORMANCE ANALYSIS

Surface Modulation Scheme

Thermal deformation has always been one of the challenges faced by synchrotron radiation beamlines. Studies have shown that thermal deformation can be effectively suppressed through various means, including notch structure design, advanced cooling schemes, and balanced design of cooling and heating areas. These methods have been developed to ensure that the optical instruments and equipment on the beamline maintain their shape and performance under heating load conditions.
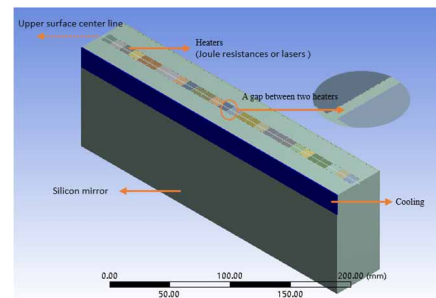
Figure 1: Multi-units surface heating-based shape modulation model.

In response to the demand for high spatial frequency modulation [16], a thermal-driven active optics mirror based on thermal deformation effects has been proposed, as shown in Fig. 1. The typical feature of this system is the overlap between the X-ray footprint and the heating driving area. Unlike traditional schemes, the fact that the position of the driving source is so close to the light-use area means that the transmission path is shorter, which is conducive to high spatial resolution. Each unit in the system is individually current-controlled, and the substrate material can be chosen as single crystal silicon, quartz, metal, etc., depending on the monochromatic and white light

ForMAX: A BEAMLINE FOR MULTI-SCALE AND MULTI-MODAL STRUCTURAL CHARACTERISATION OF HIERARCHICAL MATERIALS

J. B. González*, V. Haghighat, S. A. McDonald, K. Nygård, L. Roslund
MAX IV Laboratory, Lund, Sweden

Abstract

ForMAX is an advanced beamline at MAX IV Laboratory, enabling multi-scale structural characterisation of hierarchical materials from nm to mm length scales with high temporal resolution. It combines full-field microtomography with small- and wide-angle x-ray scattering (SWAXS) techniques, operating at 8-25 keV and providing a variable beam size. The beamline supports SWAXS, scanning SWAXS imaging, absorption contrast tomography, propagation-based phase contrast tomography, and fast tomography. The experimental station is a versatile in-house design, tailored for various sample environments, allowing seamless integration of multiple techniques in the same experiment. The end station features a nine-meter-long evacuated flight tube with a motorized small-angle x-ray scattering (SAXS) detector trolley. Additionally, a granite gantry enables independent movement of the tomography microscope and custom-designed wide-angle x-ray (WAXS) detector. These features facilitate efficient switching and sequential combination of techniques. With commissioning completed in 2022, ForMAX End Station has demonstrated excellent performance and reliability in numerous high-quality experiments.

INTRODUCTION

Both natural and man-made materials often possess a hierarchical nature, with distinct structures evident across various length scales. Understanding the relationship between structure and function in these materials necessitates characterizing the structure across these scales, coupled with sufficient temporal resolution to observe in-situ processes. The ForMAX instrument efficiently addresses this challenge by combining two complementary techniques: full-field tomographic imaging covering μm to mm scales and SWAXS targeting nm scales.

The primary technical obstacle in integrating full-field tomography with SAXS arises from spatial limitations behind the sample. In full-field tomography, one observes the x-ray beam transmitted through the sample in a forward direction. In contrast, SAXS captures the x-ray beam scattered at small angles, $\leq 3\circ$, essentially in a near-forward direction. At ForMAX, the innovative strategy is to conduct sequential tomography and SWAXS experiments. This is facilitated by a motorized detector gantry, enabling swift translation of the tomography microscope (and the WAXS detector) into and out of the x-ray beam. This design promotes a rapid and efficient transition between experimental modes.

In the following conference paper, we provide an in-depth overview of the ForMAX beamline's design. Table 1 list the main components of the beamline and their distance from source.

Table 1: Main ForMAX Components and Their Distance From Source

ForMAX Components	Distance from source (m)
Undulator	0
Front end movable mask	19.5
White-beam slits	23.9
Double multilayer monochromator	25.0
Double crystal monochromator	27.0
Vertically focusing mirror	30.2
Horizontally focusing mirror	31.0
Monochromatic slits	28.1, 32.3, 36.3, 41.5 - 41.8
Diamond window	35.8
Attenuator system	35.9
Fast shutter	36.1
X-ray prism lens	36.6
Compound refractive lenses	40.5
Experimental table	42.0
Full-field microscope	42.0 – 42.3
WAXS detector	42.1
SAXS detector	42.9-49.5

Throughout this article, we adhere to MAX IV's coordinate system: the lateral x-axis (outboard direction from the ring), the vertical y-axis (upward direction), and the longitudinal z-axis (downstream direction from the source). The direction of each rotation around the Cartesian axes (Rx, Ry, and Rz) adheres to the right-hand rule.

OPTICS

The primary optics of ForMAX comprises a double crystal monochromator (FMB Oxford), a double multilayer monochromator (Axilon), dynamically bendable vertical and horizontal focusing mirrors in Kirkpatrick-Baez (KB) geometry (IRELEC), a photon shutter (Axilon), and four diagnostic modules (FMB Oxford). These modules contain a fixed mask, a high-band-pass diamond filter for heat-load management, a white-beam stop, bremsstrahlung collimators, slits, beam viewers, and beam intensity monitors. This section explores the monochromators and mirrors. For an overview of the main components, see Fig. 1.

_____
* joaquin.gonzalez@maxiv.lu.se

SAPOTI - THE NEW CRYOGENIC NANOPROBE FOR THE CARNAÚBA BEAMLINE AT SIRIUS/LNLS

R.R. Geraldes[†], F.R. Lena, G.G. Basilio, D.N.A. Cintra, V.B. Falchetto, D. Galante,
R.C. Gomes, A.Y. Horita, L.M. Kofukuda, M.B. Machado, Y.A. Marino, E.O. Pereira, C.A. Pérez,
P.P.R. Proença, M.H. Siqueira da Silva, A.P.S. Sotero, V.C. Teixeira, H.C.N. Tolentino
Brazilian Synchrotron Light Laboratory (LNLS), Campinas, São Paulo, Brazil

Abstract

SAPOTI will be the second nanoprobe to be installed at the CARNAÚBA (Coherent X-Ray Nanoprobe Beamline) beamline at the 4th-generation light source Sirius at the Brazilian Synchrotron Light Laboratory (LNLS). Working in the energy range from 2.05 to 15 keV, it has been designed for simultaneous multi-analytical X-ray techniques, including absorption, diffraction, spectroscopy, fluorescence and luminescence, and imaging in 2D and 3D. Highly-stable fully-coherent beam with monochromatic flux up to 10^{11} ph/s/100mA-/0.01%BW and size between 35 and 140 nm is expected with an achromatic KB (Kirkpatrick-Baez) focusing optics, whereas a new in-vacuum high-dynamic cryogenic sample stage has been developed aiming at single-nanometer-resolution images via high-performance 2D mapping and tomography. This work reviews and updates the entire high-performance mechatronic design and architecture of the station, as well as the integration results of some of its modules, including automation, thermal management, dynamic performance, and positioning and scanning capabilities. Commissioning at the beamline is expected in early 2024.

INTRODUCTION

Synchrotron scanning X-ray microscopy has been established as a mature technique and a key characterization tool for scientific, technological, and engineering fields, with several beamline X-ray microscopes with beams of nanometric sizes (a.k.a. nanoprobes) being developed during this decade [1-11]. In particular, complementing techniques such as ultra-high-resolution fluorescence, the use of ptychography as a coherent X-ray diffractive imaging technique enables single-digit nanometer level spatial resolution, ultimately limited only by the beam and the sample stability during the exposure time [5, 7, 8, 11-13].

SAPOTI will be the second nanoprobe to be installed at the CARNAÚBA (Coherent X-Ray Nanoprobe Beamline) beamline at the 4th-generation light source Sirius at the Brazilian Synchrotron Light Laboratory (LNLS) [14, 15]. It has been designed for simultaneous multi-modal state-of-the-art X-ray techniques, including absorption, diffraction, spectroscopy, fluorescence and luminescence, and imaging in 2D and 3D. At 142 m from the undulator source and with achromatic optics, full benefit can be taken from the brilliance of the new-generation storage ring to reach diffraction-limited beam sizes, from 140 to 35 nm in the energy range from 2.05 to 15 keV, while optimizing the photon flux up to 10^{11} ph/s/100 mA/0.01%BW at the sample.

As comprehensively described in [15] and depicted in Fig. 1, SAPOTI will be an all-in-vacuum station, with a Kirkpatrick-Baez (KB) set of mirrors and the sample stage sharing the same ultra-high vacuum chamber. This architectural decision was made for stability, metrology and alignment purposes, and for optimization of transmission in the low-energy end. Three photodiodes (PD) for flux and absorption measurements, as well as two silicon drift detectors (SDDs) for fluorescence, are also placed inside the chamber, whereas the area detector (PiMEGA) and a complementary optical arrangement, alternatively used for an optical or a luminescence (X-ray Excited Optical Luminescence – XEOL) microscope, are placed outside vacuum, accessing the sample signals via a large beryllium window and a small glass viewport, respectively. Above the main chamber, a loading chamber comprises a load-lock system for cryogenic sample transfer, a cryogenic parking station (carousel) for sample storage, and a cryogenic pick-and-place gripper mechanism for sample loading. Cryogenic cooling at both the sample stage in main chamber and the parking station in the loading chambers is achieved by means of efficient thermal management using two pulse tube (PT) coolers.

Since the beginning of the project, the main aspect driving its mechatronic architecture has been the extreme sensitivity of the focusing optics and the sample to mechanical stability, once ultimate mapping resolution is one of the key design targets in the station. Firstly, a granite bench following the concepts developed for Sirius systems provides a stand with high mechanical and thermal stability, while allowing for basic positioning of station with respect to the beam in all degrees of freedom (DoFs) [16, 17]. Next, both the KB module and the sample stage are quasi-directly fixed to the granite bench, i.e., stiffly mounted via the bottom flange of the main chamber. Although unusual for beamline in-vacuum systems, and significantly more challenging in terms of manufacturing, assembly and baking, this solution offers unique possibilities regarding dynamics, i.e., suspension frequencies and vibration amplitudes.

---

† renan.geraldes@lnls.br

THE PROGRESS IN DESIGN, PREPARATION AND MEASUREMENT OF MLL FOR HEPS*

Shuaipeng Yue[1,2], Bin Ji[1], Ming Li[1], Qingyan Hou[1], Guangcai Chang[1,†]

[1]Institute of High Energy Physics, Chinese Academy of Sciences, 19B Yuquan Road, Beijing, China

[2]University of Chinese Academy of Sciences, 19A Yuquan Road, Beijing, China

Abstract

The multilayer Laue lens (MLL) is a promising optical element with large numerical aperture and aspect ratio in synchrotron radiation facility. The tilted MLLs are designed for the hard X-ray nano-probe beamline of HEPS. Two MLLs with 63(v)×43(h) μm² aperture and focal spot size of 8.1(v)×8.1(h) nm² at 10 keV are fabricated by a 7-meter-long Laue lens deposition machine. Ultrafast laser etching, dicing and focused ion beam are used to fabricate the multilayer into two-dimensional lenses meeting the requirement of diffraction dynamics. The multilayer grows flat without distortion. The smallest accumulated layer position error is below ±5 nm in the whole area and the root mean square (RMS) error is about 2.91 nm by SEM and image processing. The focusing performance of MLL with actual film thickness is calculated by a method based on the couple wave theory (CWT). The calculated full width at half maximum (FWHM) of focus spot is 8.4×8.2 nm² at 10 keV, which is close to the theoretical result.

INTRODUCTION

The smaller the spot of X-ray focus, the better the ability to distinguish the structure and composition of the material in a smaller spatial scale. The multilayer Laue lens has a large numerical aperture and depth-width ratio, and theoretically can focus x-rays below 1 nm [1], single-atom testing can be performed. Such high spatial resolution will enable the structure of materials to be studied at a new microscopic scale, effectively filling the gap between x-ray and electron microscopes in spatial resolution, it makes the exploration of the relationship between material structure and function more comprehensive and deepened, so it has been widely studied.

In order to improve the focusing resolution of MLL, a lot of research has been done by international researchers. In 2016, Sasa Bajt et al. carried out the fabrication and testing of wedged MLLs lens and obtained 8.4 nm × 6.8 nm at 16.3 keV [2]. In 2020, Xu et al. developed a MEMS template-based optical device for alignment of two linear MLLs, and realized a two-dimensional focusing spot of 14 nm × 13 nm at 13.6 keV photon energy [3]. In this study, we design and fabricate two MLLs with 63(v)×43(h) μm² aperture and calculate their focus performance at 10 keV.

DESIGN

The MLL consists of alternating regions made of two different materials. The thickness distribution is similar to that of a Fresnel zone plate (FZP). resulting in a focusing effect. The position of the nth layer of the film is determined by the zone plate formula:

$$x_n^2 = n\lambda f + n^2 \lambda^2 / 4 \qquad (1)$$

where x_n represents the position of the thin film, λ is the wavelength of the X-ray, and f is the focal length of the MLL. Additionally, the thickness of each layer dn can be expressed as follows:

$$d_n = x_n - x_{n-1} \approx \frac{\lambda f}{2 x_n} \qquad (2)$$

The MLL used within this study was designed at 10 keV using alternate target sputtering of WSi_2 and Si on a substrate. To achieve 8 nm focus spot for High Energy Photon Source (HEPS), the two-dimension focused MLLs are designed as follows (see Table 1).

Table 1: MLL Design Parameter

MLL@10KeV	Horizontal	Vertical
Aperture [μm]	43	63
Thickness [nm]	3.3-15	3-14
Layers	8030	13030
Optimum depth [μm]	3.5	3.3
Efficiency	8.4%	7.2%
Focal length [mm]	3	4
FWHM [nm]	8	8
Tilt angle [mrad]	7.4	8.3

The one-dimensional diffraction effect is calculated using the dynamics theory of X-ray diffraction. This was first used by Takagi and Taupin Diffraction (TTD) to describe the wavefront change of X-rays propagating when a crystal is distorted [4]. The MLLs' focusing property near focal plane is calculated using the Fresnel-Kirchhoff diffraction integral as shown in Figures 1 and 2. The intensity distribution of focal spot is shown in Figure 3.

MINERVA, A NEW X-RAY FACILITY FOR THE CHARACTERIZATION OF THE ATHENA MIRROR MODULES AT THE ALBA SYNCHROTRON

Antonio Carballedo[†1], Dominique Heinis[1], Carles Colldelram[1], Alejandro Crisol[1], Guifré Cuní[1],
Núria Valls Vidal[1], Alejandro Sánchez[1], Joan Casas[1], Josep Nicolàs[1],
Nicolas Barrière[2], Maximilien J. Collon[2], Giuseppe Vacanti[2],
Dieter Skroblin[3], Michael Krumrey[3], Levent Cibik[3], Ivo Ferreira[4] and Marcos Bavdaz[4]
[1]ALBA Synchrotron, Cerdanyola del Vallès, Spain
[2]cosine measurement systems, Sassenheim, The Netherlands
[3]Physikalisch-Technische Bundesanstalt (PTB), Berlin, Germany
[4]European Space Agency, ESTEC, Noordwijk, The Netherlands

Abstract

In this paper we present the newly built beamline MINERVA, an X-ray facility recently under commissioning at the ALBA synchrotron. The beamline has been designed to support the development of the X-ray observatory newATHENA (Advanced Telescope for High Energy Astrophysics) mission. MINERVA will host the necessary metrology equipment to integrate the stacks produced by cosine in a mirror module and characterize their optical performances. The beamline optical and mechanical design is originally based on the X-ray Parallel Beam Facility (XPBF) 2.0 from the Physikalisch-Technische Bundesanstalt (PTB), at BESSY II already in use to this effect. The construction of MINERVA is meant to significantly augment the capability to produce mirror modules.

The development of MINERVA has addressed the need for improved technical specifications, overcome existing limitations and achieve enhanced mechanical performances.

We describe the design and implementation of MINERVA that lasted three years. Even though the beamline is still under a commissioning phase, we expose tests and analysis that have been recently performed, remarking the improvements accomplished and the challenges to overcome, in order to reach the operational readiness for the mirror modules mass production.

MINERVA is funded by the European Space Agency (ESA) and the Spanish Ministry of Science and Innovation.

INTRODUCTION

The newATHENA telescope [1] is a space observatory that will address fundamental questions about energetic objects (accretion disk around black holes, large-scale structure, etc...). One of the key elements of the telescope is the innovative modular architecture of its optics subdivided by 13 concentric rings and filed by about 600 sub-systems called mirror modules (MMs) as seen in Fig. 1. These allows to maximize the effective collection area for a given geometry reducing its weight, critical aspects to be considered in space missions. The technology used to manufacture the MM is based on the Silicon Pore Optics technology

developed at cosine. Based on a modified Wolter-Schwarzschild geometry, photons in the energy range from 0.2 keV to 12 keV are reflected on two consecutive plates reaching the focal point located 12 meters further. At the focal plane, the telescope will be equipped with both imaging and spectroscopy instrumentation. Since the optics is based on the assembly of hundreds of individual and independent parts, the alignment operation is a crucial step to comply with the performance requested for the full assembled optics. At XPBF 2.0 [2], cosine is currently optimizing the method to produce MMs at large scale [3] and today MINERVA is built to strengthen and boost their production and characterization while preserving the interoperability between beamlines.
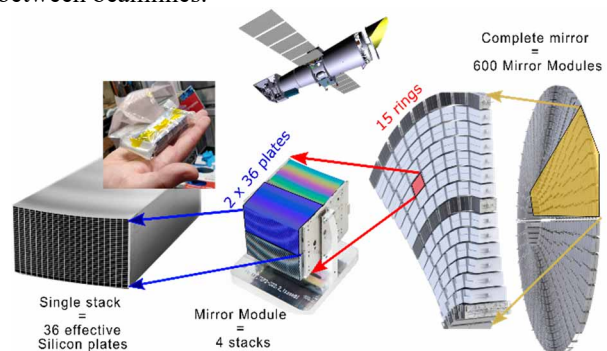
Figure 1: ATHENA Telescope Multiscale Optics Scheme

BEAMLINE OPERABILITY

MINERVA beamline works with samples consisting in a jig populated with 4 stacks composing a complete MM (Fig. 2). The relative position and orientation adjustment of an individual stack independently from the others is realized by using small hexapods. A 1 keV X-ray collimated beam impacts the optics at normal incidence. The jig is itself rigidly fixed on the top platform of a larger hexapod in order to control the 3D position of the MM respect to the incident X-ray beam. Light is then deflected and partially focused toward a 2D array detector about 12 meters further (close to the focal plane of the newATHENA optics). A complete characterization requires to repeat this operation over every single pore of the optics by mechanically moving the MM along a plane perpendicular to the input beam.

† acarballedo@cells.es

SHINING LIGHT ON PRECISION: UNRAVELING XBPMs AT THE AUSTRALIAN SYNCHROTRON

B. Lin[†], J. McKinlay, S. Porsa, Y. E. Tan, ANSTO, Australian Synchrotron, Melbourne, Australia

Abstract

At the Australian Synchrotron (AS), the need for non-destructive X-ray beam positioning monitors (XBPM) in the beamline front ends led to the development and installation of an in-house prototype using the photoelectric effect in 2021. This prototype served as a proof of concept and an initial step towards creating a customised solution for real time X-ray position monitoring. Of the new beamlines being installed at the AS, the High-Performance Macromolecular Crystallography (MX3) and Nanoprobe beamlines require XBPMs due to their small spot size and high stability requirements. However, a significant hurdle is the short distance from the source point to the XBPM location, resulting in an extremely restricted aperture to accurately monitor the beam position. Scaling down the photoelectric prototype to accommodate the available space has proven challenging, prompting us to explore alternative designs that utilize temperature-based methods to determine the beam position. This paper details insights made from investigating this alternative method and design.

INTRODUCTION

X-ray beam positioning monitoring technology plays an important role in synchrotron facilities, gaining increasing significance as light sources move towards smaller source sizes and nanoscale sample probing. The AS has been exploring this technology to develop an in-house, non-destructive white beam XBPM catered to its light source requirements. A photoemission XBPM was designed and installed by 2021 on the optical diagnostic beamline (ODB) as a proof of concept and prototype for future beamlines. The design was derived from LNLS and Soleil XBPM designs [1, 2]. However, there have been challenges with scaling this prototype to the new beamlines that need an XBPM due to their small spot size and high stability requirements, namely the Nanoprobe and MX3 beamline. Consequently, there has been a need to investigate alternative methods and designs that can cater for the requirements and specifications for the two beamlines.

PHOTOEMISSION XBPM

A photoemission prototype XBPM was fabricated and installed on the ODB with these requirements in consideration:

- Drain current from a single XBPM blade needs to be a minimum of 2 µA at 200 mA [3].
- Position resolution of < 1 µm for an undulator source at nominal beam current of 200 mA.
- Misalignment tolerance in the insertion device (ID) source point of ± 0.5 mrad in both planes.

---

† becky.lin@ansto.gov.au

XBPM Prototype Using Photoemission

The final design and assembly before the last flange was fastened can be seen below in Fig. 1 with the respective beam direction in red.
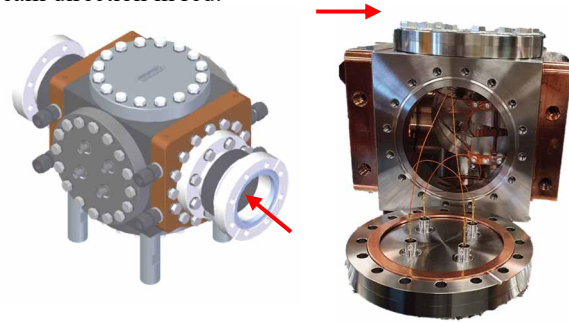
Figure 1: Final render and assembly of XBPM prototype.

The body is an ultra-high vacuum (UHV) stainless steel cube with flanged faces. Looking from upstream, the blades are mounted to the rear flange, the front flange has a pinhole mask for the beam fringes, the left and right flange both have four triaxial feedthroughs to pick up the drain current from the blades, and the top flange has a D-sub miniature (D-sub) port for temperature monitoring of the XBPM. The front and rear face of XBPM is shown in Fig. 2.
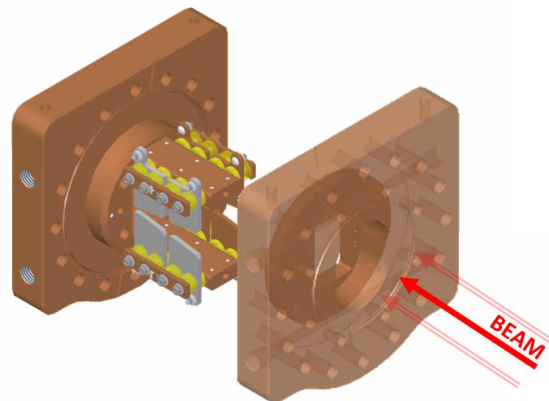
Figure 2: Front and rear flange of XBPM.

The pinholes in the mask have a diameter of 2 mm that allow the beam fringes to pass through. Theoretically, it samples the beam distribution more accurately as it strikes a more specific part of the blade, as this enables sampling of the beam at fixed points in space with a well-defined size. This allows a beam distribution to be fitted through the collected data more accurately and determine a verified centre point of the beam. Figure 3 exhibits the front view of the mask, where the pinholes are the four smaller holes adjacent to the centre window.

A SETUP FOR THE EVALUATION OF THERMAL CONTACT RESISTANCE AT CRYOGENIC TEMPERATURES UNDER CONTROLLED PRESSURE RATES

B.A. Francisco[†], W.H. Wilendorf, V.B. Zilli, G.S. de Albuquerque, D.Y. Kakizaki,

V.C. Kuriyama, A.R. Ribeiro[1], J.H.R. dos Santos[2], M. Saveri Silva

Brazilian Synchrotron Light Laboratory, Campinas, Brazil.

[1] also at Federal University of Uberlândia, Uberlândia, Brazil

[2]also at Federal University of Rio Grande do Sul, Porto Alegre, Brazil

Abstract

The design of optical elements compasses different development areas, such as optics, structures, dynamics, thermal, and control. Thermal designs of mirrors aim to minimize deformations, whose usual requirements are around 5 nm RMS and slope errors in the order of 150 nrad RMS.

One of the main sources of uncertainties in thermal designs is the inconsistency in values of thermal contact resistances (TCR) found on the literature. A device based on the ASTM D5470 standard test was proposed and designed to measure the TCR among materials commonly used in mirror systems. Precision engineering design tools were used to deal with the challenges related to the operation at cryogenic temperatures (145 K) and under several pressures rates (1~10 MPa) whilst ensuring the alignment between the specimens. We observed that using indium as Thermal Interface Material reduced the TCR in 10~42,2% for SS316/Cu contacts, and 31~81% for Al/Cu. Upon analyzing the measurements, we identified areas for improvements in the equipment, such as mitigating radiation and improving the heat flow on the cold part of the system that were implemented for an upgraded version.

INTRODUCTION

Thermal contact resistance (TCR) is a parameter that indicates the ratio between surfaces temperature gradients of two bodies in contact and the heat load and exchanged.

A heat exchange measurement setup was developed for improving our database about TCR, especially for cryogenic applications, in which uncertainties become critical for the performance of the instruments.

It is well-known that during mechanical contact between solid bodies, the surfaces typically touch each other from less than 1% to 2% of the nominal contact area [1]. This limited contact area plays an essential role in reducing the heat load exchange. The TCR is also influenced by several variables, encompassing thermal factors (material properties, interface temperature, and heat flow direction), morphological aspects (shape, roughness, finishing), as well as mechanical conditions (applied pressure between the surfaces and potential deformations) in addition to those related to the other heat transfer mechanisms: radiation (emissivity) and convection (fluid characteristics between the surfaces), which is minimized in a vacuum environment.

[†]barbara.francisco@lnls.br

An experimental approach was chosen since the diversity of models for calculating TCR values are limited to specific configurations. Among the known methods, including T-type, Infrared Thermography, Laser-Flash Method, and 3ω, the one with the lowest uncertainties (2-10%) [2] was selected: the Standard Steady-State Method. This method is comprehensively described in ASTM standard D5470-06 [3], and based on this standard, we developed a setup version for measurements at cryogenic temperatures.

EXPERIMENTAL SETUP

The standard test primarily involves column samples equipped with sensors. These samples are insulated to prevent heat loss through radiation and convection. A heat gradient is generated between the samples by using a heater, which is installed at one end, and a cooling source at the other end. A force actuator can be introduced to vary the stress across the samples. A test schematic is presented in Fig. 1. The temperature acquisition takes place after the system achieves a stationary state, and from this information, the contact region is determined.
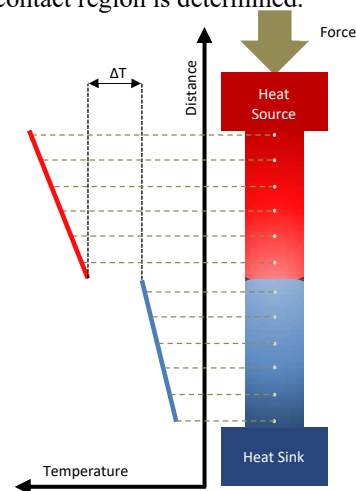
Figure 1: Diagram of how the data related to the standard steady-state method is obtained, from [4].

Thermal Management

Some adaptations were made in response to the cryogenic condition. The system was designed for operation within vacuum chambers, under a pressure level of $1 \cdot 10^{-7}$ mbar

CORE TECHNOLOGY DEVELOPMENTS

Cryogenics

ON THE PERFORMANCE OF CRYOGENIC COOLING SYSTEMS FOR OPTICAL ELEMENTS AT SIRIUS/LNLS

B. A. Francisco[†], M. P. Calcanha, L. M. Volpe, G. P. Lima, L. M. Kofukuda,
R. R. Geraldes, M. Saveri Silva

Brazilian Synchrotron Light Laboratory, Campinas, Brazil

Abstract

Several of Sirius' beamlines employ cryogenically cooled optics to take advantage of the silicon properties at low temperatures. A series of improvements has been evaluated based on our early operational experience focusing on the prevention of thermal instabilities of the optics. This work discusses the performance of the systems after optimizing the pressure of the vessels and their control logics, the effectiveness of occasional purges, and the cooldown techniques, and presents the monitoring interface. Furthermore, we introduce solutions (commercial and in-house) for achieving better beam stability, featuring active control of liquid nitrogen flow. We also propose the approach for the future 350 mA operation, including different cooling mechanisms.

INTRODUCTION

Sirius light source demands high performance instruments for ensuring photon-beam quality, especially in terms of wavefront integrity and position stability. Effective cooling of numerous silicon optical elements is essential to precisely control temperatures and related parameters, ensuring acceptable thermal effects regarding figure distortions and drifts at various timescales. Achieving the necessary precision equipment standards relies on robust thermal design. An alternative for cooling optical instrumentation in CATERETÊ [1] and CARNAÚBA [2] beamlines was described by Saveri Silva, et al [3]. This solution used open-cycle cryostats and continuous 24/7 functioning according to the diagram in Fig. 1. This approach was selected as a cost-effective alternative to closed-cycle cryocoolers for handling low-to-medium thermal loads with low vibration. Some of the adopted strategies continue to be integrated into the ongoing operation. However, during the working phase, it became evident that various instabilities occurred, posing significant hurdles to the reliable performance of the system.

The current research delves into an analysis of these instabilities and the series of tests undertaken to develop effective strategies for their mitigation. Three instances of instability were observed: temperature drifts (I) at the optics initiated after gradual variations in the temperature of the cold fingers at the end of the cryostats, variations associated with changes in the pressure (II) of the liquid nitrogen (LN2) vessels, and significant temperature spikes (III) during their refilling, as illustrated in Fig. 2.

It is believed that the explanation for all cases is related to the formation of vapor films at the cold fingers, Fig. 1. In the first case, there may be a gradual growth of the vapor film until the cold finger reaches a critical temperature, beyond
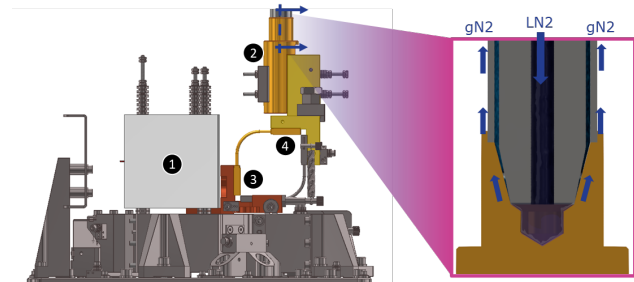
Figure 1: The second mirror (1) of CATERETE beamline is thermally connected to a cryostat (2) by a copper braid (3-4). In detail, the operation of the coupled open flow cryostat.
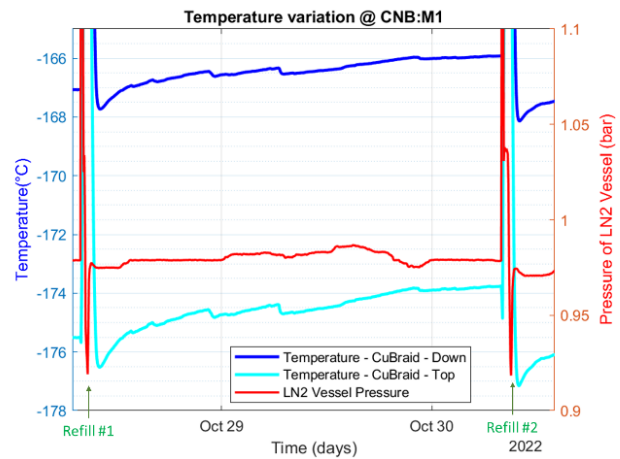
Figure 2: Temperature of a copper braid between first mirror and cold finger at CARNAÚBA beamline presenting drifts (case I), pressure-dependent variation (case II) and spikes (case III) during the refill.

which the current of the heaters that control the temperatures of the parts reaches zero and temperature variations in the optics start. In the other cases, the forced entry of vapor into the transfer line is the primary trigger for these variations [4].

It was noted that agitating the transfer line, whether through manual shaking or temporarily adjusting the flow (by a manual needle valve) and then returning it to its previous state, was sufficient to make temperatures decrease. However, this approach would require the operator to be systematically monitoring the graphs. Consequently, a general solution to these challenges could be achieved by implementing a closed-loop automatic control that adjusts the flow of liquid nitrogen based on the cold finger temperature, or, for the second and third cases, by implementing a solution that

EXACTLY CONSTRAINED, HIGH HEAT LOAD DESIGN FOR SABIA'S FIRST MIRROR*

V. B. Zilli†, B. A. Francisco, G.G. Basilio, J.C. Cezar, A.C. Pinto, V. S. Ynamassu, R.G. Oliveira,
G.R.B. Ferreira, F. A. Del Nero, G. L. M. P. Rodrigues, R.R. Geraldes, M.E.O.A Gardingo,
C. Ambrosio, L. M. Volpe

Brazilian Synchrotron Light Laboratory, Campinas, Brazil

Abstract

The SABIA beamline (Soft x-ray ABsorption spectroscopy and ImAging) will operate in a range of 100 to 2000 eV and will perform XPS, PEEM and XMCD techniques at SIRIUS/LNLS. Thermal management on these soft x-ray beamlines is particularly challenging due to the high heat loads. SABIA's first mirror (M1) absorbs about 360 W, with a maximum power density of 0.52 W/mm², and a water-cooled mirror was designed to handle this substantial heat load. To prolong the mirror operation lifetime, often shortened on soft X-ray beamlines due to carbon deposition on the mirror optical surface, a procedure was adopted using high partial pressure of O_2 into the vacuum chamber during the commissioning phase. The internal mechanism was designed to be exactly constrained using folded leaf springs. It presents one degree of freedom for control and alignment: a rotation around the vertical axis with a motion range of about ±0.6 mrad, provided by a piezoelectric actuator and measured using vacuum compatible linear encoders. This work describes the SABIA's M1 exactly constrained, high heat absorbent design, its safety particularities compared to SIRIUS typical mirrors, and validation tests results.

INTRODUCTION

Unique challenges emerged with the introduction of innovative optics instruments such as DCML [1] and the exactly constrained mirrors for the Sirius facility. The solution for SABIA's first mirror consists of an exactly constrained side bounce mirror [2] with direct internal cooling. The technical commission of SABIA Beamline (SAB) started on the early 2023. The beamline optical layout is shown on Figure 1.
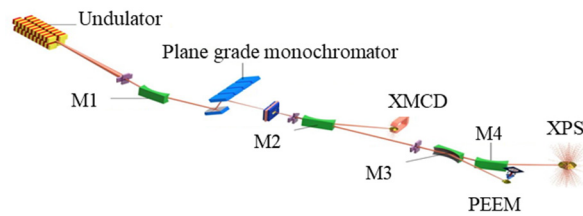
Figure 1: SABIA's optical layout.

Internal water cooling is not new for the synchrotron community, it has been proposed as a solution for previous generation sources heat management [3] but it still been used by some of the major manufacturers [4] as it can manage high heat load. Hose connections pose electronic and vacuum safety challenges, demanding meticulous mechanical isolation and leak protection. We looked at this with special attention to ensure both safety in case of coolant leakage, and mechanical decoupling on important degrees of freedoms.

THERMO-MECHANICAL DESIGN

The SAB M1 mechanism is comprised of two main parts. The first one is the granite bench, responsible for rough alignment and mechanical support for the ultra-high-vacuum vessel [5]. The other is the multifunctional internal mechanism, as it is the mirror support, short stroke for fine alignment, thermal insulator, and thermo-mechanical deformation accommodator. The main requirements for this system's internal mechanism can be found on Table 1.

Table 1: System Summarized Specs

Description	Spec
Ry range:	> 1 mrad
Ry resolution:	< 150 nrad
Resonances:	> 100 Hz
Max beam distortion	<10% nominal size
Power load @ 300mA:	~ 360 W
Cooling scheme:	Internal water flow

Figure 2 shows the complete in-vacuum parts for this system: A) the mirror with internal water channels; B) photo-collector used as indirect beam illumination over the optical face; C) the mirror support and metrology assembly, including the frame (often called *"Patrick"),* responsible for the fine mechanical motion and metrology and thermal deformation accommodator and Folded Leaf Springs (FLS); D) optical encoders RL26BVS001C30V [6], for fine metrology; E) fine rotation motion stiff actuator N-470.U PiezoMike [7]; F) water hose and vacuum guard assembly; G) water and safety vacuum inlet/outlet.

INVESTIGATION OF VIBRATIONS ATTENUATION WITH DIFFERENT FREQUENCY ALONG HEPS GROUND

Yuning Yang[1], Fang Yan[†], Zihao Wang, Xiangyu Tan

The Institute of High Energy Physics of the Chinese Academy of Sciences, Beijing, China

Xiangrong Fu, Wenjie Wu, Lan Yan, China Agricultural University, Beijing, China

Jun Lei, Peking University, Beijing, China

[1]also at China Agricultural University Beijing, China

Abstract

High Energy Photon Source (HEPS) has a strict restriction on vibration instabilities. To fulfil the stability specification, vibration levels on HEPS site must be controlled. The control standards are highly related with the vibration amplitude of the sources and the distance between sources and the critical positions. To establish reasonable regulations for new-built vibration sources, the decay patterns are investigated on HEPS site for different frequency noises. A series of experiments were conducted using shaker to generate vibrations with frequency from 1 Hz up to 100 Hz. The vibration attenuation on ground and slab were measured using seismometers and the attenuation law were analysed. Details will be presented in this paper.

INTRODUCTION

With the usage and development of high precision equipment, the impact of vibrations on large scientific facility is becoming increasingly prominent. Depending on source of the vibrations, the noises can be classified into artificial vibrations and natural vibrations [1]. Natural vibration include ground motions, wind-induced vibrations, water wave vibrations et al., while artificial vibration include vibrations generated by vehicles, light rail, building facilities, large machinery et al.. The random noise generated by these vibration sources can have a significant impact on the resolution and sampling efficiency of equipment. In severe cases, it can even cause expensive equipment or system unworkable. Therefore, controlling the internal and outside vibrations are necessary [2].

Due to the non-uniformity of the ground medium and the uncontrollability of random noise (frequency, amplitude), it is difficult to accurately predict the vibrations generated by external vibration sources using widely used Bornitz model [3]. Therefore, it is necessary to propose more reasonable prediction formulas based on the measured attenuation data on HEPS.

To ensure the validity of the measurement data, the self-noise measurement of the employed instrumentation was conducted, and compared with the environmental noise level on the foundation of HEPS storage ring and the vibration amplitude transmitted over a distance of 170 m from the shaker. Subsequently, vibrations with frequency of 1 Hz up to 100 Hz were generated using the shaker, and the ground and floor vibrations along the propagation line were measured using a seismometer. The attenuation of these vibrations was analysed and presented in this paper.

Instrumentation

The seismometers and velocimeters used in this experiment include five Gaia Code Alpha and three Guralp 3espcde all-in-one seismometers and the detailed parameters of these equipment are listed in Table 1:

Table 1: Margin Specifications

Seismometer	Frequency Ranges	Sensitivity
Alpha	0.0083~150 Hz	6000 V/m/s
3espcde	0.017~100 Hz	2000 V/m/s

ANALYSIS AND CALCULATION OF DEVICE SELF-NOISE

Seismometer Self-noise Measurement

The three-sensor coherence analysis method is a seismic instrument self-noise analysis method based on correlation analysis. Its basic principle is that when three seismometers observe the same input signal, the correlated parts of the signal are removed, and the remaining parts are considered as the device's self-noise. This analysis method requires two assumptions [4]:

1. The internal noise of the data acquisition channels is uncorrelated.

2. The internal noise of the seismometer and the environmental noise signal are uncorrelated.

The basic model is shown in Fig. 1. The calculation formula is shown in Eq. (1):

$$N_{ii} = P_{ii} - P_{ji} \cdot \frac{P_{ik}}{P_{jk}} \tag{1}$$

The experimental site for the self-noise testing of the 8 devices used in this study was located in an observation cave at the Beijing National Seismic Observatory. Each device was shielded using a simple shielding cover as shown in Fig. 2.

All the seismometers have low self-noise levels. Due to limited space, the result of one Guralp's 3espcde plotted in Fig. 3.

†yanfang@ihep.ac.cn

DESIGN AND TEST OF PRECISION MECHANICS FOR HIGH ENERGY RESOLUTION MONOCHROMATOR AT THE HEPS

Lu Zhang, Hao Liang[†,1], Wei Xu[1], Zekuan Liu, Yang Yang, Yunsheng Zhang

Institute of High Energy Physics, Beijing, China,

[1]also at University of Chinese Academy of Sciences, School of Physics, Beijing, China

Abstract

A monochromator stands as a typical representative of optical component within synchrotron radiation light sources. High resolution monochromators (HRMs), which incorporate precision positioning, stability control, and various other technologies, are a crucial subclass within this category. The next generation of photon sources imposes higher performance standards upon these HRMs. In this new design framework, the primary focus is on innovating precision motion components. Rigorous analysis and experimentation have confirmed the effectiveness of this design. This structural model provides valuable reference for developing other precision adjustment mechanisms within the realm of synchrotron radiation.

INTRODUCTION

The Nuclear Resonance Scattering (NRS) spectroscopy at High Energy Photon Source (HEPS) demands extremely high energy-resolving power better than 10^{-7}. As an optical element upstream of focusing mirror, the HRM shall maintain a high stability in terms of positioning, which could influence the energy precision as well as the beam stability at sample position, at fourth generation sources like HEPS. In the proposed monochromator configuration [1, 2], the range for fine pitch adjustment mechanism is relatively small. There also lacks an integrated angular sensing measurement device, thus real time precise tracking of fine pitch position is not possible. These factors impose constraints on the operation and performance of the monochromator. By referring to the previous design from APS and PETRA III [3-6], we have designed a new compact HRM mechanism with an *in-situ* metrology framework. This newly designed flexure mechanism is promising in increasing the stroke while minimizing errors of measurement system through highly rigid metrology devices. The developed mechanism successfully balances requirements between large travel range and high stability. In this paper, we will present the concept, simulation and offline measurements of the new HRM.

MECHANICAL DESIGN

According to the optical design, the HRM comprises two pairs of pseudo channel-cut crystals, with each pair being secured and adjusted by a pose adjustment mechanism. Consequently, the HRM is equipped with two pose adjustment mechanisms for each pair of pseudo channel-cut crystals.

As shown in Fig. 1, in response to the crystal pose adjustment requirements, each set of pose adjustment mechanisms comprises of six motion axes. These include x-axis coarse adjustment, z-axis coarse adjustment, Bragg axis adjustment, lattice matching axis tilting adjustment, and precision adjustment for crystal pitch angle and roll angle. While the first four motion axes are directly actuated by precision stages from KOHZU, the design of the last two precision adjustment mechanism is intricately linked to the ultimate performance of the monochromator and forms the core of the monochromator's structural design.
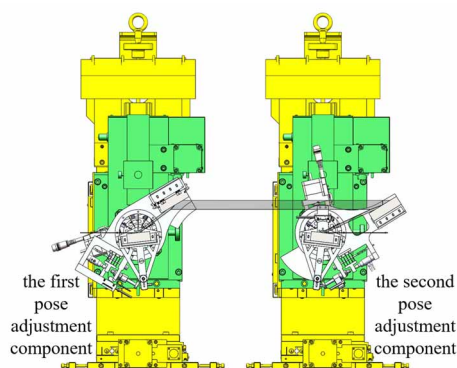
Figure 1: Mechanical design of the HRM.

In Fig. 2, we present the design of the first pose adjustment component. Due to the relatively lower resolution requirement for roll angle adjustment compared to pitch, we have directly employed a Newport 8321 picomotor as the actuator and an industrial flexible pivot as the rotational bearing. This configuration allows for the precise adjustment of the crystal's roll angle. In the design process, we carefully considered the impact of the driver's travel distance on the final angular resolution. As a result, we maximized the driver's travel distance while ensured high stability.
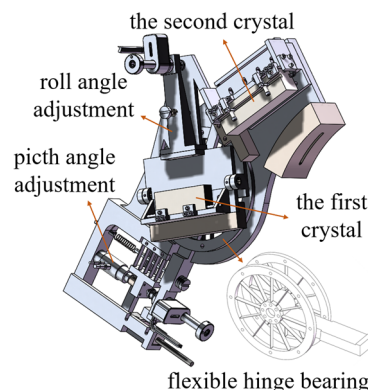
Figure 2: The first pose adjustment component.

---

† lianghao@ihep.ac.cn

DESIGN AND IMPROVEMENTS OF A CRYO-COOLED HORIZONTAL DIFFRACTING DOUBLE CRYSTAL MONOCHROMATOR FOR HEPS

Yunsheng Zhang[†], Hao Liang, Lu Zhang, Yuanshu Lu, Dashan Shen
Institute of High Energy Physics Beijing Synchrotron Radiation Laboratory, Beijing, China

Abstract

Horizontal diffracting double crystal monochromator (HDCM) are usually used in a 4th generation light source beamline due to the larger source size in the horizontal direction. This paper introduces the mechanical design and optimization of a HDCM for Low-dimension Structure Probe Beamline of HEPS. In order to achieve the high stability requirement of 50 nrad RMS, the structural design is optimized and modal improved through FEA. In order to meet the requirement of a total crystal slope error below 0.3 µrad, FEA optimizations of the clamping for first and second crystal are carried out. The vacuum chamber is optimized to become more compact, improving the maintainability. Fabrication of the HDCM is under way. The results show that the design is capable of guarantee the required surface slope error, stability, and adjustment requirements.

INTRODUCTION

HEPS is the first high energy beamline and the first 4th generation beamline in China. Thanks to the low emittance of the source, the beam source size could be as small as 10 microns. The low-dimension structure probe beamline (LODiSP) of HEPS is beamline dedicated on x-ray surface diffraction technique. The energy range of this beamline is the beamsize is in vertical and in horizontal. When a monochromator is used in horizontal diffraction mode, the tolerance of vibration in pitch direction for a double crystal monochromator could be as low as 50 nrad.
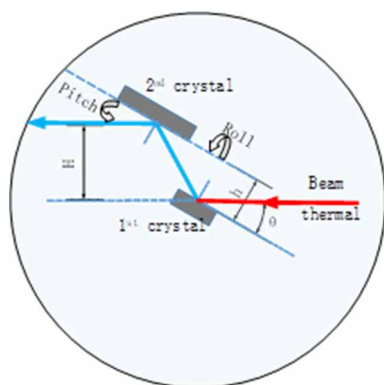
Figure 1: Beam path in a DCM.

The energy of the exit beam is a function of the Bragg angle θ (Fig. 1), and the resulting angular. and the resulting angular range with silicon crystals Si(111) is about 2.52°∼24.32° (4.8∼45 keV).

† zhangys97@ihep.ac.cn

According to Fig. 1, the spacing between reflected beam and Incident beam can be expressed as Eq. (1) [1]:

$$H = h \times 2cos\theta \qquad (1)$$

A linear slide table under the second crystal enables high requirements to be fixed. Through the bellows (Fig. 2), the vibration of the cavity and the internal components is decoupled to achieve the purpose of improving stability.
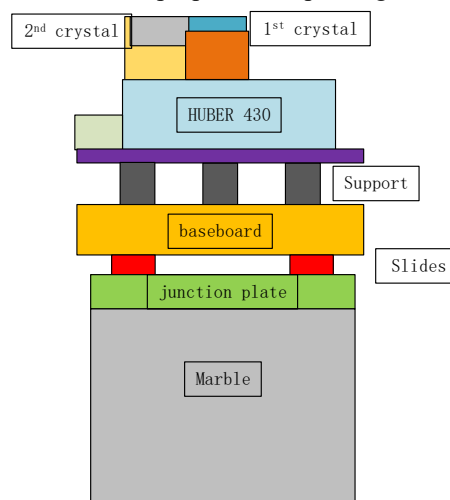
Figure 2: Monochromator construction.

DESIGN OF THE MONOCHROMATOR

The crystal slope error is an important parameter affecting the beam quality. The design of this monochromator (Fig. 3) uses a scheme in which copper blocks are clamped on both sides of the crystal [2, 3].
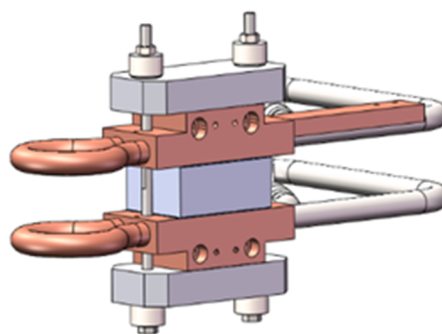
Figure 3: 1st crystal holder.

The FEA method was used to analyze the influence of different clamping positions and different thicknesses of pressure plate on it. Through multiple iterative optimizations, the clamping structure that meets the requirements of slope error is obtained, and the strain cloud diagram is shown (Fig. 4).

DEVELOPMENT AND IMPROVEMENT OF HEPS MOVER*

Shu Yang[†], Lei Wu, Chunhua Li, Zihao Wang, Siyu Chen, Yuandi Xu
Institute of High Energy Physics, Beijing, China

Abstract

High Energy Photon Source (HEPS) has been constructed after decade of research. As the first diffraction-limited storage ring light source, many advanced devices are applied in this project, including the Beam Based Alignment Mover (Mover), which support and adjust the position of the Sextupole Magnet. It undertakes to remotely online adjust the position of Sextupole to meet the Physical requirement to correct the optics coefficient of Electron beam current. The positioning accuracy, attitude angle, and coupled error of Mover with 450 kg load strictly proposed and tested during the development of Mover. There are three main types of Mover, including Four-layer with sliding guide, Three-layer with rolling guide, and Three-layer with sliding guide. This paper introduces the development and improvement of Mover.

INTRODUCTION

The High Energy Photon Source (HEPS) has been designed and constructed to be the first high energy diffraction-limited storage ring (DLSR) light source whose electron beam energy reach to 6GeV and emittance is less than 60pm·rad [1].

Movers are designed to accurately adjust the position of Sextupoles to eliminate a strong feed-down effect and so formed dominating contribution to the optics distortion [1-2]. In LCLS, EXFEL, SXFEL, and DCLS, Mover is applied to carry relative lightweight quadrupoles [3-5]. HEPS firstly apply Mover to accurately adjust the position of 450kg Sextupoles.The specific requirements are shown in Table 1.

Table 1: The physical Requirements for Mover

Content	Requirement
Positioning Accuracy	± 5 μm
Yaw	3″
Roll	3″
Pitch	2″
Coupled Error	15 μm
Natural Frequency of support system	54 Hz

Three kinds of of prototype, including four-layer with sliding guide, three-layer with rolling guide, and three-layer prototype with sliding guide are studied.

The method and result of measuring process of motion performance of batch production of Mover is described in this paper.

STRUCTURE & MANUFACTURE

The structure of Mover should be elaborately designed to possess the properties such as high precision, low velocity, good stability, resistance to radiation, long service life, and compact size.

The model of four-layer with sliding guide is firstly designed based on previous research [6]. It is basically consisted of five parts (see Fig. 1), including horizontal plate, lateral constraint guide, upper wedge plate, lower wedge plate and base plate. Three-layer with rolling guide which is driven by piezoelectric ceramic motor is designed then (see Fig. 2). It mainly consists of upper wedge plate, lower plate, base plate, and high rigidity linear guide. The structure is further simplified to three-layer prototype with sliding guide (see Fig. 3). It mainly consists of upper wedge plate, lower plate, and base plate.
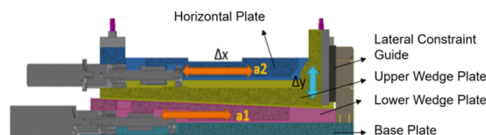
Figure 1: Four-layer with sliding guide Mover.
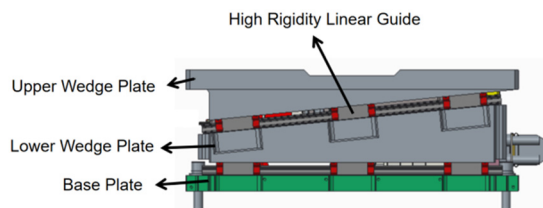
Figure 2: Three-layer with rolling guide Mover.

Figure 3: Three-layer with sliding guide Mover.

Cast iron is chose to be the material of Mover body since its properties of good resistance to vibration, stable performance and good accuracy retention, and easy to shape.

One of an important manufacture process should be scraping and grinding of sliding guide (see Fig. 4). It is helpful to decrease the residual stress in the plate so that accuracy and rigidity are enhanced. The lubricant could be reserved at series of uniform pit after scraping and grinding to form an oil film to improve friction performance and service life as a result.

THE DEVELOPMENT AND APPLICATION OF MOTION CONTROL SYSTEM FOR HEPS BEAMLINE

Gang Li, Yu Liu, Xiaobao Deng, Dianshuai Zhang,
Aiyu Zhou, Chunxia Yin, Qun Zhang, Zhenhua Gao, Zongyang Yue*
Institute of High Energy Physics, Chinese Academy of Sciences, Beijing, Peoples Republic of China

Abstract

In synchrotron radiation facilities such as the High Energy Photon Source (HEPS) beamline, thousands of motorized actuators are equipped on different optical devices, such as K-B mirrors, monochromator and transfocators, in order to acquire the specified properties of X-ray. The motion control system, as a part of the ultra-precision mechatronics devices, is used to precision positioning control, which not only has ability to realize basic motion functions but also can handle complex motion control requirements. HEPS has developed a standardized motion control system (MCS) for synchrotron radiation applications. In this paper, the structure of hardware and software of MCS will be presented, and some applications are demonstrated in detail.

INTRODUCTION

In the 15 beamlines of HEPS Phase I [1], there are thousands of actuators that required to control, including of PMSM, VCM, piezo and stepper motors. The number of stepper motors accounts for approximately 90 percent due to its high resolution ability, including two phase stepper and five phase stepper.

In order to satisfy the torque and size requirements of the optical devices, different motors must be employed, which demand that the MCS has the flexibility in configuring the driver current and micro-step. The position encoders were utilized in some motion axes for the application of close-loop to achieve the high repeatability. Therefore the MCS must be capable of supporting the different sensors, such as AqB, Biss-C and Endat2.2. Meanwhile, MCS should support the various types of limit switches, brakers and so on, to protect the mechanics devices. It is necessary to establish a uniform electrical standard, such as the connection between controller and devices (e.g. motor, encoder), the interface between controller and driver. In the aspect of field deployment, the large distances between controller and motors should be guaranteed. Besides the fundamental motion control requirements mentioned above, the complex devices in the end station of beamline especially, introduces more demanding performance criteria for MCS, include of synchronisation of multiple axis motions, complex trajectory planning, and real-time position event trigger.

Considering of the personnel resources and development costs, it's a significant challenge to satisfy all the control requirements of motion axes through a unified motion control system. It is very popular to use the VME controller in the

_____
* yuezy@ihep.ac.cn

majority of synchrotron labs worldwide, such as CLS [2], BESSY [3], and SSRF [4]. But the VxWork OS is so expensive, HEPS give up this scheme. From the perspective of HEPS and with reference to the other synchrotron labs, we have developed a novel motion control system utilizing commercial products.

In this paper, we will introduce the hardware structure of motion control system in detail. The software was developed under the Experimental Physics and Industrial Control System (EPICS) control framework [5]. Finally, several applications of MCS were demonstrated.
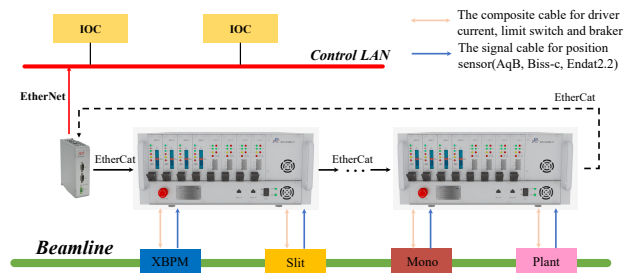
Figure 1: The overall hardware architecture of HEPS MCS.

THE ARCHITECTURE OF MOTION CONTROL SYSTEM

System Overview

The MCS is built of three main hardware components: master controller, control rack and driver board, the hardware architecture as shown in Fig. 1. A single MCS can support up to 64 axis, according to the EtherCAT fieldbus.

Figure 2: The control rack of MCS.

The MCS as the distributed system separates the control unit and driver unit. The master controller and control rack belong to the control unit. The controllers of ACS products (SPiiPlusEC and PDIcl) are the core of control unit where

DESIGN OF A LONG VERSATILE DETECTOR TUBE SYSTEM FOR PINK BEAM SMALL-ANGLE X-RAY SCATTERING (SAXS) BEAMLINE AT HEPS

Zhaoqiang Cui[†], Shanzhi Tang, Jiuchang Zhang, Zina Ou, Guang Mo, Xueqing Xing

Institute or High Energy Physics Chinese Academy of Sciences, Beijing, China

Abstract

The X-ray scattering experiment vacuum camera device is the first piping system of high-energy synchrotron radiation light source applied to pink small-angle scattering experiments, which has a variety of functions and can be used for WAXS, SAXS and USAXS experiments. This paper introduces the size, vacuum parameters, motion parameters and part of the radiation protection of the equipment, briefly summarizes how to solve the problem of the influence of uneven ground in the light source hall on the installation of the equipment, outlines how to solve the problem of maintaining good straightness of the track in a very long case, theoretically briefly analysis the influence of ground vibration on the stability of the detector, and outlines the radiation protection scheme of some vacuum cavities.

INTRODUCTION

This equipment is a small angle scattering experimental device applied to Huairou BB line station, which can perform SAXS/WAXS/USAXS, SAXS-CT and ASAXS combination experiments.

A 23m long versatile detector tube system is shown as Figure 1. Three Eiger2 detectors will be installed along the deciVe. The WAXS detector is suspended diagonally above the sample to collect about -5°~50° scattering signals. The SAXS detector, which is used to collect 0. 04°~6°, is installed in the front large tube with a diameter of 1.5 m and a length of 14 m. The detector can move freely within the tube according to experimental requirements. The distances between sample and SAXS [1] detector can be altered freely. The USAXS detector, which is used to collect 0.001°~0.1° signals, is placed at the end of tube. The vacuum degree of the tube is less than 1 Pa. The three detectors can work simultaneously to collect the whole larger angle range from 0.001°~50°. Two kinds of beamstop used for transmission mode and grazing incidence mode respectively, are installed in front of the SAXS and USAXS detectors.

Figure 1: X-ray scattering experiment vacuum camera device.

STRCTURAL DESIGN

Figure 2 shows the overall overview of the equipment. The X-ray small-angle scattering experiment vacuum camera device consists of four parts: the device for WAXS experiment, the device for SAXS experiment, the device for WAXS experiment and the vacuum chamber.
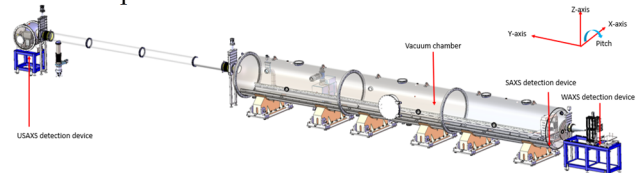
Figure 2: Overall device composition.

As shown as Figure 3, the WAXS device is located in the atmosphere and moves in a straight line in three directions of the detector. The probe's projection angle motion range is 55°. The lifting displacement table and the horizontal displacement table are spliced by processed aluminum alloy steel plates, and this structural design effectively reduces the weight of the device and effectively helps to improve the stability of the equipment structure. The base of the device is composed of square steel pipes. After the welding of the base is completed, it is treated with stress relief process, and then finished to effectively reduce the influence of welding deformation on the motion accuracy of the detector. In addition, the base is welded from Q235 square steel, which reduces the manufacturing cost. Similarly, the shelves used for the hoisting of the detectors are made of welded steel plates, which are subjected to a strain relief process of heat treatment after welding. Then drill the holes, which can ensure the concentricity of the two holes, and effectively reduce the error of detector installation.
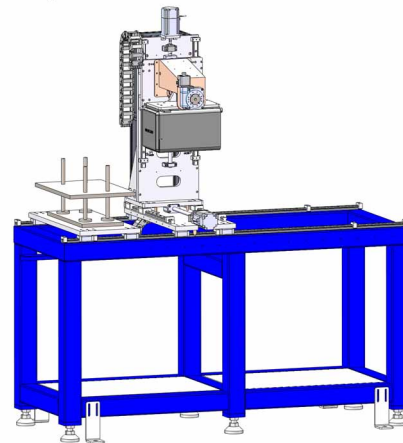
Figure 3: The device for WAXS experiment.

INFLUENCE OF THE GROOVE CURVATURE ON THE SPECTRAL RESOLUTION IN A VARIED-LINE-SPACING PLANE GRATING MONOCHROMATOR (VLS-PGM)*

Jingjing Du†, Zimeng Wang, Xuewei Du, Qiuping Wang

National Synchrotron Radiation Laboratory,

University of Science and Technology of China, Hefei, China

Abstract

Diffraction-limited synchrotron radiation (DLSR) light source with smaller source size and emittance makes ultra-high spectral resolution beamline possible. Here, we report an undulator-based beamline optical design with ultra-high spectral resolution using a varied-line-spacing plane grating monochromator (VLS-PGM), which is a well-proven design for achieving ultra-high resolution in the soft X-ray band. A VLS plane grating with a central groove density of 2400 l/mm is utilized to cover the photon energy region of 250 ~ 2000eV. VLS gratings are generally fabricated using the holographic method, but the resulting grating grooves are two-dimensionally curved curves, which can affect the resolution of the monochromator. To analyse this effect, we first use a spherical wavefront and an aspherical wavefront to generate the fringes and optimized the recording parameters. We also present a method for calculating the grooves curvature of holographic plane VLS grating grooves. Furthermore, the influence of grating grooves curvature on beamline resolution is theoretically analysed based on the aberration theory of concave grating.

INTORDUCTION

Diffraction limited synchrotron radiation (DLSR) has higher brightness and coherence. How to transmit the light from the storage ring to the experimental station with high quality is a challenge faced by beamline technology. Ultra-high spectral resolution beamlines are possible due to the smaller source size and emittance. The BL10 test beamline of Hefei Advanced Light Facility (HALF) proposed a design specification to achieve 100,000 resolving power at 400eV photon energy. In this paper, a beamline optical design based on varied-line-spacing plane grating monochromator [1, 2] (VLS-PGM) is given, which uses a VLS plane grating with a central groove density of 2400 l/mm to cover the soft X-ray photon energy region of 250~ 2000 eV。And this beamline can achieve 100,000 resolving power at 1000 eV photon energy.

There are two methods for making varied-line-spacing plane gratings, mechanically ruling method and holographic exposure method. Compared with mechanically ruled gratings, holographic gratings are simple to fabricate, easy to change the shape of the grooves, and have the advantages of no ghost lines. However, the grating grooves fabricated by the holographic method are two-dimensionally curved curves. When calculating the beamline resolving power, it is not only necessary to analyse the effects of

---

† jjdu@mail.ustc.edu.cn

aberration, entrance slit width, exit slit width, the slope error of optical elements, and diffraction limit of the grating on the monochromator spectrum broadening, but also to analyse the influence of grating grooves curvature on beamline resolution. We established a calculation model for the curvature of holographic VLS plane grating grooves. The curvature of the grating grooves is used as an important evaluation criterion when optimizing the parameters of the holographic recording system [3]. How to make the curvature of the optimized holographic grating grooves smaller is also a new challenge.

OPTICAL DESIGN

The period length of the undulator is 40mm and the total length is 3920 mm. Figure 1 shows the layout of the optical system. The total length of the beamline is 72.41 m. The first mirror is a water-side-cooled plane mirror, coated with Au, deflecting the beam horizontally by 1.6°. The monochromator consists of a varied-line-spacing plane grating and a plane mirror, which is used to change the included angle of the grating while wavelength scanning. The nominal groove density of the grating is 2400 l/mm, covering the energy range of 250 ~ 2000 eV. The toroidal mirror downstream the exit slit has a grazing incidence angle of 0.8° and is used to focus vertically and horizontally to the experimental station.
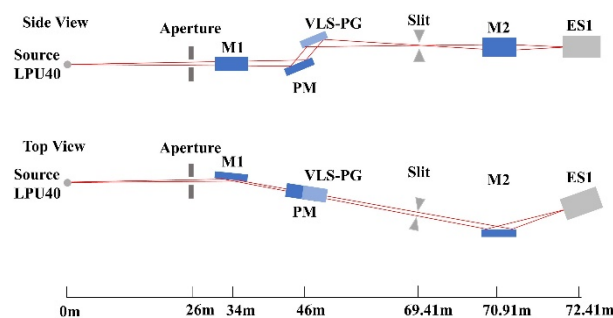
Figure 1: Layout of the optical system.

Due to the focusing characteristics of the VLS grating, a focusing mirror can be omitted upstream the exit slit, thereby improving the transmission efficiency of the beamline. The VLS grating parameters is expressed by equation $n(w)=n0(1+a_1w+a_2w^2+a_3w^3…)$, where w is the position on the grating along the light propagation direction, n(w) is the grooves density, n0 is the grooves density at the center of the grating, a_i is the space variation parameters.

According to the concave grating aberration theory, the VLS coefficient a2 can be obtained by F20 = 0. Then,

A SUBNANOMETER LINEAR DISPLACEMENT ACTUATOR

Shuaikang Jiang[†], Xuewei Du, Qiuping Wang
USTC/NSRL, Hefei, Anhui

Abstract

With the development of synchrotron radiation technology, an actuator with sub-nanometer resolution, 100 N driving force, and compatible with ultra-high vacuum environment is required. To achieve synchrotron radiation micro-nano focusing with adjustment resolution of sub-nanometer and high-precision rotation at the nano-arc level, most of the commercial piezoelectric actuators are difficult to meet the requirements of resolution and driving force at the same time. The flexure-based compound bridge-type hinge has the characteristic of amplifying or reducing the input displacement by a certain multiple, and can be used in an ultra-high vacuum environment. According to this characteristic, the bridge-type composite flexible hinge can be combined with commercial piezoelectric actuators, to design a new actuator with sub-nanometer resolution and a driving force of 100 N. This poster mainly presents the principle of the new actuator, the design of the prototype and the preliminary test results of its resolution, stroke.

INTRODUCTION

Flexure-based compliant mechanisms are wildly used due to their positive merits including free of backlash and friction, vacuum compatibility, and can achieve high-resolution motion. But the final resolution the mechanism can achieved is limited not only by flexure-based structure but also limited by the actuators.
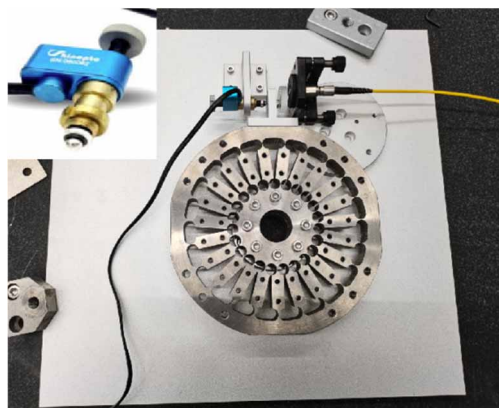
Figure 1: Preliminary resolution test of a weak-link mechanism.

As shown in Fig. 1, for example. When we use a domestic piezoelectric actuator to driven a weak-link mechanism [1] to measure the minimum angular resolution of the weak-link mechanism. The radius of the wheel-shaped flexible hinge is 200 mm. And the angular resolution we got finally is about 120 nrad, the result is limited by the minimum step size of the piezoelectric

actuator (about 15 nm). So we need an actuator with smaller minimum step size if we want to achieve a higher angular resolution.

SOLUTION AND CALCULATION

To achieve higher resolution at lower cost, a compound bridge-type hinge [2] is chosen as a pantograph mechanism to achieve smaller minimum step size by scaling down the step size of the piezoelectric actuator we have. Figure 2 shows the schematic diagram of the compound bridge type hinge, as can be seen from the figure, the bridge-type composite flexible hinge has four ends A, B, C, and D. When we fix end C and apply opposite thrust to ends B and D, end A will move along the x direction relative to end C. direction displacement.
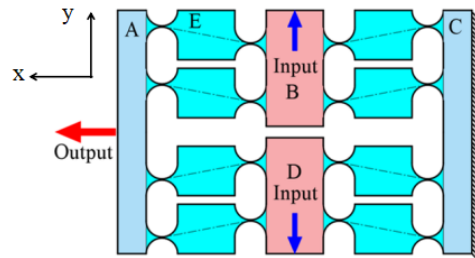
Figure 2: The schematic diagram of the compound bridge- type hinge.

In order to more accurately analyze the relationship between the relative displacement of ends B and D and the relative displacement of ends A and D, One-quarter of the model shown in Fig. 2 is taken for theoretical analysis, as shown in Fig. 3.
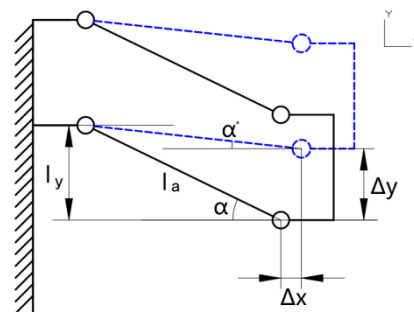
Figure 3: Simplified analysis of bridge-type composite hinge model.

In Fig. 3, l_y represents the distance (eccentricity) between the two ends of the hinge structure E in the y direction, l_a represents the arm length of the hinge structure (the length of the dotted line in Fig. 2), and α represents the angle between the arm length and the horizontal direction.

†jiangshuaikang@mail.ustc.edu.cn

THERMAL ANALYSIS SOFTWARE FOR OPTICAL ELEMENTS OF HEFEI ADVANCED LIGHT FACILITY*

Minghao Lin#, Jie Chen, Zimeng Wang, Shuaikang Jiang, Qiuping Wang, NSRL,
University of Science and Technology of China, Hefei, Anhui, P. R. China

Abstract

Thermal deformation is a key influencing factor in the surface shape of optical elements for beamline. In the process of beamline design, it is necessary not only to select different cooling schemes based on thermal loading conditions but also to extensively optimize the parameters of these cooling schemes. The traditional approach for optimizing cooling scheme design often requires significant manual effort. By integrating existing experience in optimizing cooling scheme designs, this study transforms the parameterized design tasks that are originally performed manually into automated processes using software. This paper presents the latest advancements in the automated design software for cooling schemes of beamline optical components, and the results indicate that the optimization outcomes of the existing automated design software are close to those achieved through manual optimization.

INTRODUCTION

ANSYS-based thermal analysis methodologies have found extensive application in the design of cooling strategies for optical elements employed in synchrotron radiation light sources worldwide. As the development of synchrotron radiation light sources progresses, the thermal analysis of optical elements faces two key challenges: (1) A notable increase in the quantity of high heat load optical elements, imposing a substantial burden on the engineering optimization phase of cooling system design, often demanding significant efforts from designers. (2) The need for optical elements to conform to exacting standards regarding the non-destructive transmission of radiation from the light source to the end-station, which significantly complicates the engineering optimization of cooling schemes, often necessitating iterative refinement.

Cooling methods for synchrotron optics are generally well-established, encompassing techniques such as direct cooling, indirect side cooling, and indirect liquid metal cooling [1-3]. At the Hefei Advanced Light Facility (HALF), the predominant cooling methods include direct cooling, indirect side cooling, and indirect liquid metal cooling. Within HALF, principal cooling mechanisms involve side water cooling, liquid metal bath water cooling, and side liquid nitrogen cooling. While these cooling schemes possess relatively fixed spatial structures, variations in parameters, such as the positioning and depth of Smart cut, can substantially impact the geometry of

optical elements. Consequently, the optimization of structural parameters assumes paramount importance in cooling scheme design.

To address this challenge, we have leveraged ANSYS secondary development technology [4-5] with the aim of crafting software tailored for the thermal analysis of synchrotron optics, thereby enhancing the efficiency of cooling scheme design.

SOFTWARE DESIGN

Solving Process

There are two routes for secondary development based on ANSYS: one is based on the secondary development of UPF inside ANSYS; the other is through MATLAB or python software, calling the command flow and ANSYS to solve the problem, and then return the results of the solution to MATLAB and python for further processing. We finally chose the second route for two reasons: firstly, we need to calculate the residual surface shape error and other information after obtaining the surface shape data, which is more conducive to data processing and visualization in MATLAB or python; secondly, we hope that in the future, the software can communicate with the optical calculation software, so as to obtain a more comprehensive beamline design software.
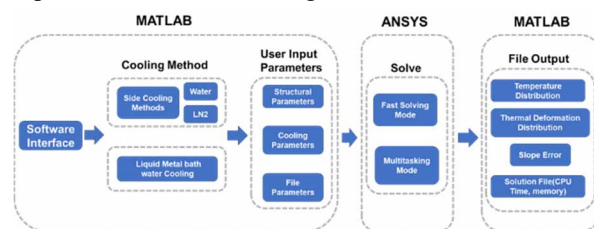
Figure 1: Computational route of the software.

The software gives priority to the service of Hefei Advanced Light Source, so the functions developed for the time being include: side cooling method (water cooling, liquid nitrogen) and liquid metal bath water cooling method. Software operation process is as follows: first of all, in the MATLAB interface to select the cooling program, and input structural parameters, cooling parameters and file location information; the parameters are processed and then written into the command flow file, and then call ANSYS to read the command flow file for the solution, after the completion of the solution, the output of the results of the file, such as the distribution of the surface type, the temperature distribution, as well as the solution of the information (such as solving time, consume memory, etc.), and finally MATLAB is used for data processing and

---

THE DESIGN OF HIGH STABILITY DOUBLE CRYSTAL MONOCHROMATOR FOR HALF

Zhanglang Xu, Jie Chen, Yang Peng, Xuewei Du, Qiuping Wang, National Synchrotron Radiation Laboratory (NSRL), University of Science and Technology of China (USTC), Hefei 230026, China

Abstract

The monochromator is known to be one of the most critical optical elements of a synchrotron beamline, since it directly affects the beam quality with respect to energy and position. Naturally, the new 4th generation machines, with emittances in the range of order of 100 pm rad, require even higher stability performances. A high stability DCM (Double Crystal Monochromator) is under development at the HALF, the new 4th generation synchrotron. In order to achieve high stability of tens of nano radians, as well as to prevent unpredicted mounting and clamping distortions, simulation are proposed for crystal angular vibration and thermal management. This paper gives an overview of the DCM prototype project including specifications, Mechanical design, heat load management and stability consideration.

INTRODUCTION

In the recent years it has become clear to the Diffraction Limit Storage Rings (DLSR) that the stability performance of DCMs would turn out to be one of the main bottlenecks in the overall performance of many X-rays beamlines. With the arrival of the diffraction-limited ring, This is because the instabilities in the DCM affect the position and the size of the virtual source, and, consequently, the spot size and the position of the beam at the sample. The angular instability between the two crystals is the most critical one because its effects on the virtual source scales with the lever-arm between the monochromator and the source [1].

Of the ten lines in the HAFL pre-construction, two of them use crystal monochromators. One of them has an energy range of 2-8 keV, and they both have high requirements for stability. In order to ensure that the stability required to meet the target requirements, this paper briefly describes the design of the DCM from the convenience of mechanical structure design, thermal stability analysis (1st crystal slope and temperature distribution of the core module) and vibration analysis. Detailed finite element analysis ensures that stability requirements and optical requirements (energy range, resolution and luminous flux) can be met. This prototype is designed to meet basic engineering needs.

SPECIFICATIONS

Depending on the energy, stability and coherence requirements of the beamline, an prototype of a high stability vertical DCM (Double Crystal Monochromator) with angular range between 14 and 81 degrees (equivalent to 2 to 8 keV with Si(111)) has been developed at the National Synchrotron Radiation Laboratory. Table 1 summarizes the main functional specifications of this DCM.

Table 1: Main Specifications for the DCM Prototype

Parameter	Description
type	Vertical DCM
Beam offset	20 mm
Angular range	14° - 81°
Angular resolution	0.5 µrad
Crystal	Si (111): 2 to 8 keV
Crystal Cooling	1st crystal: Indirect LN2
	2nd crystal: Copper straps
Beam size	4×3.3 mm^2
Input power	38.9 W

STRUCTURE DESIGN

The DCM can be divided in the following parts: support, vacuum vessel, rotary system and core (Fig. 1). The DCM is divided into the following parts: support, vacuum chamber, rotation system and core mechanism. The main axis mainly realises the crystal Bragg angle adjustment for energy selection and regulation. The crystal assembly contains the clamping, cooling, and adjustment of the first and second crystals, which directly affects the face shape, stability, and adjustment accuracy of the crystals. The granite support pedestal mainly realises attitude adjustment, provides support, ensures high stability, and at the same time carries out the exchange of crystals to achieve energy expansion. The cooling pipeline mainly provides liquid nitrogen delivery, and the reasonable design can control the vibration problem caused by the fluid. Cavity components mainly contain vacuum chamber, providing various types of vacuum interfaces and monitoring role.
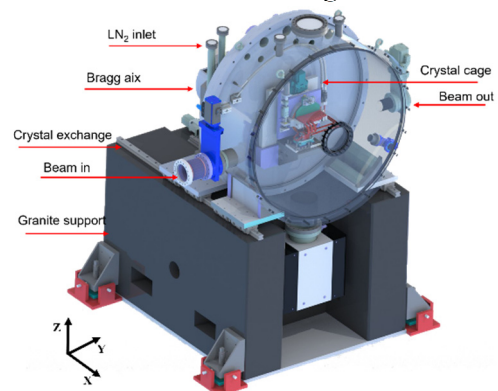
Figure 1: DCM assembly.

PRECISION MECHANICS

Mechatronics

AN ARGON-OXYGEN OR ARGON-HYDROGEN RADIO-FREQUENCY PLASMA CLEANING DEVICE FOR REMOVING CARBON CONTAMINATION FROM OPTICAL SURFACES

Hongjun Yuan[†], Xuewei Du, Qiuping Wang, National Synchrotron Radiation Laboratory,
University of Science and Technology of China, 230026 Hefei, China

Abstract

Due to synchrotron radiation, carbon contamination on the surfaces of optical elements inside the beamlines, such as mirrors and gratings, remains an issue. Future beamline designs will select more optical element surface coating materials according to the specific needs, including gold, platinum, chromium, nickel, and aluminum, and a single cleaning method will not be able to adequately address the demands. We have studied the radio-frequency (RF) plasma cleaning of optical elements. After the Ar/O_2 or Ar/H_2 gas mixture was injected into the chamber, glow discharge was carried out, and the carbon on the surface of the inert metal-coated optical element and oxidation-prone metal-coated optical element was removed by the oxidation or reduction reaction of radicals. In order to optimize the discharge parameters, it utilizes a differential mass spectrometry system and an optical emission spectrometer to monitor the cleaning process. This poster introduces the principles of the two cleaning methods as well as our existing cleaning device.

INTRODUCTION

Carbon contamination is a typical issue for high flux optical elements in synchrotron radiation beamlines. Short-wave light irradiation cracks the hydrocarbons, which then deposit a layer of carbon deposition on the surface of the optical element. This causes a decrease in reflectivity in the vacuum ultraviolet and soft X-ray regions as well as a loss of photon flux.

More varieties of coated mirrors and gratings will be chosen for the Hefei Advanced Light Facility (HALF) beamline in order to attain high performance. When the mirror coating is made of inert metal, such as Au or Pt, the carbon contamination could be removed using Ar/O_2 RF plasma cleaning. However, the reflectivity in the soft X-ray area may be decreased due to oxidation of the metal surface when the coating material is readily oxidized metal, such as Ni, Cr, or Al. The RF plasma cleaning approach using Ar/H_2 was suggested to clean optical elements in order to prevent the loss of reflectance by the oxidation of coating materials [1-3].

Based on the aforementioned reasons, Ar/O_2 and Ar/H_2 RF plasma cleaning system is constructed, equipped with cleaning parameter optimization system, which can achieve the optimal cleaning rate under varied operating conditions.

EXPERIMENTAL SETUP

Figure 1 shows the principle of cleaning carbon contamination with RF plasma. Under the influence of RF discharge, the mixed gas produces active free radicals that oxidize or reduce the carbon on the surface of the optical element to produce the volatile gas, such as CO_2, or CxHy, which could be removed by the vacuum pump.
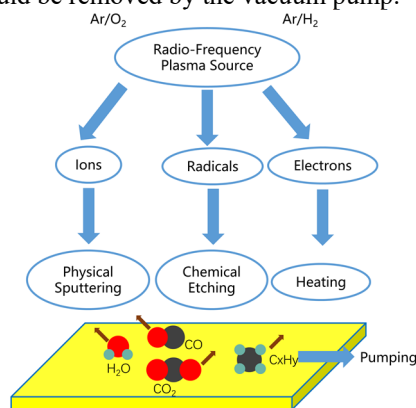
Figure 1: Schematic diagram of cleaning carbon contamination with RF plasma.

As seen in Fig. 2, the experimental device utilizes the laboratory's current RF plasma cleaning technology. The experimental equipment includes: cleaning chamber, gas mixing chamber, RF power supply and RF matching device, vacuum pumping system, etc. Ar/O_2 or Ar/H_2 enter the gas mixing chamber with a certain ratio through the mass flow meter. The mixed gas enters the cleaning chamber through the needle valve. By adjusting the needle valve and the pumping speed of the molecular pump unit, the cleaning chamber is maintained at a certain pressure. Turn on the RF power supply, adjust the RF matcher to find the appropriate discharge power, and perform glow discharge.
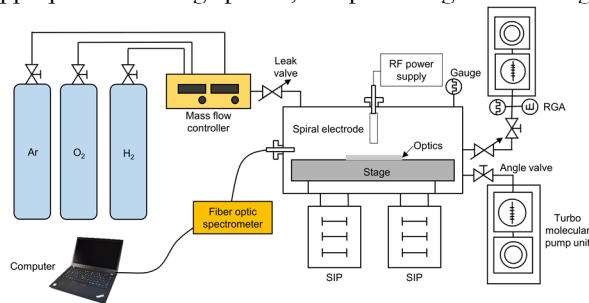
Figure 2: Setup for carbon contamination cleaning with RF plasma.

† yuanhj@mail.ustc.edu.cn

MECHANICAL DESIGN OF MULTILAYER KIRKPATRICK-BAEZ (KB) MIRROR SYSTEM FOR STRUCTURAL DYNAMICS BEAMLINE (SDB) AT HIGH ENERGY PHOTON SOURCE (HEPS)

Ruiying Liao [†], Haihan Yu, Lidan Gao, Zina Ou, Bingbing Zhang, Shanzhi Tang
Institute of High Energy Physics, Chinese Academy of Sciences, Beijing, China

Abstract

SDB aims in-situ real-time diagnosis in dynamic compression science and additive manufacturing. Nano-experimental environment requires highly multilayer KB mirror system in thermal deformation and stability of mechanism. This paper illustrates the KB cooling scheme and mechanical design. Only using variable-length water cooling to control the temperature and thermal deformation of mirror has limitations here. First, the installation of cooling system should be non-contact so that the surface shape can be sophisticatedly controlled without deformation of chucking power. Second, the distance between the HKB and the sample stage is too small to arrange the cooling pipe. Third, the KB mirror has multi-dimensional attitude adjustment. Cu water cooling pipe would be dragged with adjustment thus it has to be bent for motion decoupling, which occupies considerable space. Thus, the Cu cooling block and water cooling pipe are connected by copper braid. Eutectic Gallium-Indium fills a 100 µm gap between the cooling block and KB mirror to avoid chunking power deformation. Finally, the structural stability and chamber sealability are analyzed.

INTRODUCTION

Structural Dynamic Beamline (SDB) at High Energy Photon Source (HEPS) [1] intends to realize in-situ real-time diagnosis of dynamic and non-reversible processes in dynamic compression science and additive manufacturing fields [2]. The beamline station includes a micro-beam hutch, a large-spot hutch, and a nano-beam hutch. The multilayer Kirkpatrick-Baez (KB) mirror system is located at the last nano-beam hutch, which focuses the secondary source at 95.5 m on 210 m to form a 60 nm light spot. The nano experimental environment requires multilayer KB mirror system highly since any chunking power or thermal source would deform the KB mirror surface shape. The mechanical structure of multilayer KB mirror system was meticulously designed, especially the cooling scheme. Water or liquid nitrogen [3] cooling with oxygen-free high-conductivity (OFHC) copper braid [4] or copper stripe [5] is a common method for beamline station equipment, such as Fresnel zone plates (ZP) microscope modules [6] and monochromators [7]. Considering the installation space limitations and the surface shape requirement of the KB mirror, a water cooling scheme combining copper braids and eutectic GaIn [8] was utilized to remove thermal load. Deep calculation and finite element analysis (FEA) have been operated.

The remaining parts of this paper are organized as follows: Section 2 gives the overview of mechanical structure design. Section 3 depicts the cooling scheme and thermal ansys results. The conclusions are reported in Section 4.

MECHANICAL STRUCTURE DESIGN

The overview of mechanical structure design is shown in Fig. 1. The length, width, and height of the whole KB mirror system are 1430 mm, 740 mm, and 1150 mm respectively. The size of horizontal Kirkpatrick-Baez (HKB) is 70 mm×40 mm×50 mm and of vertical Kirkpatrick-Baez (VKB) is 120 mm×40 mm×40 mm. Except for the KB mirror, the multilayer KB mirror system includes pose adjustment mechanism, a gantry, and cooling system. The fishbone flexure hinge and U-frame flexure hinge mechanism are used for position and attitude adjustment respectively, which fulfill the movement requirement in Table 1. The granite air-bearing table outside the chamber controls the whole KB mirror system moving in X and Z-axis directions.
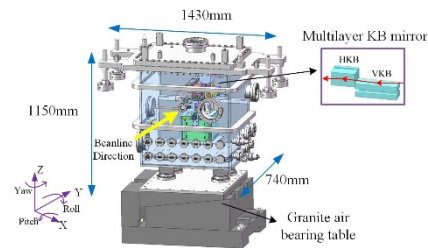
Figure 1: The mechanical structure.

Table 1: Adjustment Parameter Index for HKB, VKB, and Whole KB Mirror System

	Movement	Resolution	Range
HKB	X-axis	1µm	±0.5mm
	Yaw	1µrad	±10mrad
VKB	Z-axis	1µm	±0.5mm
	Y-axis	1µm	±0.5mm
	Pitch	1µrad	±10mrad
	Roll	10µrad	±20mrad
Whole System	X-axis	1µm	±5mm
	Z-axis	1µm	±5mm

A stable invar gantry shown in Fig. 2(a) is designed for metrology and to solve the problem of the limited installation space for HKB. By lightweight design, the gantry mass is only 188.3 kg. The granite stage is sufficiently stiff to not amplify vibrations. In FEA modal simulation, the resonance frequency is over 140 Hz. The first modal analysis and the direction of rigid motion are performed in Fig. 2(b). To avoid interference with the sample stage, the

_____
† email address : liaory@ihep.ac.cn

A DESIGN OF AN X-RAY PINK BEAM INTEGRATED SHUTTER FOR HEPS*

Sai Liu, Guang Mo†, Qingfu Han, Aiyu Zhou

Institute of High Energy Physics, Chinese Academy of Sciences, Beijing, China

Abstract

The main function of the shutter is to accurately control the exposure time of the sample so that the sample as well as the detector can be protected. In order to cover the high thermal load and high energy working environment, we designed an integrated shutter device. The device includes a thermal absorber shutter, a piezoelectric ceramic fast shutter, a vacuum chamber and an adjustable height base. Firstly, SPECTRA and ANSYS were used to verify the device's institutional temperature reliability at a thermal power density of 64 W/mm^2. In addition, the device is suitable for both monochromatic and pink light operation with a horizontal pitch of 15 mm. The device is also compatible with both vacuum and atmospheric working environments, and the recollimation of the device is not necessary when switching modes. Finally, the thermal absorber shutter is also able to function as a beam profile monitor, and the position of the spot can be monitored through a viewing window on the cavity.

INTRODUCTION

The high energy photon source (HEPS) is a fourth-generation synchrotron radiation facility and has characteristics of high brightness, high flux, and high coherence [1].

The integrated shutter is designed for the small angle X-ray scattering station, which is under construction at HEPS and characterized by a pink beam with enormous high photon flux. In order to solve the problem of the vacuum heat dissipation and at the same time ensure a fast response, we proposed the following schematic design. Firstly, as shown in Fig. 1, the integrated shutter is comprised of a thermal absorber shutter in series with a piezoelectric ceramic fast shutter. It works as follows: in the off-work state, the thermal absorber shutter is responsible for taking away the heat from the pink beam to protect the piezoelectric ceramics. When working, the thermal shutter is opened first, and then the piezoelectric ceramic shutter turns on, at the same time the detector starts sampling. After the exposure time, the detector and the piezo shutter turn off first, after that the thermal shutter is closed and continues to absorb the heat. By coordinating their different opening and closing times, the exposure time of the sample can be controlled.

The monochromatic beam and pink beam in SAXS can be switched through moving in and out of the monochromator and there is 15 mm in the horizontal direction between the two beams. In order to ensure that the position of the integrated shutter does not need to be adjusted after switch-

---

ing modes, we designed two pass-through holes in the piezo shutter, which can meet the passing of pink beam as well as monochrome beam.

In addition, after being coated with fluorescent powder, the thermal absorber shutter is also able to function as a beam profile monitor and the position of the spot can be monitored through a viewing window on the cavity.
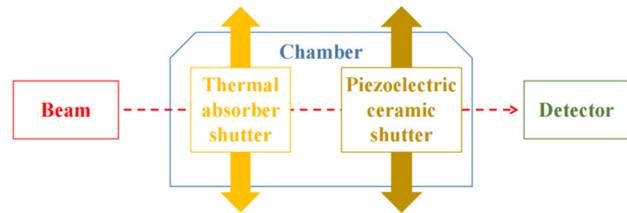
Figure 1: Schematic diagram of integrated shutter.

DESIGN

Overall Description

The integrated shutter consists of three parts: a thermal absorber shutter, a piezoelectric ceramic fast shutter and a stainless-steel vacuum chamber. The assembly drawing is sketched in Fig. 2.
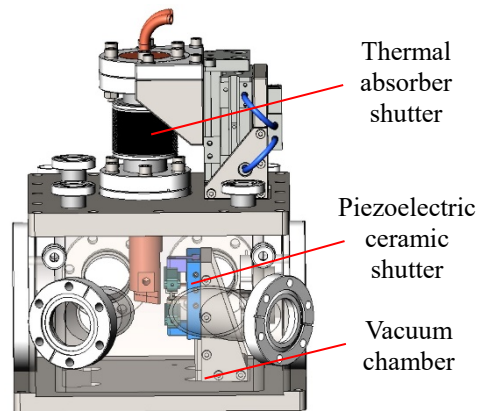
Figure 2: Schematic diagram of integrated shutter.

Thermal Absorber Shutter

At this position the spot size of pink beam is 500 μm and the thermal power density is 64 W/mm^2. It will be a burden for the thermostat system if the heat is emitted directly into the experimental hutch. For this reason, we decided to use water cooling instead of natural cooling. The thermal absorber shutter is driven by an LCG cylinder slide with a stroke of 5 mm, as shown in Fig. 3 and the response time of the cylinder slide is less than 0.1 seconds. The material of water-cooled absorber is OFHC, and the light-receiving surface of the absorber is angled at 45° to the optical axis.

A DESIGN OF AN X-RAY MONOCHROMATIC ADJUSTABLE SLIT FOR HEPS BEAMLINES*

Sai Liu[1], Qingfu Han[†], Zhe Li, Junliang Yang, Qihui Duan,
Zongyang Yue, Zebin Zhang, Qun Zhang
Institute of High Energy Physics, Chinese Academy of Sciences, Beijing, China

Abstract

The monochromatic slit is a commonly used device in HEPS beamlines. It can limit the synchrotron beam-spot within a desired size required by the downstream optical equipment. In addition, the four-blade structure is the most widely used form of slit. The slit with this form usually consists of a pair or two parallel tungsten carbide blades. With their edges close to each other, a slit can be formed, and the size of which can be controlled by micromechanical guides. This structure is very suitable for the case of large beam size. In this work, we have designed a monochromatic slit based on the four-blade form for BF beamline in HEPS. It can be used in ultra-high vacuum, high luminous flux working environment. The maximum opening range is up to 30*10 mm² (H*V), while it can allow a white beam of 136*24 mm² (H*V) to pass through. Furthermore, we adopted a point to surface contact design, which can effectively avoid the over-constraint problem between two guide rails.

INTRODUCTION

The test beamline (ID42) is under construction at HEPS. Its main function is to perform comprehensive testing and evaluation of some high-performance optical elements and detectors before they go online [1]. That means it can provide various modes of beam, including white, pink, monochromatic, and focused beam [2]. Therefore, the design of general optical equipment on this beam is usually very challenging: we have to consider the compatibility between different modes.

This monochromatic slit is designed for the test beamline. Its major functional requirements are that the maximum opening range is up to 30*10 mm² (H*V), while it can allow a white beam of 136*24 mm² (H*V) to pass through. The working environment is ultra-high vacuum, and the energy range is 5-45 keV.

DESIGN

Overall Description

The monochromatic slit consists of three parts: horizontal tungsten blade module, vertical tungsten blade module, vacuum chamber and a height-adjustable granite base. The assembly drawing is sketched in Fig. 1. It is well known that one of the most important technical parameters of an adjustable slit is the parallelism between the blades, which directly affects the spot quality. For this reason, drive and guide components with good precision are essential [3]. At present, there are many technologically mature products with integrated drive and guide on the market, and their

motion accuracy can even reach the manometer level [4]. Considering practicality and economy, we mainly choose these standard products as driving and guiding components.
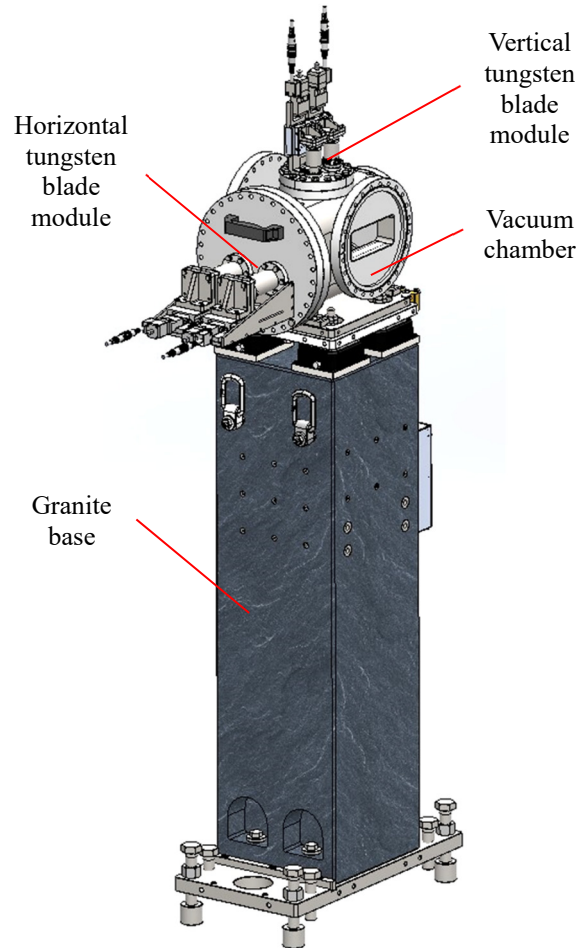
Figure 1: Overview of the monochromatic adjustable slit.

Horizontal Tungsten Blade Module

The design of the horizontal tungsten blade module is shown in Fig. 2, which consists of two KOHZU slide models (SXA0575-R01) as drive components to move the tungsten blades in the vacuum chamber by a connecting rod. The blade holder is located on an AML slide. In this way, the parallelism between the two tungsten blades depends on the parallelism between the two slide guides. However, the motion guidance of the slide itself can be over-constrained with the guide rails inside the vacuum. For this reason, a flexible connection is proposed. As shown in Fig. 3, the end side of the connecting rod is machined into

THE DESIGN OF TEST BEAMLINE AT HEPS

Junliang Yang[†], Quanjie Jia, Ming Li, Peng Liu, Ye Tao
Institute of High Energy Physics, Chinese Academy of Science, Beijing, China

Abstract

This paper describes the design of a test beamline for a new generation of high-energy, high-flux, and high-coherence synchrotron radiation beamlines. The beamline will be built at ID42 of HEPS. The beamline includes two sources, a wiggler and an undulator, to provide high-energy, high thermal power, large size, and high-coherence, high-brightness X-ray beams, respectively. In the current design, the beamline mainly has optical components such as monochromators, CRLs, and filters. With different combinations of sources and optical components, the beamline can provide various modes, including white, monochromatic, and focused beam. Using a Si(111) double-crystal monochromator (DCM), the beamline covers a wide photon energy range from 5 to 45 keV. In the future, the beamline will be capable of providing monochromatic beam with photon energy higher than 300 keV. And the wiggler's white beam can provide high thermal load test conditions over 1 kW. The beamline offers high flexibility and versatility in terms of available beam size (from 1 μm to over 100 mm), energy resolution, and photon flux range. Various experimental techniques including diffraction, spectroscopy, imaging, and at-wavelength measurement can be performed on this beamline. At present, the construction of the radiation shielding hutch for the beamline has been completed.

INTRODUCTION

For the fourth-generation synchrotron source (SR), high brightness, high flux, and high coherence are its main characteristics. To match the advanced performance of the fourth-generation SR, the use of the highest performance optical elements and detectors is necessary. However, these optical elements and detectors are not widely used, and their quality and performance cannot be fully guaranteed. To ensure successfully operate the beamline, comprehensive testing and evaluation before the equipment goes online is essential. Furthermore, even with the highest performance optical elements and detectors in current state of the art, it is difficult to achieve certain extreme performance limits of the fourth-generation SR. Therefore, continue research and development (R&D) are needed to improve the performance of various optical elements and detectors. Testing is a necessary step in the R&D of new equipment [1, 2]. To achieve these goals, a test beamline has been designed at high energy photon source (HEPS). This paper mainly introduces the sources, beamline layout, and expected performance of the beamline.

SOURCE OF THE BEAMLINE

The HEPS design has an electron operating energy of 6 GeV, a beam current of 200 mA, and a natural horizontal

emittance of smaller than 60 pm·rad, which can accommodate up to 48 straight sections [3]. The test beamline occupies a straight section with a total length of approximately 6 m, located at ID42. From upstream to downstream, arrange two sources, an undulator source with a length of 1.94 m and a wiggler source with a length of 1.05 m, as well as a reserved space of approximately 1.5 m that can be used for future light source performance upgrades. The main parameters of the HEPS storage ring and the straight section where the test beamline are summarized in Table 1. The design of the test beamline's sources considers the requirements of HEPS engineering tests and various experimental methods as much as possible. The undulator source is designed to provide conditions such as high brightness, high coherence, and micro-focusing. The wiggler sources are used to provide conditions such as continuous spectrum, large spot size, and high thermal load.

The undulator source is cryogenic permanent magnet undulator (CPMU), with a gap range of 7.2-16.0 mm, a magnetic period of 22.8 mm, a number of periods of 85, and a maximum peak magnetic field $B_0 = 1.18$ T. Table 2 provides the basic parameters of the CPMU22.8 source. Figure 1 shows the brightness and coherent flux spectrum of the CPMU22.8 source, and the results show that its brightness can reach 2.5×10^{21} phs/s/mr2/mm2/0.1%BW, with a maximum coherent flux of 0.9×10^{14} phs/s/ 0.1%BW.

Table 1: The Main Parameters of the HEPS Storage Ring and the Straight Section where the Test Beamline

Parameter		Value
Electron energy		6 GeV
Beam current		200 mA
Circumference of the storage ring		1360.4 m
Natural horizontal emittance		<60 pm·rad
	βx	10.12 m
	βy	9.64 m
Parameters of	σx	17.74 μm
straight sections	$\sigma x'$	1.753 μrad
	σy	5.48 μm
	$\sigma y'$	0.568 μrad

The wiggler source is permanent magnet wiggler (PMW), with a gap range of 11−46.5 mm, a magnetic period of 73 mm, a number of periods of 14, and a peak magnetic field of 1.64 T. Table 3 provides the basic parameters of the PMW73 source. Figure 2 shows the energy spectrum of the PMW73 source at different gaps and the angular distribution of flux density at different energy values at the minimum gap. The results show that it can provide photons with energy above 300 keV. The light source size of

USABILITY STUDY TO QUALIFY A MAINTENANCE ROBOTIC SYSTEM FOR LARGE SCALE EXPERIMENTAL FACILITY

J. Y. Zhang[†,1,3], J. X. Chen[2], L. Kang[1], R. H. Liu[2], J. B. Yu[2]

[1]Institute of High Energy Physics, Chinese Academy of Sciences, Beijing, China

[2]Spallation Neutron Source Science Center, Dongguan, China

[3]University of Chinese Academy of Sciences, Beijing, China

Abstract

The primary stripper foil device is one of the most critical devices of The China Spallation Neutron Source Project Phase-II (CSNS-II), which requires regular foil replacement maintenance to ensure its stable operation. To mitigate the potential hazards posed to workers by prolonged exposure to high levels of radiation, a maintenance robotic system has been developed to perform repetitive and precise foil changing task. The proposed framework encompasses various aspects of the robotic system, including hardware structure, target detection, manipulator kinematics design, and system construction. The correctness and efficiency of the system are demonstrated through simulations carried out using ROS Moveit! and GAZEBO.

INTRODUCTION

Nowadays, the role of robotics in industrial and scientific applications is growing exponentially, one of which is the usage of maintenance robotic systems in large experimental facilities such as Synchrotron Radiation Equipment and Instrumentation [1].

The China Spallation Neutron Source Project Phase-II (CSNS-II) poses ongoing challenges in terms of both its upgrade and remodelling. The primary stripper foil device is one of the most critical devices of CSNS-II, which undergoes significant changes due to the increased beam injection energy from 80 MeV to 300 MeV, as well as the radiation dose in the injection zone is expected to be further amplified (see Table 1). During the maintenance process, the foil components that are being exchanged need to be placed in radiation shielding containers until the radiation dose has decayed to a safe level before new foils can be installed.

Table 1: Downtime Dose Statistics

Shut-down Time	Proton-Induced Dose Rate	Dose Rate in 1 W/m Mode	Total Dose Rate
0 s	0.5 mSv/h	2.2 mSv/h	2.7 mSv/h
1 h	0.3 mSv/h	1.3 mSv/h	1.6 mSv/h
1 day	0.23 mSv/h	1.0 mSv/h	1.23 mSv/h
1 week	0.18 mSv/h	0.77 mSv/h	0.95 mSv/h
1 month	0.13 mSv/h	0.55 mSv/h	0.68 mSv/h

From the maintenance work described above, this paper presents a usability study that aims to evaluate a maintenance robotic system for large-scale experimental facilities.

The findings of this study will contribute to the development of robust and reliable robotic system, which would emerge as viable industrial solutions to replace humans in executing construction tasks that are safe, efficient, and precise.

SYSTEM FRAMEWORK

The overall framework of the robotic system is depicted in Fig. 1, which consists of a vision and image processing system, a ROS operating system, a hardware system, and a host computer system.
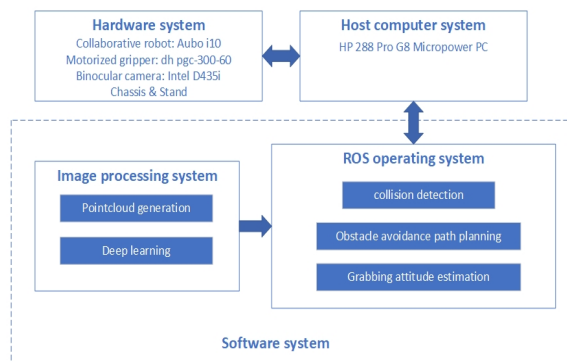
Figure 1: Robotic system framework.

Leveraging the Robot Operating System (ROS) platform, the proposed robotic system exhibits the capability to successfully execute target recognition and motion planning tasks for a 6-degree-of-freedom tandem robotic arm, as well as the ability to transition to a solid robot configuration. The system workflow diagram is illustrated in Fig. 2.
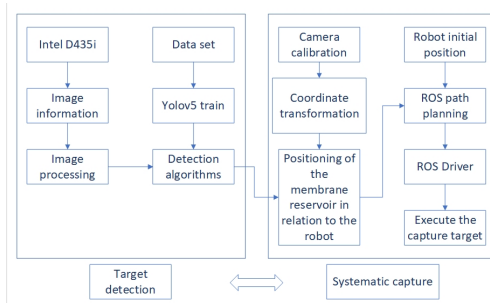
Figure 2: System workflow diagram.

Hardware Component Design

The entire system is installed in the CSNS Experiment II Testbed (see Fig. 3). Considering the workspace and

† zhangjingyu@ihep.ac.cn

DESIGN OF LIQUID INJECTION DEVICE FOR THE HARD X-RAY ULTRAFAST SPECTROSCOPY EXPERIMENT STATION*

Linghao Li, Bing Li, Xing Liu, Jianwei Meng, Ruixue Zhu, Kaiyu Zhang, Tsu-Chien Weng[†]

Center for Transformative Science, ShanghaiTech University, Shanghai, China

Abstract

The Hard X-ray Ultrafast Spectroscopy Experiment Station (HXS) of the Shanghai high repetition rate XFEL and extreme light facility (SHINE) requires the design and manufacture of a specialized liquid sample injection device when studying the liquid phase state of matter. Due to the damage caused by high-repetition-rate XFEL pulses on the sample, it is necessary to ensure that the liquid sample is refreshed before the next pulse arrives. In order to reduce the impact of liquid film thickness on pump-probe ultrafast spectroscopy experiments, it is required that the liquid film thickness be less than 20 μm. This article describes the use of oblique collision of two jets, from simulation calculation to the construction of experimental device, and the use of absorption spectroscopy principle to construct a thickness characterization system. This system can stably produce ultrathin liquid films with thickness ranging from 3-20 μm. The article proposes views on the limitations and future improvements of this device.

INTRODUCTION

The Shanghai high repetition rate XFEL and Extreme light facility (SHINE) is equipped with a high-quality electron beam continuous wave superconducting linear accelerator with an energy of 8 GeV. The energy wavelength coverage of this device is 0.4-25 keV, and the pulse repetition rate can reach up to 1 MHz. The device has the characteristics of high brightness, short pulse, high repetition rate, and high coherence [1]. The main experimental platform of the Hard X-ray Ultrafast Spectroscopy Experiment Station (HXS) located in FEL-III is the high-energy resolution X-ray photo-in-photo-out (PIPO) spectrometer, which can achieve femtosecond time resolution by combining pump-probe technology. The reactions involved in the liquid phase state of matter are currently an important research area in the fields of chemistry and biology [2], and are also an important research direction of HXS. Therefore, it is necessary to build a liquid sample injection device that meets the requirements of the experiment station.

After in-depth analysis of the characteristics of X-ray free-electron lasers and samples, we propose the following requirements for the in-situ environment of liquid samples: Firstly, due to the high repetition rate and radiation damage characteristics of X-ray free-electron lasers, sample replacement is necessary. Therefore, we need to establish a system that can continuously deliver samples to ensure that the pulse of the X-ray free-electron laser is not wasted.

Secondly, in order to control the impact of liquid film thickness on the pump-probe time resolution within 66 fs, the liquid film thickness must be less than 20 μm. At the same time, the outline of the liquid sample should be much larger than the light spot of the X-ray beam to ensure that the detector receives the signal after passing through the liquid sample.

This article designs and implements a super-thin liquid film generation device, and verifies the stability and thickness of the generated liquid film through the construction of a test optical path, which meets the experimental requirements. This research provides an important experimental foundation for subsequent research in related fields.

EXPERIMENTAL METHODS

Liquid Film Generation Device

In recent years, the principles of generating flowing liquid films suitable for X-ray spectroscopy research mainly include the following three types:

Slit jetting [3]. This method involves spraying liquid through a slit to overcome the surface tension of the liquid and form a liquid film. However, this method is limited by the size of the tube wall, and the production of microfluidic tubes with dimensions of a few microns can easily encounter problems such as clogging during use.

Liquid flow collision [4-6]. This method utilizes two liquid flows that collide with each other to form a liquid film through interaction, and has high stability. This method has broad application prospects in pump-probe ultrafast spectroscopy experiments.

Gas focusing [7-9]. This approach is similar to gas-dynamic focusing virtual nozzle (GDVN), which requires gas pressure to change the cross-sectional shape or size of the liquid flow, typically serving the needs of lower dimensions. This approach is not further discussed in this article.

Based on the principle of liquid flow collision, this study built an experimental platform as shown in Figure 1. Using an HPLC pump to provide power for liquid transport and control the liquid flow rate, a liquid pipeline was constructed at the output end of the pump, using PEEK tubes, liquid-phase connectors, T-shaped tees, stainless-steel tubes, and other parts.

A HIGH REPETITION RATE FREE-ELECTRON LASER SHUTTER SYSTEM

Jiacheng Gu, Yajun Tong[†], Zhen Wang, Huaidong Jiang

School of Physical Science and Technology, ShanghaiTech University, Shanghai, China

Abstract

The Shanghai High repetition rate XFEL and Extreme light facility (SHINE) is the first high repetition rate XFEL in China. It is a powerful tool for scientific research. The high repetition rate XFEL has not only high peak power but also high average power. The high average power will cause the distortion of optics and make the diagnostics failure. To measure the distortion of optics, the diagnostics, such as wavefront sensor, imager, should be working properly. A fast shutter system is designed to protect the diagnostics and to make the diagnostics working properly. It can control the number of pulses and average power on the diagnostics. The time window of shutter can be as small as 10 milliseconds. It can absorb most of FEL power.

INTRODUCTION

X-ray free electron laser (XFEL) is a new generation of advanced light source based on particle accelerators, with excellent characteristics such as ultra-short pulses, ultra-high brightness, high coherence, and continuously adjustable output wavelength. It has made significant progress in the past decade [1], and the XFEL facility has also become a powerful tool for cutting-edge research in life sciences, materials science, physics, and other fields [2]. The Shanghai High repetition rate XFEL and Extreme light facility (SHINE) is the first hard X-ray free electron laser facility in China, with a maximum electron energy of 8 GeV and a maximum repetition rate of 1 MHz. In the phase-I, it offers a photon energy range of 0.4-25 keV. SHINE's accelerator parameters are listed in Table 1 [3].

However, high repetition rate XFEL has both peak power and average power, and its high peak power can cause damage to the devices in the optical path. High average power can bring thermal load on the devices and cause thermal distortion to the optics, affect the beam transportation and focusing, and cause diagnostics failure. Therefore, how to diagnostics the distorting beam under high repetition rate is particularly important.

M. Renier and colleagues previously designed an X-ray shutter for the European Synchrotron Radiation Facility (ESRF) [4]. It can control the shortest exposure time achieved 3 milliseconds. However, it was not suitable for operation under high vacuum conditions. In a different endeavour, Chang Yong Park and collaborators designed a shutter tailored for high vacuum environments [5]. Their shutter realized the use of vacuum environment but their stopper cannot withstand 100W laser's heat load for a long time. To address this critical need, we have designed a shutter system based on M. Renier's design, but it can work in

vacuum. The shutter's aperture is 4mm which is suitable for the small beam size of hard X-ray beamline, with a minimum time window of 10 milliseconds. To ensure efficient heat conduction within the stoppers and free falling, liquid metal is employed for cooling purposes.

Table 1: The Main Parameters of SHINE

Parameters	Nominal	Objective
Beam energy [GeV]	8	4~8.5
Bunch charge [pC]	100	10~300
Peak current [kA]	1.5	0.5~3
Slice emittance [µm·rad]	0.4	0.2~0.7
Max repetition rate [MHz]	1	1
Beam power [MW]	0.8	0~2.4
Photon energy [keV]	0.4~25	0.2~25
Pulse length [fs]	66	3~600

SHUTTER DESIGN

Basic Principle of the Device

The shutter consists of two sandwiched stoppers, as illustrated in Fig. 1. Each stopper is guided to move linearly along a track and is driven by a combination of an electromagnet and its own gravity. The system operates in the following states:

(a) State 1: In this configuration, both stoppers are positioned at their lowest point, and they are actively cooled. Notably, stopper 1 is responsible for absorbing the thermal load.

(b) State 2: When the need arises to create an time window, both stoppers are raised to their highest position, and at this point, neither receives cooling. This state typically lasts for less than 1 second.

(c) State 3: The electromagnets of the two stoppers begin to fall at different time, forming a defined time window. Eventually, both stoppers return to their lowest position, effectively reverting to the configuration of State 1.

The stopper is designed as a sandwich structure, comprised of three key components: a radiation damage resistant block (diamond), a burn-through detector, and a tungsten block, as depicted in Fig. 2. The burn-through detector serves the purpose of identifying whether the radiation damage resistant block has experienced burn-through. Its fundamental operational principle relies on the interaction of incident light with a YAG crystal, resulting in the generation of visible fluorescence. A photodiode is employed to detect this optical signal, which is subsequently transmitted as an interlocking signal through the connecting lead wire. Meanwhile, the tungsten block is deployed

---

† tongyj@shanghaitech.eud.cn

DESIGN AND CALCULATION OF VACUUM SYSTEM FOR WALS STORAGE RING*

Chengyin Liu, Jian Li[†], Geng Wei, Jianhua He, Haohu Li, Yuan Chen, Jike Wang, Yuancun Nie, Ye Zou, Xuerui Hao, Yuxin Zhang, Jingmin Zhang, Pai Xiang, Hui Li, Yong Wang, Yuhai Xu
Wuhan Advanced Light Source Research Center, Wuhan University, Wuhan, China

Abstract

Wuhan Advanced Light Source (WALS) is a fourth-generation synchrotron radiation facility with 1.5 GeV designed energy and 500 mA beam current. The storage ring vacuum system has to be designed in such a way which is compatible with a multi-bend achromat (MBA) compact lattice. the new technology of non-evaporable getter (NEG) coating was used, which is more and more popular in accelerator equipment.

The design of the whole vacuum chamber and the necessary calculations were posted in the paper. The results indicated that the design of the vacuum system can meet the design requirement.

INTRODUCTION

Wuhan Advanced Light Source (WALS) is a fourth-generation synchrotron radiation facility with 1.5 GeV designed energy and 500 mA beam current. The storage ring vacuum system has to be designed in such way which is compatible with a multi-bend achromat (MBA) compact lattice. The emittance of WALS is less than 230 pm·rad, which can provide high brilliance lights to experimental stations. To achieve these objectives, the aperture of the various types of the vacuum chambers to be much smaller and more compact than that of the 3th generation light source, which is complexity of the design of vacuum chamber [1].

The general requirements for vacuum chamber have to be considered for the cost, performance, and required maintenance, these factors will lead to a design by which the details of the chamber construction various according to local spatial constraints and synchrotron radiation (SR) loading [2].

In this paper, the design of the whole vacuum chamber is introduced, the vacuum distribution results calculated by PTMC and the SR heat loads calculated by FEM indicated that the design of the vacuum system is reasonable.

THE OBJECTIVES AND THE LAYOUT OF THE WALS VACUUM SYSTEM

The parameters of the storage ring in WALS are show in Table 1. The Ring circumference is 180 m with 8 cells. Thus, the length of each cell is 22.5 m, contains 6.8 meters of insertion devices. The internal aperture of vacuum chamber is 32 mm (except Super-bend combination magnet section). Each cell contains 12 BPMs, including 7 BPM with bellows in each side, connected with vacuum chamber

---

through knife flanges, and other 5 BPMs directly soldered to the vacuum vessels. The layout of the cell is show in Fig. 1.

Table 1: Parameters of the Storage Ring

Parameter	Value
Beam energy [GeV]	1.5
Current [A]	0.5
Ring circumference [m]	180
Max. magnet field strength [T]	3.5
Total synchronous radiation power [kW]	54.35
Photon desorption coefficient [molecules/photon]	2×10^{-6}
Linear photon airborne [Pa×L/s×m]	2.66×10^{-5}
Static pressure [Pa]	$< 5 \times 10^{-8}$
Dynamic pressure [Pa]	$< 2 \times 10^{-7}$
Vacuum box beam aperture [mm×mm][H×V]	Ø 32 (standard vacuum box)
	12×30 (SuperBend combination magnet vacuum box)
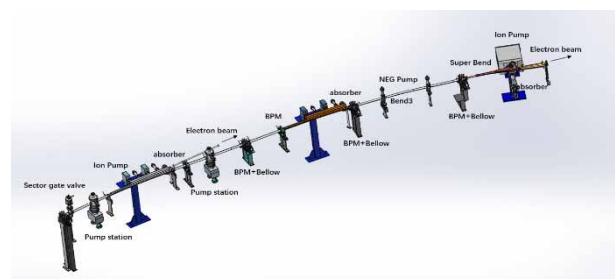
Figure 1: Layout of the 1/2 cell of WALS vacuum system.

According to the overall design requirements, the vacuum system should meet the requirements of static vacuum less than 5×10^{-8} Pa and dynamic vacuum less than 2×10^{-7} Pa. Due to the small aperture of the vacuum chamber, traditional methods with lumped pumping station can

PROGRESS OF WALS NEG COATING EQUIPMENT AND TECHNOLOGY*

Geng Wei, Yuan Chen, Jian Li, Chengyin Liu, Jianhua He, Haohu Li, Jike Wang, Yuancun Nie,
Ye Zou, Xuerui Hao, Yuxin Zhang, Jingmin Zhang, Pai Xiang, Hui Li, Yong Wang, Yuhai Xu
Wuhan Advanced Light Source Research Center, Wuhan University, Wuhan, P. R. China

Abstract

The objective of WALS (Wuhan Advanced Light Source) is to establish a world-class radiating light source. For the entire storage ring vacuum vessels, chromium-zirconium-copper has been selected as the primary material. Additionally, the magnetron sputtering (PVD) process has been employed to apply NEG (Non-Evaporable Getter) coatings to the inner surfaces of the copper vacuum chambers. This coating process enhances the vacuum performance.

Currently, the coating laboratory has taken shape and includes various components such as a standard cleaning platform, a coating platform, an ultimate vacuum test platform, an extraction rate test platform, and a coating microstructure test process. In terms of coating equipment, a bias power supply and customized ceramic components have been integrated to provide additional functionality. Multiple electrode control is utilized to manage different target materials, and experiments are conducted to deter-mine the composition of multilayers for various deposition ratios. Furthermore, sample tube bias control access is maintained during the coating process, and diverse combinations of target materials and bias parameters have been thoroughly investigated. Coating is presently in progress, and specific test results are underway.

INTRODUCTION

Process Difficulty Introduction

The 1.5 GeV storage ring vacuum system designed by WALS has a circumference of 180 m. According to the characteristics of physical design, the storage ring vacuum system was divided into 8~cells (standard segment) and 8 straight segments of 6.8 m. Chromium-zirconium-copper was chosen as the primary material for the entire ring vacuum vessel [1, 2]. At the same time, 316L was selected as the material for the pumping, bellows unit, and BPM mechanical shell.
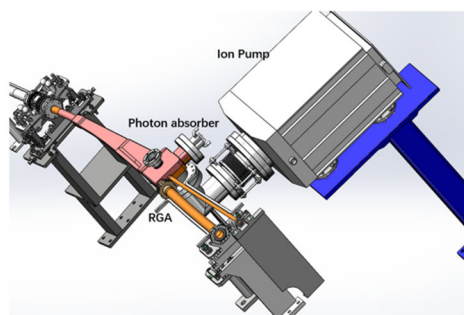
Figure 1: Model of vacuum chamber (Super Bend composite magnet).

One of the major challenges of WALS vacuum system design is magnet clearance small aperture (14 mm). The vacuum chamber (Super Bend composite magnet) has an oval profile with an inner diameter of 30×12 mm, a wall thickness of 1 mm, and a front chamber structure, which is a vacuum chamber about 1.8 m long, where the bending angle at the bipolar magnet is $10.8°$, and the reverse bending is $1°$, as shown in Fig. 1. The corresponding sample tube with the NEG coating [3] deposited on the inner wall is shown in the *Technical Status* section.

COATING MACHINE EQUIPMENT

Currently, the coating laboratory has taken shape and includes various components such as a standard cleaning platform, a coating platform, an ultimate vacuum test platform, an extraction rate test platform, and a coating microstructure test process, as shown in Fig. 2.

Figure 2: The coating laboratory.

Figure 3 shows the schematic diagram of the vacuum coating system [4]. The copper alloy pipe to be plated reaches vacuum through the flange and the auxiliary vacuum box at the lower end, and an appropriate amount of high-purity krypton gas is injected into the pipe as the discharge gas. The sputtering cathode target is made of a wire wound with a diameter of 1 mm. The end of the sputtering cathode target is fitted with a ceramic sheet to ensure insulation from the inner wall of the pipe. The magnetic field is provided by an external solenoid coil, which generates an adjustable magnetic field of $0.03 - 0.08$ T at the central axis.

Three feasible research directions for NEG coating have been pursued:

1. Different target materials were controlled by means of multi-electrode control, while experiments were performed on deposited compositions of different ratios of multilayers,

CURRENT STATUS OF VIBRATION MONITORING SYSTEM AT SOLARIS

M. Piszak*, SOLARIS National Synchrotron Radiation Centre, Cracow, Poland

Abstract

Solaris synchrotron radiation centre, despite being relatively new facility, began enlargement of its experimental hall in 2022 in order to accommodate new beamlines. The construction works were carried out along with regular accelerators and beamlines operation and generated high levels of vibration. To better understand the influence of vibrations on electron and x-ray beams' stability, an accelerometer-based monitoring system was designed and implemented. The system consists of a triaxial measurement point equipped with seismic accelerometers located on bending magnet inside storage ring and a central signal conditioning and acquisition point. The results of long-term vibration data collection and analysis will be presented along with plans for the future system development.

INTRODUCTION

Low vibration environment is crucial for an optimal operation of storage rings and beamlines at synchrotron light sources. Evaluation of background vibrations in synchrotron facilities is typically carried out using accelerometers in short-term survey measurement campaigns [1]. Some facilities decide on permanent monitoring systems installation [2]. The Vibration Monitoring System (VMS) at SOLARIS synchrotron radiation centre has been developed in order to provide continuous diagnostic data of vibration conditions in the storage ring.

The VMS started operation in the beginning of 2023 and the commissioning period ended in September 2023 (due to long component delivery schedules). Along with the development of the system, the enlargement of the experimental hall and related construction works were carried out. The VMS has played an important role during accelerators and beamlines operation coinciding with heavy construction equipment works that generated high levels of vibrations. When established vibration limits were exceeded, actions were taken: the problematic construction methods were changed to lower the impact of vibrations; the activities were rescheduled to take place during less-critical time periods.

SYSTEM DESIGN

Hardware

Currently, the VMS consists of a single Measurement Point (MP) located inside the storage ring on Double-Bend Achromat (DBA) cell in section 01. Measurement point consists of three PCB Piezotronics Model 393B31 seismic accelerometers (nominal sensitivity: $1 \text{ V m}^{-1} \text{ s}^2$, frequency

---

* marcel.piszak@uj.edu.pl

range: 0.1 Hz to 200 Hz). Transducers are fixed to a custom-build, triaxial adapter that allows for axial alignment with respect to the DBA cell. The MP's orientation was chosen accordingly: the x-axis of the MP is normal to the electron beam at the DBA center, the y-axis is tangential to the beam and the z-axis is oriented vertically (Fig. 1).
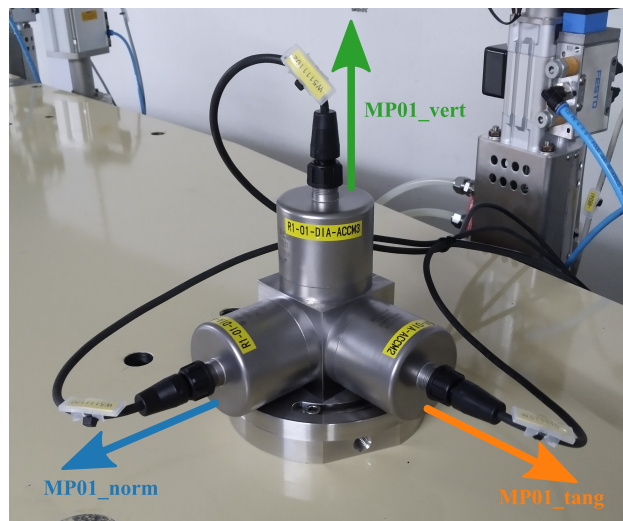
Figure 1: Triaxial measurement point with custom adapter mounted on the top surface of a DBA cell.
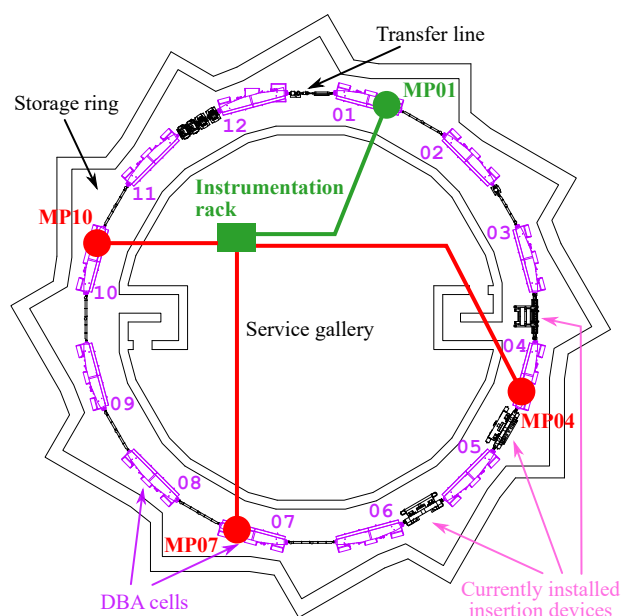
Figure 2: VMS arrangement view over the storage ring area (green color indicates existing infrastructure; red color indicates planned measurement points).

MECHANICAL DESIGN OF THE BEAM GAS IONISATION (BGI) BEAM PROFILE MONITOR FOR CERN SUPER PROTON SYNCHROTON

M. T. Ramos[†], W. Andreazza, P. Bestmann, H. Bursali, N. S. Chritin, W. Devauchelle,
A. Harrison, G. Khatri, M. McLean, C. Pasquino, F. Sanda, P. Schwarz, J. W. Storey,
R. Veness, W. Vollenberg, C. Vollinger
CERN, Meyrin, Switzerland

Abstract

The Beam Gas Ionisation (BGI) instrument of the Proton Synchrotron (PS), presently installed and operational, has been re-designed for the Super Proton Synchrotron (SPS), the following machine along the Large Hadron Collider (LHC) injector chain at CERN accelerator complex. Using the same detection technology, Timepix3, the SPS-BGI infers the beam profile from the electrons created by the ionisation of rest gas molecules and accelerated onto an imaging detector. This measurement method will allow for continuous, non-destructive beam size measurement in the SPS. In view of the upgrade, the design has been simplified and validated for integration, radio-frequency & impedance, high-voltage, and ultra-high vacuum compatibility.

INTRODUCTION

Accurate time-resolved measurements of the transverse beam profile are required to identify the causes of emittance growth. A new generation of Ionisation Profile Monitors (IPM) based on the detection of ionisation electrons with Hybrid Pixel Detectors (HPD's) installed directly inside the accelerator beam pipe, are currently being designed, produced, installed, and commissioned along the LHC injector chain [1]. Furthermore, in the scope of the High-Luminosity Large Hadron Collider (HL-LHC) upgrade, IPM's based on this technology are under development. Henceforth, the present proceeding will focus on the design phase of the new IPM's for the Super Proton Synchrotron accelerator – which at CERN are called Beam Gas Ionisation (BGI) profile monitors.

The working principle of the BGI for SPS is presented in Fig. 1. Electrons (and ions) are released by the interaction of the beam with residual gas. An electric field of 357 kV/m, formed by a cathode at -30 kV and a grounded anode, accelerates electrons onto an imaging device. The density of detected electrons is a direct measure of the transverse beam profile. The corresponding ions are transported through a hole – called the ion trap – to prevent the production of background electrons. A 0.26 T magnetic field, parallel to the electric field, ensures that the transverse position of the electrons is maintained, mitigating the effects of electron drift caused by electric field imperfections, the ionisation process, and the beam space-charge [1].

† teresa.ramos@cern.ch
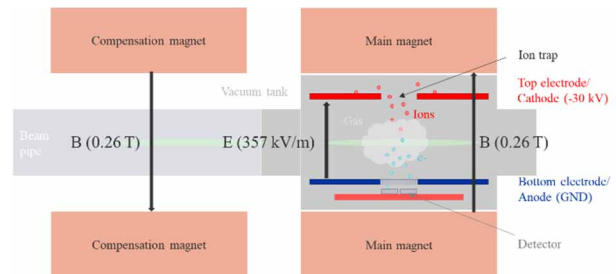
Figure 1: SPS-BGI working principle.

INSTRUMENT OVERVIEW

In the following section, a general overview of the instrument installed inside the vacuum tank will be described. The explanation will focus on the main function of the components listed in Fig. 2. The particular design features that have been implemented to address issues of radio-frequency (RF) & impedance, high-voltage (HV) and ultra-high vacuum (UHV) compatibility requirements will be described in the corresponding sections.

Structural Components

The BGI structural components are those that shape and give rigidity to the arrangement. Among them, these parts stand out: the support arms, the front reinforcement, and the Ultra-High Vacuum ConFlat (UHV CF) rectangular flange, a technology developed at CERN in 2015 for the first prototype of the BGI instrument [2].

Field Cage Design

The BGI field cage is required to provide a homogeneous electric field, protect the hybrid pixel detectors from background electrons, and shield the readout electronics from electromagnetic interference from the beam [3].

As illustrated in Fig. 2B, two parallel electrodes hold a potential difference of 30 kV. The top electrode or cathode, at -30 kV, is mechanically connected and electrically insulated from the support arm with ceramic spacers. To supress the formation of background electrons, a slit – called the ion trap – allows the corresponding ions to pass through and be directed onto the back of the cathode, where secondary (background) electrons will find no path back to the pixel detector. The bottom electrode or anode is grounded by means of fingerstock gaskets. A square pattern provides an opening in the faraday cage to allow the electrons to reach the surface of the chips, while protecting the electron detection system from electromagnetic interference.

APPLICATION OF QXAFS IN THE MEDIUM-ENERGY X-RAY ABSORPTION SPECTROSCOPY

Y.H. Xia[†], G.K. Zhang, F.F. Yang, J.F. Chang, H.Y. Zhang, S.H. Liu, L. Zheng, S.Q. Chu, J. Zhang

|Institute of High Energy Physics, Chinese Academy of Sciences, Beijing, China

Abstract

A quick scanning X-ray absorption fine structure spectroscopy (QXAFS) system has just been installed in 4B7A, a general medium-energy X-ray beamline at Beijing Synchrotron Radiation Facility (BSRF). This system is independent so that the QXAFS system can be employed by other beamlines equipped with a double-crystal monochromator (DCM) to achieve quick scanning and data acquisition. Continuous scanning is available in this system to satisfy the time scale from a few seconds to several minutes, depending on the energy range to be scanned. In this case, our QXAFS system applied to medium-energy X-ray beamlines will broaden the application of time-resolved measurement to a greater range of elements, thereby benefiting a wider user community.

INTRODUCTION

Time-resolved X-ray absorption fine structure (XAFS) measurements play a crucial role in studying in situ dynamic processes. Numerous techniques have already been applied to many synchrotron radiation beamlines to shorten the acquisition time of a XAFS spectrum down to a few seconds or even milliseconds. Among these, quick scanning XAFS is one of the successful modes.

QXAFS maintains a full compatibility with the step-by-step mode, based on the double-crystal monochromator, that is commonly used for general XAFS experiments. In QXAFS, one key difference from traditional XAFS methods is that the crystal monochromator continuously and rapidly rotates, significantly reducing the collection time of the spectrum. More importantly, it is easily compatible with various sample conditions. Therefore, with the development of photon sources and mechanization, QXAFS has the potential to become a primary method in the future.

Up to now, QXAFS has mainly been applied to hard X-ray beamlines, with limited applications in the lower energy range. However, in the medium-energy X-ray regime, there is a pressing need for a time-resolved XAFS experimental technique to investigate dynamic processes occurring within short time frames, especially elements like sulfur that are active in the field of electrochemistry.

In this paper, we will introduce the QXAFS system built at 4B7A, where can conduct medium-energy XAFS experiments at BSRF. The newly equipped QXAFS will be applied in the total electron yield experimental mode, providing a new and reliable experimental platform for various in-situ experiments in the future [1].

---

† xiayh@ihep.ac.cn

BEAMLINE OVERVIEW

The 4B7A beamline, completed in 2005 at BSRF, is dedicated to experiments in the medium-energy X-ray range [2]. BSRF is the first-generation synchrotron radiation facility of China, with its storage ring supporting high-energy physics experiments (Beijing Electron Positron Collider) and synchrotron radiation research. After an upgrade project in 2008, BSRF now operates in 2.5 GeV full-energy injection and top-up mode with 250 mA beam current in dedicated synchrotron radiation mode. Beamline's source is the No. 7 bending magnet in region 4 of storage ring. The bending magnet generates a magnetic field of 0.808 T and has a critical energy of 3358.6 eV. The source size is approximately 1.5 mm (H) × 0.4 mm (V). At the critical energy, the vertical divergence of the source is around 0.28 mrad. The maximum horizontal acceptance angle is 5 mrad, defined by the apertures in the front-end section.

As shown in Fig. 1, this beamline is equipped with a fixed-exit DCM, and usually used crystals are Si(111) and InSb(111). The corresponding energy range is from 1.75 to 3.5 keV while using InSb(111), and from 2.1 to 6.0 keV for Si(111), the useful Bragg angle is about from 19° to 71°, only one pair of crystals can be used at the same time. The energy resolution power (E/ΔE) was higher than 5000 at 3206 eV and 1800 at 5465 eV. The measured flux at the sample is higher than 3×10^{10} photons/s/250 mA in the energy region of 1.75–6.0 keV. The measured beam size at the sample position is about 5 mm (H) × 1.5 mm (V). Finally, due to diffraction forbiddance, Si(111) cannot emit even-order harmonics of X-rays. This will allow the experimental station to obtain high-purity monochromatic light.
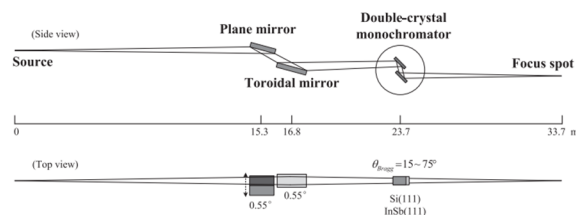
Figure 1: Schematic layout of beamline 4B7A.

QXAFS SYSTEM AND PERFORMANCE

For time-resolved XAFS experiments, QXAFS converts the motion mechanism of the monochromator and improves the data acquisition system. The 4B7A beamline has been equipped with a fixed-exit Si(111) DCM. The angle position is rotated through a stepper motor and recorded by

A VACUUM ASPIRATED CRYO COOLING SYSTEM (VACCS)

G. Duller, B. Olafsson, M. Nagy, Diamond Light Source, Didcot, United Kingdom
D. Magrath*, Brompton Bicycles, Greenford, United Kingdom

Abstract

The use of liquid nitrogen for cooling of synchrotron equipment is widespread. The cryogenic sub-coolers commonly employed come with some significant drawbacks such as cost, complexity, stiffness of distribution lines, and vibration induced by pressure variations. The typical sub-cooler is capable of handling 2 to 3 kW of absorbed power whilst many optics require no more than 50 to 150 W of cooling. We present a Vacuum Aspirated Cryo-cooling System (VACCS) which overcomes many of these disadvantages and which allows cryo-cooling to be implemented more widely. The VACCS system uses a vacuum, generated with no moving parts, to draw LN2 through a heat exchanger. Thus the system does not have to be pressure rated. We describe our designs for highly flexible distribution lines. A simple control system offers variable temperature at the heat exchanger by varying the flow rate of LN2. A system is installed at Diamond which allows the independent control of three zones. A test rig has demonstrated cooling capacity in excess of 100 W for a monochromator crystal assembly and controlled temperatures −194 to −120 °C.

INTRODUCTION

Many synchrotron optics require some sort of cooling. Cryogenic cooling is often an attractive choice due to, for instance, the enhanced properties of silicon and copper which can be accessed. Equally, scientific goals commonly demand that sample environments are held at cryogenic temperatures (77 K and above).

As a result closed-cycle cryogenic cooling systems are frequently employed where the high cost of implementation can be warranted. Unfortunately these systems come with some significant drawbacks, including high capital and running costs, take up a substantial footprint, have a tendency to excite vibrations due to pressure fluctuations, and require high stiffness distribution lines. These sub-coolers circulate liquid nitrogen (LN2) at elevated pressures to increase the boiling point of the fluid, thus allowing the coolant to extract power from the heat exchanger without inducing local boiling. Commonly rated at 5 to 10 bar, these pressures demand that all distribution lines are constructed to withstand these pressures whilst having minimal thermal losses, and vacuum vessels equipped with these systems require safety assessment and protection (burst disc or similar). These sub-cooler systems are typically rated at 2 to 3 kW cooling power, significantly in excess of the requirements of a typical beamline. In our tests the majority of monochromators require cooling of less than 100 W.

_____

* daniel.magrath@brompton.co.uk

We have developed a novel cryocooling system, the Vacuum Aspirated Cryo-Cooling System (VACCS), with the goal of addressing many of the issues associated with sub-cooler systems and have demonstrated its cooling ability up to 100 W. This has been implemented at the Diamond Light Source (DLS) beamline, VMXm, to control three independent end-station zones and will shortly be implemented in a monochromator.

DESIGN

Principles of Operation

The VACCS system is designed with a focus on simplicity and cost-effectiveness, aiming to cool assemblies down to cryogenic temperatures using basic components. As the name implies, flow of LN2 is induced by generating partial vacuum at the exhaust. This is achieved by using an ejector pump and the basic function of it is shown in Fig. 1, where suction is generated by a motive fluid (pressurised air in our case), entering from the left side. The converging/diverging nozzle increases the velocity of the motive fluid and the kinetic energy is balanced by a drop in pressure, thereby generating suction at the bottom inlet [1].

A schematic of the VACCS system is shown in Fig. 2 which illustrates its principle components. The dewar supplying the LN2 to the system is vented to atmosphere. By placing a temperature sensor on the heat exchanger (device to be cooled), flow of LN2 can be adjusted via a PID controller by varying the pressure of the compressed air entering the ejector pump to achieve a desired temperature. Alternatively, the flowmeter in front if the ejector pump can used as a set point for control.

Taking advantage of the latent heat of vaporisation to cool the device, most of the LN2 is expected to have transformed to gaseous form (GN2) as it exits the heat exchanger. The purpose of having an exhaust heater after the heat exchanger is to heat the nitrogen to ambient temperature, allowing for uninsulated pipework to be used beyond this point, and thereby increasing the system's flexibility and ease of installation. Additionally, a standard calibrated flowmeter for air can be used, making it more cost-effective.
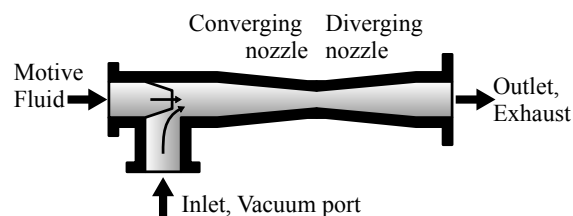
Figure 1: An illustration of an ejector pump (Figure based on a diagram from the product sheet in [2]).

MAGNETIC LEVITATION ON A BUDGET: A STUDENT DISCOUNT

J. H. Kelly, M. Hurlstone, S. Farrelly, D. Crivelli
Diamond Light Source, Harwell Science & Innovation Campus, Harwell, UK

Abstract

The successful mechatronics development i. e. modelling, simulation, design, build and test of a magnetic levitation stage at the Diamond Light Source is presented. The concept was to use a low control bandwidth across the 6 degree of freedom MIMO system, to provide both an alignment stage and vibration isolation. The project simultaneously upskilled staff and developed a proof-of-concept system demonstrator at a low cost. The final motion stage was constructed for a component cost of less than £15,000.

INTRODUCTION

The Diamond Light Source (DLS) is the UK national synchrotron facility. Numerous beamlines focus X-ray beams to less than 100 nm and hence require relative sample & optics stability to be a fraction of this. The new flagship beamline I17 to be built as part of the Diamond II upgrade has extreme stability requirements yet to be achieved on existing beamlines. The sample position jitter specification is ± 0.5 nm Peak – Peak, 1-1000 Hz relative to the beam. To even come close to this performance significant mechatronics modelling, simulation, testing will be required. A component of this research and development has been performed by Year-in-Industry engineering students. The primary goal of their project was to deliver the knowledge & processes required to design a magnetically levitating motion stage (maglev), as this had never been done before at DLS. This paper details the significant achievements of two students to model, simulate, design, build and test a magnetic levitation stage suitable for synchrotron endstation vibration isolation.

The benefit of an active maglev solution as compared to a passive isolator is that the amplification at resonance can be eliminated, the system stiffness and damping adjusted in software and the isolation also provides a compact parallel kinematic 6 degree of freedom (DOF) system which may be stepped or rotated about any arbitrary co-ordinate system. The downside is the inherent mechanical system instability and complexity.

REQUIREMENTS

The top-level requirements defined for the project were:
- Load capacity > 10 kg
- Low profile ∼ 0.5 × 0.5 × 0.2 m maximum envelope
- Vibration transmission < 10% from 10 – 500 Hz
- Provide 6 DOF motorised alignment
- Position Stability ± 500 nm, 1-1000 Hz Peak-Peak
- Angular Stability ± 500 nrad, 1-1000 Hz Peak-Peak
- Travel Range XYZ ± 1 mm, Pitch/Roll/Yaw ± 1 mrad

PROJECT PROCESS

A clear Mechatronics workflow was followed; requirements specification, hand calculations, literature review, concept simulation, design iteration, final system simulation including the motion control software and hardware, Dynamic Error Budget, build, commission, test, validate & update the original model to improve the process.

SYSTEM DESIGN

It was decided to use commercial voice coils (Motion Control Products AVA2-20-0.5) with sufficient clearance to meet the desired motion requirements rather than manufacturing custom coils to save resources. The flat rather than cylindrical design enabled the co-location of the position sensor. The design is deliberately symmetric with the centre of mass located at the geometric centre. The nominal required control bandwidth was calculated to be ∼10 Hz via hand calculations [1]. The bracketry was designed to have a 1st mode above 100 Hz i.e. 10 times the fundamental rather than the usual 3-5 time rule-of-thumb so a higher bandwidth could be tested.

GRAVITY COMPENSATOR

Most magnetically levitating motion stages employ a gravity compensator to minimise the power required to resist gravity [2–4].
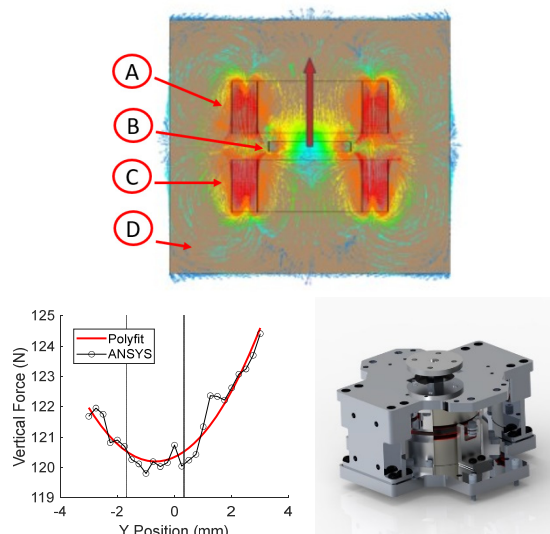
Figure 1: ANSYS Magnetostatic simulation of permanent magnet gravity compensator magnetic field vectors (Top) A) Upper fixed ring magnet, B) Floating magnet, C) Lower fixed magnet, D) Simulation space. Predicted vertical force variation with vertical translation (bottom left) and gravity compensator 3D design (bottom right).

DEVELOPMENT OF LOW-FREQUENCY SUPERCONDUCTING CAVITIES FOR HIGH ENERGY PHOTON SOURCE

X.Y. Zhang[1]*, J. Dai, L. Guo[1], Q. Ma[1], F.B. Meng, P. Zhang[1], H.J. Zheng[1]

Institute of High Energy Physics (IHEP), Chinese Academy of Sciences (CAS), Beijing, China

[1]also at University of Chinese Academy of Sciences, Beijing, China

Abstract

A low-frequency superconducting cavity is one of the most critical devices in the High Energy Photon Source (HEPS), a 6 GeV diffraction-limited synchrotron light source under construction in Beijing. A higher-order-mode (HOM) damped 166.6 MHz β=1 quarter-wave superconducting cavity, first of its kind in the world, has been designed by the Institute of High Energy Physics. Compact structure, excellent electromagnetic and mechanical properties and manufacturability were realized. An enlarged beam pipe was proposed allowing HOMs to propagate out of the cavity and be subsequently damped by a toroidal beamline HOM absorber at room temperature. Mounted with a forward power coupler, a tuner, two thermal break beam tubes, a collimating taper transition, two gate valves and some shielded bellows, the jacketed cavity was then assembled into a cryomodule. Two cryomodules were later required to fit into HEPS straight sections with a length limitation of 6 meters, which posed a significant challenge for the design of the cavity string. The success of the horizontal test also verifies the design of the cavity string. This article presents the design, fabrication, post-processing, system integration, and cryogenic tests of the first HOM-damped compact 166.6 MHz superconducting cavity module.

INTRODUCTION

High energy photon source (HEPS) is a diffraction-limited synchrotron light source designed by the Institute of High Energy Physics [1]. It is a 6 GeV kilometer-scale light source. The construction of HEPS began at Beijing in Jun 2019 and is expected to be completed in 2025. Five 166.6 MHz superconducting rf (srf) cavities will be installed in the storage ring as main accelerating cavities. The frequency of 166 MHz was chosen to implement a novel beam injection scheme proposed by physics [2], while compromising with the kicker technology [3]. The main parameters of HEPS are listed in Table 1.

A proof-of-principle (PoP) cavity has been successfully developed in HEPS-Test Facility (HEPS-TF) project [5, 6]. A HOM-damped 166.6 MHz β=1 quarter-wave superconducting cavity was proposed for HEPS storage ring [4, 7]. Mounted with a forward power coupler (FPC), a tuner, two thermal break beam tubes, a HOM absorber, a collimating taper transition, two gate valves and some shielded bellows, the jacketed cavity was then assembled into a cryomodule. In this paper, the design, fabrication, post-processing, system

---

* Email: zhangxinying@ihep.ac.cn

Table 1: Main Parameters of the HEPS [4]

Parameter	Value	Unit
Circumference	1360.4	m
Beam energy	6	GeV
Beam current	200	mA
Total energy loss per turn	4.14	MeV
Total power loss to radiation	828	kW
Forward RF frequency	166.6	MHz
Total RF voltage (main)	5.16	MV
3rd harmonic RF frequency	499.8	MHz
Total RF voltage (HC)	0.91	MV
Transmitter power per rf station	260	kW

integration, and cryogenic tests of the first HOM-damped 166.6 MHz cavity module were introduced in detail.

DESIGN OF THE CAVITY STRING

Layout of the Cavity String

A total of four layouts for the cavity string were analyzed and finally layout1 was chosen as the baseline scheme [8], as shown in Fig. 1. The total loss factor of this setup was calculated to be 5.2 V/pC. Synchrotron light can be nicely collimated, producing sufficient shadow for downstream components.
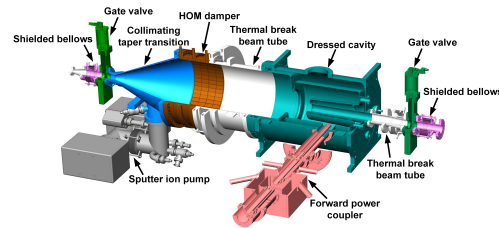
Figure 1: The 166 MHz cavity string.

Component Design of Cavity String

The Jacketed Cavity The jacketed 166 MHz cavity was fabricated by Beijing HE-Racing Technology Co., Ltd. There are 44 individual components. Grade-2 titanium was chosen to join the jacket and the NbTi flanges by using electron beam welding. The inlet flange was located at the bottom of the vessel and the feed pipe with a diameter of 8 mm guides the liquid helium into the LHe vessel. The outlet of the gas helium with a diameter of 160 mm was traditionally located on the top of the vessel. The welded cavity with helium jacket dressed are shown in Fig. 2.

CHALLENGES AND SOLUTIONS FOR THE MECHANICAL DESIGN OF SOLEIL-II

K. Tavakoli[†], F. Alves, G. Baranton, Y. Benyakhlef, A. Berlioux,
J. Dasilvacastro, M-E. Couprie, S. Ducourtieux, Z. Fan, C. Herbeaux,
C. Kitegi, F. Lepage, A. Loulergue, V. Leroux, A. Mary, F. Marteau,
A. Nadji, V. Pinty, M. Ribbens, A. Carcy, S. Pautatd, S. Thoraud, A. Lejollec
SOLEIL-II TDR team, Synchrotron SOLEIL, L'Orme des Merisiers, Saint-Aubin, France

Abstract

The Synchrotron SOLEIL is a large-scale research facility in France that provides synchrotron radiation from terahertz to hard X-rays for various scientific applications. To meet the evolving needs of the scientific community and to remain competitive with other European facilities, SOLEIL has planned an upgrade project called SOLEIL-II. The project aims to reconstruct the storage ring as a Diffraction Limited Storage Ring (DLSR) with a record low emittance which will enable nanometric resolution.

The mechanical design of the upgrade project involves several challenges such as the integration of new magnets, vacuum chambers, insertion devices and beamlines in the existing infrastructure, the optimization of the alignment and stability of the components, and the minimization of the downtime during the transition from SOLEIL to SOLEIL-II. The mechanical design is mainly based on extensive simulations, prototyping, and testing to ensure the feasibility, reliability, and performance of several key elements.

INTRODUCTION

SOLEIL is the French third generation light source operated for users since 2008 with an electron beam emittance of 4 nm·rad at an energy of 2.75 GeV in high intensity (500 mA, multibunch) [1].

The current lattice of the SOLEIL storage ring is composed of 16 modified two-bend achromat cells, 8 of which have short straight sections between the dipoles, altogether giving a total of 24 straight sections. After years of successful operation, a series of feasibility studies were initiated for a possible upgrade of the storage ring with a significantly lower emittance.

The SOLEIL Upgrade project, known as SOLEIL-II aims to design and build a 2.75 GeV diffraction-limited synchrotron light source preserving the actual infrastructure, 29 beamlines (far-IR to hard X-rays) and the 500 mA uniform filling pattern. The lattice of the new storage ring presented in CDR report [1] is built over a non-standard combination of twelve 7BA cells and eight 4BA cells [2, 3]. The main comparison parameters are listed in Table 1.

Table 1: Main SOLEIL-II Lattice Parameters

	Actual	**Upgrade**
Emittance (2.75 GeV)	4 nm·rad	84 pm·rad
Circumference	354.1 m	353.5 m
Straight section number	24	20
Long straight length	12 m	8.0/8.3 m
Medium straight length	7 m	4.25 m
Short straight length	3.8 m	3.0 m

Figure 1 shows the arrangement of the magnets in the 7BA cell and the 4BA cell of SOLEIL-II lattice. The length of the 7BA cell is rather short (~16 m) containing 52 magnets, depending on the lattice version, and including 7 dipoles. This very high density of multipoles increases the problem of compactness and creates implementation difficulties.
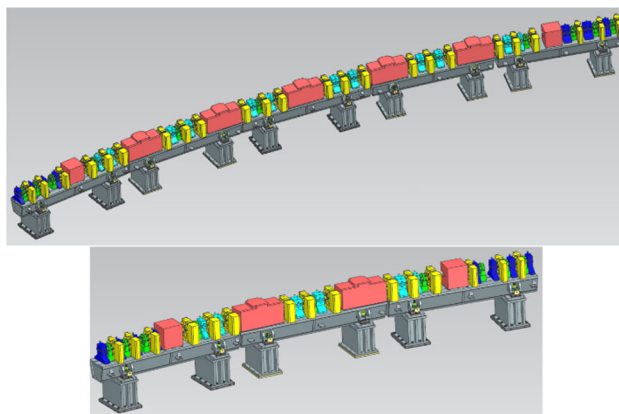
Figure 1: Engineering layout of the 7BA cell type of the new MBA-ARC (top) and the 4BA cell (bottom).

GIRDER DESIGN

The design of the girders is the result of a compromise between the vibration and thermal stability, adjustment precision and overall fabrication costs. After few iterations, SOLEIL mechanical engineers came up with a design based on four girder length families. Each girder family can be assembled in different configurations carrying single or double dipole [4].

The specification defined by accelerator physicists for the first modal frequency is around 40 Hz under load. Figure 2 shows the FE simulations on one of girder families in two different configurations.

---

† Keihan.tavakoli@synchrotron-soleil.fr

DEVELOPMENT OF THE BENT FOCUSING MIRROR IN HEPS FROM DESIGN TO TEST

Minwei Chen[†], Ming Li, Fugui Yang, Shanzhi Tang
Institute of High Energy Physics, CAS, Beijing, China

Abstract

The focusing mirrors are important for each beamline in the 4th generation photon source. One bent focusing face-down mirror in HEPS is taken for an example to be introduced from the design to the test. The effect of the gravity of the mirror is considered in the design. Moreover, for the sake of the compromise between the processing and the precision, the polygonal structure is adopted. Also, the iteration of the solution is improved to increase the design efficiency. The results reveal that the theoretical precision of the mirror after bending can reach less than 100 nrad RMS. In the aspect of the mechanics, the scheme of four roller bender comes out to avoid the parasitic moment, and the movable component in the bender are all coated with the MoS_2. As the type of the measurement is facing side which is different from the type of the actual condition, the effect of the gravity must be included in the metrology results. In the meantime, the stability and the repeatability are also measured. The result can be converged to around 200 nrad RMS, which is less than the required error. The stability, $\Delta R/R$, can be constrained under the 0.6%, showing the outstanding performance.

INTRODUCTION

Since the small spot and the high brightness, people around the world engage in pursuing the 4th synchrotron radiation facility (SRF). Bent mirror is one of the most significant optical element in the SRF, which can not focus the light but also decrease the error induced by other elements in the beamline. High energy photon source (HEPS) is one of the establishing 4th SRF, of which the circumference is about 1360 m and the emittance is 34 pm·rad [1].

This paper is dedicated to illustrating one focusing bent mirror in the HEPS beamline from design to test, which is seldom explained in other articles. The method used in the design is one kind of new iteration algorithm to increase the efficiency [2]. And the outstanding performance of the whole system is shown in the off-line testing.

DESIGN METHOD

Since the bent mirror is vertical reflection, the influence of the gravity is nonnegligible in this design. In order to decrease the cost of the bent mirror, the gravity compensation is also considered, thus the polygonal profile is adopted. The width of the mirror can be described as

$$b(x) = \frac{M(x) + M_g(x)}{EI_0 C(x)} b_0 , \qquad (1)$$

† chenmw@ihep.ac.cn

where $b(x)$ is the width varying with the position of the mirror, $M(x)$ is the moment of the mirror, $M_g(x)$ is the moment caused by gravity, E is the elastic module, $C(x)$ is the curvature of the mirror shape, b_0 and I_0 are the width and the inertia moment at the mirror center, respectively.

The solution on mirror width is utilized by the method in this article [2], which can improve the efficiency of the calculation.

DESIGN RESULTS

The active area of the bent focusing mirror used in HEPS is 605×20 mm^2. The requirement for the total slope error is less than 0.3 µrad. The final width can be solved by the theory above, and the results of the performance of the mirror are also shown as following.

The mirror width is plotted in Fig. 1. For sake of the processing convenience, the mirror edge is divided into 5 segments. Due to its direction of reflection, the distribution of the width shows a concave polygon. This width shape can effectively reduce the influence of the gravity.
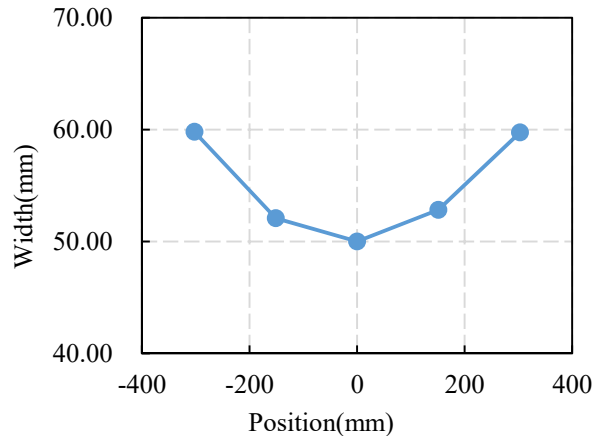
Figure 1: Mirror width along the position.

The design result of the slope error is shown in Fig. 2. The curve fluctuates between -0.03 µrad and 0.03 µrad, indicating the excellent performance of the mirror. The RMS (root mean square) of the slope error is about 14 nrad that is a very low value. Besides the design error, the material error, fabrication error and mechanical error are all included in this stage. The total error can be controlled around the 140 nrad RMS, which meets the requirement for less than 300 nrad RMS.

THE DESIGN AND PROGRESS OF THE NETWORK AND COMPUTING SYSTEM FOR HEPS

H. Hu, F. Qi, X. Wang, Y. Cheng, Q. Hu, H. Zhang, Y. Hu, S. Zeng
Institute of High Energy of Physics, Beijing, China

Abstract

China's High Energy Photon Source (HEPS) is the first national high-energy synchrotron radiation light source. The 14 beamlines for the phase I of HEPS will produces about 300 PB/year raw data, it represents significant challenges in data storage, data access, data analysis and data exchange. HEPS Computing and Communication System (HEPSCC), is an essential work group responsible for the IT R&D and services for the facility, including IT infrastructure, network, computing, analysis software, data preservation and management, public services etc. This paper mainly introduces the design and progress of HEPSCC's work in addressing the data challenges faced by HEPS from various aspects, including machine room, network, storage, computing, and scientific software of data management and data analysis.

MANUSCRIPTS

HEPS is the first national high-energy synchrotron radiation light source and soon one of the world's brightest fourth-generation synchrotron radiation facilities [1], has been constructed from 2019 in Beijing's Huairou District, and will be completed in 2025. The 14 beamlines for the phase I of HEPS will produces about 300 PB/year raw data (see Table 1). Efficiently storing, analyzing, and sharing this huge amount of data presents a significant challenge for HEPS.

Table 1: Estimated Data Volume of HEPS at Phase I

Beamlines	Burst output(Byte/day)	Average output(Byte/day)
B1 Engineering Materials Beamline	600TB	200TB
B2 Hard X-ray Multi-analytical Nanoprobe (HXMAN) Beamline	500TB	200TB
B3 Structural Dynamics Beamline (SDB)	8TB	3TB
B4 Hard X-ray Coherent Scattering Beamline	10TB	3TB
B5 Hard X-ray High Energy Resolution Spectroscopy Beamline	10TB	1TB
B6 High Pressure Beamline	2TB	1TB
B7 Hard X-Ray Imaging Beamline	1000TB	250TB
B8 X-ray Absorption Spectroscopy Beamline	80TB	10TB
B9 Low-Dimension Structure Probe (LODISP) Beamline	20TB	5TB
BA Biological Macromolecule Microfocus Beamline	35TB	10TB
BB pink SAXS	400TB	50TB
BC High Res. Nanoscale Electronic Structure Spectroscopy Beamline	1TB	0.2TB
BD Tender X-ray beamline	10TB	1TB
BE Transmission X-ray Microscope Beamline	25TB	11.2TB
BF Test beamline	1000TB	60TB
Total average:		**805.4TB/day, 24.16PB/month**

HEPS Computing and Communication System (HEPSCC), also called HEPS Computing Center, is an essential work group responsible for the IT R&D and services for the facility, including IT infrastructure, network, computing, analysis software, data preservation and management, public services etc. Aimed at addressing the significant challenge of large data volume, HEPSCC has designed and established a network and computing system, making great progress over the past two years.

As the most fundamental part of the IT infrastructure, a deliciated and high-standard machine room, with about 900 m² floor space for more than 120 high-density racks in total, has been prepared for production since this August. The power system has two transformers for dual power supply and has a total capacity of 2,500KVA, with the UPS providing 800KVA of power capacity and offering a half-hour backup during emergencies. Row-Air conditioning with natural cooling is used for the refrigeration of the machine room, which can greatly reduce the energy consumption.

For the data center network, we designed it as a spine-leaf architecture which makes it very easy to scale out. The backbone bandwidth of the data center network can support speeds up to 4*400 Gb/s, which can fully meet the demands of high-speed data exchange. Meanwhile, we also support RoCE [2] (RDMA over Converged Ethernet) to provide a lossless and high-performance network environment for scientific workload in HEPS data center. Previous test evaluations showed that RoCE can reach the same performance as InfiniBand (IB) in both point-to-point and collective tests.

In order to balance the cost-effectiveness of storage devices and realize the high reliability of data storage, a three-tier storage is designed for storing experimental data, including beamline storage, central storage, and tape. There is a storage policy for data preservation (see Fig. 1), the raw data and processed data are stored on the beamline storage for a maximum of 7 days, on the central storage for a maximum of 90 days, and only the raw data are archived to tape for long-term storage with two copies. Of course, this data storage policy could be adjusted according to the actual data volume and funding situation of HEPS. The beamline storage utilizes distributed all-flash SSD arrays to achieve high data input/output speeds, while offering a total storage capacity of 800 TB. The central storage leverages distributed high-density HDD arrays to get medium-high speed data IO, providing a total capacity of 30 PB. The tape storage is compliant with the LTO9 [3] standard, and provides 2 PB at the first stage although we have no budget for tape.
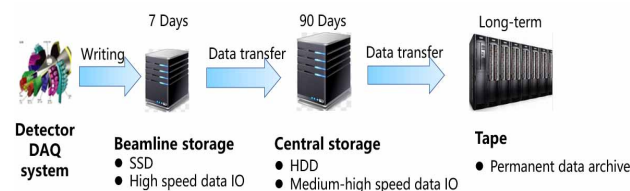
Figure 1: Storage policy for HEPS data.

To meet the requirements of data analysis scenarios for HEPS, a computing architecture has been designed and deployed in three types (see Fig. 2), including Openstack [4], Kubernetes, and Slurm. Openstack integrates the virtual cloud desktop protocol to provide users with remote

ADVANCING SIMULATION CAPABILITIES AT EUROPEAN XFEL: A MULTIDISCIPLINARY APPROACH

F. Yang*, D. La Civita, M. Di Felice, B. Friedrich, N. Kohlstrunk, M. Planas, M. Wuenschel,
L. Samoylova, H. Sinn, European XFEL, Schenefeld, Germany
T. Stoye, DESY, Hamburg, Germany

Abstract

At European XFEL, computational techniques such as finite element analysis (FEA) and computational fluid dynamics (CFD) are widely applied in various scientific and engineering fields, such as damage simulation due to heat load, bleaching effect study of gas attenuator, optimization of fluid cooling system for detectors and characterization of liquid sheet jets for sample delivery system. Without being constrained by experimental conditions, the multiphysics and multiscale models in simulation could virtually replicate the interaction process of XFEL beam with different materials, taking into consideration heat transfer, structural deformation and phase transition. In this contribution, to gain comprehensive insights into the fluid behaviors of the detector cooling system, as well as the performance of reduced order modelling solvers, parametric studies are conducted using CFD simulation code. Furthermore, a realistic simulation requires a secured process of Verification and Validation (V&V) of the computational model. Specific guides and standards need to be followed to ensure the credibility and accuracy of the simulation results. Besides following the FAIR principle (Findable, Accessible, Interoperable, and Reusable), a smart simulation data management system using machine learning algorithm is under construction. Moreover, the large amount of data from the simulations in the past can be utilized to train the machine learning model, which can be used for simulation results prediction without running further simulations. Further AI and machine learning tools are going to be employed to set up generative design workflow and digital twin scheme for the beamline components, serving as a new safety constraint for monitoring and optimizing of the facility operation.

VERIFICATION, VALIDATION AND UNCERTAINTY QUANTIFICATION

The goal of setting up a systematic verification, validation and uncertainty quantification (VVUQ) for all simulations is to build a common agreement based on corresponding ISO standard [1–3] regarding the reliability of simulation results. This topic is increasingly important when many models could be reused for new applications. As an example, to characterize the thickness change of the CVD diamond of the spectrometer, simulation results using various numerical methods are compared in Fig. 1. It shows that the divergence between these methods is obvious. Without having possibility to validate with experimental results, it
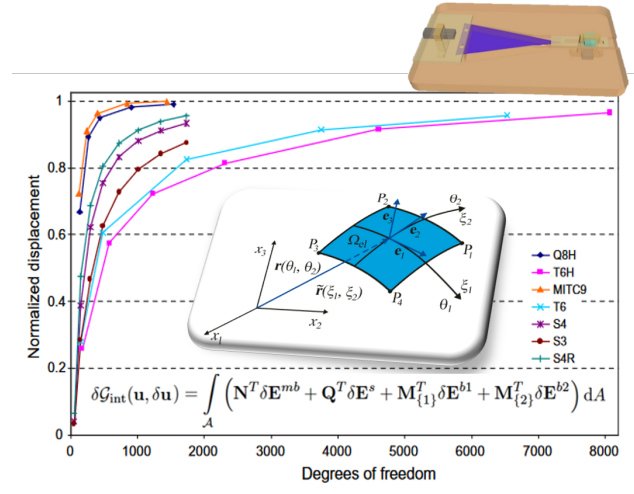
Shell element to avoid shear locking phenomena

Figure 1: Characterization of thickness change of bending crystal.
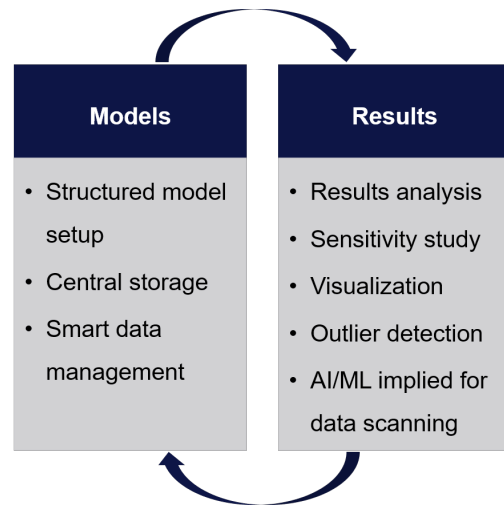
Figure 2: Simulation data management Scheme.

is important to execute a VVUQ process. The comparison shows that the element using convective coordinates which include the 2nd order bending moment is the most precise and efficient computational model. But since the elements in commercial code are only based on Cartesian coordinates, finer meshing is needed for a precise results [4]. Therefore, a standard workflow is essential, to ensure the credibility of the simulation models and results as following: (a) Purpose and Scope (b) Model Development (c) Verification and

___
* fan.yang@xfel.eu

SIMULATION

FEA methods

THERMAL CALCULATION AND TESTING OF SLS 2.0 CROTCH ABSORBERS

Xinyu Wang[†], Colette Rosenberg, Romain Ganter, André Weber, Markus Maehr, Samuel Bugmann

Paul Scherrer Institut, Villigen, Switzerland

Abstract

After 22 years of operation, the Swiss Light Source (SLS) was recently shut down on September 30, 2023, and the construction of SLS 2.0 has commenced. The storage ring of SLS2.0 based on a multibend achromat lattice will have the maximum electron energy of 2.7 GeV. SLS 2.0 crotch absorbers are designed to have two water-cooled, toothed jaws made of Glidcop to dissipate a maximum heat power of 6 kW. Finite element analysis has been conducted to validate the thermal and mechanical strength of the absorber's mechanical design. A conjugate heat transfer (CHT) simulation was performed to verify the water cooling concept. Furthermore, a prototype absorber underwent testing in an e-beam welding chamber. This paper describes numerical simulation and thermal testing of SLS 2.0 absorber.

INTRODUCTION

The storage ring of SLS 2.0 will feature a 40-fold increase in hard X-Ray brilliance, achieved through a low-emittance magnet lattice and a beam pipe with smaller aperture [1, 2]. The majority of over 100 pieces of absorbers is designated to dissipate synchrotron radiation power from normal bend dipoles [3]. The normal incidence power density is at a maximum of 600 W/mm² for a total power up to 3.5 kW. This absorber was initially designed using the age-hardenable CuCrZr alloy with two individually water-cooled upper and lower parts with saw-tooth surfaces. The idea was to produce the absorbers by wire erosion with a directly machined Conflat type knife edge in the absorber body. As no welding or brazing procedure would be necessary, this was expected to reduce material and fabrication costs [4-6]. From the 5 T superconducting magnets, a total power of about 7 kW is generated with the normal incidence power reaching as high as 1100W/mm². A different design and material is required, and Glidcop® AL-15 alloy was chosen due to its higher thermal conductivity and better resistance to thermal stress. The jaw has an inclination of 1° with a number of flat teeth and intermediate grooves. The teeth of upper and lower jaws interleave without contacting each other. In this way, the power was distributed to the upper and lower jaws, so that the power density is reduced to less than 30 W/mm². The two jaws are water-cooled and brazed into a stainless-steel flange.

WATER COOLING MODELLING

The cooling concept of SLS1 absorber has been adapted: the inlet water is guided by a stainless steel tube to the end of the pin hole and flows back through the helical channel on outer surface of the tube. Each jaw has three 10 mm pin-holes, and the tube has a diameter of 6 mm (inner) and 8 mm (outer). The average water velocity is limited to 1.5 m/s due to corrosion concerns, which corresponds to a flow rate of 15.3 l/min for an absorber with 6 channels.

In thermal calculations, water cooling can be simulated as forced convection using a heat transfer coefficient with a constant water temperature. Alternatively, water flow can be modeled using 1D thermal fluid elements, taking into account temperature changes in the water. For most common pipe geometries and flow conditions, the heat transfer coefficient can be estimated from correlations, such as Dittus-Boelter, Sieder-Tate, etc. Ultimately, the Computational Fluid Dynamics (CFD) analysis can be employed to investigate heat transfer between the solid and fluid.

A conjugate heat transfer simulation of a full absorber body including six stainless steel water pipes in parallel and with fluid water, would be very complex and time-consuming. Therefore a sub-model contains one water pipe with the lower-left part of the absorber, which removes more than ¼ of total heat power, has been analysed [7]. The Fluent model contains 3.7 million zones and 9.5 million nodes for the fluid, and 197'000 zones and 847'000 nodes for the solid. The turbulence model used was SST k-omega.
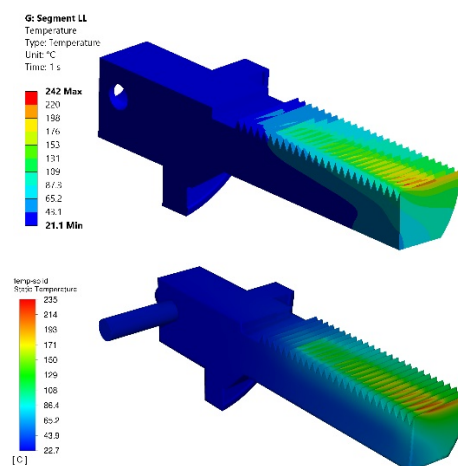
Figure 1: Temperature distribution in °C, from a): mechanical thermal model (top) and b): CFD model (bottom).

The adiabatic boundary condition was applied on the horizontal cutting face, as heat transfer between the upper and lower parts of the absorber is negligible. On the vertical section face, a convective boundary condition was applied to simulate the heat transfer to the colder, cut portion of the absorber jaw. Further simplification includes uniform distribution of heat flux on the surfaces. The thermal

---

DESIGN, MODELING AND ANALYSIS OF A NOVEL PIEZOACTUATED XY NANOPOSITIONER SUPPORTING BEAMLINE OPTICAL SCANNING

Lingfei Wang*, Guangcai Chang, Zongyang Yue, Lu Zhang, Shanzhi Tang

Institute of High Energy Physics, Beijing, P. R. China

Abstract

In recent years, with the advancement of X-ray optics technology, the spot size of synchrotron beamlines has been reduced to 10nm or even smaller. The reduction in spot size and the emergence of ultra-bright synchrotron sources necessitate higher stability, resolution, and faster scanning speeds for positioning systems. This paper presents the design, analysis, and simulation of an XY piezoelectric driven nanopositioning platform that supports high-precision optical scanning systems. To achieve fast and highly precise motion under the load of an optical system, a design scheme based on a hollow structure with flexible amplification and guiding mechanisms is proposed. This scheme increases displacement output while minimizing coupling displacement to ensure a high natural frequency. The rationality of this platform design is verified through modeling and finite element simulation.

INTRODUCTION

The High Energy Photon Source (HEPS) is a new generation light source that offers enhanced brightness and performance capabilities. The hard x nanoprobe beamline is primarily utilized for nanoscale scientific research. The minimum spot size can be less than 10 nm. Owing to the limitations inherent in conventional stepper motors, piezoelectric actuators have emerged as the preferred choice in this field, offering advantages such as exceptional positioning accuracy, rapid response times, compact dimensions, and lightweight construction.

The piezoelectric actuators utilized in synchrotron radiation light sources can be broadly categorized into two groups. One category encompasses the piezoelectric stick-slip actuators, which operate based on the principle of frictional inertia [1, 2]. These actuators are predominantly employed for large-scale position adjustments. One is the direct drive piezoelectric scanning platform [3–5], which is mostly used for sample scanning. This paper introduces an XY scanning platform specifically designed for nano-scanning experiments conducted at light sources. Subsequent chapters will provide detailed explanations on the structural design, static modeling, and simulation analysis of the XY scanning platform.

DESIGN OF THE MECHANICAL STRUCTURE

The schematic diagram of the nano-positioning platform driven by a piezoelectric stack is illustrated in Fig. 1. The nano-positioning platform features a symmetrical structure, comprising a bridge amplifying mechanism, two sets of guiding mechanisms, a piezoelectric stack, and a central moving stage. The piezoelectric stack is integrated into the bridge amplifying mechanism through a preload bolt, while the end of the bridge mechanism is connected to both the base and central moving stage via two sets of guiding mechanisms, ensuring optimal platform stiffness. The central moving stage adopts a hollow structure design with screw holes at the four corners, which facilitates scanning experiments and the installation of position feedback lenses.
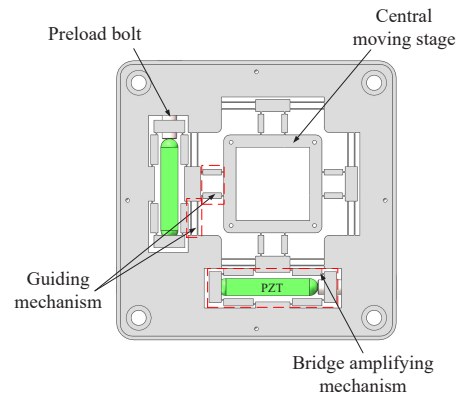
Figure 1: Schematic diagram of the XY positioning platform.

MODELING AND ANALYSIS

The amplifying mechanism analyzed in this paper is a planar mechanism, thus only the deformation of flexible hinges within the plane needs to be considered. The model diagram of the prismatic beam hinge is illustrated in Fig. 2. The thickness, width and length of the hinge are expressed by h, t_b and l_b, the loads on the prismatic beam flexure hinge are F_{xi}, F_{yi} and M_{zi}. and the flexibility matrix of the prismatic beam hinge can be obtained by considering it as a cantilever beam.

The expression of the flexibility matrix of the prismatic beam hinge [6] is as follows:

$$\begin{bmatrix} \delta x \\ \delta y \\ \delta \theta \end{bmatrix} = \begin{bmatrix} c_{11} & c_{12} & c_{13} \\ c_{21} & c_{22} & c_{23} \\ c_{31} & c_{32} & c_{33} \end{bmatrix} \begin{bmatrix} F_{xi} \\ F_{yi} \\ M_{zi} \end{bmatrix} \quad (1)$$

$$\begin{bmatrix} c_{11} & c_{12} & c_{13} \\ c_{21} & c_{22} & c_{23} \\ c_{31} & c_{32} & c_{33} \end{bmatrix} = \begin{bmatrix} \frac{l_b}{Eht_b} & 0 & 0 \\ 0 & \frac{4l_b^3}{3Eht_b^3} + \frac{l_b}{Ght_b} & \frac{6l_b^2}{Eht_b^3} \\ 0 & \frac{6l_b^2}{Eht_b^3} & \frac{12l_b}{Eht_b^3} \end{bmatrix} \quad (2)$$

THE STATUS OF THE HIGH-DYNAMIC DCM-Lite FOR SIRIUS/LNLS

G. S. de Albuquerque*, T. R. S. Soares, J.P. S. Furtado, N. P. Hara, M. Saveri Silva
Brazilian Synchrotron Light Laboratory, LNLS, Campinas, Brazil

Abstract

Two new High-Dynamic Double Crystal Monochromators (HD-DCM-Lite) are under installation for QUATI (superbend) and SAPUCAIA (undulator) beamlines at Sirius. The HD-DCM-Lite portrays an updated version of Sirius LNLS HD-DCMs not only in terms of being a lighter equipment for sinusoidal scans speeds with even higher stability goals, but also bringing forward greater robustness for Sirius monochromators projects. It takes advantage of the experience gained from assembly and operation of the previous versions during the last years considering several work fronts, from the mechanics of the bench and cooling systems to FMEA, alignment procedures and control upgrades. In this work, those challenges are depicted, and first offline results regarding thermal and dynamical aspects are presented.

INTRODUCTION

In recent years, LNLS has successfully developed and operated a cutting-edge high dynamic double crystal monochromator (HD-DCM) tailored for 4th generation light sources, representing a significant leap forward in terms of mechanical design and control. This innovation has yielded a state-of-the-art product, distinguished by its stability, both for fixed-energy and scan work [1–3]. The success of the first units in MANACA and EMA beamlines has driven the design of two new units, containing improvements designed [4] and assembled entirely by the LNLS team. Such enhancements focused on enabling high-speed sinusoidal scans capabilities [5] as required by QUATI [6], adapting to the energy range of the new beamlines (QUATI and SAPUCAIA), increasing stiffness, implementing control and FPGA optimizations [7], and applying Design for Manufacturing and assembly (DFMA) techniques to minimize the efforts required during mounting and offline commissioning phases.

Figure 1 shows the complete system's in-vacuum parts, highlighting its subcomponents, namely: the granite bench (GRA) (1); the goniometers rotary stages (ROT) (2) with their cooling systems; the goniometer frame (GOF) (3) for the crystal module mounting; the first crystals (CR1) (6), Si(311) and Si(111), which are fixed on the Metrology Frame 1 (MF1) (5), where the interferometer mirrors (IFM) are placed; the Auxiliar Frame 1 (AF1) (4), supporting the MF1; and the ShortStroke (SHS) (8), for mounting the second crystals (CR2) (7), elastically connected to the Short Stroke Frame (SSF) (9). The lower image offers an upstream view of the monochromator, showcasing the Upstream Mask (10) and the Cryogenic Pump (11). For a more detailed and functional explanation, please refer to [4].

---

* guilherme.sobral@lnls.br
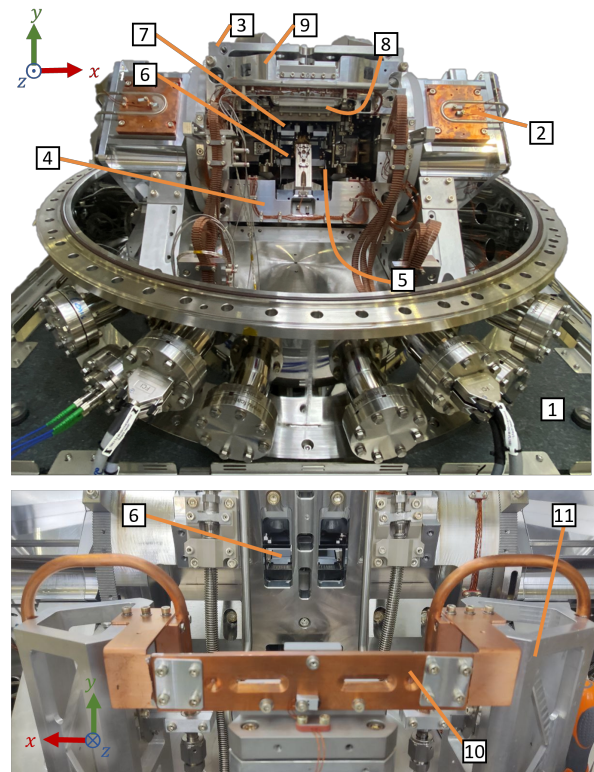
Figure 1: Overview of the assembled SAPUCAIA's HD-DCM-Lite with annotated subparts.

KEY DESIGN MODIFICATIONS

Drawing upon the insights gleaned from the design, assembly, and commissioning of previous HD-DCMs, we have implemented several design updates with the goals of enhancing performance, streamlining the production process, and facilitating the assembly phase. For example, we attest that improvements in the granite base, such as new routing parts, equipment protection components, and features designed to facilitate the placement of feet during assembly, played pivotal roles in the the assembly phase. Specific details regarding some updates will be elaborated upon in the subsequent subsections.

Rotary Stages

To meet the requirements of the QUATI (quick-EXAFS) beamline, a redesign of the rotary stage system was necessary. In addition to doubling the number of actuators to achieve extended scanning speeds, scans of longer duration required the implementation of a specialized thermal solution. This solution took the form of a water cooling system using machined copper components, as illustrated in Figure 1 under item (2).

The use of two mechanically coupled rotary stages intro-

CORE TECHNOLOGY DEVELOPMENTS

Others

HIGH HEAT LOAD TRANSFOCATOR
FOR THE NEW ID14 ESRF BEAMLINE

Laurent Eybert, Philipp Brumund, Juan Reyes Herrera, Noel Leve
ESRF, Grenoble, France
Miguel Lino Diogo dos Santos, CERN, Geneva, Switzerland

Abstract

X ray refractive lenses (CRL) are powerful in line optics for focusing/collimating x-rays. They offer many advantages such as compactness, a comfortable working distance, robustness, and are suitable for use in a wide range of energy. In the scope of the new nuclear resonance ID14 beamline at ESRF, a new **white beam transfocator** (WBT) was developed. This transfocator benefits from the previous experience of ESRF's transfocator to withstand the high heat load power densities (645 W/mm^2) and total power (405 W) generated by the future CPMU18. A thermal load analysis was carried out to optimize the cooling design. The tight alignment specifications within the same CRL (Compound Refractive Lenses) stack assembly and between different assemblies was achieved thanks a good machining of both lenses unit mechanical assembly and reference V shaped rail. High positioning repeatability of CRLs actuator is assured thanks to an optimized flexor and a good alignment procedure. The transfocator vessel is installed on a granite and on a 4-DOF alignment table.

INTRODUCTION

The mission of new ID14 beamline at ESRF is to carry out nuclear resonance scattering experiments. ID14 have 2 optic hutch (OH1) and (OH2). OH1 is a white beam hutch used for pre-conditioning of the X-ray beam for downstream high resolution optics as high resolution monochromators and a Synchrotron Mossbauer Source installed in OH2.

OH1 LAYOUT

In OH1 a high-heat-load monochromator (HHLM), a **white-beam transfocator** (WBT) and a monochromatic-beam transfocator are installed (see Fig. 1).
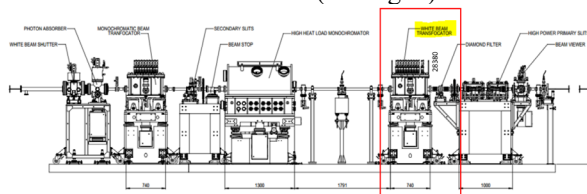
Figure 1: The white beam transfocator is installed in OH1 at 28.5 m from source.

WHITE BEAM
TRANSFOCATOR OVERVIEW

The only purpose of the white beam transfocator installed on ID14 is to avoid flux loss by matching the divergence of the collimated beam into the acceptance of the

Si(111) reflections used in HHLM. Figure 2 shows the collimation of the beam with 1D lenses.
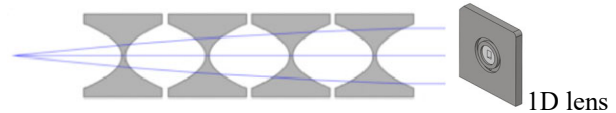
Figure 2: Use of Be CRL to collimate the beam.

Only a moderate, not an ultimate collimation is required to keep effective focusing. Focusing will be done downstream, in experimental hutches using KB mirrors. HHLM works in horizontal scattering plane so WBT collimates beam in horizontal plane only with 1D Beryllium lenses. Exceptions are 2D lenses for very high energies, where 1D lenses with very small radius (0.05) are not available. For the EBS machine, horizontal and vertical divergences are both about 14 µrad.

Table 1: Ω Angular Acceptance of HHLM - ΔΘ Divergence after Collimation [1] (Courtesy A. Chumakov)

Energy [keV]	type	R_A [mm]	N_{CRL}	T [%]	A [mm]	A_{eff} [mm]	$\Delta\theta$ [µrad]	Ω [µrad]	X
14.412	1D	0.50	3	93.6	1.39	1.35	6.8	17.5	0.45
21.541	1D	0.30	5	93.3	1.08	1.05	4.5	11.8	0.32
22.494	1D	0.20	4	94.7	0.88	0.86	3.5	11.3	0.25
23.879	1D	0.20	4	94.8	0.88	0.86	4.7	10.7	0.33
25.614	1D	0.20	5	93.8	0.88	0.86	3.9	10.0	0.28
27.78	1D	0.20	5	96.5	0.88	0.86	5.4	9.2	0.38
35.46	1D	0.20	12	88.0	0.88	0.83	3.6	7.2	0.10
37.13	1D	0.20	12	88.1	0.88	0.83	3.6	6.9	0.17
39.58	1D	0.20	12	88.4	0.88	0.83	3.6	6.5	0.27
67.408	2D	0.05	12	85.0	0.44	0.42	3.6	3.8	0
89.571	2D	0.05	21	76.9	0.44	0.41	3.6	2.9	0

As the Table 1 above shows, the type and number of lenses must be changed as the energy varies. This is the role of the transfocator (see Fig. 3). A maximum of 3 lenses casings are used simultaneously. They are installed next to each other.
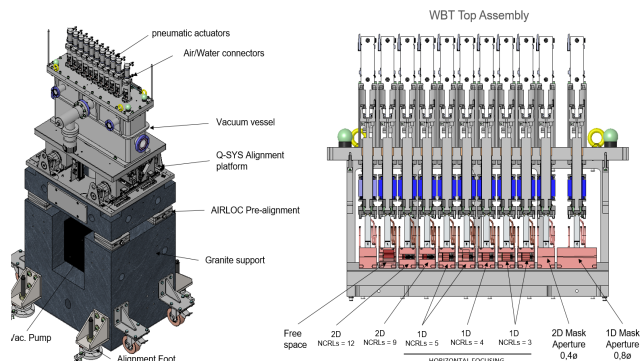
Figure 3: 11 axis water cooled transfocator.

POLAR SYNCROTRON DIFFRACTOMETER

G. Olea, N. Huber, J. Zeeb

HUBER Diffraction GmbH & Co.KG, Rimsting, Germany

Abstract

A new product for research purposes aiming to work in a 4th generation synchrotron facility (APS-U) after its upgradation has been recently developed. POLAR-Dm was conceived on a traditional 6C (C-circles) geometry, maintaining the common kinematic structural principle of the family. With the addition of several interchangeable devices, the multipurpose system is expanding the spectrum of possible investigations, maintaining the precision of setups. Mainly, it consists of two customized sample (S) modules for high-precision versatile sample manipulation and a dovetail detector arm (D) module for manipulating the detector, optics (polar analyzer), slits, etc. An alignment base (Ab) module stable supports the above modules and roughly adjusts the motions towards the incoming X-ray beam. In addition, a planar non actuated manipulator is facilitating the cable management during the work. The kinematic, design and precision concepts applied, together with the obtained test results are all in detail presented.

INTRODUCTION

The advanced synchrotron investigations require not only improved beam characteristics and/or new modern techniques, but dedicated instruments adapted to the specificity of the applications.

Advanced Photon Source (APS) research facility is currently under an upgradation process (APS-U) [1]. Apart from several improved characteristics e.g., emittance, coherence, etc for new / enhanced beam lines, an appreciable number of experimental stations (hutches) are to be developed and/or improved, as well. Several beamlines will be allocated to magnetic materials (MM) group from X-ray Science Division (XRS). After its completion, the 4-ID (POLAR) beam line will investigate the emergent electronic properties (e.g., inhomogeneity) of advanced magnetic and ferroelectric functional materials, relevant to quantum and energy technologies, using spectroscopy and/or X-ray magnetic scattering techniques [2].

A request to develop a dedicated diffractometer has been issued for one of the end stations (G) [3]. The intention was to use a common fife-circle (5C) diffractometer architecture adapted with the geometry for horizontal scattering (Q-range access) for a superconducting magnet (2T) and low vibration for thin films, under extreme conditions - low temperature (cryo) and high pressure (HV) investigations. In addition, adequate support for a vacuum polarizer analyzer and area detector has to be included. The new Dm has to offer not only heavy load/small manipulation capabilities, but (high) precision features, as well [4].

The main features of the final product (prototype) are described below, including most important aspects related to kinematics, design and precision concepts.

POLAR DM

Dm should accommodate with the use of x-ray techniques based on spectroscopic (absorption, polarized dependent resonant) and magnetic (XRMS) scattering principles. A 2T magnet sample (120 kg), sample cells (30 kg) and (15 kg), together with small (200 g) one must be manipulated by the two sample positioning systems. 1D/point (5 kg) detector and the polarized analyzing optics (100 kg) are to be manipulated, as well. The manipulation errors must be inside of the Sphere of Confusion (SoC < 50μm).

Kinematics

Basically, from a kinematic point of view, the chosen Dm (POLAR) architecture belongs to 5C (2D + 3S) class – two $(C_i, i = 1,2)$ for detector(D) and three $(C_i, i = 3…5)$ for the sample (S) actuated circles, respectively [5]. However, as (S) comes with two independent setups called manipulators (S_1, S_2), each of them is composed from another actuated circle $(C_6)_i, i = 1...2$. Thus, the structure became a 6C (2D + 4S). However, there are also another three (3) circles inside of the polar analyzer $(C_7 - C_9)$, so the entire system falls into a multi-circles Dm class.

Mainly, it has two distinct (kinematics) chains (K_D, K_S) supported by another (K_B), Fig. 1. The experimental investigations are based on the corelated motions (positioning) of the two (K_D, K_S) relative to X-ray (incident/scattered) fixed beam, respecting the diffraction law (Bragg).
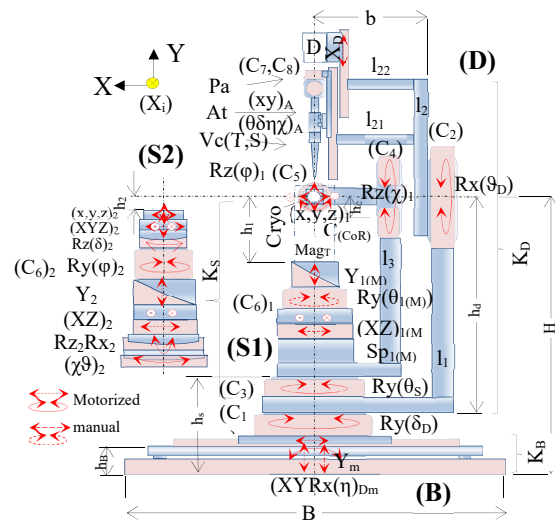
Figure 1: POLAR-Dm kinematics.

The detector (D) manipulator kinematic chain (K_D) mechanism consists of two active rotational joints $C_1 (\delta_D)$ and $C_2 (\vartheta_D)$ linked together through (l_1). In addition, a dove

THE MID INSTRUMENT OF EUROPEAN XFEL: UPGRADES AND EXPERIMENTAL SETUPS

G. Ansaldi[†], A. Schmidt, U. Boesenberg, J. Hallmann, J. Möller, J.-E. Pudell,
K. Sukharnikov, T. Andersen, J. Wonhyuk, R. Shayduk, A. Bartmann,
A. Rodriguez-Fernandez, A. Zozulya, A. Madsen
European X-Ray Free-Electron Laser Facility, Schenefeld, Germany

Abstract

This article provides examples of setups and upgrades currently under development at the Materials Imaging and Dynamics (MID) instrument of the European X-Ray Free-Electron Laser (Eu. XFEL) concerning the X-ray Scattering and Imaging Setup (XSIS):

- The Multi-environmental multi-Detector Setup (MDS_2) is a set of setups designed to integrate in the MID Instrument an additional detector chamber (the Multi Detector Stage, MDS) to be used in parallel with the AGIPD detector, allowing simultaneous coverage of the wide- (WAXS) and small-angle X-ray scattering (SAXS) regions by use of several area detectors. It can also be used in Large Field-of-View (LFOV) configuration.
- The Multi-Purpose Chamber 2 (MPC-2) is an evolution of the current MPC and includes design upgrades of both the exterior of the vessel as well as some internal improvements concerning simultaneous use of optical laser excitation of the sample and Nano-focusing X-ray optics.

Both upgrades will improve the capabilities of MID and enable new types of experiments.

- We also show examples of recent developments of dedicated setups for experiments at MID, as well going in the simultaneous multi-detector-use direction.

THE MULTI-ENVIRONMENTAL MULTI-DETECTOR SETUP (MDS_2)

Environment

The MDS_2 at (Eu. XFEL) [1,2] is an important addition to the instrumentation at MID. The integration is currently in progress allowing to use and move an additional detector chamber (MDS) simultaneous the common detector AGIPD [3] in several positions of MID high-quality floor. It has been designed to be compatible with the current XSIS [1,2], but expands the capabilities of the instrument in three areas:

- AGIPD in WAXS geometry: in this case the MDS is situated on the Support Structure Girder Assembly (SSG) (see Figs. 1 and 2) with its own sliding carts and rails and movable using air pads along the beam axis for SAXS applications or direct beam imaging. The AGIPD detector on the XSIS arm can be freely positioned in the usual WAXS geometry.

- AGIPD in SAXS geometry: in this case the MDS will be mounted onto the XSIS arm using the SSG interchangeable rails, behind the AGIPD detector in SAXS position, see Fig. 3.
- LFOV: in this configuration the MDS will also be mounted onto the XSIS Arm behind the AGIPD detector, but in LFOV configuration (see Fig. 4).

For further information about the MDS, see also the paper of A. Schmidt in this conference.

Design

The MDS_2 Setup, designed and partly realized for the aforementioned three Environments consists of the following assemblies (see the **Poster** of this Paper: Nr. **WEPPP010** and Figs. 1-4):

MDS_2 SSG has been designed, simulated by FEA (see Poster WEPPP010, Fig. 1), and manufactured to withstand the expected static and dynamic loads. The motion concept has been successfully tested by moving it on its air pads.

MDS_2 Upstream Adapter Flange (UAF) has been designed, simulated by FEA (see Poster WEPPP010, Fig. 1), and manufactured to withstand foreseen vacuum load. It has been successfully tested sealing the vacuum of the MDS. It is connected to the other MPC_2 assemblies via a central DN250CF rotatable flange and features 4x DN160ISO-K viewports for visual inspection of the the detectors inside.
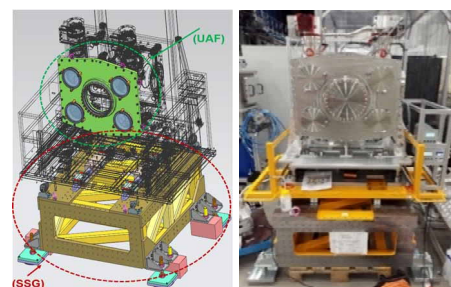
Figure 1: left) design of the Support Structure Girder Assembly moved on airpads (SSG) and Upstream Adapter Flange (UAF), in green. right): manufactured MDS_2 installation during air pads motion and vacuum tests.
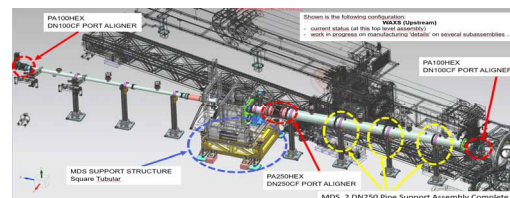
Figure 2: MDS_2 Environment in WAXS Configuration.

MULTIPLE DETECTOR STAGE
AT THE MID INSTRUMENT OF EUROPEAN XFEL

A. Schmidt, G. Ansaldi, A. Bartmann, U. Boesenberg, T. Falk, J. Hallmann,
J. Möller, K. Sukharnikov, A. Madsen
European X-Ray Free-Electron Laser Facility, Schenefeld, Germany

Abstract

The Multiple Detector Stage (MDS) is an ancillary detector setup for the Materials Imaging and Dynamics (MID) instrument at the European X-Ray Free-Electron Laser Facility (EuXFEL). It is developed to improve the current capabilities concerning X-ray detection and make entirely new experiments possible.

A unique feature of the MID instrument is the large flexibility in positioning of the AGIPD detector relative to the sample. This enables a large variety of instrument configurations ranging from small-angle (SAXS) to wide-angle (WAXS) X-ray scattering setups. A recurrent request from the users, which is currently not enabled, is the option of simultaneously recording both wide- and the small angle scattering by using two area detectors.

The aim of developing MDS is to provide this missing capability at MID so that SAXS and WAXS experiments can be performed in parallel. The MDS will not be installed permanently at the instrument but only on request to provide as much flexibility as possible.

In this article, the background and status of the MDS project is described in detail.

INTRODUCTION

The basis for the MDS is a vacuum chamber which can host two small area detectors simultaneously. The detectors inside the vacuum chamber can be arranged differently with the help of two translation stages. The full chamber is assembled on a platform which includes a vertical motion. The platform also carries electronics required for the X-ray detectors, motors, and the vacuum system.

An important feature of MDS is that it can be positioned either on the existing arm of the XSIS instrumentation at MID [1], together with the AGIPD detector [2], or as a standalone device on a separate girder (Figs. 1 and 2). The girder stands on air pads, suitable for the floor in the MID experimental hutch. With this the MDS can be positioned inside the hutch and operated in parallel with the AGIPD detector. Space constrains and cable routing are limiting factors for the positioning. As day-1 configuration the MDS is used only in SAXS geometry, either mounted behind AGIPD on the XSIS arm, or on its own girder if AGIPD is positioned in WAXS.
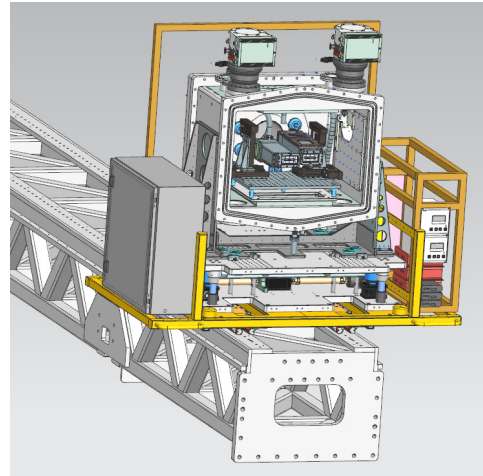
Figure 1: Vacuum chamber with detectors and platform with electronics of the MDS on the arm of the AGIPD at the MID instrument (CAD model).

Figure 2: Assembled mechanics of the MDS on separate girder with air pads.

CONFIGURATIONS

The recurrent request of the user community for simultaneous wide- and small-angle scattering capabilities is the motivation behind the MDS project.

Experiments, where information about the scattering sample is required in-situ on both atomic (nm and sub-nm)

MECHANICAL DESIGN AND INTEGRATION OF THE SXP SCIENTIFIC INSTRUMENT AT THE EUROPEAN XFEL

V. Vardanyan[†], P. Grychtol[1], E. Tikhodeeva[1], D. Doblas-Jimenez[1], J. Ohnesorge[1],

N. Kohlstrunk[1], J. Buck[2,3], S. Thiess[3], M. Dommach[1], D. La Civita[1], M. Vannoni[1],

K. Rossnagel[2,3], G. Schönhense[4], S. Molodtsov[1,5,6], M. Izquierdo[1]

[1]European XFEL, Schenefeld, Germany
[2]Ruprecht Hänsel Laboratory, Deutsches Elektronen-Synchrotron DESY, Hamburg, Germany
[3]Institut für Experimentelle und Angewandte Physik, Christian-Albrechts-Universität Kiel,
Kiel, Germany
[4]Institut für Physik, Johannes Gutenberg Universität Mainz, Mainz, Germany
[5]Institute of Experimental Physics, TU Bergakademie Freiberg, Freiberg, Germany
[6]Center for Efficient High Temperature Processes and Materials Conversion (ZeHS),
TU Bergakademie Freiberg, Freiberg, Germany

Abstract

The European XFEL provides femtosecond X-ray pulses with a MHz repetition rate in an extended photon energy range from 0.3 to 30 keV. Soft X-rays between 0.3 and 3 keV are produced in the SASE3 undulator system, enabling both spectroscopy and coherent diffraction imaging of atoms, molecules, clusters, ions and solids. The high repetition rate opens the possibility to perform femtosecond time-resolved photoelectron spectroscopy (TR-XPES) on solids. This technique allows the simultaneous understanding of the evolution of the electronic, chemical and atomic structure of solids upon an ultrafast excitation. The realization with soft X-rays requires the use of MHz FELs. In this contribution, we present the mechanical design and experimental realization of the SXP instrument.

The main technical developments of the instrument components and the TR-XPES experimental setup are described.

INTRODUCTION

The SXP Scientific Instrument is designed as an open port were users' provided stations can be integrated [1, 2].
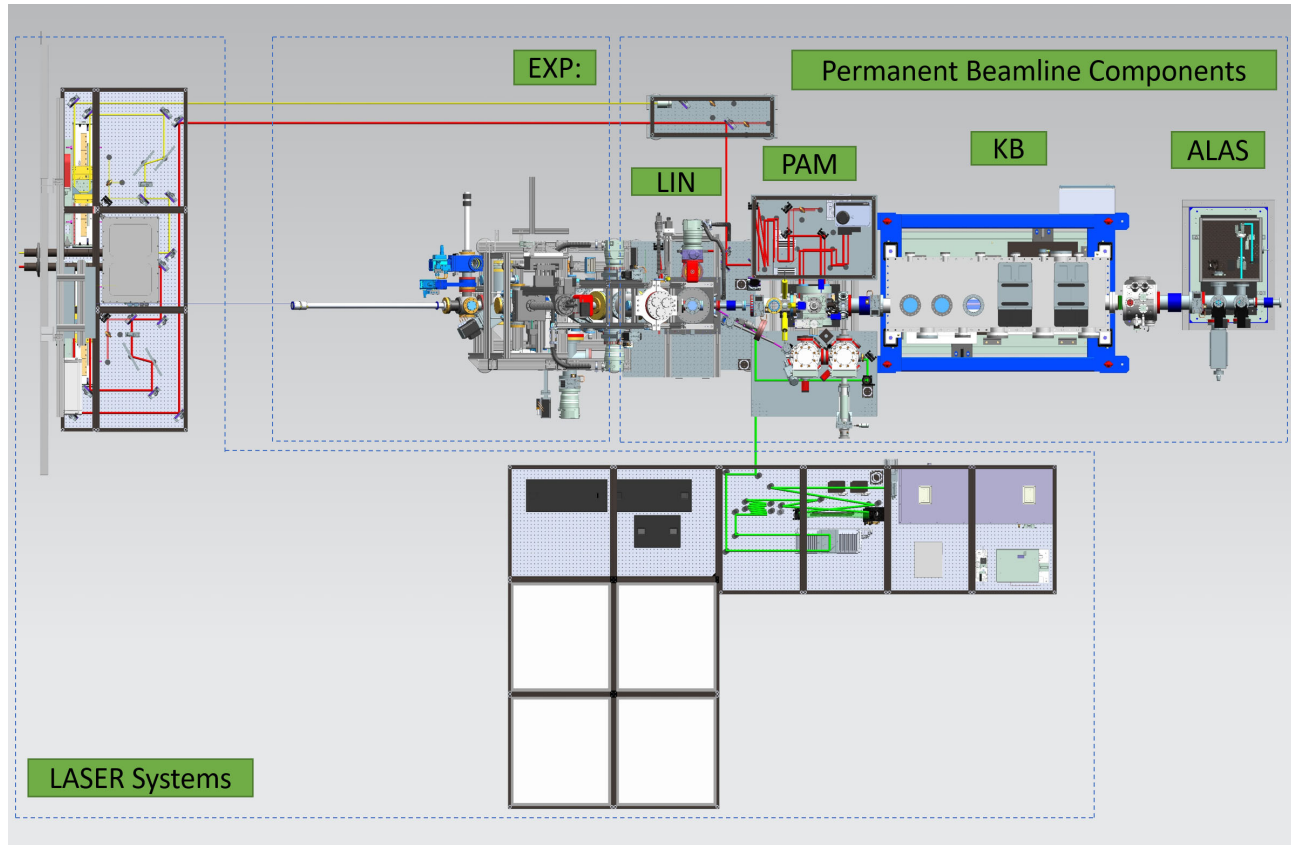
Figure 1: Layout of the SXP Scientific Instrument.

PROGRESS OF FRONT ENDS AT HEPS

Hong Shi[†], Ping Luo, Yaxin Ma, Heying Wang, Yinglei Tan

Institute of High Energy Physics (IHEP), Chinese Academy of Sciences, Beijing, China

Abstract

High Energy Photon Source (HEPS) is a 6 GeV synchrotron radiation facility building in Huairou, with a storage ring perimeter of 1390.6 m and 41 straight sections. In phase I, 15 front ends will be installed, including 14 insertion device front ends and 1 bending magnet front end. These front ends are divided into three types: the Undulator front end, the Wiggler front end, and the BM front end. The U-type front end will receive 766 W/mrad^2 of peak power density and 25 kW of the total power. The design of the W-type front end is based on compatibility with various insertion devices, including undulators and wigglers. In this paper, the designs and the progress of HEPS front ends are presented.

INTRODUCTION

HEPS is a 6 GeV synchrotron radiation facility building in Huairou, storage ring has 48 straight sections, and 41 of them that are 6 m long can extract user beams, as 7 are required for injection and RF straights. Therefore, there is a capacity for 41 Insertion Device (ID) Front Ends and 41 Bending Magnet Front Ends to be installed. Fifteen beamlines are being built in Phase I of HEPS project. One of them is BM beamline, others use ID as light source. These front ends are divided into three types: the Undulator front end (UFE), the Wiggler front end (WFE), and the BM front end (BFE). The UFE will receive 766 W/mrad^2 of peak power density and 25 kW of the total power. The design of the WFE is based on compatibility with various insertion devices, including undulators and wigglers.

GENERAL LAYOUT

Front ends at HEPS are divided into three types: Undulator Front End (UFE), Wiggler Front End (WFE), and Bending Magnet Front End (BFE). There are 12 UFEs, 2 WFEs, and 1 BFE. Due to the implementation of a unified standardized design, the layout of the three types of front ends is similar. The main components of front ends are: (1) Pre-Mask, (2) Low Power Photon Shutter, (3) All-metal Fast Valve, (4) 1st Fixed Mask, (5) XBPM, (6) Photon Shutter, (7) Slits, (8) Filters, (9) Safety Shutter, (10) Ratchet Wall, (11) 2nd Fixed Mask, (12) Be Window. Figure 1 shows the layout of UFE. Table 1 summarizes the front end parameters.

COMPONENTS

Pre-Mask

The isolation valve on the crotch leg of the storage ring is followed by the Pre-Mask which is to reduce dipole radiation to downstream 1st Fixed Mask. The absorber of the Pre-Mask is made of OFHC and cooled by water. The mechanical module of the Pre-Mask is shown in Fig. 2.
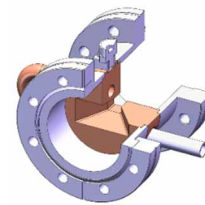
Figure 2: Mechanical module of the Pre-Mask.
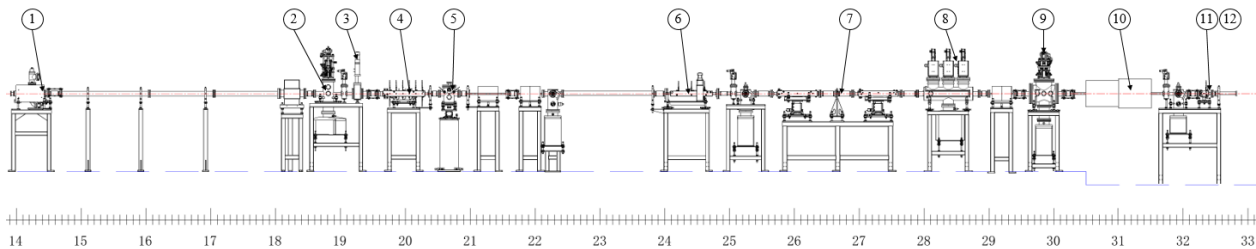
Figure 1: Layout of the UFE.

Table 1: The Parameters of Front Ends at HEPS

	UFE	WFE	BFE
Length [m]	18.9	18.9	22.2
Beam Size at Entrance [mrad]	3.1×1.3	3.1×1.3@ID19, 3.2×1.5@ID42	3.3×1.5
Beam Size at Exit [mrad]	0.2×0.2	1.0×0.9@ID19, 2.0×0.3@ID42	2.0×0.4
Peak Power Density [kW/mrad^2]	766	414	0.18 kW/mrad
Total Power [kW]	25	9	

---

† shihong@ihep.ac.cn

MECHANICAL DESIGN OF XRS AND RIXS MULTI-FUNCTIONAL SPECTROMETER AT THE HIGH ENERGY PHOTON SOURCE

Jiuchang Zhang, Yujun Zhang, Zina Ou, Ruzhen Xu, Zhiying Guo, Shuoxue Jin, Xun Jia, Shanzhi Tang, Weifan Sheng, Wei Xu

Beijing Synchrotron Radiation Facility and High Energy Photon Source, Institute of High Energy Physics (IHEP), Chinese Academy of Sciences, Beijing, China

Abstract

The integration of an X-ray Raman spectroscopy (XRS) spectrometer and a Resonant Inelastic X-ray scattering (RIXS) spectrometer at HEPS is described. The XRS has 6 regular modular groups and 1 high resolution modular group. In total 90 pieces of spherically bent analyzer crystals are mounted in low vacuum chambers with pressure lower than 100 Pa. On the other hand, the RIXS spectrometer possesses one spherically bent analyzer crystal configured in Rowland geometry whose diameter is changeable from 1 m to 2 m. The scattering X-ray photons transport mostly in helium chamber to reduce absorption by air. The RIXS and the high resolution module can be exchanged when needed. Six air feet are set under the granite plate to unload the weight when the heavy spectrometer is aligned. The natural frequency and statics of the main granite rack were analyzed and optimized to maintain high stability for the HEPS-ID33 beamline at the 4th generation source. A type of compact and cost-effective adjustment gadget for the crystals was designed and fabricated. Economic solutions in selection of motors and sensors and other aspects were adopted for building the large spectrometer like this.

INTRODUCTION

The inelastic X-ray scattering spectroscopy in the hard X-ray(>6 keV) regime is an indispensable tool for studying electronic excitations in condensed matter physics. The incident energy can either be in resonance with the binding energy of core-levels, or near the backscattering energy of crystal optics. The former is called resonant inelastic X-ray scattering (RIXS) and the latter is non-resonant inelastic X-ray scattering (NRIXS), also known as X-ray Raman scattering (XRS). To perform RIXS [1] and XRS [2], an energy-analysis spectrometer should be employed. More strictly, the RIXS also requires momentum-analysis, e.g. for studying the dispersion of magnons. Instrumentally, the spectrometers for both techniques are in common, based on the principles of Rowland circle, on which the sample, crystal analyzers and detectors are strictly aligned. Nevertheless, the RIXS spectrometer should sweep over the region of interest in the energy spectrum of scattered energy; while the XRS spectrometer can be static during data acquisition, in so-called "inverse scanning geometry" mode.

The ID33 beamline at High Energy Photon Source is the first beamline dedicated to inelastic X-ray scattering at HEPS. As is designed, the XRS and RIXS techniques will be operated in the same experimental hutch. To be cost-effective, it is reasonable to share the same focusing mirrors and sample stages. In this contribution, we will describe the mechanical design of the spectrometers and the concept for integrated spectrometer for beamlines targeting RIXS and XRS techniques together.

Integration of XRS and RIXS

This spectrometer integrates two functions, an X-ray Raman spectroscopy (XRS) spectrometer and a Resonant Inelastic X-ray scattering (RIXS) spectrometer, on one site, running separately at different time periods as needed.

The XRS has 6 regular modules and 1 high resolution module as planned. Each of them has a low vacuum chamber with pressure lower than 100Pa. A total of 90 pieces of spherical bent analyzer crystals evenly distributed across six chambers. Three modules rotate around sample point in vertical sliding on an arch bridge with a range -35°～163°. Other modules rotate around sample point in horizontal sliding on a base board and are separated by the vertical group on the bridge. The base board has two semicircles with different radii. The larger radius half supports the high-resolution module as well as regular. The XRS is showed in Fig. 1 below.
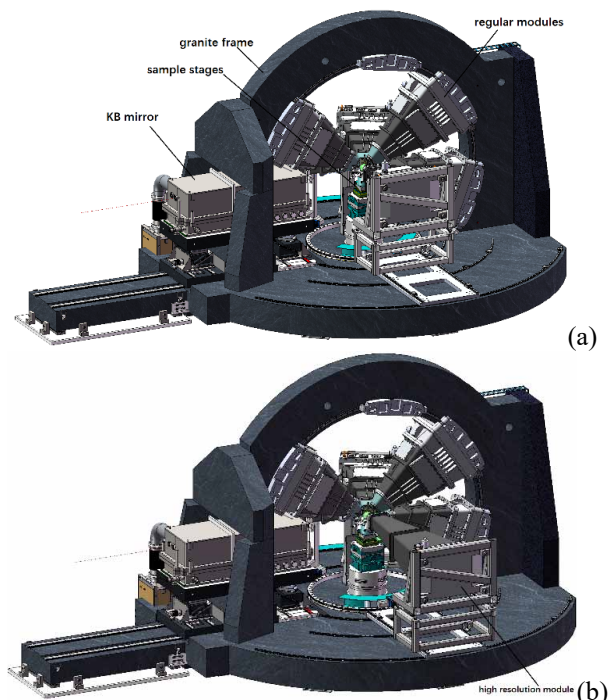
Figure 1: a) XRS with a regular resolution module; b) XRS with a high energy resolution module.

COATING REMOVAL OF SILICON-BASED MIRROR IN SYNCHROTRON RADIATION BY SOLUBLE UNDERLAYER

Q. Y. Hou[†], S. P. Yue, G. C. Chang, B. Ji, M. Li
Institute of High Energy Physics, Chinese Academy of Sciences, Beijing, China

Abstract

Multilayer optics is widely used for the x-ray beam monochromatization, focusing, and collimation in synchrotron light source. However, the multilayer coatings might be damaged by the high heat loads, the poor film adhesion, the high internal stress, or the inadequate vacuum conditions. As a result, it is essential to develop a method to make the optical substrate reusable without compromising its quality. In our published work, we successfully prepared a W/B$_4$C multilayer coating with a 2 nm Cr buffer layer on a small-sized Si wafer. The coating was stripped from the Si substrate by dissolving the Cr buffer layer using an etchant. After the etching process, the sample's roughness was comparable to that of a brand-new substrate. We have since utilized this method to clean the multilayers on the surface of a 20 cm × 5 cm silicon-based mirror for High Energy Photon Source (HEPS). The surface roughness and shape were measured, and they reached the level of a brand-new mirror.

INTRODUCTION

The surface of the mirror is coated with a single or multilayer coating of different materials, so that the mirror has high reflectivity or spectral selectivity. Monocrystalline silicon is an ideal substrate for synchrotron radiation optics due to its low density, high mechanical strength, and good thermal stability. Silicon substrates are typically polished to a roughness of only a few angstroms and have an excellent surface shape before being coated with a single or multilayer coating. After long-term service, the coating will deteriorate or even fail due to contamination, mishandling, instantaneous temperature changes, poor adhesion between the coating and the substrate, and high internal stress of the film. The optics need to be updated after a period of service. Therefore, there is a need to study ways to remove optical films to make the expensive high-precision Si substrates reusable.

There are many ways to remove films, such as liquid etching, vapor etching, laser etching, and soluble underlayers [1]. In the preparation of optics with coating in synchrotron radiation, researchers usually prepare a Cr buffer layer on the substrate, and then prepare various optical thin films to reduce the stress of the film and enhance the adhesion force. Therefore, for synchrotron radiation optics, there is an inherent advantage to using the method of soluble underlayers to remove the film. In our published work in Optics Express [2], we successfully prepared a W/B$_4$C multilayer coating with a 2 nm Cr buffer layer on a small-sized (2 cm × 1 cm) Si wafer. As is shown in Fig. 1, the coating

_____
† Email address: houqy@ihep.ac.cn

was stripped from the Si substrate by dissolving the Cr buffer layer using an etchant. After the etching process, the sample's roughness was comparable to that of a brand-new substrate. The W/B$_4$C multilayer coatings with a Cr buffer layer were recoated on the etched samples, and the results of X-ray reflection (XRR) show that the interface roughness was not damaged by the etching process.
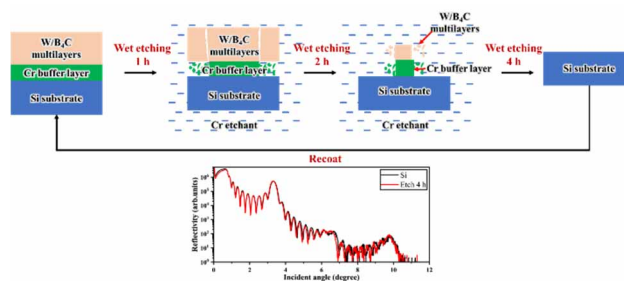
Figure 1: Schematic diagram and XRR results of a refurbished coated silicon wafer with a Cr buffer layer.

The optics used in synchrotron radiation are usually large-size silicon stripes, it is necessary to investigate the applicability of the method of soluble underlayers for refurbishing large-size silicon strips. We have since utilized this method to clean the multilayers on the surface of a 20 cm × 5 cm silicon-based mirror for High Energy Photon Source (HEPS), and the surface roughness and shape at different stages were measured.

EXPERIMENTAL

Films were deposited on the surface of a 20 cm × 5 cm silicon-based mirror by magnetron sputtering at the Platform of Advanced Photon Source Technology R&D (PAPS) in Huairou, Beijing. The deposition parameters of the Cr buffer layer and W/B$_4$C multilayer film and the etching process were the same as those previously applied on small-sized wafers. To compare the effects of the etching process on different coatings, Pt/ B$_4$C multilayer film with a Cr buffer layer were also deposited in different areas of the same silicon strip. A mask was used to allow the film to be deposited in a designated area of the silicon stripe. The deposition parameters of the Cr buffer layer in both coatings are the same. The surface roughness was investigated using a non-contact 3D optical surface profiler. The optical figure was measured by Long Trace Profiler (LTP).

RESULTS AND DISCUSSION

Figure 2 is the image of the coated silicon stripe. The W/B$_4$C multilayer coating was intact, while the surface of the Pt/B$_4$C multilayer coating was crazing, which might be caused by the high internal stress in the film. Figure 3 shows the etching process. Figure 3(a) shows that the

DESIGN OF A HARD X-RAY NANOPROBE BASED ON FZP*

Keliang Liao, Maohua Song, Panyun Li
Jinan Hanjiang Opto-Electronics Technology Company Ltd., Jinan, China
Ping Zhou, Wenqiang Hua[†]
Shanghai Advanced Research Institute, Chinese Academy of Sciences, Shanghai, China
Qili He, Peiping Zhu[†]
Institute of High Energy Physics, Chinese Academy of Sciences, Beijing, China
Liang Luo, Tsinghua University, Beijing, China

Abstract

A high-resolution hard X-ray nanoprobe (HXNP) based on Fresnel Zone plate (FZP) was designed. The HXNP relies on a compact, high stiffness, low heat dissipation and low vibration design philosophy and utilizes FZP as nanofocusing optics. The optical layout and overall mechanical design of the HXNP were introduced. Several important modules, such as probe module, sample module, interferometer module and vacuum chambers were discussed in detail.

INTRODUCTION

In recent years, X-ray nanoprobe operating in the hard X-ray regime has achieved rapid improvements based on the development of a lot of advanced X-ray optics, such as Fresnel zone plate (FZP) [1], multilayer Laue lens (MLL) [2], nanofocuisng K-B mirror. With outstanding quantitative non-destructive three-dimensional (3D) imaging capabilities, the hard X-ray nanoprobe (HXNP) has attracted significant interest across many different disciplines. In previous work, a prototype of HXNP with about 70 nm spacial resolution was constructed and tested at Shanghai Synchrotron Radiation Facility (SSRF) [3]. Driven by the needs of observing and analyzing the internal fabrication defects of the chips with feature size smaller than 28 nm, this paper introduced the recent development of a new HXNP based on FZP.

INSTRUMENT DESIGN

Optical Layout

As depicted in Fig. 1(a), the FZP was chosen as the nanofocusing optics. In order to select the -1st diffraction order of the FZP, a central beamstop (BS) and an order sorting aperture (OSA) were also utilized. The BS, FZP, OSA and their corresponding adjustment components together constituted the probe module. The coherent X-ray from the upstream of the beamline could be focused by the above probe module to form an X-ray nanoprobe, which was also the illumination probe for the ptychographic imaging.

The sample was located near the focus of the FZP. With XY two-dimensional (2D) scan of the sample, a series of diffraction patterns could be acquired by the far-field detector. As the over-sampling condition is satisfied, the 2D electron density distribution of the sample over the fully scanning area could be reconstructed. Moreover, by combining with the CT technology, the 3D sample information could be revealed. An in-line visible light microscope (VLM) was placed behind the sample for coarse adjustment of the FZP and fast calibration of the sample.

According to the functional requirements of the instrument, the freedom of motion required by the HXNP was also shown in Fig. 1(b).
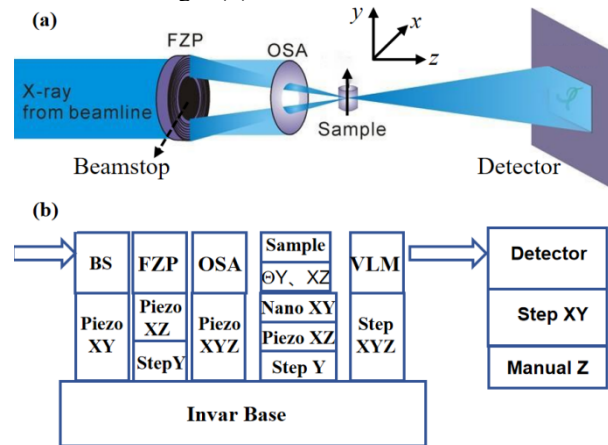
Figure 1: The optical layout of the HXNP.

Overall Scheme of the HXNP

The 3D mechanical design of the HXNP optimized for ptychographic imaging was shown in Fig. 2. The HXNP mainly consists of several important modules, including the welding supporting frame, the marble supporting base, the imaging module, the vacuum chamber and the detector module, which have been marked clearly in Fig. 2. The following was a further introduction.

First, a set of welding frame with high-rigidity was designed as the supporting base for the vacuum chamber. In order to decouple the vibration of the optical vacuum chamber from that of the imaging module, a more stable marble base was utilized for the supporting of the imaging module.

Second, the imaging module is composed of the probe module, the sample module, the interferometer module and

APPLICATION OF CuCrZr IN THE FRONT-END OF SHANGHAI SYNCHROTRON RADIATION FACILITY

Shuai Wu, Jun-Nan Liu, Jin-Wei Wang, Yong-Jun Li

Shanghai Advanced Research Institute, Chinese Academy of Sciences, Shanghai, China

Abstract

At present, Glidcop® Al-15, oxygen-free high thermal conductivity（OFHC）copper and other materials are mainly used in the front-end of the Shanghai Synchrotron Radiation Facility (SSRF). CuCrZr has high heat load capacity, high yield strength and tensile strength, good thermal conductivity, and low vacuum outgassing rate. At present, it has been used as the heat sink material in the heat exchanger of nuclear reactors. Due to the above characteristics, CuCrZr has the basic ability to be an excellent substitute material for synchrotron radiation heat load. However, there are also some problems in the application of CuCrZr materials. The softening temperature is not high enough. Because the brazing process is needed in the processing engineering of the heat load absorber, the brazing process needs more than 500 °C, so the brazing process cannot be used in the processing of the absorber. In this paper, based on the previous process exploration, the front-end absorber is made of CuCrZr material, and the technical scheme of integral processing of flange and absorber is adopted. The thermal stress and deformation of CuCrZr absorber are analyzed by finite element method, and the processing of CuCrZr absorber is completed, and it is applied to the SSRF BL04U&04W canted front-end. After a period of electron beam cleaning, vacuum and temperature tests were carried out under high thermal load power, and the characteristics of the material in practical use were analyzed, which proved that CuCrZr material can be used for the high heat load at SSRF font end.

INTRODUCTION

The main materials used for thermal radiation absorption in the front end of synchrotron radiation light source are Glidcop® Al-15, oxygen-free high thermal conductivity（OFHC）copper and other materials. OFHC is usually used as a material for synchrotron radiation absorbers, especially in the first and second-generation synchrotron radiation light sources. However, the third-generation synchrotron radiation light source uses more insert devices, and the power density of the synchrotron radiation light source is improved. OFHC cannot handle the higher power and higher power density thermal power. Glidcop® Al-15 material has high tensile strength and is used as the material of high heat load absorber. At present, Glidcop® Al-15 material is used as the fixed mask (FM) at the front end of most beamline in SSRF. Glidcop® Al-15 material is an Al_2O_3 dispersed copper oxide material developed by Hoganas, USA. Generally, it is provided in standard size, non-standard size can only be customized, and the cost of customization is so high. CuCrZr material has high heat load capacity, high yield strength and tensile strength,

good thermal conductivity and low vacuum outgassing rate. At present, it has been used as a heat sink material in the heat exchanger of nuclear reactors. Due to the above characteristics, CuCrZr has the basic ability to be an excellent substitute material for synchrotron radiation heat load. The mechanical properties, photo desorption properties and vacuum properties of CuCrZr have been tested [1–3]. It is proved that the material can be used for absorption of synchrotron radiation light source.

However, there are also some problems in the application of CuCrZr materials. The softening temperature is not high enough. Because the brazing process is needed in the processing engineering of the heat load absorber, the brazing process needs more than 500 °C, so the brazing process cannot be used in the processing of the absorber. SSRF is the first third-generation synchrotron radiation light source in China. Most of the absorbers at the front end of the beamline use Glidcop®AL15 material as the main heat absorption material. At present, CuCrZr is a good alternative material to meet the needs of high heat load in the front-end. The main beamlines of SSRF are divided into three types, bending magnet beamline, insert device beamline and Canted beamline. The Canted beamline is generally composed of two insertion beamlines. The general insert device is the undulator, and the angle between the two beamline stations is 6 mrad.

DESIGN OF BL04U&04W FRONT-END

Physical Parameters of Insert Devices

The BL04U and BL04W beamline stations are Canted beamline. BL04U uses a vacuum undulator (IVU20), which is located upstream of the insert device center, and BL04W uses a wiggler, which is located downstream of the insert device center. The angle between the beamlines and the center line of insert device is 4 mrad, and the angle between beamlines is 8 mrad. Incident angle BL04U, BL04W are shown is Table 1.

Table 1: Incident Angle of BL04U&BL04W

Beamline	Insert device	Output angle (mrad²)	Input angle (mrad²)	Power (kW)
BL04W	Wiggler	1.8×0.18	4×1	9.287
BL04U	IVU	0.3×0.15	2×1	2.62

Design of PreM

Generally, the PreM only bears the light source from bending magnet, and the main body adopts OFHC material. However, the horizontal tracing of the BL04U & 04W front-end, the PreM bears the appropriate beam source

A NOVEL FLEXIBLE DESIGN OF THE FaXToR END STATION AT ALBA

L. Ribó[†], A. Patera, N. Gonzalez, L. Nikitina

ALBA Synchrotron Light Source, Cerdanyola del Valles, Spain

A. Mittone, Argonne National Laboratory, Illinois, US

Abstract

FaXToR is one of the beamlines currently in construction and commissioning phase at ALBA, dedicated to fast hard X-ray imaging. It will offer absorption and phase contrast imaging to users. Possible applications of the beamline include 3D static and dynamic inspections in a wide range of applications. FaXToR aims to provide both white and monochromatic beam of maximum 36x14 mm (HxV) at sample position with a photon energy up to 70 keV. The optical layout of the beamline will tune the beam depending on the specific experimental conditions. Among the required optical elements, there is a multilayer monochromator, the cooled slits, the filtering elements, the intensity monitor and the beam absorption elements. The end station will be equipped with a rotary sample stage and a detector system table to accommodate a dual detection thus simultaneously scanning the samples with high spatial and temporal resolutions. On top of it, a motorized auxiliary table dedicated to complex sample environment or future upgrades will translate along the total table length, independently from the two detector system bridges. The design and construction process of the beamline will be presented.

INTRODUCTION

The FaXToR - Fast X-ray Tomography and Radioscopy beamline at ALBA will operate a micro-tomography station working in the hard x-ray regime. The beamline will provide users with sub-second computed tomography capabilities in both absorption and phase-contrast imaging regimes [1]. FaXToR will give service for material science and engineering, health, biology, food science, archaeology, cultural heritage, geology, paleoethology, environment. The capability of performing simultaneous fast 3D acquisition with a multi-resolution approach and the presence of a versatile detector environment will make the beamline unique thus providing the opportunity to users to access a novel data package, which can be reconstructed and analysed directly at the facility site or remotely.

FaXToR LAYOUT

FaXToR source is an in-vacuum multipole wiggler. The front-end angular opening is set to 1×0.4 mrad^2 (H×V). The main optical element of the beamline is a Double Multilayer crystal Monochromator (DMM). No other optics elements besides attenuators, slits and diagnostics are included in the design.

The experimental hutch includes a beam conditioning elements table holding the sample slits, a second CVD diamond window and a fast shutter. It follows a fly tube

equipped with Kapton foil windows to minimize the air absorption at lower x-ray energies and the exhaust ozone in white beam conditions. Such a pipe will be directly link to the tomography stage, located at 36.5 m from the source. Samples of different dimensions up to 5 cm in diameter and 30 cm in height will be located on top of the rotary stage, reaching a maximum speed of 750 rpm depending on the sample weight. The detector table is 4 meters long and is supporting two detection systems: a triple magnification microscope and a low resolution macroscope, together with a dedicated positioning stage and an auxiliary table. All those mentioned elements are able to be displaced along the beam direction. FaXToR foresees two detectors and four cameras to be positioned at a short distance from the sample (for scanning in absorption mode) or at a longer distance (to implement the free space propagation modality in the case of low absorbing matters). Such a configuration is easily interchangeable according to the user experimental requirements. Figure 1 represents the previously mentioned elements.
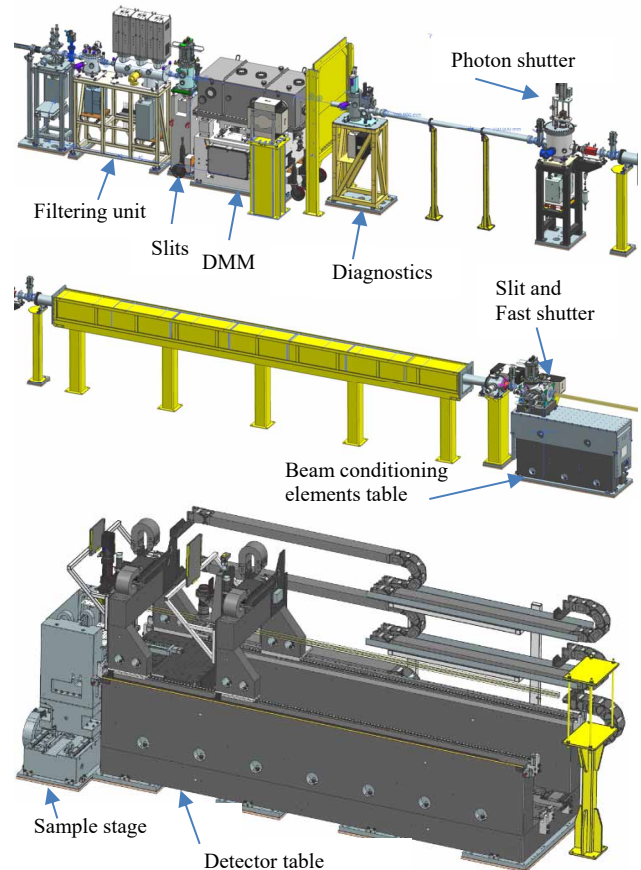
Figure 1: Layout of FaXToR: optics (top), shielded transfer pipe (middle) and end station (Bottom).

† lribo@cells.es

MAX IV – MicroMAX DETECTOR STAGE*

S. Benedictsson[†], M. Al-Najdawi[1], O. Aurelius, G. Felcsuti, J. Lidon-Simon, M. Milas, T. Ursby

MAX IV Laboratory, Lund, Sweden

[1]also at SESAME, Allan, Jordan

Abstract

The MicroMAX beamline at MAX IV Laboratory will employ two detectors to be used independently and move along the beam depending on the diffraction target resolution, starting close to the sample hanging partially over the sample table. The X-ray beam can be deflected by Kirkpatrick-Baez (KB) mirrors in the horizontal and vertical directions or pass undeflected.

The MAX IV Design office designed a detector stage as an in-house project based on the ALBA table skin concept to switch between the two detectors and accurately position the selected detector, either with or without the KB mirrors.

To achieve stability and precision during translations, a large granite block is used, as well as preloaded linear and radial guides, and preloaded ball screws with stepper motors and, in most cases, a gear box. Flexures are used to allow linear motion's pitch and yaw angles. The various motions are layered so that alignment to the beam axis can be done first, and then sample-to-detector distance can be adjusted independently.

A Finite Element Analysis (FEA) were performed to achieve a stable design and measurements of resonance frequencies on the finalized stage were done to verify it.

INTRODUCTION

The MicroMAX beamline at MAX IV Laboratory is designed for macromolecular crystallography and will employ two detectors: the DECTRIS Eiger 2 X CDTe 9M and the Paul Scherrer Institute (PSI) developed Jungfrau 4M. The X-ray beam can be deflected by Kirkpatrick–Baez (KB) mirrors in the horizontal and vertical directions by 6 mrad, or it can pass undeflected. Beam Conditioning Unit (BCU), Diffractometer and the detector stage are designed to align with the beam. The individual detector should have a variable positioning along the beam path, depending on the target resolution of the diffraction data collection.

SPECIFICATION

The stage shall align the active detector to match either the deflected or undeflected beam following in line with the sample. Translations needs to be performed at a fast enough speed to avoid unnecessary waiting times, this is mainly important for the longitudinal translation that is long and can vary within one experimental setup. The detector stage is designed to accomplish the specifications (Table 1). All motion needs to be motorized. The table shall allow for a passthrough vacuum pipe to be manually placed between the detectors to allow the beam to pass to a second experimental hutch.

Table 1: Specifications

	Vertical	Horizontal	Longitudinal	Pitch	Yaw
Range	10 mm	382.5 mm	940 mm	±0.5°	±0.5°
Resolution	10 µm	10 µm	100 µm	10 µrad	10 µrad
Repeatability	50 µm	50 µm	100 µm	50 µrad	50 µrad
Resonance frequency f_0	>55 Hz				
RMS displacement	<7.5 µm (<10 % of pixel size)				

DESIGN

Inspired by the ALBA table skin concept design [1] a stage was designed around a grouted granite block. Two opposing steel plates are attached with linear guides for vertical translation. On the top part of the plates a thin neck is milled to create a flexure, allowing pitch by moving the two sides by different amounts. The sides are connected by a horizontal plate stiffened by two longitudinal side plates and a centre beam, together forming the vertical/pitch table. On top the other translations are worked out step by step, first horizontal translation for sideways adjustment and to switch between detectors and passthrough pipe. The horizontal is followed by yaw, using radial linear guides motorized by a linear translation translated into an angle by a flexure and then compensating the offset rotation centre with the horizontal axis (Fig. 1). Finally, the two longitudinal stages move each detector independently (Fig. 2) to find the correct focus and keep the unused detector out of the way in the centre of the table where it has less impact on the resonance frequencies. All translations are done with preloaded linear and radial guides and preloaded ball screws with stepper motors and all except for the motion of the detector along the X-ray beam also use a gear box to increase the resolution.

PHOTON SLITS PROTOTYPE FOR HIGH BEAM POWER USING ROTATIONAL MOTIONS

X. Liu [†], W. Cheng, A. Walters, L. Hudson, H. Patel, Diamond Light Source, Didcot, UK

Abstract

A new slits prototype utilising a rotatable oxygen-free high thermal conductivity (OFHC) copper block to absorb high heat load is developed for the Diamond-II upgrade. The slits will be used at front end of Diamond I13 X-ray Imaging and Coherence beamline which has two canted beamline branches. Required by the beamline optics, the front end slits function as virtual sources for the 250 meters long beamline. Working for the dual beam geometry, these specialised slits can vary the size of one x-ray beam with rotational motions while allowing the second beam to pass through unaffected. The rotational operations of the slits are achieved by an innovative commercial flex pivot and a unique in-house designed pivoting flexure.

INTRODUCTION

This paper describes the prototype design of a new slits utilising a rotatable OFHC copper block to absorb high heat load. The prototype is part of Diamond-II upgrade pre-development for three front end applications. The design case picked is to prototype for Diamond I13 X-ray Imaging beamline.

The I13 X-ray Imaging and Coherence beamline has two canted beamline branches. The front end slits function as virtual sources which is required by the I13 beamline optics in the long insertion straight of I13. It is essential to place the opposite beam defining blades at close proximity to collimate the x-ray beam. Diamond traditional white beam slits are not suitable for this function. In the traditional layout, the virtual focal point required by the beamline optics cannot be formed because the opposite slit blades are placed at a great distance due to one 'L' shaped blade being fixed onto an upstream copper assembly and another 'L' shaped blade being fixed onto a downstream copper assembly.

The newly developed slits prototype utilises a rotatable copper block assembly with the integration of a pair of 'L' shaped slits blades in one brazed copper block. The pair of 'L' shaped blades are placed at close proximity which is the perfect solution for creating the needed virtual source at the front end. The design concept is inspired by Schmidt's design of "Variable aperture photon mask (slits) for canted undulator beamlines at the Advanced Photon Source" [1]. Working for the dual beam geometry, these specialised slits can vary the size of one x-ray beam with rotational motions while allowing the second beam to pass through unaffected. The rotational operations of the slits are achieved by innovatively designed pivoting flexure and commercial flex pivots. Since the slits are used in the front end, the rotatable slits block is required to handle high beam power

from the undulator insertion device of I13 beamline. To consider other Diamond-II applications, we developed the slits to be capable of carrying out raster scanning.

DESIGN
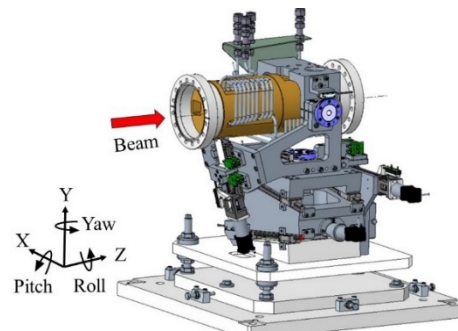
Figure 1: Slit assembly and the coordinate systems.

The overview of the slit assembly is shown in Fig. 1. The slits are installed at 18.4 meters from the source. The dual beam geometry is shown in Fig. 2. At the location, the photon beam size of the I13 Imaging branch is 4.1 × 4.1 mm, and the beam size is 3.7 × 3.7 mm for the Coherence branch. The separation distance of the two canted photon beams is 64.7 mm. The slits vary the size of Imaging beam while allowing the Coherence beam to pass through unaffected. The slit is also required to scan the beam. When carrying out the scanning, the slits are opened a set amount and then driven across the beam in a vertical or horizontal motion.
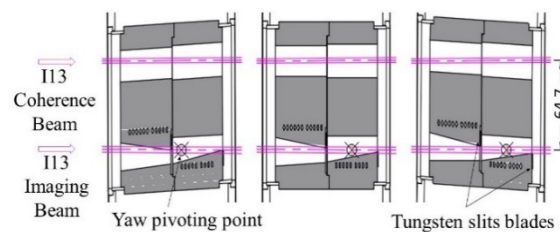
Figure 2: Anamorphic view of sections in X-Z plane showing yaw rotations of the slits. Left: closed position; Middle: neutral position; Right: open position.

Slits Rotary Motions

In normal operation mode, slits are only required for varying opening apertures. Using the concept from Schmidt [1], the variation of slit aperture is achieved by rotating the slit block horizontally (yaw rotation) and vertically (pitch rotation). Two unique pitch and yaw rotary stages (Figs. 3 and 4) are designed to control the slit width in the vertical and horizontal direction. The rotary stages are driven by a linear drive with the rotary motion produced by a flexure link between linear and rotary motion. The

† xia.liu@diamond.ac.uk

ALBA EXPERIMENTAL SET UP FOR THE EVALUATION OF THERMAL CONTACT CONDUCTANCE UNDER CRYOGENIC AND VACUUM CONDITIONS

O. Traver[†], J.J. Casas, C. Colldelram, J. L. Frieiro, B. Molas, M. Quispe, M. Sanchez
ALBA-CELLS Synchrotron, Cerdanyola del Vallès,

Abstract

The Thermal Contact Conductance (TCC) between two surfaces plays a very important role in the design of components in particle accelerators. The TCC depends on many variables such as surface finish, type of material, pressure, temperature, etc. As a general rule, the TCC comes from experimental results reported in the specialized literature. However, it is not always possible to find this information, especially if components are designed to operate in cryogenic and vacuum conditions, for this reason, assumptions are made that render results with high uncertainty. In this context, ALBA has designed an experimental set up to carry out axial heat flow steady state experiments for the evaluation of TCC under vacuum and cryogenic conditions. The minimum pressure achievable in the set up will be 1e-5 mbar while the temperature may vary between 80 and 300 K. The results will provide inputs to further optimize ALBA designs, including ALBA II, our ongoing fourth-generation synchrotron upgrade project. This paper describes the experimental setup, the thermal and mechanical design considerations and experimental validation tests.

INTRODUCTION

Real engineering surfaces exhibit a complex three-dimensional landscape, characterized by peaks and valleys of diverse sizes and shapes. A "flat surface" contains microscopic irregularities which compose its roughness and macroscopic irregularities such as waviness and deviation from flatness [1, 2, 3]. Consequently, when two surfaces are pressed together, they touch each other at only limited discrete points separated by large gaps. Thus, the *real* contact area is found to be much smaller than the *geometrical* contact area (1-2% for metallic contact) [2]. The remaining space between the contact points can be filled with an interstitial medium, such as air or a vacuum.

Thermal contact conductance (hj), also known by the acronym TCC, can happen through conductance along three primary pathways: the real contact spots (h_c), conduction through the interstitial fluid (h_g) and thermal radiation (h_r).

$$h_j = h_c + h_g + h_r .$$ (1)

Conceptually, hj is defined as the ratio of the heat power (Q) per unit area (A) flowing across the interface and the temperature drop (ΔT) at the interface.

$$h_j = \frac{Q/A}{\Delta T} .$$ (2)

† otraver@cells.es

If the heat transfer takes place in vacuum conditions, the conduction through the interstitial fluid can be neglected. Radiative heat transfer can also be disregarded in the current context, as it becomes significant only above 400 ºC [3].

$$h_j \approx h_c = \frac{\frac{Q}{A}}{\Delta T} .$$ (3)

According to [4], hj increases proportionally to the applied load at the interface since the real contact area is proportional to the load. When the load increases the average contact spot size remains relatively stable. However, the quantity of contact spots changes.

The hj dependence on temperature varies over different temperature ranges. From 30 K to 200 K, hj approaches a linear dependence with T, above this range it tends to a temperature-independent conductance value.

To determine hj, experimental research is fundamental, as it can provide realistic results compare to theoretical studies. Obtaining information on hj under cryogenic and vacuum conditions is often challenging. In this context, at ALBA an experimental setup has been built to evaluate hj values in these special conditions. This work describes relevant aspects of its design, its operating principle and the first validation tests.

EXPERIMENTAL SET-UP

Description

The experimental setup (Figs. 1 and 2). consists of a heating block (1), a cold finger (2), an insulating block (3) an insulating ring (4), a load cell (5), a mechanical loading system (6), a vacuum system (7) and two specimens (8).

The heating block is a cylindrical copper block of Ø25 mm with its cylindrical surface covered by two 45 W kapton heaters foils, which are powered by a current source. The cold finger is a cylindrical copper block of Ø25 mm x 150 mm with a hole of Ø8 mm x 110 mm where liquid nitrogen circulates. In order to avoid losses and ensure one dimensional heat flow, an insulating block made of PEEK has been provided at the top of the heating block and an insulating ring has been provided at the bottom of the cold finger. Between the heating block and the cold finger, the two specimens, with a cylindrical shape (Ø25 mm x 48 mm high) and which can be fabricated from any material of interest for the experiment are brought in contact. One of the specimens is heated, the other one is cooled, allowing the generation of a downward axial heating flow. The experimental set-up aims at measuring the TCC

DESIGN AND FLUID DYNAMICS STUDY OF A RECOVERABLE HELIUM SAMPLE ENVIRONMENT SYSTEM FOR OPTIMAL DATA QUALITY IN THE NEW MICROFOCUS MX BEAMLINE AT THE ALBA SYNCHROTRON LIGHT SOURCE

M. Quispe[†], J.J. Casas, C. Colldelram, D. Garriga, N. González, J. Juanhuix, J. Nicolàs, Y. Nikitin

ALBA-CELLS, Cerdanyola del Vallès, Spain

M. Rabasa, ESEIAAT, Terrassa, Spain

Abstract

XAIRA is the new microfocus MX beamline under construction at the ALBA Synchrotron Light Source. For its experiments, data quality will be optimized by enclosing all the end station elements, including the diffractometer, in a helium chamber, so that the background due to air scattering is minimized and the beam is not attenuated in the low photon energy range, down to 4 keV. This novel type of chamber comes with new challenges from the point of view of stability control and operation in low pressure conditions while enabling the recovery of the consumed helium at the ALBA Helium Liquefaction Plant. Besides, the circuit includes a dedicated branch to recirculate the helium used by the goniometer bearing at the diffractometer. This paper describes the fluid dynamic conceptual design of the Helium chamber and its gas circuit, as well as numerical results based on one-dimensional studies and Computational Fluid Dynamics (CFD).

INTRODUCTION

The new microfocus beamline BL06-XAIRA at ALBA, in commissioning phase, will have a chamber enclosing the goniometer that holds the sample, the detector, a cryostream, and other sample environment elements. The setup allows the experiments to be performed either in air or in helium atmosphere, and both at room temperature or under cryogenic conditions. The helium atmosphere not only reduces the background noise, thus increasing data quality for the whole energy range, but also prevents flux loss at low energies, providing the optimal conditions for anomalous phasing and elemental analysis experiments [1].

From the point of view of fluid dynamic engineering, a description of the design of this special chamber, as well as its adjacent gas circuit, is presented in the following sections. This design includes the possibility to recycle the helium, directing it to the ALBA Helium Liquefaction Plant.

PIPING AND INSTRUMENTATION DIAGRAM (PID)

Figure 1 shows the PID of the gas distribution. The design has been based on the requirement to operate in three modes: sample in helium atmosphere at a nominal cryogenic temperature of 95 K (mode 1), sample in helium

atmosphere at room temperature (23 ºC, mode 2); and sample surrounded by nitrogen gas at a nominal cryogenic temperature of 100 K (mode 3) [2]. For modes 1 and 2, a helium purity of 95% is required (experimental criterion).

The elements of the circuit are distributed inside and outside the experimental hutch (marked in green in Fig. 1) and regulate the different beamline components that blow helium into the helium chamber (bold black line). In the Fig. 1 the circuit for helium gas is highlighted with black lines (mode 1), while the distribution lines for air and nitrogen gas are marked in grey.

Under steady state regime, the balance of helium gas inside the chamber is conserved according to the following input and output conditions: (1) Gas input to the chamber from the detector. This component, has to be connected to a dry air (or nitrogen, or helium) source to avoid humidity and condensation damage. The gas first enters the detector (0.167 l/min, 296 K and 2.5 bar ABS), then is distributed inside the chamber; (2) Injection of pure helium gas from the cryostream to the sample, under nominal conditions 2.74 l/min, 95 K and 1.2 bar ABS; (3) Helium gas input from the goniometer. The rotation movement of this component requires helium gas under the conditions 5.61 l/min, 296 K and 5.5 bar ABS. During its operation, the goniometer "loses" approximately 5% of gas, which becomes a gas supply to the chamber; and (4) A single output is fixed, represented in the PID with an output arrow on the left side of the chamber.

For the circulation of helium gas, two compressors are required. One of them is dedicated exclusively to supplying helium to the goniometer under its working conditions; the other compressor, located on the exit branch of the chamber, takes the exit gas and then distributes the helium in three branches: one towards the detector, another towards the aspiration of the other compressor (to recover the 5% of "lost" gas inside of the chamber), and the last one towards the Helium Liquefaction Plant, for recovery. Under ideal fluid balance conditions, the recovery line should recover the same amount of gas injected by the cryostream into the chamber.

The system has 12 bottles of pure helium gas, each of 50 litres at 200 bars of pressure. This assembly will feed gas directly to the cryostream during experimentation. An individual bottle of helium gas, connected to the chamber (He pressure control unit), has been added to inject helium in case of gas losses during the operation.

DATA PREPROCESSING METHOD OF HIGH-FREQUENCY SAMPLING XAFS SPECTRA COLLECTED IN A NOVEL COMBINED SAXS/XRD/XAFS TECHNIQUE*

Yunpeng Liu [1], [†], Zhongjun Chen [1], Guang Mo [1], Zhonghua Wu [1], [2]

[1] Beijing Synchrotron Radiation Facility, Institute of High Energy Physics,
Chinese Academy of Sciences, Beijing 100049, China

[2] University of Chinese Academy of Sciences, Beijing 100049, China

Abstract

High-frequency (HF) sampling X-ray absorption fine structure (XAFS) spectra with a time-resolution of ~8 s were collected in our newly developed synchrotron radiation small-angle X-ray scattering (SAXS)/X-ray diffraction (XRD)/XAFS combined technique. Restoring the HF XAFS spectrum which contains hundreds of thousands to millions of data points to a normal XAFS spectrum consisting of hundreds of data points is a critical step for the subsequent neighbor structure analysis. Herein, the data preprocessing method and procedure of HF XAFS spectra were proposed according to the absorption edge of the standard sample and the rotation angular velocity of the monochromator. This work is expected to facilitate the potential applications of HF XAFS spectra in a time-resolved SAXS/XRD/XAFS experiment.

INTRODUCTION

To achieve the goals of controllable synthesis and performance optimization [1, 2], the knowledge of the structural evolution of materials in the processes of synthesis or service is a prerequisite. During the material synthesis and some dynamic changes, the synthesized material structures often be hierarchical. Tracking the entire material synthesis process and capturing useful information on all possible metastable precursors and intermediates will facilitate the controllable synthesis of materials. However, it is difficult for a single technique to meet all the detection requirements of hierarchical structure. It is very necessary to develop in-situ combined techniques to obtain simultaneously time-resolved hierarchical structural information on a dynamic reaction process.

Recently, we developed a novel SAXS/XRD/XAFS combined setup [3], where an area detector, a curved detector, and a point detector are, respectively, used for the detections of SAXS, XRD, and XAFS signals. This kind of combining technique can be used to track the changes [4] ranging from the molecular (local coordination state) to nanoscale (primary units) to microscale (crystallite formation) dimension during the crystallization process of samples. It should be noted here that, an ion chamber (IC) is often used detector to collect XAFS signals due to its good linear response to the X-ray intensity. However, for this compact combined setup, it is a failure to collect the

XAFS spectra using IC as a result of its large volume. Intelligently, silicon PIN photodiodes [5] (SPPD) and diamond detectors[6] (DD) were used to substitute for IC due to their small size and good performance. Furthermore, to meet the time-resolved dynamic detection requirements, a high frequency (HF) sampling transmission scheme based on the high-speed counting cards (HSCC) was adopted to collect quick XAFS (QXAFS). However, the HF sampling XAFS data are very different from the conventional XAFS data in terms of abscissa and data points. Thus, the abscissa conversion and data reduction must be properly performed for the raw HF sampling scheme XAFS data.

Herein, the data preprocessing method of HF XAFS spectra will be proposed in detail according to the absorption edge of the standard sample and the rotation angular velocity of the monochromator. The data batch preprocessing program based on MATLAB code will also be introduced.

COLLECTION AND PREPROCESSING OF HF SAMPLING XAFS DATA

Data Collection

All the data was collected at beamline 1W2B of Beijing Synchrotron Radiation Facility (BSRF). The X-ray photon flux is about 1.0×10^{12} photons/s at Cu K-edge (8979 eV) with an X-ray spot size of about 0.8 (H) × 0.5 (V) mm^2 at the sample position. In HF sampling XAFS transmission mode, DD is used to monitor the X-ray intensity (I_0) in front of the sample, and DD or SPPD is used to monitor the X-ray intensity (I) behind the sample. For a sample with a thickness of d, the absorption coefficient (μ) can be written as:

$$\mu(E) = \ln(I_0/I)/d \tag{1}$$

The high-speed counting module [5] (NI 9223) instead of the 974 counter was used for the Cu K-edge XAFS measurements of Cu foil at a sampling frequency of 10 kHz. Here, the sampling frequency represents the number of times that an experimental signal (here it is the X-ray intensity) was repeatedly read out in one second. A higher sampling rate can greatly improve data quality by raising statistics. Figure 1 clearly shows the raw data of an HF sampling XAFS spectrum for standard Cu foil at the sampling frequency of 10 kHz. Figures 1a and 1b clearly show the dependences of I_0, I, and μ on counting (0~80,000). Based on the data acquisition frequency, the abscissa can also be expressed in terms of time t:

EXPERIMENTAL METHODS BASED ON GRAZING INCIDENCE AT THE 1W1A BEAMLINE OF THE BEIJING SYNCHROTRON RADIATION FACILITY AND ITS APPLICATION IN CHARACTERIZING THE CONDENSED STATE STRUCTURE OF CONJUGATED POLYMERS

Yu Chen[1]*, Hongxiang Li[2†], Pei Cheng[2‡], Yanchun Han[3§]

[1] Institute of High Energy Physics, Chinese Academy of Sciences, Beijing, China
[2] School of Polymer Science and Engineering, Sichuan University, Sichuan Province, China
[3] Changchun Institute of Applied Chemistry, Chinese Academy of Sciences, Jilin Province, China

Abstract

The Beijing Synchrotron Radiation Facility (BSRF) 1W1A Diffuse X-Ray Scattering Station can conduct grazing incidence wide/small angle scattering (GIWAXS/GISAXS) experimental method characterization, which is an important method for characterizing the condensed structure of conjugated polymers. To this end, we have upgraded and optimized the experimental method of grazing incidence. After updating the EIGER 1M area detector and reducing stray light interference, the exposure time of a single sample was reduced from 300 seconds to 30 seconds. And we have developed a remote rapid sample change platform, which can achieve remote testing operations outside of the hutch, greatly reducing testing time, and enabling users to remotely conduct online testing operations in their own labs. Subsequently, we further established in-situ steam treatment, in-situ thermal annealing, in-situ drip coating, in-situ spin coating, in-situ scraping coating, and GISAXS testing platforms, enriching the beamline's grazing incidence methods. In the future, relying on the 1W1A diffuse X-ray scattering station, more in-depth research can be conducted on the crystallization behavior, film formation process, crystallization and phase separation size, and film structure of solution processed conjugated polymers.

INTRODUCTION

The Wiggler insert 1W1 in the storage ring I area of the Beijing Synchrotron Radiation Facility has led out two stations: 1W1A diffuse scattering and 1W1B-XAFS experimental stations (Fig. 1(a)). The 1W1A station utilizes the dual focusing monochromatic X-ray provided by the beam line to conduct structural research on crystals and thin film materials. This station can be operated in both dedicated and parasitic modes. The main optical components of the 1W1A beam line include an asymmetric cut crystal monochromator and a vertical bent reflector. The asymmetric cut crystal monochromator is 19 meters away from the light source, achieve monochromatization and horizontal focusing of the beam, and splitting with the 1W1B beam. The vertical bent reflector is located 1.6 meters behind the monochromator, used to realize vertical focusing of the beam

and effectively suppress high-order harmonics. This beamline can conduct experiments such as high-resolution diffraction (XRD), low angle reflection (XRR), grazing incidence diffraction (GIXRD), GIWAXS, and GISAXS.
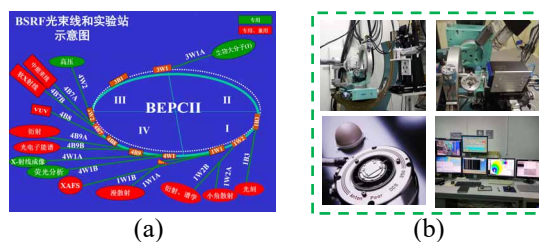
Figure 1: (a) Schematic diagram of BSRF Beamline Station; (b) Multiple experimental platforms of the 1W1A.

Recently, we optimized the detectors, flight channels, attenuators, beamstop, etc., and reduced the exposure time of a single sample from 300 seconds to about 30 seconds. And we have developed a remote rapid sample change platform for grazing incidence experiments. Subsequently, we further established a series of in-situ steam treatment, in-situ thermal annealing, in-situ drip coating, in-situ spin coating, in-situ scraping coating, and GISAXS testing platforms, enriching the grazing incidence experimental methods (Fig. 1(b)).

REMOTE OPERATION GRAZING INCIDENCE EXPERIMENTAL PLATFORM

This experimental platform is equipped with a fast sample change device, which saves time for calibration of the sample in grazing incidence mode. Paired with E63 intelligent lightweight 6-degree of freedom modular collaborative robot, it can achieve continuous sampling without entering the hutch, and can achieve continuous testing of hundreds of samples (Fig. 2). Utilization of remote control software, users can realize remote operation of the experiment, greatly reducing the testing time for conventional thin film samples and simplifying the testing steps. (http://202.122.38.138/docs/1w1aremote.mp4).

Figure 2: Remote operation GIWAXS platform.

* chen_yu@ihep.ac.cn, † lihongxiang@scu.edu.cn,
‡ chengpei@scu.edu.cn, § ychan@ciac.ac.cn

THE JOY OF VIBRATION MITIGATION

J. H. Kelly, D. Crivelli, S. Beamish, S.G. Alcock
Diamond Light Source, Harwell Science & Innovation Campus, UK

Abstract

As part of the Diamond-II facility upgrade, a new Optics Metrology Lab has been built at Diamond Light Source. This replaced the old lab which will be demolished to make space for a "flagship" beamline. However, the location for the new lab has intermittent 100 times higher floor velocity in the range 50-150 Hz compared to the original. This paper describes the engineering developments to successfully mitigate vibrations within the new lab. The raft of measures includes: 'skyhook' damping (i.e. active damping using geophone velocity feedback) and novel 2-stage passive vibration isolation. New vibration isolation & damping systems have been installed and will enable ultra-sensitive metrology tests to continue in the new lab.

INTRODUCTION

Diamond Light Source is the UK's national synchrotron light facility. Each beamline uses a range of optics to focus and monochromate the ultra-intense X-ray beams created by the synchrotron. Prior to beamline installation, all X-ray optics are assembled and characterised in the Optics Metrology Laboratory (OML1). This cleanroom lab contains a suite of state-of-the-art metrology instruments to measure X-ray optics with sub-nanometre precision. These sensitive instruments require a mechanically and thermally stable environment. After > 15 years of operation, OML1 is to be demolished to make space for a new flagship beamline. To continue optical metrology operations and prepare for the improved-quality X-ray optical systems required for Diamond-II beamlines, a new lab (OML2) has been built. However, due to space limitations within the Experimental Hall, the location for OML2 has an intermittent 100 times higher floor velocity in the range 50-150 Hz compared the original. Such vibrations are caused by nearby plant, including a large, motorised dewar store. The engineers were given the task of finding isolation solutions to mitigate these increased levels of disturbances and provide an ultra-stable environment for the optical metrology instruments. Commercial passive vibration isolated tables only provide transmission data over a limited frequency range (e.g., Newport™ S-2000A from 0.8 to 30 Hz) and the supplied plots look like simple 1D lump mass models. Active damping options were also investigated, but they were not considered to be cost-effective, or provide the required damping bandwidth. Therefore, in-house damping solutions were designed and built.

PASSIVE VIBRATION ISOLATION

To replace existing air-isolation optical benches, a concept using spring isolators (from Farrat) was developed. The design re-used unwanted optical breadboards, which were supported via an intermediate granite block with two isolation stages i.e. floor to granite, and granite to table. This provided an attachment method that did not over-constrain the breadboard as well as providing a steeper isolation slope with frequency, as shown in Fig. 1. The performance of the vibration isolation system is significantly different from a simple 1D lump mass model since the higher-order vibration modes cross-couple. Rotation modes are measured as translations with amplitudes that depend upon the modal lever [1]. A 3D modal analysis of the proposed design was performed using ANSYS software to both visualise the mode shapes and to generate a reduced order model (ROM) for input into Simulink®. The sensor location was close to, but not exactly at, the centre of the table, as with the measured data. This prevents symmetry from making modes unobservable. The simulated vibration transfer function depends upon the point of measurement and the variation of spring rate across isolators. A random distribution of a realistic ± 10% spring rate causes higher-order modes to become more significant.
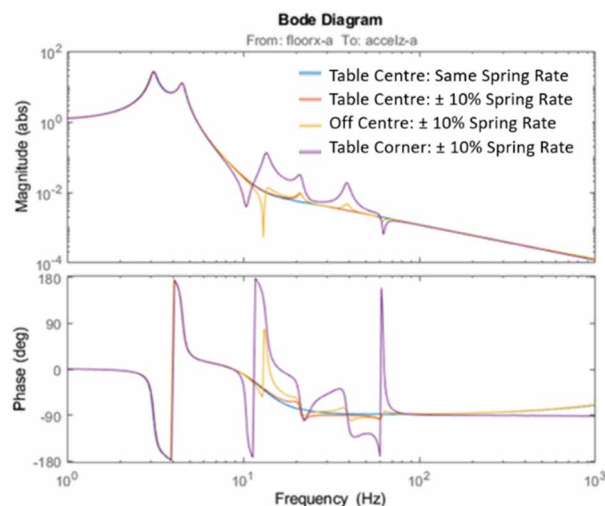
Figure 1: Simulated floor to tabletop transfer functions showing the effect of varying the spring stiffness and sensor location.

Passive Vibration Test Results

A measured transmissibility plot of the installed table, to compare with Fig. 1, is given in Fig. 2. The very low coherence is caused by the acoustic disturbance which is comparable to the floor vibration. Significant energy is passing through the air which is not measured by the floor accelerometer corrupting the transmissibility ratio. That said the measured data does show the simulated 2 resonant peaks below 10 Hz which amplify the floor acceleration and vibration isolation above 6-8 Hz.

DEVELOPMENT OF HIGH POWER DENSITY PHOTON ABSORBER FOR SUPER-B SECTIONS IN SSRF*

Qisheng Tang[†, 1], Changyu Jin[2], Qinglei Zhang[1], Yeliang Zhao[1], Yiyong Liu[1]
[1]Shanghai Advanced Research Institute, CAS, Shanghai, China
[2]SKY Technology Development Co., Ltd., CAS, Shenyang, China

Abstract

There are two symmetrical standard bend (standard-B) sections been upgraded to super-B sections in the storage of Shanghai Synchrotron Radiation Facility (SSRF). Photon absorbers made up of CuCrZr were used for absorbing radiation with very high power density in the super-B sections. Meanwhile, CuCrZr absorbers were also used as beam chamber and pump port for the lattice of super-B section is very compacted. The absorbing surface was designed as serrate structure in order to diminish the power density. CuCrZr was cold-forged before machining to enhance its strength, thermal conductivity and hardness. Friction welding is adopted for absorber fabrication to avoid material properties deterioration. Rectangle flanges of absorbers were designed as step rather than knifer for vacuum seal. These high power density photon absorbers have been installed on the storage ring, both pressure and temperature being in accordance with design anticipation under the condition of 240 mA beam.

INTRODUCTION

The purpose of upgrading 2 symmetric standard-B sections to super-B sections is to provide hard X-ray with the energy of 18.7 keV for users in SSRF [1], as shown in Fig. 1. Moreover, short straight sections in which insert devices can be installed to provide photon for beamline laboratories were added in super-B sections of which the total length is same with that of standard-B sections. Compare to standard-B, much stronger magnetic field can be generated by super-B, the power of synchrotron radiation being much higher. Furthermore, the majority of synchrotron radiation has to be absorbed in much compact space.
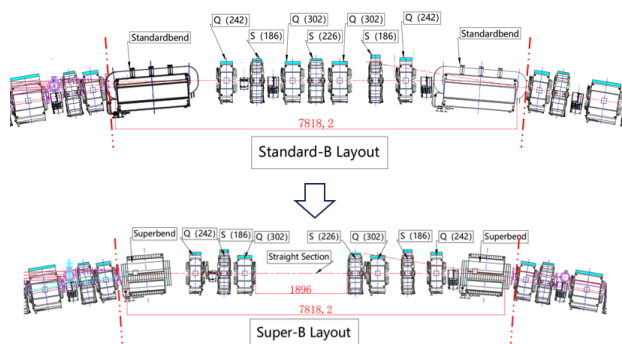
Figure 1: Standard-B section upgrade to super-B section in SSRF.

The density of photon power is much higher because of limited absorbing space and much stronger magnetic field. CuCrZr photon absorbers were developed to absorb photon with high power density in super-B sections. Friction welding was adopted to fabricate these absorbers with complex structure. The comparison of main specification between standard-B and super-B is shown in Table 1.

Table 1: Main Specification of Standard-B and Super-B

	Standard-B	**Super-B**
Arc length (mm)	1440	832.5
Magnetic field (T)	1.27	2.29
Magnet gap (mm)	50	30
Bending angle (°)	9	9
Radiation Power (kW)@300mA	10.9	18.8

ABSORBERS DISTRIBUTION AND MATERIAL

There are just five absorbers distributed in each super-B section and downstream because of very limited available installing space. The lattice of super bend magnet 2 downstream haven't been changed. However, original absorbers have been replaced by two new absorbers (absorber 4 and absorber 5) to absorb high power density radiation from super bend magnet 2, vacuum chambers also being redesigned, as shown in Fig. 2.
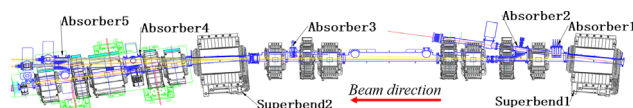
Figure 2: Absorbers distribution on super-B section.

All absorbers were installed at clearance of each couple of magnets. Ion pumps were installed next to these absorbers to enhance pumping efficiency. The maximum heat flux density on absorber 2 is yet up to 43 W/mm^2 @300 mA after structure optimization, as shown in Table 2.

Oxygen free copper (OFHC) is widely adopted to fabricate absorbers on storage rings because of its high thermal conductivity. However, it can't endure so high power density. Glidcop is another kind of absorber material for absorbing photon with high power density in some light source [2, 3]. However, Glidcop imported is very expensive. CuCrZr is attractive material for fabricating high power density photon absorbers because of its high thermal conductivity [4], high softening temperature and good mechanical properties [5-8]. Domestic CuCrZr was chosen as material for these absorbers finally. Properties of the

PARTICLE-FREE ENGINEERING IN SHINE SUPERCONDUCTING LINAC VACUUM SYSTEM

Y.L. Zhao†, Y.Y. Liu, Y.F. Liu, Q.S. Tang, L.X. Yin
Shanghai Advanced Research Institute, CAS, Shanghai, China

Abstract

The Shanghai high-repetition-rate XFEL and extreme light facility (SHINE) is under design and construction. The linac of SHINE facility is superconducting accelerating structures of high gradients, whose performance is closely related to the cleanliness of superconducting cavities. Therefore, the beam line vacuum system has extremely high requirement for particle free to avoid particles down to submicrometric scale. To control particle contamination, particle-free environment has been built for cavity string assembly and other beam line vacuum components installation, clean assembly criterion has been established. Furthermore, the particle generation of vacuum components (valve, pump, etc.) has been studied. Moreover, dedicated equipment and component (slow pumping & slow venting system, non-contact RF shielding bellow) have been developed for particle-free vacuum system.

INTRODUCTION

SHINE is a new hard-XFEL facility under construction in China, which is designed to accelerate electron beams to 8 GeV by 600 1.3 GHz 9-cell cavities working in continuous wave mode, and the cavities is installed in 75 cryomodules [1]. Cleanliness is essential in the preparation of field emission free, high gradient, low loss superconducting cavities [2], therefore, not only the cavities but also the beamline vacuum components adjacent to cryomodules has extremely high cleanness requirement. The design, fabrication, cleaning, assembly, testing process of these components must be followed the cleanliness requirement.

In SHINE linac, the total length of particle-free zone is 1.2 km, including cryomodules and room temperature (RT) beamline. For cryomodules, the vertical test of single cavity, cavity string assembly and cryomodule horizontal test are all carried out in SHINE. For RT beamline vacuum components, most pre-cleaning is performed at supplies. For integrated equipment like collimators, profile monitors wire scanners, e.g., the particle-free assembly is carried out at supplies. For standard components like vacuum gauges, valves, pumps, the cleaning before final assembly is carried out in SHINE.

INFRASTRUCTURES, EQUIPMENTS AND TECHNOLOGIES

A 400 m² cleanroom have been built in 2019 for SHINE superconducting cavity string assembly, which has 300 m² ISO 4 class area and 100 m² ISO 5 class area.(Fig. 1 top).

The cleanroom includes ultrasonic cleaning, high press rinsing (HPR), cavity drying areas, and the cavity string assembly area is capable for up to 8 persons to assembly 2 cavity strings at the same time (Fig. 1 bottom).
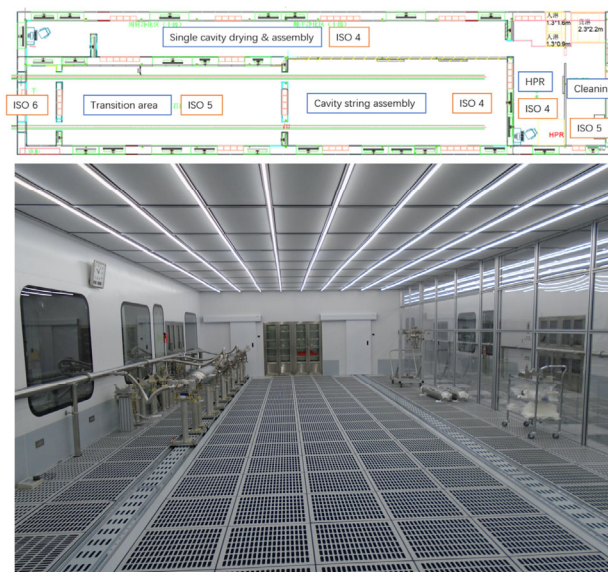
Figure 1: ISO 4 class cleanroom for cavity string assembly.

Various moveable laminar flow booths have been used for particle-free operation at cryomodule horizontal test, cavity vertical test, beam line vacuum components, e.g. High Efficiency Particulate Air (HEPA) filter was used in all of these booths, so as to obtain a local cleanness higher than

Figure 2: Moveable laminar flow booths for local particle-free assembly.

INSTALLATION PROCESS EXPERIMENT OF HEPS STORAGE RING EQUIPMENT

C. H. Li†, Z. H. Wang, S. Lu, L. Dong, S. Yang, S. Y. Chen, Y. D. Xu, Y. F. Wu, F. S. Chen,
M. Yang, L. Wu, G. Feng, Institute of High Energy Physics, Beijing, China

Abstract

HEPS is a new generation synchrotron radiation source under construction in China. In order to complete high-precision installation of the 1.4 km storage ring within a limited construction period, it is necessary to identify and solve potential issues in various aspects, including operation space, installation process, alignment scheme, and unit transportation, prior to the regular batch installation. Therefore, a full-process installation experiment was performed and the feasibility of relevant schemes are verified. Batch installation is currently in progress based on the experimental experience.

INTRODUCTION

The High Energy Photon Source (HEPS) is the fourth-generation synchrotron radiation source currently under construction in China, characterized by high energy and extremely low emittance. The circumference of the storage ring is approximately 1.4 km, and compact 7BA achromats is adopted [1], which brings lots of challenges to the installation. In order to complete high-precision installation within a very limited construction period, it is necessary to identify and solve potential issues in various aspects, including installation operation space, alignment installation process, pre-alignment precision, and transportation reliability, before the regular installation in batches.

The experiment object is a standard 7BA cell, as shown in Fig. 1, which includes 6 pre-alignment units, 5 BLG magnets, 1 ID beamline, and 1 BM beamline.
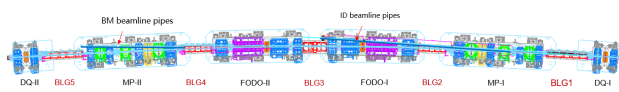
Figure 1: A standard 7BA cell.

The experiment was performed in a laboratory adjacent to HEPS. The pre-alignment was carried out in a thermostatic room, while other processes were conducted in the hall. The experiment lasted for approximately 4 months.

PRE-ALIGNMENT SCHEME

The magnet pre-alignment errors are required to be less than 30 µm, which accumulate from several processes such as measuring, magnet positioning, magnet opening/closing, and transportation. The magnet positioning deviation between magnets within a girder is required to be less than 10 µm, and much higher measuring accuracy and precise alignment mechanism of micron level are needed.

† lichunhua@ihep.ac.cn

Measuring Accuracy

The laser tracker, which is the most popular instrument in accelerator alignment, cannot meet such high precision requirements directly. Therefore, a laser tracking interferometer system is developed and the measuring accuracy can be improved to 6 µm [2].

Based on multi-lateration measurement principle, four laser trackers are arranged in a specific layout, as shown in Fig. 2, to measure one target point simultaneously. Only distances are extracted from the measuring parameters, which is more accurate than the angles in the laser tracker measurement, for calculating the coordinates of the targets. Meanwhile, the target coordinate is displayed on the screen in real-time, and the magnet position can be adjusted precisely by operating the alignment mechanism.

Figure 2: Laser tracking interferometer system.

Pre-alignment Process

Before installation, wipe the mounting surface to ensure there are no debris, stickers, or other foreign objects. Ensure that the six support points of the girder body bear force evenly, and then assemble a group of magnets on this girder into a pre-alignment unit.

Basic pre-alignment procedure includes following steps:

1. Transport the unit into the thermostatic room for temperature stabilization. At least 4 hours are needed before measurements to eliminate the influence of environmental temperature on the equipment.

2. Level and tighten the girder on the plinth, and establish a coordinate system based on the girder as the alignment reference.

3. Measure the position of each magnet and fit it with the theoretical values to determine the adjustment amount for each magnet.

4. Select a magnet as the alignment reference, usually is the magnet located in the middle of the girder and with

DESIGN OF MULTIPLE EXPERIMENTAL MODELS FOR PINK SAXS STATION

Guang Mo[†], Zhihong Li, Xueqing Xing, Zhongjun Chen, Yunpeng Liu, Ye Tian, Zhaoqiang Cui, Zhonghua Wu, Institute of High Energy Physics, Chinese Academy of Sciences, Beijing, China

Abstract

Pink small angle X-ray scattering station is dedicated to performing scattering related experiments. A classical in air planar undulator is adopted as the beam source. The fundamental radiation can be adjusted within 8-12 keV through altering the magnetic gaps. Monochromatic beam and pink beam can be switched through moving in and out of the monochromator. Three set diamond compound refractive lenses with different curvatures are employed to focus the 12 keV monochromatic beam to achieve different focusing modes. With the help of a flexible vacuum detector tube, varies experimental models could be carried out easily.

INTRODUCTION

Small angle X-ray scattering (SAXS) is a powerful technique for studying nano materials [1]. As for numerous scattering experiments, different experimental demands are proposed by users. For example, as monochromatic beam is not necessary for some SAXS measurements [2], they prefer higher beam flux to shorten exposure time and to carry out higher time resolved scattering experiments at the expense of sacrificing energy resolution and beam size. Conversely, some researchers hope to carry out fine experiments with higher energy resolution and small beam size. In order to accommodate these seemingly contradictory needs of diverse users, a muti-functional SAXS station is under construction at HEPS.

HEPS [3] (high energy photon source), which is a 6 GeV synchrotron radiation facility with low emittance, provide perfect conditions for meeting these requirements. The high flux pink beam, which is from the fundamental radiation of the undulator, will be used directly after reflected by a pure silicon reflector to perform high time-resolution experiments. Monochromatic beam, which is obtained by a horizontal double Si(111) crystal monochromator, also can be used alternately to perform high energy resolution experiments. With the help of flexible monochromator, focusing element and a SAXS tube, the main parameters of SAXS station can be adjusted conveniently, which are reflected in the following aspects. First, the pink beam and monochromatic beam can be switched through moving in and out a horizontal double crystal monochromator. Second, the incident beam energy can be altered through adjusting the gaps of undulator at the range of 8-12 keV with the help of a monochromator. Third, for the commonly used 12 keV monochromatic beam, four types of focusing

modes can be changed through changing on-line diamond CRLs. Four, the different range of scattering angle can be altered easily by the help of a flexible tube. This design can meet the vast majority needs of users. The main specifications of the SAXS beamline is shown in Table 1.

The available experimental techniques include single SAXS, WAXS, USAXS, SAXS-CT, ASAXS and combined SAXS/WAXS/USAXS, etc. The measuring mode includes transmission and grazing incidence, static and dynamic (in situ, time resolved) measurements. The time resolution lies in microseconds to seconds based on different sample environments and detectors. Some sample environmental devices, including in-situ heating, in-situ growing, in-situ tension, will be equipped in our station.

Table 1: Main Specifications of the SAXS Beamline at HEPS

Pink beam	
Energy range	8-12 keV
Flux at sample	$\sim 10^{15}$ ph/s
Beam size @sample	500 μm × 500 μm
Energy resolution	1.5 %
Scattering angle	0.001°~50°
Monochromatic beam	
Energy range	8-30 keV
Flux at sample	$\sim 10^{13}$ ph/s
Beam size @sample	300 μm × 300 μm
	14 μm × 6 μm;
Energy resolution	$\sim 2 \times 10^{-4}$

DESIGN

Overall Description

The basic idea of design, sketched in Fig. 1, is that the monochromator and the focusing devices (CRL) can be moved in and out of the beamline. Without monochromator and CRLs, the quasi monochromatic beam from the fundamental radiation of the undulator also can be directly collimated to measure the sample. A set of three-slits is used to reduce the scattering background, which are not drawn in the diagram.

We specify the beam source as the starting position (0 m). The front-end of the beamline is about 32 m long, which is mainly used to provide radiation protection and heat reduction to the downstream devices. The beamline starts from the front-end ratchet wall exit (32 m from the source) and ends at 49.9 m, which is located in the first optical

QUICK SCANNING CHANNEL-CUT CRYSTAL MONOCHROMATOR FOR MILLISECOND TIME RESOLUTION EXAFS AT HEPS

Yuanshu Lu, Hao Liang, Yunsheng Zhang, Zekuan Liu, Dashan Shen, Yang Yang, Shan Zhang, Zheng Sun, Institute of High Energy Physics, Chinese Academy of Sciences, Beijing, China

Abstract

The design and capabilities of a Quick scanning Channel-Cut monochromator (QCCM) for HEPS are presented. The quick scan and step scan are realized by a torque motor directly driven Bragg axis, controlled by a servo controller. This design allows easy and remote control of the oscillation frequency and angular range, providing comprehensive control of QXAFS measurements. The cryogenically cooled Si(311) and Si(111) crystals, which extends the energy range from 4.8 keV-45 keV. The dynamic analysis verifies the rationality of the mechanical structure design. The device was fabricated and tested, results show an oscillation frequency up to 50 Hz with a range of 0.8, and a resolution of 0.2 arcsecond in step scan mode. This device demonstrates the feasibility of large range quick scan and step scan by a single servo control system.

INTRODUCTION

An X-ray Absorption Spectroscopy (XAS) is a standard method at synchrotron radiation sources to study solid or liquid, crystalline and non-crystalline matter [1, 2]. The Quick scanning Extended X-ray Absorption Fine Structure (QEXAFS), reduces the scanning time of a single spectrum from 10 minutes to 10 milliseconds [3, 4, 5]. It has become one of the ideal methods for in situ investigations of the kinetics of chemical reactions. Highly optimized for general use and perfect compatibility with conventional XAFS beamline structures [6, 7].

High energy photon source (HEPS) is one of the world's lowest emissivity, highest brightness of the fourth generation of synchrotron radiation light source. The electron beam group emissivity of HEPS will be lower than 60 pm·rad, providing a very small light source size and extremely high brightness and other excellent performance, the excellent characteristics of synchrotron radiation light source makes the monochromator working conditions worse. We have constructed a dedicated beamline X-ray absorption spectroscopy stations (B8 beamline) at the HEPS. It is a high-performance hard X-ray beamline based on X-ray absorption spectroscopy and related derivative experimental methods. Target energy covering 4.8 keV-45 keV.

DESIGN OF THE MONOCHROMATOR

The QCCM, as shown in Fig. 1, contains: high precision rotating axes system, crystal components, vacuum chamber system and base adjustment system.

The High Precision Rotating Axes System

The high-precision rotating axes system, as shown in Fig. 2 relies on the torque motor (KEDE CNC,

GTMH0360WS-50) to drive the rotation axes and the crystal components to rotate, the peak torque of the motor is 756 N m, the continuous torque is 516 N m, the stator is provided with a water-cooling channel, and the heat generated during the motor movement is taken away by circulating cooling water. The torque motor transmits the torque to the vacuum chamber through the magnetic seal unit (Rigakual). An RESM150 angle encoder system (Renishaw) is installed on the atmospheric side of the rotating axes system, and an RESA150 absolute angle encoders (Renishaw) is installed on the vacuum side, which are used for measuring the angle of the crystal during step scanning and quick scanning.
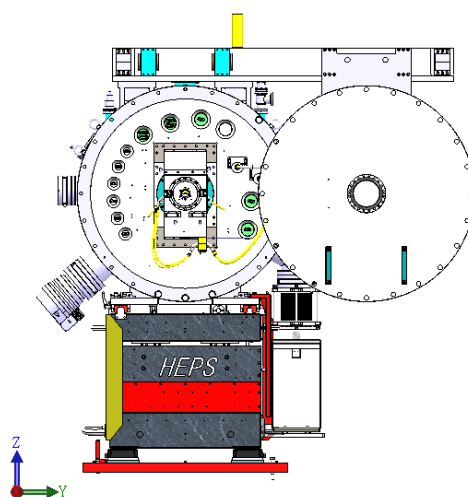
Figure 1: The show of QCCM.
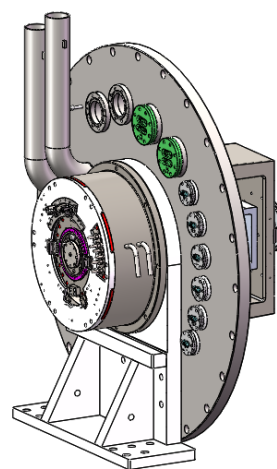
Figure 2: Diagram of rotating axes system.

THE DESIGN OF A 2 m LONG COPPER LIGHT EXTRACTION VESSEL AT DIAMOND LIGHT SOURCE FOR THE DIAMOND-II UPGRADE

V. Danielyan[†], M.P. Cox, P. J. Vivian, R. Fielder, S. L. Hodbod, T. Lockwood
Diamond Light Source, Didcot, Oxfordshire, UK

Abstract

The design of a 2 m long light extraction copper vacuum vessel for Diamond-II (D-II) storage ring upgrade in Diamond Light Source (DLS) is described. Initially, an aluminium vessel with two discrete copper absorbers was considered, further studies have shown the concept was not capable of handling high heat loads making the aluminium vessel arrangement an unworkable solution. Therefore, it was decided to change the design concept from an aluminium vessel to a copper vessel. The main difference between two concepts is that the copper vessel has integrated absorbing surfaces instead of discrete absorbers. Due to the change, it was possible not only to reduce the power densities of the absorbing surfaces, but also it allows placing active cooling directly on the high heat loaded areas. These two factors contributed to a significant reduction of the peak temperatures. Synchrotron light raytracing, thermal analysis, vacuum performance, beam impedance, prototyping and next steps of the new copper vessel are also covered in this paper.

INTRODUCTION

The D-II Storage ring vacuum system comprises 48 arcs and 48 straights [1]. There are 4 main types of arc girder vessel strings: MS, SM, ML and LM girder vessel strings. The above-mentioned copper vessel is located on the upstream end of the LM girder vessel string, vessel 2 shown in Fig. 1. There are 6 LM Girders in the whole storage ring, which means 6 LM vessel 2 are required for various light extractions. The vessel is designed in a way that it covers all 6 cases, hence no special vessels are required. The most challenging case is the LM girder vessel 2 for I05 light extraction.

Figure 1: Diamond II LM girder vessel string.

The main challenges associated with the design of this vessel at that particular location are, firstly, the heat loads of I05 beamline upgrade involving the installation of a powerful and highly divergent APPLE-knot quasi-periodic (QP) insertion device (ID) [2]. Second aspect is the requirement of a homogeneous NEG (non-evaporable getter) coating on the complex internal geometry of the vessel. Detailed FEA analysis shows the peak temperature is

---

† vahe.danielyan@diamond.ac.uk

reduced from 446°C to 71°C for the copper vessel as compared to the aluminium vessel discrete absorbers. The change from an aluminium vessel to a copper vessel will not only reduce the peak temperatures, thereby making it a workable solution according to DLS FEA criteria [3], but has the added benefits of improved vacuum performance, reduced beam impedance, reduced capital and operating cost, as well as reduced manufacturing risks due to splitting of vessels into three separate sub-vessels.

DESIGN AND PROTOTYPING

Figure 2 shows the design of both aluminium (a) and copper (b) versions of LM girder vessel 2. Many features of the original aluminium vessel design have been reused on the copper vessel, particularly regions of multipole magnets, downstream pumping, and crotch absorber section etc. Key differences between two vessel designs are listed in the Table 1. The copper vessel is comprised of 3 separate sub-vessels: vessel 2_a, _b, and _c, where vessel 2_b is the highest heat loaded section.
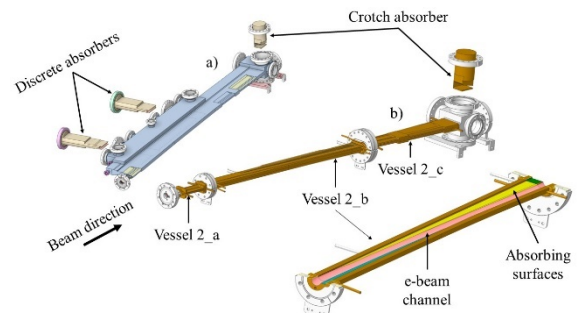
Figure 2: LM girder vessel 2 design versions: a) aluminium and b) copper.

Table 1: Design Differences Between Al. and Cu Vessels

Features	Al. Vessel	Cu Vessel
Antechamber	yes	no
Discrete absorbers	yes	no
Bimetallic flanges	yes	no
Int. Absorbing surfaces	no	yes
Water cooled	no	yes
NEG coated	no	yes
Manufacturing method	welded	brazed

There are two sets of beam position monitor (BPM) buttons at the entry and exit flanges. Vessel 2_a upstream flexible flange allows movements of +2 mm extension, -5 mm compression, and ±0.25 mm of lateral offsets. The design constraints are different for each sub-vessel (e.g. available space, power load etc.), and these factors are dictating the design of both internal and external geometries. Figure 3

VIBRATION ANALYSIS OF STORAGE RING GIRDER FOR THE KOREA 4GSR*

G. W. Hong [†], H. G. Lee, T. Ha, H. S. Han
Pohang Accelerator Laboratory (PAL), Pohang, Republic of Korea

Abstract

Ensuring the mechanical stability of the girder for a 4th generation storage ring (4GSR) is crucial to provide a high-quality photon beam to users because the mechanical motion should be maintained at less than 10 % of the electron beam size which is expected to be sub-micrometer. One of the key roles of the girder is to provide structural rigidity and temperature stability while effectively suppressing vibrations from the ground during accelerator operation. The Korea 4GSR girder is being designed to have the first natural frequency above 50 Hz to minimize the effect of the ground vibration. In order to maintain better mechanical stability, it is necessary to conduct research not only on the natural vibration evaluation of the girder but also on external vibrations to the girder structure. In this paper, we introduce the result of the harmonic analysis of the girder structure using the finite element method.

INTRODUCTION

The Korea 4GSR girder system is designed to conform to a storage ring circumference of approximately 800 m to conform to stable accelerator design variables. Alignment mechanisms such as motor-driven cam moves, wedge jacks, and motor-driven wedge jacks are used in the case of circular synchrotron accelerator girder systems that are driven worldwide. The girder system for the PLS-II of the third-generation circular accelerator used an alignment mechanism through screw jacks to secure a wide driving range and mechanical rigidity [1]. The Korea 4GSR girder system was developed using a ball screw jack with improved moving accuracy and durability instead of the existing TM screw jack for the girder body adjustment. In addition, it was developed using a motor control drive and a displacement sensor for convenience in precise alignment of the accelerator [2]. This research explains the design concept of Korea 4GSR and structural design to secure rigidity [3], natural frequency evaluation [4], and structural stability due to random frequency [5] using Finite element analysis (FEA) to analyse mechanical characteristics.

Requirement for the Girder System

Beam physical requirements must be satisfied for the design of the Korea 4GSR girder system. In the global cases where upgrades from 3rd generation to 4th generation circular accelerators have been made, vibration characteristics of the ground and characteristics of the accelerator building should be reliably identified in order to build a successful synchrotron accelerator. Korea 4GSR should be operated stably for the external environment, and development that meets the following requirements should be carried out for the girder system.

- Electron beam height: 1.4 m.
- High flatness of girder top and low deformation for installation and operation of accelerators.
- Securing high primary resonant frequencies for limited conditions.
- Motor driven alignment mechanisms.
- Optimal girder design for free space in storage-ring tunnels.
- Securing mounting holes for installing various devices.
- Ensuring thermal stability.

The main parameters for developing the girder system of Korea 4GSR are as follows.

Table 1: Main Parameters for the Girder System [6]

Parameter	Value	
Number of cells	28	cells
Circumference	798.8	m
Beam height	1.4	m
Levelling range (Vertical)	± 10	mm
Lowest natural frequency	50	Hz
Adjustment method	Motorized (Vertical)	
Positioning accuracy	± 10	μm

Design Layout

The girder design is heavily influenced by the beam physics design and device configuration. There is a total of 28 cells at about 800 m around the storage ring, and the types are normal cells and high beta injection (HBI) cells, each cell was developed into five girders. The layout of the girder system is also composed of two types because the normal cell consists of symmetrical upstream and downstream based on the central bending section, and the HBI cell has a non-symmetric configuration [7]. There are three types of girder for installing the storage ring accelerator. All girder adjustment devices are designed in the same mechanism with 4 points motor-driven in the Y direction and 3 points in the X and Z directions being manually adjusted. For a normal cell, three girders based on the center of each cell are designed to be 4.8 m in the longitudinal direction, and the girders at both ends of the cell are designed to be 3.8 m. The HBI cell is designed with the three

PERMANENT MAGNET IN SOLEIL II

A. Berlioux[†], Y. Benyakhlef, C. Kitegi, F. Marteau, A. Mary, E. Raimon, M. Ribbens, K. Tavakoli

Synchrotron SOLEIL, Saint-Aubin, France

Abstract

Twenty years after SOLEIL Synchrotron was established, the facility needs to adapt to follow new scientific fields that have emerged since. The proposed new lattice for upgrading SOLEIL storage ring will reduce the horizontal emittance by a factor 50 to reach less than 100 pm·rad.

This new lattice presents significant challenges and requires compact magnets that provide strong gradients. As a result, PM (permanent magnet) technology is preferred over electromagnet (EM) technology whenever possible. All sextupoles and octupoles will be EM to ensure efficient optic correction. However, all dipoles, reverse bends and quadrupoles will be PM.

The replacement of aging infrastructure and the use of permanent magnets (PM) will lead to a noticeable reduction in SOLEIL's electric power consumption and environmental footprint.

SOLEIL II lattice consists of 116 dipoles with gradient and 354 PM quadrupoles which can also be used as reverse bends. All PM multipoles have been designed by SOLEIL's Mechanical Engineering Group in close collaboration with the Magnetic and Insertion Devices Group.

INTRODUCTION

Since its inception in 2008, SOLEIL has proudly represented the cutting-edge of French third-generation light sources. This facility harnesses an electron beam emittance of 4 nm·rad, fueled by an energy of 2.75 GeV, delivering intensity at 500 mA in a multibunch configuration [1].

Having achieved years of successful operation, SOLEIL embarked upon an ambitious project dedicated to advancing its capabilities. The project, known as SOLEIL II, aspires to reduce the horizontal emittance of the electron beam less down to 100 pm·rad at 2.75 GeV. Our mission is to design and construct a fourth-generation synchrotron light source while preserving the existing infrastructure, including 29 beamlines spanning from far-infrared to hard X-rays.

The lattice of the new storage ring consists of alternating 7BA and 4BA High Order Achromat type cells, including more than twelve hundred magnets. To achieve such challenge, magnet design compactness is a key parameter. Permanent Magnets (PM) technology offers us a great balance between space and magnetic strength. Dipoles, reverse-bends and quadrupoles have been designed with such technology. Table 1 list the main materials used.

Table 1: Main Materials

Class	Designation
Magnets	Sm_2Co_{17}
Iron	XC06 (or ARMCO)
	Permendur (Fe-Co)
	34CrMo4
Stainless Steel	316L (μ<1.01)
Aluminium	2017A T4
Mu-metal	$NiFe_{15}Mo_5$

DIPOLES

Within the SOLEIL II storage ring lattice, there are eight distinct categories of dipoles, including four normal short dipoles (DNC) and four normal long dipoles (DNL). Table 2 is listing their main characteristics [2].

Table 2: Main Dipoles Parameters

Dipole	Diamater (mm)	Deviation (mrad)	Mag. Length (mm)	On axis field (T)	Gradient (T/m)	Quantity
DNC1	23	42.22	460	0.921	-18.7	22
DNC2	23	40.09	460	0.874	-18.7	16
DNC3	23	41.85	460	0.912	-18.7	1
DNC4	23	48.43	460	1.061	-18.7	1
DNL1	19	68.86	940	0.593 / 1.2 / 0.593	-21.57 / 0 / -21.57	58
DNL2	19	65.39	940	0.563 / 1.2 / 0.563	-21.57 / 0 / -21.57	16
DNL3	19	69.02	940	0.593 / 1.2 / 0.593	-21.57 / 0 / -21.57	1
DNL4	19	68.51	940	0.593 / 1.2 / 0.593	-21.57 / 0 / -21.57	1

Short Dipoles

DNC are used at the upstream and the downstream of 7BA and 4BA cells [3]. Their poles are curved with a hyperbolic profile, adding a transverse gradient. Low carbon steel is used for all magnetics parts and an aluminium bloc enable the transmission of forces. Mu-metal plates are used as a magnetic shield. They are fixed on both sides of the dipole to prevent crosstalk with the very close magnets next to it. Figure 1 shows the actual 3D model of the DNC.

---

† anthony.berlioux@synchrotron-soleil.fr

DEVELOPMENT AND QUALIFICATION OF MICROMETRE RESOLUTION MOTORIZED ACTUATORS FOR THE HIGH LUMINOSITY LARGE HADRON COLLIDER FULL REMOTE ALIGNMENT SYSTEM

M. Noir * [1], M.Sosin † [1], P.Biedrawa [2], S.Fargier [1], W.Jasonek [2]

[1]CERN, Geneva, Switzerland

[2]AGH, University of Science and Technology, Krakow, Poland

Abstract

In the framework of the High-Luminosity Large Hadron Collider project at CERN, a Full Remote Alignment System (FRAS) is under development, integrating a range of solutions for the remote positioning of accelerator components. An important component of FRAS is the motorized actuator allowing the remote adjustment of accelerator components with a micrometre resolution. These actuators need to fulfill multiple requirements to comply with safety rules, and be highly reliable and maintenance free as thus are located in a harsh environment.

The integration of the safety functions required for the FRAS was crucial, with the motorized actuators able to provide an absolute position monitoring of the available stroke, integrating electrical end-stops and having an embedded mechanical stop as a hardware safety layer. In addition, the design has been elaborated to allow a rapid, in-situ re-adjustment of the nominal stroke in order to cope with potential readjustment requirements, following long-term drifts caused by ground motion.

This paper describes the design approach, prototyping and qualification of these motorized actuators.

INTRODUCTION

The High-Luminosity-Large Hadron Collider (HL-LHC) project is an upgrade of the current LHC that aims to increase its integrated luminosity by a factor of 10. In order to achieve such a luminosity, components of the Long Straight Sections (LSS) will be replaced around the two major detectors (ATLAS and CMS), representing a major modification of 1.2 km of beam line [1, 2].

The increased luminosity will generate higher radiation levels in the LSS and prevent from an easy and safe access in the area. In order to reach the required physics performance, the LSS components will have to be aligned within +/- 0.3 mm (1 sigma) over a 450 m length. The alignment will be performed by the Full Remote Alignment System (FRAS) [3, 4]. It consists of a set of sensors and actuators allowing a micrometre position monitoring and remote adjustment of the accelerator components.

To perform their adjustment, the heaviest components, like magnets, will be installed on a set of 3 standardised jacks (each jack providing 2 degrees of freedom of adjustment). The following chapters describe the design, prototyping and

---

* michel.noir@cern.ch

† mateusz.sosin@cern.ch

qualification of the radial and vertical motorized adapters used for the accurate adjustment of each jack position.

SYSTEM CRITICALITY DUE TO REMOTE OPERATION

During the alignment operations in HL-LHC, the available stroke of the vacuum interconnection bellows linking adjacent components of the beam lines must be taken into account before a relative movement. As the FRAS will be operated remotely, a safety strategy has been implemented to protect the machine from unexpected relative movements that could lead to major failures. Two safety functions, representing the major challenges in the adapters design, have been assigned to the motorised adapters:

- They shall provide at anytime the absolute position of the adapter within its stroke, to control that the displacement at the level of the bellows is performed within the limits of ±2.5 mm.
- A mechanical end-stop shall block any motion if the nominal stroke of ±2.5 mm is exceeded. This additional feature represents a challenge regarding the developed force of the adapters (up to 17 500 kg).

MOTORISED ADAPTERS DESIGN

Vertical Position Adjustment

Each vertical adapter has been designed to withstand loads up to 17.5 T, to fit into small jack adapter volume (Figure 1). The compactness of the overall design was one of the major challenges which is why a quasi-hydraulic actuation solution has been selected. The main concept relies on the deformation of a polyurethane pastille in the actuator head. A pushing finger driven by a self-locking thread-nut system deforms radially the pastille taking the full chamber space and lifting the piston to adjust the jack position as per an hydraulic cylinder (see Figure 2). This system, already used today in the LHC, provides a micrometre position adjustment.

Radial Position Adjustment

For the radial actuation, the motion is performed by the jack mechanism itself, consisting of a screw-nut actuation system linked to a high-ratio worm gear (see Figure 1). Hence, the radial motorized adapter role is to provide a high resolution rotary motion and to measure it in an absolute way. The global stroke of the actuator to perform the ±2.5 mm final motion corresponds to 58 revolutions.

SmarGon MCS2: AN ENHANCED MULTI-AXIS GONIOMETER WITH A NEW CONTROL SYSTEM

W. Glettig, D. Buntschu, E. Panepucci, M. Wang, Paul Scherrer Institute, Villigen PSI, Switzerland
A. Omelcenko, SmarAct GmbH, Oldenburg, Germany

Abstract

As an improvement on the commercially available SmarGon multi-axis goniometer (SmarAct GmbH), the Macromolecular Crystallography (MX) Group at the Paul Scherrer Institute (PSI) has been pursuing a further development of the system. In addition to suggesting mechanical improvements to SmarAct for improved ruggedness and reliability, PSI has developed a brand-new and flexible control system for better customization, reliability, and control. Calibration routines were implemented to reduce systematic errors, and the system has been tailored for practical beamline usage. SmarGon is a six degree-of-freedom positioning device, allowing positioning of a sample and orientation around any given point, with < 5 µm sphere of confusion diameter. It was purpose-built for protein-crystallography experiments but, as will be presented here, was also re-purposed for other applications. Two devices have been in continuous 24/7 use for two years at the MX Beamlines PXI & PXII at SLS.

INTRODUCTION

Initially developed based upon PSI's 6-axis-goniometer for protein crystallography PRIGo [1], SmarAct GmbH's SmarGon is a further developed and commercially available positioning device [2] allowing 4 mm translational XYZ motion and three angles of rotation ω: $[-\infty, +\infty]$, χ: $[0, 90°]$, φ: $[-\infty, +\infty]$ around any arbitrary point in space (Fig. 1). Positioning resolution is 1 nm and spheres of confusions are achievable of below 1 µm for ω, and well below 7 µm for χ & φ. [2]

Figure 1: SmarGon with a representation of the rotations ω: $[-\infty, +\infty]$, χ: $[0, 90°]$, φ: $[-\infty, +\infty]$.

SmarGon is used to position and orientate a sample with respect to the X-ray beam, and is one of the central components of a macromolecular crystallography (MX) beamline setup [3]. It was purpose built for MX experiments, but has also been used in other applications.

INITIAL RELIABILITY ISSUES

While offering advantages over the PRIGo Goniometer in terms of compactness and build simplicity, a big challenge in daily operation was to preserve SmarGon's reliability over extended periods of time. MX beamlines are often set up for high throughput and can process hundreds of samples a day. They are often controlled remotely, and now increasingly in unattended automatic operation [4]. In such cases, downtime must be avoided, and all systems must be as remotely monitorable and controllable as possible, without any need for physical human intervention.

The initial version of SmarGon posed problems: Due to its fine mechanical structure it was prone to mechanical damage caused by rough human manipulation during manual sample mounting, or unforeseen collisions during robotic sample mounting [5]. User-prepared samples can sometimes present unpredictable defects, leading to mis-gripped samples and ice-related slipping and sticking issues.

Another limitation was the inability to customise the control system for different modes of operation, like permitting flexible recovery in case of problems during remote access. Or in tweaking the calibration routine. Or modifying interfaces, to extend remote system diagnostics or to collect usage statistics.

Improvements both on the mechanical side as well as on the control side were strongly requested.

MECHANICAL IMPROVEMENTS

Over the initial design of the SmarAct goniometer, several simple mechanical improvements were implemented by SmarAct GmbH, primarily to increase robustness and reliability of the mechanism, and by improving processes for more repeatable assembly tolerances. These improvements are now standard in the latest SmarGon devices. Revisions to the pivot and ball joints were made and hard stops were added to prevent dislodging. Both during manual interaction and during robotic sample mounting, misaligned or mis-gripped samples can cause large forces on the goniometer, which can lead to plastic deformation of the mechanical structure. The design of a critical area of high stress, and the choices of materials were revised. Holding forces of the SmarAct piezo stick-slip positioners were taken into account, so that during a physical interaction the compliance in the structure would be in the sliders, and not as a plastic deformation of the structure.

OVERALL PROGRESS ON DEVELOPMENT OF X-RAY OPTICS MECHANICAL SYSTEMS AT HIGH ENERGY PHOTON SOURCE (HEPS)

Shanzhi Tang [†, 1], Jianye Wang, Weifan Sheng [1], Haihan Yu, Zhongrui Ren, ZinaOu, Ruzhen Xu,
Ruiying Liao, Luhan Ma, Xiaohui Kuang, Hao Liang, Ming Li [1], Hanjie Qian, Yuhui Dong[‡, 1]
Institute of High Energy Physics, Chinese Academy of Sciences Beijing, China
[1] also at University of Chinese Academy of Sciences, School of Nuclear Science and technology,
Beijing, China

Abstract

High Energy Photon Source (HEPS) regarded as a new 4th generation synchrotron radiation facility, is under construction in a virgin green field in Beijing, China. The X-ray optics/mirror mechanical systems (MMS) play an important role, which would be expected to be designed carefully and rigidly for the extremely stable performance requirement of HEPS. In addition, there are indeed big challenges due to so many types of mirror systems, such as white beam mirror (WBM), harmonic suppression mirror (HSM), combined deflecting mirror (CDM), bent mirror, Nano-KB, and the transfocator of Compound refractive lens (CRLs), etc. Therefore, overall progress on design and manufacture of the MMS is introduced, in which a promoting strategy and generic mirror mechanical system as a key technology is presented and developed for the project of HEPS. Furthermore, ultra-stable structure, multi-DOF precision positioning, Eutectic Galium Indium (E-GaIn)-based vibration-decoupling water-cooling, clamping, and bending have always been prior designs and considerations.

INTRODUCTION

To meet the extreme requirement of 4th generation synchrotron radiation facility, many efforts and design considerations on the X-ray optics mechanical system are presented, such as an ultra stability mirror system or benches [1-7], a better mounting and water-cooling of mirror [8], and an improved bender [9].

HEPS is a new and under construction 4th generation synchrotron radiation facility. It has a 6 GeV storage ring with a circumference of 1360.4 m and a natural emittance of 34.2 pm [10]. The ground stability of vibration should be required to 25 nm @1~100 Hz. So, the stability of mechanical engineering design of synchrotron instrument and device becomes a critical important issue. Besides, there are 15 beamlines in Phase I of HEPS, which has so many types of mirror systems, such as white beam mirror (WBM), harmonic suppression mirror (HSM), combined deflecting mirror (CDM), bending mirror, Nano-KB, and the transfocator of Compound refractive lens (CRLs), etc. This bring out another big challenge. So, to deal with the problems, a promoting strategy is presented at HEPS. The

steps as follows: firstly, a high-performance generic mirror mechanical systems (GMMS) is first proposed and developed. Secondly, GMMS-based variable mirror mechanical system or Transfocator will be designed and manufactured. Actually, GMMS would been also applied for the main mechanical system of Laue double bent crystal monochromator (LDBM). Finally, lots of specific mechanical designs in vacuum will be implemented, including bender, water cooling, support and clamping, and other custom-made mechanisms.

OVERALL DESIGN STRATEGY

It is well known that base support, positioning, and clamping are the three common main functions of the mirror mechanical system (MMS), although the types of MMS are different. So, a high-performance MMS is presented and developed, which not only features ultra-stable, bust also has a high accuracy attitude adjustments and stress-free mirror mounting. More importantly, it is expected to be a generic MMS (GMMS) for a large number and variety mirrors at HEPS. Therefore, a strategy of GMMS is proposed as shown in Fig. 1. Moreover, a customized GMMS-based design scheme will be formed as shown in Fig. 2.
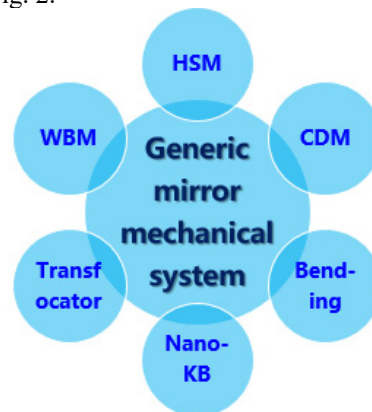
Figure 1: The promoting strategy of design for MMS.

Compared to the existed mirror mechanical systems, the vibration stability of ≤ 25 nrad rms@1-120 Hz and 5-DOF positioning-motorized are extracted as the main technical parameters of GMMS. And it must be compatible for horizontal reflection mirror and vertical reflection mirror as shown in Fig. 3. It is that the performance of yaw adjustment mechanism is equivalent to pitch. Be-

MODELING THE DISTURBANCES AND DYNAMICS OF THE NEW MICRO CT STATION FOR THE MOGNO BEAMLINE AT SIRIUS/LNLS

G. S. Baldon*, G. S. de Albuquerque†, F. Ferracioli, G. B. Z. L. Moreno, R. R. Geraldes

Brazilian Synchrotron Light Laboratory (LNLS), CNPEM, Campinas, Brazil

Abstract

At the 4th generation synchrotron laboratory Sirius at the Brazilian Synchrotron Light Laboratory (LNLS), MOGNO is a high energy imaging beamline, whose Nano-Computed Tomography (CT) station is already in operation. The beamline's 120 nm × 120 nm focus size, 3.1 mrad × 3.1 mrad beam divergence, and 9×10^{11} ph/s flux operated at 21.5 keV, 39.0 keV, and 67.7 keV energies, allow experiments with better temporal and spatial resolution than lower energy and lower stability light sources. To further utilize its potential, a new Micro-CT station is under development to perform experiments with $0.5\,\mu m - 55\,\mu m$ resolution, and up to 4 Hz sample rotation. To achieve this, a model of the disturbances affecting the station was developed, which comprised: i) the characterization and simulation of disturbances, such as rotation forces; and ii) the modeling of the dynamics of the microstation. The dynamic model was built with the in-house developed Dynamic Error Budgeting Tool, which uses dynamic substructuring to model 6 degrees of freedom rigid body systems. This work discusses the trade-offs between rotation-related parameters affecting the sample-to-optics stability and the experiment resolution in the frequency domain integrated up to 2.5 kHz.

INTRODUCTION

The MOGNO beamline [1] is the hard x-ray micro- and nano-computed tomography (CT) beamline at Sirius, the 4th generation synchrotron light source at the Brazilian Synchrotron Light Laboratory (LNLS). As illustrated in Fig. 1, the beam is generated at a dipole, passes through a slit, and is primarily focused in the horizontal plane with an elliptical mirror (M1). Next, the beam's focus size (120 nm×120 nm) and position, 3.1 mrad conical divergence, and energy (21.5 keV, 39.0 keV, and 67.7 keV), is finally achieved through a Kirkpatrick-Baez (KB) mirror system, with two stripes and multi-layer coating (Tungsten and Boron Carbide), which allows the beam to reach the sample with a photon flux of 9×10^{11} ph/s. The main detector of the beamline is a PiMega 135D [2], located 27 m away from the focus, which delivers a maximum frame rate of 2×10^3 fps with a 85 mm × 85 mm sensor consisting of a 1536 × 1536 pixel array.

The sample may be at one of the two experimental stations of the beamline: the nanostation, currently under commissioning; or at the microstation, now under construction, and whose error budget is the main subject of this work. Both take advantage of the high photon flux and high frame rate

* gabriel.baldon@lnls.br
† guilherme.sobral@lnls.br
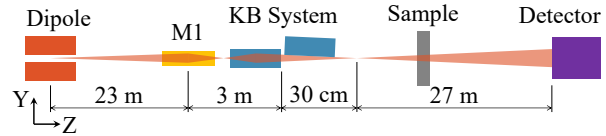
Figure 1: The MOGNO beamline layout. Approximate distances. Z is parallel to the beam, and Y is the vertical upwards.

of the detector to execute time-resolved CT scans, where they can be acquired periodically to observe transient phenomena in in-situ experiments, such as flow through porous media. The time resolution for the nanostation is limited at 5 s, and, for the microstation, at 0.5 s. Additionally, both stations were designed to allow high-throughput CT scans, where the samples are exchanged by a robot without the need of the researcher doing it manually, which greatly improves the speed of experiments with large batches.

The main difference between the stations is the resolution and field of view (FOV): the nanostation was designed to perform CT scans at higher resolution at the cost of smaller FOV and smaller sample sizes. Its sample stage allows movement on a 7 m-long granite rail along the beam direction, resulting in experiments that can range from 120 nm to 13 µm resolution and from 150 µm to 20 mm FOV; the microstation will have a 30 m-long rail, resulting in resolutions between 500 nm and 55 µm, and from 800 µm to 85 mm FOV.

In this work, the objective is the development of a model to analyze the disturbances and the error budget of the microstation. As source and detector stabilities have been designed to meet the more demanding requirements of the nanostation, the main source of error for the microstation is the vibration of the sample itself.
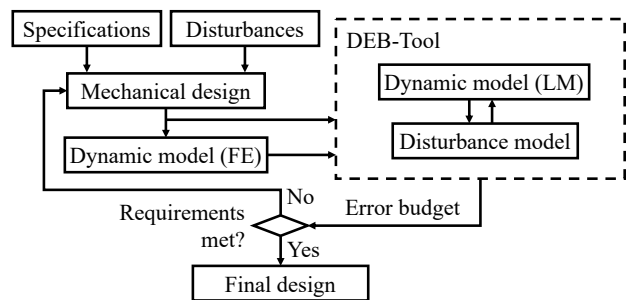
Figure 2: The specifications and disturbances are boundary conditions to the design, which is iterated to meet the requirement, attested through models. Here, FE means finite element, and LM means lumped mass. Adapted from [3].

FIRST RESULTS OF A NEW HYDROSTATIC LEVELING SYSTEM ON TEST PROCEDURES AT SIRIUS

W. R. Heinrich[†], G.R.S. Gama, G.J. Montagner, E. Teixeira, S.P. Oliveira

Setup Automação, Campinas, Brazil

R. B. Cardoso, L. R. Leão, S. R. Marques, R. T. Neuenschwander

LNLS/CNPEM, Campinas, Brazil

Abstract

The Hydrostatic Leveling System (HLS) is commonly employed in Structural Health Monitoring (SHM) to anticipate issues in large-scale structures. Particularly in structures like particle accelerators, it is used in high-precision alignment, where small differences in elevation such as terrestrial tides, could affect machine operation. This study outlines the development and evaluation of the first HLS based in Linear Variable Differential Transformer (LVDT) and were used to monitor the structure at LNLS/CNPEM, Brazil, from 2020 to 2023. A comparative analysis with a capacitance-based off-the-shelf HLS was executed, and experimental data analyzed through Fast Fourier Transform (FFT) confirmed the presence of tidal components in both HLS's data. Additionally, the correlation between level and temperature data was demonstrated by Pearson coefficient. The Setup-HLS device, developed with support from Brazilian national resources, exhibited accurate measurements in building tilt and diurnal and semi-diurnal Earth tide variations. Future researches include a calibration jig and an online verification system. This research provides a viable alternative to existing HLS systems.

INTRODUCTION

The Hydrostatic Leveling System (HLS) is a precision measurement and monitoring system designed to detect differences in elevation between points in the system, typically achieving submicrometric precision and repeatability on the order of microns. This is accomplished by measuring the fluid's height difference, usually water, contained in a recipient, and the inclination between two points in the system where two sensors are located. Various technique principles are employed in HLS systems, including fiber optic and interferometric methods [1], ultrasonic technologies [2], capacitance and dielectric measurements [3], as well as mechanical and optical approaches [4].

The system is applied in diverse fields such as monitoring sea levels, water reservoirs, groundwater, dams, seismic events, building foundations, tunnels, traffic of heavy vehicles, and alignment of particle beams in accelerators. Generally, HLS is widely used in Structural Health Monitoring (SHM) to predict potential structural issues in large-scale equipment and facilities.

During the development of this system, it is crucial to meticulously isolate specific phenomena and sources of uncertainty that may influence measurement results,

including tidal forces. Tidal forces result from spatial gradients in the gravitational field strength originating from celestial bodies. This gravitational phenomenon induces the elongation of the body experiencing the tidal force along the axis aligned with the center of mass of the attracted body.

The consequences of tidal forces encompass various occurrences on Earth, such as ocean tides, earth's rotation, tidal heating, tidal locking and terrestrial tides (or solid-earth tides). Careful consideration of tidal forces is essential for accurate and reliable HLS measurements.

On Earth, the principal manifestation of this gravitational interaction arises from the Moon's and Sun's gravitational influences, leading to the periodic oscillation of the semidiurnal of terrestrial tide, with a typical amplitude of approximately 0.55 meters [5]. Moreover, terrestrial tides and localized gravitational field variations contribute to minute perturbations in particle accelerator systems, on the order of 1 millimeter, as evidenced by measurements conducted in Geneva at the Large Electron-Positron Collider (LEP). The standard model of electroweak interactions requires precise knowledge of the LEP beam energy with an accuracy of 20 ppm. However, small fluctuations, induced by tidal effects, resulted in a beam energy variation of approximately 120 ppm [6].

HLS has been employed to precisely measure the tidal effect, which has well known periods and frequency components, so detecting these frequencies in the results measured by the HLS is a step in the sensor validation.

This study introduces a novel and robust HLS, denoted as Setup-HLS, which represents a pioneering application of the Linear Variable Differential Transformer (LVDT). The device is capable to quantify terrestrial tidal influences on level variations at the micrometer scale and was used for testing and structural monitoring at the Laboratório Nacional de Luz Síncrotron (LNLS-CNPEM) in Campinas, São Paulo, Brazil, from the years 2020 to 2023 [7, 8].

DEVICE CONCEPT

The Setup-HLS system employed in this study is an innovative Brazilian HLS, funded by FAPESP/FINEP. It was specifically designed for implementation at the Sirius facility and achieved a Technology Readiness Level of 9 (TRL 9) during its development, indicating proven functionality in an operational environment [9]. The configuration of the Setup-HLS comprises a cylindrical enclosure made of anodized aluminum, housing instrumentation responsible for converting analog water

DEVELOPMENT OF A MIRROR CHAMBER FOR SHINE PROJECT

F. Liu†, T. Wu, S. He, H. Yuan, X. Zhang, Z. Wang, W. Li

Center for Transformative Science, ShanghaiTech University, Shanghai, China

L. Zhang, J. Chen, W. Zhu

Shanghai Advanced Research Institute, CAS, Shanghai, China

Abstract

A 5-DOF mirror chamber test system was developed to adjust offset mirror or distribution mirror for the SHINE project. Two linear guides were used for horizontal translation and coarse pitch adjustments. Three vertical gearboxes were used for height, roll and yaw adjustments. In the vacuum, a fine flexure structure was engineered for the fine pitch adjustment with a piezo actuator. To prevent the cooling vibrations, the cooling module was separately fixed and the heat from the mirror was conducted by Ga/In to the cooling blade. Pitch angular vibration were measured by several equipment under different conditions. Results showed that the pitch angular vibration was below 40 nrad above 1 Hz without active vibration control, and below 10 nrad with active vibration isolation system.

INTRODUCTION

Shanghai HIgh repetitioN rate XFEL and Extreme light facility (SHINE) started the ground breaking on 27th April, 2018. The whole facility is 3.1 km long installed in the tunnels about 29 meters underground. The whole facility was shown in Fig. 1. The first 1.5 kms were for the linac to accelerate the electron bunches up to 8 GeV, and generate X rays in the range between 0.4~25 keV within 3 beamlines. In the Near Experimental Hall (NEH) and Far Experimental Hall (FEH), 10 endstations were built in the first phase. As shown in Fig. 1, there was highway lying along the facility, and a river passing across the tunnel between Shaft 3 and Shaft 4, and a subway Line 13 running right above the tunnel between Shaft 4 and Shaft 5. To investigate the vibration transfer between the ground to the optics, a mirror chamber system was developed according to the requirements of M1 adjustments.

MIRROR CHAMBER SETUP

According to the requirements for the M1 adjustments, the specifications were listed in Table 1 and the schematic of the mirror chamber was shown in Fig. 2. The X translation was used to move the mirror in and out of the beam when necessary, the Z translation was intended to change the stripe of the mirror, however, considering the ground settlement of the tunnel, 100 mm adjustment range was designed. To make a stable and reliable chamber system, most of the adjustments were put outside the vacuum, and the vacuum chamber was supported separately.

The whole mirror chamber system was shown in Fig. 3, the base was made of two granites, in between were four air bearings, and two linear translations were installed in the two ends. When the translation move in the same direction, horizontal movement was realized, when they move in opposite directions, a pitch angle would appear (detailed in Fig. 4) [1]. For the vertical translation and the roll and yaw adjustment, since no fine adjustments were necessary, ordinary gearboxes were employed, however, the stiffness in the radial directions were carefully designed to meet pitch angle stabilities. And the contacts of the three kinematic supports were also optimized for better stability issues. To minimize the influence by water cooling, the mirror was cooled by a copper blade inserted in an Indium Galium eutectic bath on the mirror, and the cooling tubes were fixed to a separate support decoupled to the mirror holder as shown in Fig. 5. Considering the vertical translation when exchanging the stripes on the mirror, the water cooling movement was coupled to the vertical translation of the mirror holder by connecting the two gearboxes with a shaft.

Figure 1: Topview of the SHINE facility.

† liufang@shanghaitech.edu.cn

ANALYSIS OF HAZARDS IN A FLAMMABLE GAS EXPERIMENT AND DEVELOPMENT OF A TESTING REGIME FOR A POLYPROPYLENE VACUUM WINDOW

S. Bundrock, E.X. Li, D.M. Smith, B.E. Billinghurst

Canadian Light Source Inc., Saskatoon, Canada

Abstract

Far Infrared Spectroscopy (Far-IR) is a bend magnet infrared beamline at the Canadian Light Source. The beamline utilizes a gas cell loaded with experimental gas which light is bounced through and a spectrometer to measure the absorption of the gas. For an experiment at Far-IR utilizing methane and nitrogen at 100 K temperatures, issues with icing and inconsistent absorption gradients were noted at the Polymethylpentene Rigid Plastic (TPX™) window separating the cell filled with the flammable gas mixture from the vacuum of the spectrometer. The possibility of replacing the existing windows with new 50-micron thick polypropylene window was investigated. Material properties were not available for polypropylene at the operating temperature of the experiment. Due to the hazardous nature of the gas being held back a hazard analysis was carried out to identify potential risks and mitigations for the change. Additionally, with material properties unavailable, a testing regime was established to ensure the polypropylene could survive in the experimental environment. The experiment was successfully completed. using the modified window assemblies.

INTRODUCTION

The Far-IR beamline uses several different Fourier Transform Infrared Spectroscopy (FTIR) methods during operation. When a FTIR method is to be utilized with a gas the beamline is equipped with gas cells of a known light path length. Some experiments require the use of flammable or potentially hazardous gasses. For safe handling of these gasses the beamline is equipped with a hazardous gas exhaust system; an explosion proof vane pump is used for post-experiment gas removal into the dedicated exhaust system. Far-IR's 2 m gas cell has a volume of 300 L and includes a cold nitrogen gas cooling system used to maintain cell contents at cryogenic temperatures when required. The 2 m cell is separated from a Bruker© spectrometer by a pair of windows; several window materials can be used. One such material is Polymethylpentene Rigid Plastic (TPX™). The windows separate the rough vacuum of the spectrometer from the cell's experimental conditions while simultaneously allowing synchrotron light to pass through. The 2 m cell and Bruker© spectrometer can be seen in Fig. 1.

In one instance, complications with the TPX windows at cryogenic temperatures interfered with the collection of quality data. A proposed modification of the windows to address these complications introduced uncertainty as to whether the modified windows could survive the experimental operating conditions.

Figure 1: Far-IR 2m gas cell and Bruker© spectrometer.

BACKGROUND

Two primary issues arose with the 6.6 mm thick TPX windows during an experiment. This experiment used the 2 m cell with a 1 atm methane mixture at 100 K. Ice would form in-vacuum on the spectrometer side interfering with transmission through the windows. TPX has a temperature-dependant absorption spectrum and as the methane moved within the cell, the temperature of the windows would fluctuate. This fluctuation produced inconsistent experimental conditions and unrepeatable results. Therefore, alternate window solutions were investigated. A requirement for a new window material was transparency in the visible range as a laser is used to align optics prior to an experiment. The FAR-IR beamline staff proposed 50 µm polypropylene windows as they had been observed to have better absorption spectra in previous published work [1].

OBJECTIVES

1. Design a new window assembly to eliminate icing and minimize absorption problems.
2. Complete a hazard analysis of risks introduced by window modification.
3. Test if proposed polypropylene windows can safely withstand experimental conditions.

FINAL DESIGN AND CONSIDERATIONS

The new window assemblies featured numerous modifications from the original TPX window to address the issues observed. To address ice formation, a two-window design with internal vacuum break was adopted. This design is pictured in Fig. 2. The added vacuum gap minimized icing by reducing heat transfer from the methane, maintaining the spectrometer side window at a higher and more stable temperature. Creating a smaller vacuum space reduced the

FEM SIMULATIONS FOR A HIGH HEAT LOAD MIRROR

J. Seltmann†, H. Geraissate, M. Hoesch,

Deutsches Elektronen-Synchrotron DESY, Hamburg, Germany

Abstract

At the variable polarization XUV beamline P04 of PETRA III the first mirror is used to switch the beam between the two branches of the beamline. The heat load on this white beam mirror is dependent on the degree of polarization and the energy of the first harmonic of the synchrotron radiation. For this project the water cooled "notched" mirror approach by Khounsary, and Zhang et al., has been evaluated with FEM simulations. These show promising results for linear horizontal (LH) polarization in which the heat load profile is aligned with the mirror length. For linear vertical (LV) polarization the heat load is concentrated in the mirror centre, which violates the basic concept of the "notched" mirror design and therefore the simulation results indicate only poor performance. To compensate for this a secondary cooling loop has been implemented and will be shown to improve the performance for the LV case significantly. Additionally, a new design approach is evaluated to reduce the peak temperatures of the mirror, which otherwise ranged at 140-180 °C.

P04 VARIABLE POLARIZATION XUV BEAMLINE

Beamline P04 at the 6GeV storage ring PETRA-III is a XUV to soft x-ray facility in the range of 250-3000 eV. The 5 m long APPLE-II undulator allows to change polarization rapidly while achieving high brightness and coherence. The frontend consists of several apertures of which the smallest has a diameter of 4mm. A set of a vertical and a horizontal slit can be used to further reduce the footprint of the beam. The first set of optics at 35 m from the undulator is used to switch between the two branches of the beamline.
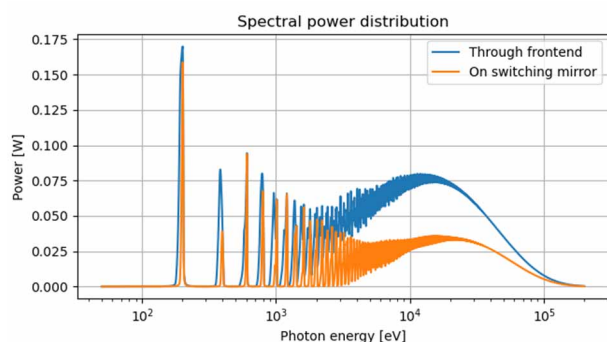
Figure 1: Spectral power distribution with open frontend apertures (blue) and on the mirror (yellow).

This switching mirror unit (SMU) consists of two mirrors facing each other, were one mirror at a time is used to reflect horizontally into its beamline branch at a grazing incidence of 0.8° [1].

---

† Joern.seltmann@desy.de

HEAT LOAD CONSIDERATIONS

High K (up to K=7.1) operation of the undulator combined with the high electron energy of the storage ring results in high on-axis heat load due to higher harmonics contributions. Figure 1 shows the simulated spectral power distribution done with SPECTRA [2].

The high flexibility in terms of polarization of the APPLE-II undulator leads to different power distributions for each polarization setting, as the plots in Fig. 2 from OASYS-SRCalc show [3-4].
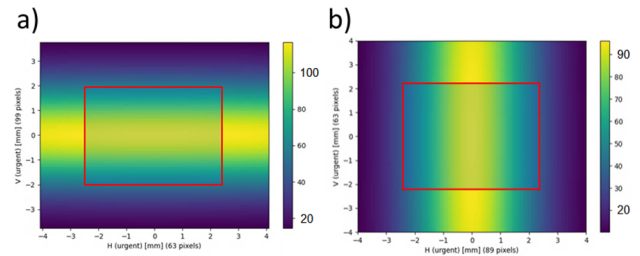
Figure 2: Power density [W/mm²] distribution with open frontend apertures for a) LH and b) LV polarized light. The footprint on the mirror is marked in red.

For LH polarization we expect the highest power on the mirror which will be distributed along the whole length of the mirror (400 mm). LV polarized light has lower absolute values but the power density is focussed in the centre of the mirror (Table 1).

Table 1: Polarization Cases

Polarization	LH	LV	Circular
Total power [kW]	3.90	3.21	0.6
Mirror power [kW]	2.1	1.5	0.3
Max. power den. [W/mm²]	1.66	1.30	0.13

Besides LH and LV polarization all other linear orientations are also possible but aren't broached by this study. The case of circular polarization is easier in terms of heat load considerations, since the higher harmonics are distributed radially and therefore easily cut by the frontend apertures.

NOTCHED MIRROR DESIGN

The water cooled "notched" mirror approach by Khounsary [5] and Zhang et al. [6] has been chosen instead of an internal cooling design as shown by Reininger et al. [7]. This design uses the bulk material of the mirror for stabilization, by cooling only on a small segment on the mirror sides, separated by a notch. By changing the depth of the notch, the profile of the mirror centreline can be shaped for a known heat load. This design favours a uniform heat load distribution along the mirror length, which is incompatible with varying heat loads at first.

DEVELOPMENT OF A VACUUM CHAMBER DISASSEMBLY AND ASSEMBLY HANDCART

X. J. Nie*, J. X. Chen, H. Y. He, L. Liu, R. H. Liu, C. J. Ning, G. Y. Wang, J. B. Yu,
Y. J. Yu, J. S. Zhang, Institute of High Energy Physics (IHEP CSNS) China
also at Spallation Neutron Source, Dongguan, China
L. Kang, Institute of High Energy Physics (IHEP) Accelerator Center, Dongguan, China

Abstract

This paper developed a dedicated disassembly and assembly handcart for CSNS magnetic alloy cavity vacuum chamber. The optimal supporting section structure was determined by the use of ANSYS to analyze the strength of different sections. The stress situation of the handcart was improved by adding an extension rod at the end of the handcart. The installation position of the handcart was determined by the center position of the associated equipment. The development of the disassembly and assembly handcart structure was completed through structural optimization, disassembly and assembly process analysis, and positioning scheme design. The development of a handcart can improve the positioning accuracy of the vacuum chamber and prevent damage to the vacuum chamber during disassembly and assembly process.

INSTRUCTIONS

Magnetic alloy cavity is an important device for CSNS power increase. The length of its vacuum chamber is about 1.8 m with the weight of 75 kg. The vacuum chamber needs to pass through several cavities during the assembly-disassembly of it. And it is necessary to protect the insulating ceramics in the middle of the vacuum chamber. Meanwhile, just one small gap was left between the vacuum chamber and cavity to ensure the performance of the cavity. The smallest gap was only 3.5 mm. These factors make disassembly and assembly of the vacuum chamber very difficult and challenging. So, a dedicated handcart was developed for the disassembly and assembly of vacuum chamber.

OVERALL STRUCTURE DESIGN

The overall structure of the handcart is determined by the functions it is intended to achieve and working conditions [1]. First, the handcart is used to support the vacuum chamber steadily. And then it is required to smoothly move to the installation position of the vacuum chamber. To achieve the above functions, the overall handcart structure is designed as the following picture, which is composed of a base, support part, and guide part. The structure of the handcart is shown in Figure 1.

SUPPORT STRUCTURE DESIGN

The support beam is extended into the interior of the vacuum chamber during disassembly and assembly, support-
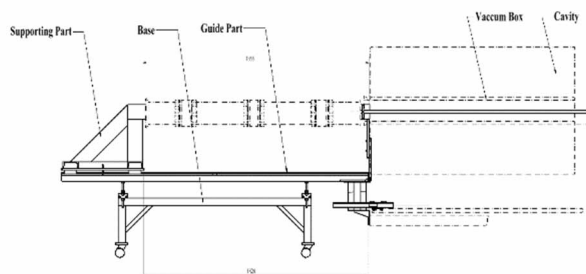
Figure 1: Overall structure of the handcart.

ing the weight of the vacuum chamber. Its strength and deformation need to be within a reasonable range. Based on the working condition of the support beam, it is determined that the force acting on the support beam is a cantilever structure. Several different cross-sectional shapes of support beams were selected for comparison. And the one with the best stress conditions was determined as the support beam. I-beams, rectangular tubes, and circular tubes were selected for comparison in usual materials. One end of the support beam was fixed and the load of the vacuum chamber was uniformly acted on the supporting surface [2]. The calculation results were shown in Table 1.

Table 1: Stress and Deformation for Support Beams with Different Cross-sectional Shapes

Cross-sectional shapes	Maximal stress [MPa]	Maximal deformation [mm]
I-beam	17.6	0.67
Rectangular	21.0	0.97
Circular	26.6	1.12

The distribution of stress and deformation on the supporting beams of each section is shown in Figure 2.

From above results, it can be concluded that under the same load, I-beam has the best stress state. And it can also be found that there is still significant deformation under cantilever structure for I-beam. If the cantilever structure can be eliminated, the stiffness of the support beam can be greatly improved. Figure 3 shows the stress and deformation distributions of the support beam under two fixed ends. The maximum deformation is only 0.02 mm, and the maximum stress is only 4.9 MPa.

---

* niexj@ihep.ac.cn

OPTIMIZING INDIRECT COOLING OF A HIGH ACCURACY SURFACE PLANE MIRROR IN PLANE-GRATING MONOCHROMATOR*

Jie Chen#, Zimeng Wang, Xuewei Du, Minghao Lin, Qiuping Wang

NSRL, University of Science and Technology of China, Hefei, Anhui, P. R. China

Abstract

For the cooling of the plane mirror in VIA-PGMs (variable-included-angle plane-grating monochromators), the top-side indirect cooling based on water is preferred for its advantages, such as cheaper, easier to use, smart notches, etc, when compared to the internal cooling. But it also arises challenges to control the RMS residual slope error of the mirror, whose requirement is less than 100 nrad. This requirement is even hard to fulfill, when combined with 1) the asymmetry thermal deformation on the meridian of the footprint area during the energy scanning, 2) the high heat load deduced by the synchrotron light and 3) the no obvious effects of the classical optimizations, such as increasing footprint size, cooling efficiency or adding smart notches. An effective way was found after numerous attempts, which is to make the footprint area far from the mirror's edge to reduce the asymmetry of the thermal deformation except for leading to a longer mirror. This paper will illustrate how the asymmetry affects the mirror's residual slope error and then, focus on the relationship among the asymmetry of cooling and the distance to provide a reference for optical cooling.

INTRODUCTION

In recent years, numerous light sources are developing synchrotron facilities with higher brightness, smaller divergence angle and more stability. During the development, the researching of the optics cooling of the beamline has draw much attention for the crucial role to realize these goals. There are so many articles focus on the cooling art of the first mirror because it bears the highest heat load among all the optics in a beamline [1-5]. However, for some VIA-PGMs in the downstream of the first mirror, few report about the cooling of optics in the PGM was found. And the cooling of the VIA-PGM had become an issue in some synchrotron facilities with high brightness and ultra small divergence angle, not only for its thermal working condition and high accuracy surface requirement of the mirror but also for its different optimization of cooling, compared to first mirror. This article will briefly list the common optimizations for the cooling of first mirror as references; then, based on a high heat load mirror of a beamline of Hefei Advanced Light Facility (HALF) [6], the limitation of these optimization are introduced; and at last, the reason and resolution are provided.

OPTIMIZATIONS FOR INDIRECT COOLING OF THE FIRST MIRROR

For water cooling solutions, indirect cooling technology is still the first choice in design, when considering drawback of the internal cooling optical components, such as the long supply period, expensive, difficult to maintain, etc. [7]. Further, the indirect cooling has the capacity to utilize the reverse thermal moment, local heat compensation, etc to improve the slope error of thermal deformation. This part briefly introduces the common optimization method of the first mirror cooling of the beamline.

From 1996, Khounsary et al. adjusted the width of the cooling area and the bias and the depth of the notches on the side of the first deflection mirror to change the temperature distribution, which diminished the meridian slope error of the central part of the footprint (Fig. 1(a)) [1, 7, 8]. The principle of the two method are same. The bending of the mirror can be substantially reduced or reversed by a reverse thermal moment generated from the temperature difference between different uniform temperature region. And the notch has a more obvious effect because it makes the temperature difference between the uniform temperature region larger, and thus the expands the balanced thermal moment.

From 2013, Zhang Lin et al. reported the method on cooling length tuning to optimize the edge effect of the first mirror and upgrade it via heaters, as shown in Fig. 1(b) [4, 9]. At the two ends of the spot area, the heat flow reduced and became zero out of the area. This sharp change in heat flow leaded to a large slope error in these area, which named the edge effect on meridian. The effect also affected the inner zone of the spot area except for the edge area. Zhang's method made the cooling length shorter than the spot length, which can rise the temperature of the two end locations, to compensate the effect.

In 2016, Corey Hardin et al. reported a cooling method based on liquid metal bath and surface shape tuning technique for horizontal deflection mirrors. This method decoupled the effect of fluid induced vibration to optical components during cooling. As Fig. 1(c), although the optical element used unilateral cooling, the structure of the mirror still retains a symmetrical design [10].

In 2022, Wang Shaofeng and Gao Lidan et al. illustrated another cooling method for horizontal deflection mirror. Different from the design of Corey Hardin, this is a structure of unilateral cooling, notches and asymmetry to simplify the processing and assembly, as in Fig. 1(d) [11].

Beyond the mentioned above, the slope error of thermal deformation can also be decreased by improving the cool-

OPTIMIZATION OF THERMAL DEFORMATION OF A HORIZONTALLY DEFLECTING HIGH-HEAT-LOAD MIRROR BASED ON eInGa BATH COOLING *

Jie Chen[#], Xuewei Du, Zimeng Wang, Minghao Lin, Qiuping Wang

NSRL, University of Science and Technology of China, Hefei, Anhui, P. R. China

Abstract

The synchrotron facilities are developing towards higher brightness, lower divergence, narrower pulse, higher stability, etc. Therefore, the requirements of the first mirror of the beamline, who bear high-heat-load, were also upgraded, and the performances of the mirror become affected easily by other factors, such as flow induced vibration, clamping force, etc. Indirect water cooling based on eInGa bath is regarded as an effective mean to solve these thorny problems in designing of the first mirror cooling. However, for the case a horizontal deflection mirror, the unilateral cooling method is usually adopted, resulting in some changes in the structure of the mirror. In this paper, a first mirror horizontally deflecting of Hefei Advanced Light Facility (HALF) are taken as an example to introduce the optimization method to achieve ultra-low slope error in the meridian direction. The results show that this optimization method provides a rapid design process to design the cooling scheme of the horizontally deflecting mirror based on the eInGa bath.

INTRODUCTION

In synchrotron facilities, the first mirror of the beamline has the advantages of substantially reducing the heat load of downstream optics, suppressing high order harmonics and radiation shielding [1]. The cooling method of the first mirror, depended on the heat load power density and total heat load on it, can adopt direct water cooling, indirect water cooling or liquid nitrogen indirect cooling schemes [2-5]. Since the power density on the first mirror has a good uniformity and symmetry in the meridian direction, an indirect water cooling, combined with the thermal deformation optimization method via passive reverse thermal moments, were developed [6, 7]. With the improvement of the brightness, stability and low divergence of the synchrotron light source, the surface shape requirement of the first mirror of the beamline has reduced to the order of hundreds nano-radian, which also leads challenges, such as the flow induced vibration caused by the coolant, the clamping deformation caused by the liquid cooled copper plates when cooling the mirror and the non- uniformity of the thermal conductance between contact blocks, etc. The indirect water-cooling scheme based on eInGa bath is regarded as an effective means to solve these problems [8, 9]. However, for the case that the first mirror is a horizontal deflection one, the

optimization method is different because of the changes of cooling structure, such as: 1) the side of the mirror needs to be slotted for holding eInGa; 2) the cooling area changes from bilateral to unilateral. These factors will significantly affect the design and optimization of the mirror and its cooling structure. Taking a high-heat-load first mirror of the beamline of Hefei advanced light source (HALF) as an example, this paper introduces the optimization method to achieve the ultra-low meridian slope error in the meridian direction of the high heat load horizontally deflecting mirror.

THERMAL DEFORMATION OPTIMIZATION METHOD BASED ON eInGa BATH COOLING

The eInGa bath cooling method for the first mirror of the beam line has many advantages [8, 10]. First, the eInGa liquid metal has a very high and uniform heat transfer coefficient at the contact interface between components, up to 100,000 W/m²K [10]. Although the thermal conductivity is only 28 W/m•K, it still turn out to be an excellent thermal interface material. Secondly, the viscosity of eInGa liquid alloy is very low, only 1.99×10^3 Pa•s, a factor of two greater than that of water [11], makes the vibration transfer ability extremely bad, which can effectively decouple the flow induced vibration transmitted from the water-cooled copper plate to the optical element. Third, the liquid metal can avoid the clamping force on the optics since no direct contact between the cooling mechanism and the mirror. However, the application of cooling based on the eInGa bath will also have some influences on the mirror body and the cooling structure.

Limitation

In the first mirror of vertical deflection, eInGa grooves can be applied on the top surface and near the edges of it [8]. This cooling topology is similar to the cooling efficiency of the double-sided clamping structure [12]. The difference is that since the insertion of the cooling structures in the mirror body, the depth of the notches will also increase, but the level of the reverse thermal moment on each side will not change much.

However, in the first mirror of horizontal deflection, the eInGa groove can only be applied on the top surface of the mirror, i.e., on one side of the incident plane, as shown in Fig. 1. This cooling structure is very different from the previous: 1) The cooling efficiency is reduced. As the cooling structure is changed to one side, the cooling efficiency is reduced by twice compared with the two-

THE HEAT LOAD CALCULATION IN THE GRATING-BASED BEAMLINE AT HEFEI ADVANCED LIGHT FACILITY (HALF) *

Zimeng Wang[†], Jie Chen, Xuewei Du, Qiuping Wang and Donglai Feng, National Synchrotron Radiation Laboratory, University of Science and Technology and China, Hefei, Anhui, China

Abstract

The light emitted by the 4th generation synchrotron radiation (SR) light source is more concentrated. Therefore, its heat load causes more severe thermal deformation on the beamline optics than the 3rd generation SR light source. The requirement on the optical element surface quality is also higher to achieve better spectral resolution, coherence preservation and focusing. The precise calculation of heat load on the optical elements is fundamental for the thermal analysis including cooling method and thermal deformation simulation. A heat load calculation code has been developed for SR beamline optics, which consists of SR source calculation module for precise power density distribution, mirror reflectivity module and grating efficiency module. Therefore, it can be applied to mirrors, crystals and gratings.

This code has been used to calculate the heat load of BL10 - the Test Beamline optics at Hefei Advanced Light Facility (HALF). The heat absorbed by the first three optical elements are precisely calculated, including a toroidal mirror, a plane mirror and a plane grating.

INTRODUCTION

To quantitatively calculate the heat load on the synchrotron radiation (SR) beamline optical elements, it is necessary to combine the angular distribution calculation of the source power density with the calculation of optical element transmission efficiency, including the reflectivity of the mirrors and the diffraction efficiency of the gratings. SRCalc [1, 2] is one of the software that calculates the optical elements. However, SRCalc only contains mirror and crystal heat load calculation. Currently, there is still no software available that enables the calculation of grating heat load. Therefore, in beamline design, the calculation of grating thermal load is often estimated.

The light source and efficiency calculation programs mentioned earlier have been completed. Therefore it is possible to achieve precise calculations of the heat load for all optical elements, including the gratings. This paper will take the Test Beamline (BL10) in Hefei Advanced Light Facility (HALF) [3] as an example of heat load calculation including mirrors and gratings.

HALF TEST BEAMLINE HEATLOAD CALCULATION

HALF is a 4th generation SR light source with the emittance of 73.2 pm•rad in both x and y directions. The storage ring energy is 2.2 GeV and the current is 350 mA. The Test Beamline (BL10) is an undulator-based beamline. The undulator consists of 98 periods with 40 mm as its period length.

The Test Beamline aims to use a grating monochromator with extra high spectral resolving power of 10^5@400 eV, ranging from 275 eV to 1500 eV in the first-version optical design. High-quality optical surface is required with overall slope error from 100 – 200 nrad (rms). In order to control the thermal-induced slope error, the precise heat load distribution absorbed by the optical elements should be calculated, which is fundamental for cooling system design and simulation. Here, the undulator source angular power density distribution up to 80th order is calculated.

Optical Design

The Test Beamline adopted the collimated SX-700 grating monochromator as shown in the Fig. 1. The toroidal mirror M$_1$ collimates the source light in the vertical direction and focus it onto the exit slit in the horizontal direction. The plane mirror (PM) reflects the incoming light from M$_1$ to the centre of plane grating GR. The light diffracted from GR is focused by the cylindrical mirror M$_2$ to the exit slit in the vertical direction. The grazing incident angle and M$_1$ and M$_2$ are 2°.The heat load of M$_1$, PM and GR will be calculated at 275 eV.
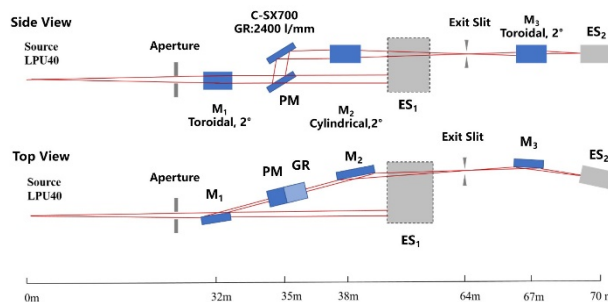
Figure 1: The beamline optical design.

Mirror Heat Load Calculation

The heat load of the mirrors is calculated by combining the source property and mirror reflectivity calculation. The spatial power density distribution can be calculated from the angular distribution of the source power density $\frac{d^2 P_{\sigma,\pi}^n}{d\varphi d\psi}$ [4]:

MECHANICAL ANALYSIS AND TESTS OF AUSTENITIC STAINLESS STEEL BOLTS FOR BEAMLINE FLANGE CONNECTION

T. T. Zhen, L. J. Lu†, S. Sun, R. B. Deng, F. Gao, H. X. Deng
Shanghai Advanced Research Institute, Chinese Academy of Sciences, Shanghai, China

Abstract

Cryogenic tests of 1.3 GHz superconducting accelerator cryomodule for the Shanghai Hard X-ray Free Electron Laser Installation Project (SHINE) are in progress. For better performance, a study of mechanical analysis and tests of austenitic stainless steel bolts for beamline flange connection has been done in preliminary work. In order to satisfy the residual magnetism and strength, high-strength austenitic stainless steel bolts are selected. For higher sealing performance, the torque coefficient is determined by compression test, the lower limit of yield of the bolts is obtained by tensile test, then the maximum torque applied to the bolts under real working conditions can be obtained according to the relationship between preload and torque. A finite element model is established to get the deformation curve of the gasket, and the measured results of gasket thickness are compared to ensure the reliability of the simulation. The deformation curve of the gasket is used to calculate the change of compression force under the temperature cycling load (cool down and warm-up). Finally, the results of residual magnetism show that the bolts have a negligible effect on magnetic field.

INTRODUCTION

1.3 GHz superconducting accelerator is characterized by extremely good vacuum condition [1-3]. Many of the flanges that are along the beamline immersed in the insulation vacuum. The connection construction is shown in Figure 1, which has to guarantee a reliable sealing performance both at room and cryogenic temperature, also after warm-up.
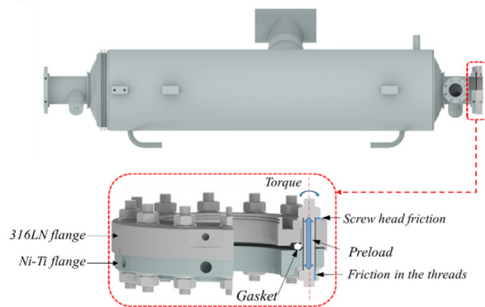
Figure 1: Beamline flange connection.

The mechanical properties, the applied torque, the preload changes with temperature of the bolts, etc., all affect sealing quality.

† lulj@sari.ac.cn

TENSILE TEST

For the requirement of the residual magnetism and higher fracture toughness at cryogenic temperature, 316LN high-strength bolts are selected. The mechanical properties of the bolts prepared by a domestic and a foreign company respectively have been tested at room temperature. The size [4] of the tensile samples is shown in Figure 2. Four samples are tested and the average value is used for discussion.
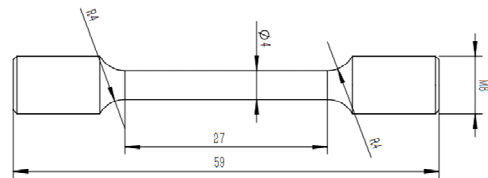
Figure 2: Sampling map.

All samples are tested for mechanical properties at room temperatures. The engineering stress-strain curves of some tensile samples are shown in Figure 3.
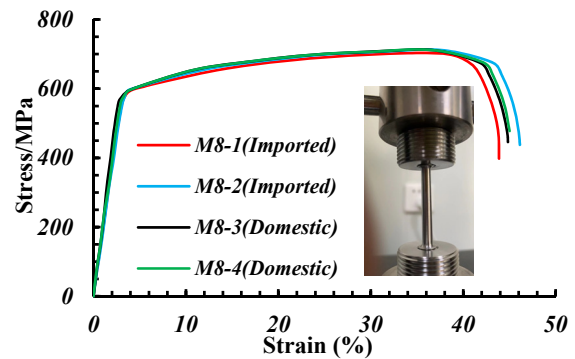
Figure 3: Engineering stress-strain curves of the samples.

The results including R_{el} (Lower limit of yield), UTS (Ultimate tensile strength) and EL (Elongation), are shown in Table 1. From Table 1, it can be seen that the average R_{el} of the bolts is 595 MPa, and the EL is greater than 40 %.

Table 1: Tensile Test Results at Room Temperature

Coding	R_{el} MPa	UTS MPa	EL %
Imported-1	598	711	44
Imported-2	596	710	46
Domestic-3	586	704	45
Domestic-4	603	712	45

SHAPE OPTIMIZATION DESIGN OF MONOCHROMATOR PRE-MIRROR IN FEL-1 AT S³FEL*

Zhongmin Xu†, Chuan Yang, Yinpeng Zhong, Weiqing Zhang[1]

Institute of Advanced Science Facilities, Shenzhen, China

[1]also at Dalian Institute of Chemical Physics, Chinese Academy of Sciences, Dalian, China

Abstract

For the monochromator pre-mirror in FEL-1 at S³FEL, the deformation induced by high heat load result in severe effects on the beam quality during its off-axis rotation. To meet the pre-mirror shape error requirement for X-ray coherent transport, an integration of passive cooling and active heating systems for thermal management of the monochromator pre-mirror has been proposed, developed, and modelled. An active heating system with multiple electric heaters is adopted to compensate for the pre-mirror shape further. Finally, using MHCKF model, the optimization of multiple heat fluxes generated by all electric heaters was accomplished. The results show that the thermal management using passive cooling and active heat schemes is effective to obtain high-precision surface shape for the pre-mirror.

INTRODUCTION

The Shenzhen Superconducting Soft X-ray Free Electron Laser (S³FEL) is a new light source under construction phase at Institute of Advanced Science Facilities (IASF), Shenzhen. S³FEL consists of 2.5 GeV CW superconducting linear accelerator and four initial undulator lines, aiming to generate X-rays between 40eV and 1 keV at rates up to 1 MHz [1]. According to the Maréchal Criteria [2], in order to meet the needs of FEL wavefront coherent transmission, the height error RMS of the pre-mirror mirror should be less than 0.9 nm and the slope error RMS should be less than 100 nrad, which are more stringent than those of the mirrors in synchrotron radiation facilities. Therefore, it is necessary to choose an appropriate shape control scheme.

PRE-MIRROR MODEL AND BOUNDARY CONDITIONS

The structure of the monochromator shown as Figure1 is different with that of LCLS-II, European XFEL [3]and SwissFEL. It consists of a front plane mirror and plane variable-line-spacing grating. During the course of the pre-mirror off-axis rotation, the spot centres of different wavelengths on the surface of are moving. Meanwhile, the pre-mirror will absorb high heat load, resulting in serious local bulging and bending deformation. If the traditional cooling

methods are adopted, the mirror shape is unlikely to meet all of the working conditions.
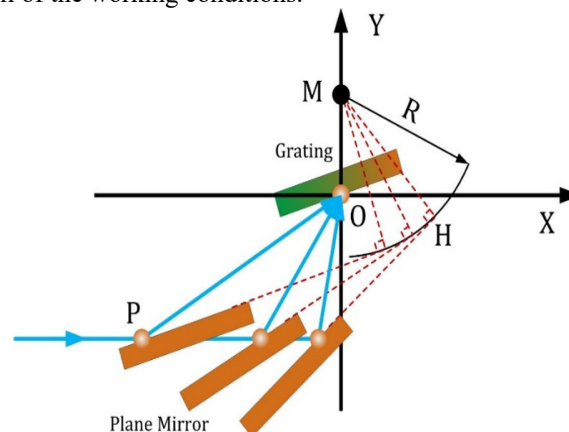
Figure 1: Structure of Grating monochromator in FEL-1.

Power density distributions of wavelength 1-3 nm absorbed by the pre-mirror in beamline FEL-1 are shown Figures. 2, 3 and 4. And the footprints information for three wavelengths are listed in Table 1. Footprint centre of 2 nm X-ray is located at the centre of pre-mirror, while those of other two wavelengths on either side. Though their maximum power density for each wavelength is not much different, the absorbed power of each wavelength is quite different.

Table 1: Footprints Information for Three Wavelengths

Wavelength	Length of Footprint	Absorbed Power
1 nm	150 mm	5.46 W
2 nm	174 mm	11.2 W
3 nm	200 mm	16.65 W
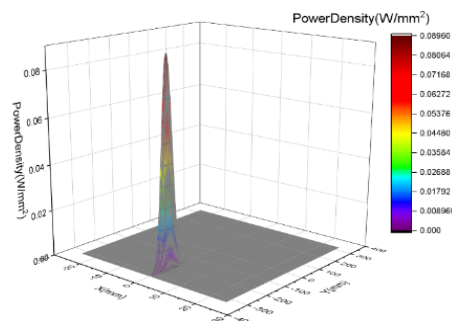
Figure 2: Power density distribution of wavelength 1 nm.

STUDIES ON THE INFLUENCES OF LONGITUDINAL GRADIENT BENDING MAGNET FABRICATION TOLERANCES ON THE FIELD QUALITY FOR SILF STORAGE RING

J. Zhu[†], M. Zhang[†], C. Wang, D. Liang, Y. Shi

Institute of Advanced Science Facilities, Shenzhen, China

Abstract

The advanced storage ring of 4th generation synchrotron radiation facility, known as the diffraction-limited storage ring (DLSR), is based on multi-bend achromat (MBA) lattices, which enables an emittance reduction of one to two orders of magnitude pushing beyond the radiation brightness and coherence reached by the 3rd generation storage ring. The longitudinal gradient bending (LGB) magnets, with multiple magnetic field stages in beam direction, are required in the DLSR to reduce the emittance. The permanent magnet based LGB magnets are selected for the Shenzhen Innovation Light-source Facility (SILF) due to the advantages of operation economy, compactness and stability compare to the electro-magnet. In this paper, the influences of typical LGB magnet fabrication tolerances on the field qualities are presented using a dedicated parameterized finite element (FE) model, including the poles height tolerances, the pole tip inclination (in different orientations).

INTRODUCTION

Benefit from supporting the cutting-edge researches in various disciplines and industry applications, such as physics, material, bioscience, medicine, electronics, chemistry, etc., the advanced storage ring of 4th generation synchrotron radiation facility based on multi-bend achromat (MBA) lattices (also known as the diffraction-limited storage ring, DLSR) is emphasized and constructed world widely, pushing beyond the radiation brightness and coherence attained by the 3rd generation storage ring [1]. In the Institute of Advanced Science Facilities (IASF, Shenzhen, China), a storage ring of this type in Shenzhen Innovation Light-source Facility (SILF) is proposed and under preliminary design [2]. The longitudinal gradient bending (LGB) magnets, with multiple field stages in beam line direction, are required in DLSR design to reduce the electron beam emittance. Concerning the advantages of operation economy, compactness and stability compare to the electro-magnet, the permanent magnet (PM) based LGB magnets are selected and designed for SILF storage ring.

Typical structure of the LGB magnet is shown in Fig. 1. Field of five stages is first designed by adjusting the PM block number, size and easy magnetization direction in each module. The pole profile is optimized to fulfill the field quality requirements in good field region, i.e. the homogeneity of the field in transverse direction and / or the integrated field in beam direction (denoted as TFH and IFH respectively). The C-shape design has an open access to the magnet gap which simplifies the beam pipe installation and

† email address: zhujiawu@mail.iasf.ac.cn; zhangmiao@mail.iasf.ac.cn

field measurements. Sm_2Co_{17} is selected as the PM material, which has small temperature coefficient and good magnetic performance. The pole, yoke, shielding plates and field tuning bolts are made of soft iron DT4. The material of the bolts for the back yoke fixation is carbon steel. The Fe-Ni alloy with high temperature coefficient (grade 1J30) is introduced at the magnet opening side to compensate the field changes result from the temperature variations. The field tuning bolts provide an additional approach to actively adjust the fields afterwards.
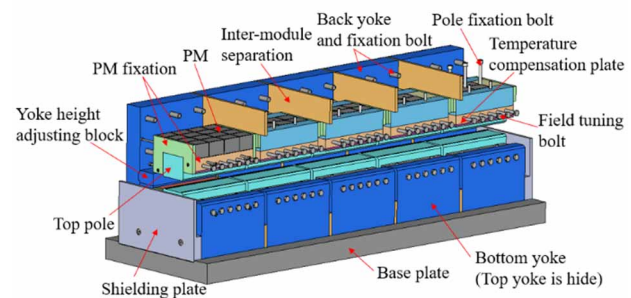
Figure 1: Typical structure of LGB magnet for SILF (5 modules assembled).

The five magnet modules have similar structures as shown in Fig. 1. Aluminium blocks fill the remain voids between the poles and yokes to support the PMs. The magnet modules are assembled separately at first and then combined as entire structure by bolting to the base plate and separated longitudinally by thin aluminium plates.

The fabrication and assembly tolerances of the LGB magnet will inevitably affect the final field quality, in order to conduct the LGB magnet manufacturing process in this regard, the influences of LGB magnet fabrication tolerances on the field quality are investigated using a dedicated parameterized finite element (FE) model, including the pole height tolerances, the pole tip inclination in transverse and longitudinal directions. The influences of the mesh sizes on field quality are firstly studied in order to find a compromise between the computation accuracy and efficiency with respect to the FE model size.

PARAMETERIZED FE MODEL

A parameterized FE model of the entire typical LGB magnet is firstly developed in Opera-3D®, however, the computation time turns out very long. We therefore reduce the model size to has only one module, i.e. the one for the highest field stage with the shielding plates at both ends, as shown in Fig. 2. The model size reduction is under the assumption that the relative change of the TFH / IFH results from a particular fabrication tolerance is the same for

A SPECIAL-SHAPED COPPER BLOCK COOLING METHOD FOR WHITE BEAM MIRRORS UNDER ULTRA-HIGH HEAT LOADS

J. Liu, X. Yan, H. Qin[†], Institute of Advanced Science Facilities, Shenzhen, Guangdong, China

Abstract

In order to fulfil the more stringent requirements of optical figure accuracy for cooled X-Ray mirrors imposed to high heat loads, especially from advanced insertion devices in the diffraction limited storage rings (DLSR), investigations on the cooling system for white beam mirrors are conducted in this paper. A special-shaped copper block (SSCB) cooling method is proposed, using eutectic indium-gallium alloy as heat transfer medium. The SSCB cooling technology can keep a 550 mm-length mirror slope error of 0.2 µrad (RMS) under 230 W absorption heat power, showing great advantages in the accuracy and flexibility for thermal deformation minimization when compared with the traditional ones.

INTRODUCTION

The diffraction limited storage ring generates high-quality X-Ray with more collimated, brighter and coherent beams, showing novel technical superiority and greatly expanding the synchrotron radiation applications [1-3]. However this also poses a serious challenge on the cooling mechanism design of beamline optics [4-6]. How to efficiently carry away the heat on optical components, and achieve the very closely ideal mathematical surfaces (e.g. ellipsoids, paraboloids, etc.) is one of the key problems in the DLSR beamline transportation system [7, 8].

Various efficient cooling technologies have been developed to solve thermal release issues for water-cooled white beam mirror (WBM) [9-14], including top-side contact water cooling, In-Ga bath and water-cooling, mirror geometry optimization (smart notch structure), variable-length cooling, electric heater compensation, and so on. The top-side contact cooling scheme has been a routine way for most WBMs at third generation synchrotron radiation beamline. The design of the In-Ga bath and water-cooling copper blade is applied under more intense X-Ray beams due to better thermal conductivity, which can achieve sub-nano surface shape control combining with the notch structure and electric heater compensation method. However, the latter demands complicated mirror process, mounting, relatively high sensitivity power control algorithms and costs. How to achieve efficient thermal release and meet higher optical profile requirements, in practice, has become an urgent challenge.

In this article, a cooling scheme for WBMs called special-shaped copper block (SSCB) cooling, is presented. We describe the cooling model and optimize the cooling mechanism geometry by finite element analysis (FEA). It can achieve precise control on mirror surface optical profile by adjusting the layout of local thermal resistance of the mirror cooling mechanism. The quantitative correspondence between cooling mechanism, temperature distribution, and thermal deformation is studied by finite element methods.

OPTIMIZATION OF THE COOLING MECHANISM

The grazing-incidence X-Ray mirror can be considered as a one-dimensional mechanical beam. The thermal slope error of the mirror can be calculated from Eq. (1).

$$\theta(x) = -\frac{12}{WH^3} \int_0^x \frac{1}{E} \left[\int_{-H/2}^{H/2} \int_{-W/2}^{W/2} \alpha E T(x, y, z) z \, dy \, dz \right] dx \quad (1)$$

where W is the mirror width;
H is the mirror thickness;
α is the coefficient of thermal expansion;
E is the elastic modulus;
T(x, y, z) is the temperature-coordinate distribution.

The cross-section of a WBM imposed to an intense X-Ray beam can be divided into three parts, the central part and two parts at mirror ends. A half model with temperature distribution is shown in Fig.1 [15]. The central part is affected by illuminated beam, causing a tendency of convex warping owing to the upper hot and lower cool temperature distribution, based on Eq. (1). However, the situation is just on the opposite at both ends, since the top-side contact cooling generates a descent temperature gradient from lower to upper. As in Eq. (1), a negative value is obtained at the side parts, which offsets with the central one during the integration. The overall thermal deformation close to flat can be easily achieved along the beam footprint length, while hard to eliminate local fluctuations. It is obviously unreasonable to adopt a globally consistent cooling mechanism along the mirror length in order to minimize the thermal slope error.
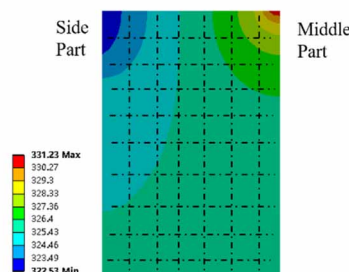
Figure 1: Half of the mirror cross-section

A cooling scheme of SSCB is proposed, which is expected to achieve thermal deformation control precisely by introducing grooves on the heat transfer path of the cooling blades properly. For the cooling mechanism with In-Ga eutectic alloy as heat transfer medium, the position of the heat

---

† qinhongliang@mail.iasf.ac.cn

MECHANICAL DESIGN OF THE NOVEL PRECISE SECONDARY SOURCE SLITS

X. Yan, J. Liu, Z. Ji, Y. Gong, H. Qin[†], Institution of Advanced Science Facilities, Shenzhen, China

Abstract

High-precision slits are extensively adopted in coherent or nano-focusing beamlines as the secondary source, which can accurately define or achieve a beam size at the micron or sub-micron scale, while maintaining high stability. This paper presents the design of a set of precise slits based on a flexure hinge mechanism, which enables a nano-scale resolution and a stroke of hundreds of microns simultaneously. The coarse or fine adjustment motion of each blade can be accomplished with or without a displacement amplification mechanism, which is driven by a piezo actuator. Furthermore, the kinematic and dynamics models are investigated through finite element analysis (FEA) and numerical analysis successively, yielding consistent results. The optimized slits system can provide a linear stroke of up to 400 μm with a resolution of 10 nm both in horizontal and vertical directions, whose first Eigen frequency is 130 Hz.

INTRODUCTION

As an important component of the beamline, the secondary source slit has the function of shaping the beam size and preventing scattering X-rays. With the increasing demands for smaller beam size in hard X-ray beamlines at diffraction-limited storage ring, the performance requirements for secondary source slits have become more challenging [1-2]. The aim of this work is thus the development of an innovative design of a large stroke compact slits system with nano scale beam shaping capability. The following sections will introduce design and analysis of the secondary source slits.

DESIGN OF THE SLITS

Specifications

Table 1: The Overall Specifications of Secondary Source Slits

Item	Specification
Vacuum	$\leq 10^{-9}$ mbar
Y/Z motion range	10 mm
Y/Z resolution	1 μm
Y/Z repeatability	± 2 μm
Parallelism between blades	≤ 0.2 μm
Range of rotary adjustment	± 0.5º
Slits blade motion range	−20 ~ 200 μm (H)
	−20 ~ 200 μm (V)
Slits resolution	0.01 μm
Slits repeatability	± 0.03 μm

† qinhongliang@mail.iasf.ac.cn

Mechanical Design

The overall slit system consists of five parts, including (1) the slit motion adjustment mechanism, (2) the chamber, (3) the vertical movement (Z direction), (4) the horizontal movement (Y direction) and (5) a marble support, as shown in Fig. 1 (see the specifications in Table 1).

The main mechanism containing slit motion and parallelism adjustment are integrated in a compatibility of ultra-high vacuum (UHV) chamber. There are two sets of slit motion adjustment components, positioned perpendicular to each other and slightly offset along the beam direction. These components enable horizontal and vertical slit openings, with each set comprising two translational mechanisms and one rotating mechanism. Figure 2 shows a motion adjustment assembly. One tungsten carbide blade is mounted on each translational mechanism, which is driven by a piezo actuator via a linear flexure hinge. Two translational mechanisms are symmetrically connected with the inner part of the flexible rotating mechanism, i.e. a circular flexible hinge, by which the pair of blades can be aligned to X-Ray beam accurately. The outer part of the rotating mechanism is fixed on the chamber bottom using silvered screws. Herein, there is a manual flexible hinge mechanism connected to one of the blades for parallelism alignment during installation.
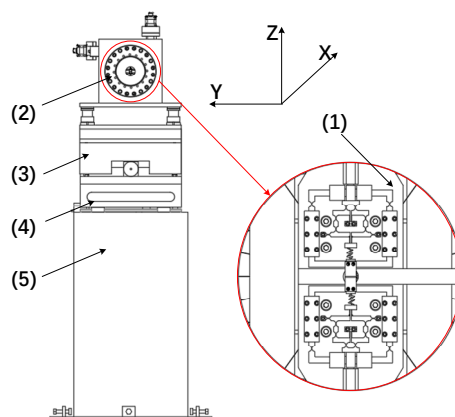
Figure 1: Schematic diagram of the secondary source slits.

There are two operation modes for the slit translational motion, corresponding to coarse or fine adjustment. (1) Displacement amplification mode. When the electromagnets are power-off, then the piezo actuator directly drives the hinge to accomplish the output displacement amplification. The blade fixed on the displacement output structure is connected to the hinge output end with a preload spring. (2) Non-displacement amplification mode. When the electromagnets are charged, it will clamp the rod fixed on the translational hinge input end, the blade is moved directly with the displacement output structure driven by the

NUMERICAL AND EXPERIMENTAL STUDIES TO EVALUATE THE CONSERVATIVE FACTOR OF THE CONVECTIVE HEAT TRANSFER COEFFICIENT APPLIED TO THE DESIGN OF COMPONENTS IN PARTICLE ACCELERATORS

M. Quispe†, J. J. Casas, C. Colldelram, M. Sanchez, ALBA-CELLS, Cerdanyola del Vallès, Spain

R. Capdevila, M. Rabasa, G. Raush, ESEIAAT, Terrassa, Spain

S. Grozavu, Universidad Politecnica de Madrid, Madrid, Spain

H. Bello, La Romanica, Barberà del Vallès, Sabadell, Spain

Abstract

The fluid boundary condition applied to the design of components in particle accelerators is calculated as a global variable through experimental correlations coming from the literature. This variable, defined as the convective heat transfer coefficient, is calculated using the conventional correlations of Dittus and Boelter (1930), Sieder and Tate (1936), Petukhov (1970), Gnielinski (1976), among others. Although the designs based on these correlations work properly, the hypothesis of the present study proposes that the effectiveness of these approximations is due to the existence of a significant and unknown conservative factor between the real phenomenon and the global variable. To quantify this conservative factor, this work presents research based on Computational Fluid Dynamics (CFD) and experimental studies. In particular, recent investigations carried out at ALBA confirm in a preliminary way our hypotheses for circular pipes under fully and non-fully developed flow conditions. The conclusions of this work indicate that we could dissipate the required heat with a flowrate lower than that obtained by applying the conventional experimental correlations.

INTRODUCTION

Nowadays, in particle accelerator engineering and in engineering in general, numerical simulations, such as FEA (Finite Element Analysis) and CFD (Computational Fluid Dynamics), are decisive to approve the viability of a proposed design. Although its importance is recognized, it is also known that the results of numerical simulations have a strong dependence on the precision and good approximation of other variables such as the geometric model, physical properties, boundary conditions, etc. In this context, the content of this work is oriented to the study of one of the boundary conditions commonly used in design: the convective heat transfer coefficient (h) for internal flow in cooling channels. In particular, at ALBA we are studying the conservative factors inherent in the "h" coefficient, currently obtained from experimental correlations reported in the literature. Our main working hypothesis considers the existence of a significant and not yet quantified conservative factor in the calculation of the "h" coefficient. The results of this study will be relevant for the design of the new components of ALBA II, our current project to become a fourth-generation accelerator. From the point of view of

accelerator engineering, we will have the challenge of designing the new components for higher power densities, compared to ALBA I. In this new scenario, it will be important to know with a better precision the value of the "h" coefficient to avoid oversizing in the new designs.

For general engineering applications, the "h" coefficient is obtained from experimental correlations from the literature, reported by authors such as Dittus and Boelter (1930), Sieder and Tate (1936), Petukhov (1970), Gnielinski (1976) [1], among others. The design engineer must choose between those authors to obtain this coefficient, whose value is not unique depending on the selected experimental correlation. For example, for a hypothetical case of water at 23 ºC circulating in a pipe with an internal diameter of 10 mm and assuming a dissipation of 7 kW in the water, there is a difference of approximately 10 % between the values of "h" calculated with the correlations of Dittus – Boelter and Petukhov.

Another aspect to highlight of the "h" coefficient is the condition of its approximation: the experimental correlations have been formulated for thermal and hydraulic fully developed flow conditions. In real applications of particle accelerators, we rarely have fully developed flow, because the geometries are small in size, such as the cooling channels of mirrors, monochromators, front end masks, radiation absorbers, etc. These real geometries would increase the unknown conservative factor with respect to the case of fully developed flow, according to our hypothesis. On the other hand, from the point of view of the real phenomenon, conventional correlations assume homogeneity of the coefficient along the cooling channel, which is not true because this variable has local behaviour and its distribution is influenced by the geometry of the channel, by the flow conditions (especially for transient and turbulent cases), and by the temperature of the fluid.

In the same line of research, another variable to study is the approximation of the hydraulic diameter concept. In many applications we are forced to design cooling channels with non-circular cross sections. In these cases, the application of the hydraulic diameter concept suggested by conventional references introduces, in our opinion, a new conservative factor with respect to the case of a circular tube.

The investigations of this paper are based on CFD calculations, Heat Transfer (HT) simulations, and preliminary experimental studies in setups developed at ALBA. The HT simulation approximates the heat transfer in the fluid

---

†mquispe@cells.es

THE PRE-ALIGNMENT OF HIGH ENERGY PHOTON SOURCE STORAGE RING

Shang Lu[†], Lan Dong, Jing Liang[1], Lingling Men, Tong Wang[1], Xiaolong Wang

Institute of High Energy Physics, Beijing, China

[1]also at Spallation Neutron Source Science Center, Dongguan, China

Abstract

In order to achieve 10 μm pre-alignment accuracy of storage ring in transverse and vertical, four laser trackers were used for set up a four-station μm measurement system. Experiment results show that the relative displacement measurement accuracy is better than 3 μm in 3-meter workpiece range, which can satisfy the real-time position feedback accuracy of the magnets in the process of ultra-high-precision pre-alignment. After two years of research and development, three pre-alignment standard workstations have been established. And the laser multilateration measurement method is adopted to the pre-alignment of the three, five and eight magnet girders in the storage ring of HEPS. Currently, 240 out of 288 girders have been pre-aligned after half a year of work.

INTRODUCTION

In order to improve the installation efficiency and accuracy of the storage ring for Chinese High Energy Photon Source (HEPS), each girder is usually pre-aligned in the laboratory, and then transported to the storage ring to participate in the tunnel alignment. Based on physical design of the accelerator, the standard deviation for the pre-alignment adjustment of magnets on one girder with respect to each other in transverse and vertical must below 10 μm.

In the particle accelerator field, laser tracker, such as the Leica AT930, is one of the most commonly used instruments for component fiducialization and alignment [1-3]. However due to the influence of the 15μm +6μm/m angle measurement accuracy, the three-dimensional coordinate measurement accuracy of the AT930 reaches 15μm +6μm/m. To improve its accuracy, numerous attempts have been made [2, 4]. However, these methods still cannot avoid the measurement of angle.

So, we build a four-station laser trackers multilateration measurement system for magnet pre-alignment. We first built a multilateration measurement system using four laser trackers. Then, the self-calibration of the system was completed by measuring more than 12 target points. Next, the front intersection is realized in combination with the Super-Cat's Eye, which realizes the real-time measurement of the coordinates of the magnet fiducial points. Finally, through careful adjustment, the pre-alignment of a girder with 8 magnets is completed, and the alignment standard deviation of transverse and vertical is within 6 μm.

BASIC PRINCIPLE OF FOUR-STATION MULTILATERATION MEASUREMENT METHOD

The measurement principle of the multilateration measurement method mainly includes two parts: Self-calibration and Intersection measurement.

Self-calibration: The system parameters, that is, the coordinates of the four stations, are solved by measuring enough points.

Front intersection: Calculate the coordinates of the under-test point. After the system parameters are determined, four stations are used to measure the distance to the under-test point at the same time, and then the coordinate of the point can be calculated based on the distance.

There are four stations and n target point in the space, as shown in Fig. 1. Four stations were employed simultaneously to measure the distance to the target point. The center coordinate of the i-th station is $S_i = (X_i, Y_i, Z_i)$ ($= 1, 2, 3, 4$) the coordinate of the j-th target point is $P_j = (X_j, Y_j, Z_j)$ ($j = 1, 2, 3, …, n$) the observed value between S_i and P_j is D_{ij}. The error equation group can be expressed as:

$$D_{ij} + v_{ij} = \sqrt{(X_i - x_j)^2 + (Y_i - y_j)^2 + (Z_i - z_j)^2} \quad (1)$$

where v_{ij} is the error corresponding to the observed value.
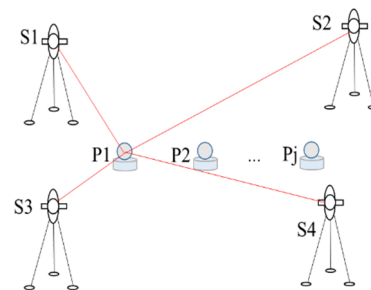
Figure 1: The principle of multilateration measurement method.

Expand Eq. (1) according to Taylor series and omit higher-order terms to obtain the error linear equation:

$$v_{ij} = f_{ij}\delta X_i + g_{ij}\delta Y_i + h_{ij}\delta Z_i - f_{ij}\delta x_i$$
$$-g_{ij}\delta y_i - h_{ij}\delta z_i - (D_{ij} - D_{ij}^0) \quad (2)$$

As the self-calibration process was completed, the coordinate of the four stations S_i ($i = 1, 2, 3, 4$) and the target points P_j ($j = 1, 2, 3, …, n$) were obtained in one coordinate system [5]. Then assuming that the coordinate of under-test points is $W(X, Y, Z)$, the measurement distance between the four stations and under-test point W is L_i ($i =$

† lushing@ihep.ac.cn

DESIGN AND TEST OF A NEW CRYSTAL ASSEMBLY FOR A DOUBLE CRYSTAL MONOCHROMATOR*

Yang Yang[1], Hao Liang† [1,2], Dashan Shen[1], Zekuan Liu[1], Yunsheng Zhang[1], Shan Zhang[1],
Yuanshu Lu[1], Lu Zhang[1]
[1]Institute of High Energy Physics, Beijing, P. R. China,
[2]University of Chinese Academy of Sciences, School of Physics, Beijing, P. R. China

Abstract

A vertical diffraction double crystal monochromator is a typical optical component in synchrotron radiation beamlines, its main requirements and characteristics are high angular adjustment resolution and stability. Due to the development of the 4th generation light sources, those requirements get even more challenging. This paper mainly introduces the design and test of a new crystal assembly design in a vertical diffraction double crystal-monochromator. The designed scheme has been fabricated. The surface slope error of the first both crystals was measured and below 0.1 μrad RMS. The motion adjustment test of the second crystal module has been carried out under atmosphere, vacuum and cryocooled conditions, and the results are much better than required ones. The stability of the monochomator was measured, and results below 10 nrad RMS were observed under cooling conditions.

INTRODUCTION

HEPS is a 4th generation light source which employs multi-bend achromat lattices and aims to reach emittance as low as 60 pm•rad with a circumference of about 1360 m [1]. The vertical diffracting double crystal monochromator (VDCM) described in this paper will be serving the X-ray microscopic imaging line station of HEPS. The monochromator hosts 2 Si(111) crystal, covers an energy range of 5 keV to 15 keV. It works in fixed exit mode. The maximum heat load is 435 W, thus the monochromator is liquid nitrogen cooled. The relative pitch stability requirement is 100 nrad RMS. This paper mainly introduces the design and test of the crystal assembly of the monochromator. The crystal assembly includes 2 main sub-components, the first crystal component and the second crystal component. The first crystal component mainly includes the first crystal cooling and clamping, using micro-channel side cooling and flat plate clamping schemes. The second crystal component provides gap, coarse pitch and roll, fine pitch and roll for the second crystal. At the same time, the Angle monitoring system is designed (Fig. 1).
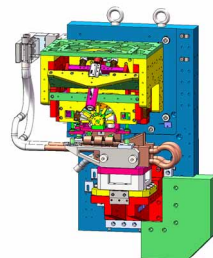
Figure 1: Crystal module design model.

The First Crystal Components

The first crystal component mainly includes the first crystal cooling and clamping component, crystal heat insulation component and crystal support structure.

Indirect cooling of the first crystal has been proven effective for high heat load monochromators around the world [2, 3]. Therefore, the crystal cooling in this scheme follows the microchannel edge cooling design, and the crystal clamping adopts the disc spring plate clamping mechanism. The two plates rely on the disc spring to provide compression force. Each disc spring is compressed by 0.2 mm, and six unilateral superpositions are used. The unilateral compression can be 1.2 mm, and the maximum force can be 814 N. The heat insulation of the crystal is designed with a machinable ceramic design, which is placed between the bottom of the crystal and the support structure. The heat leakage and mode analysis of the whole monocrystalline component are carried out. The overall heat leakage is 3.3 W, and the first-order angle direction mode is 312 Hz (Fig. 2).
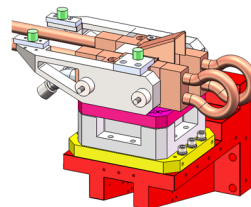
Figure 2: The first crystal components design model.

The design scheme was processed and assembled, and the crystal surface shape was measured (Fig. 3). The normal temperature result is less than 0.1 μrad, which meets the requirements of use.

MOTORIZED UNIVERSAL ADJUSTMENT PLATFORM FOR MICROMETRIC ADJUSTMENT OF ACCELERATOR COMPONENTS

M. Noir [*][1], M. Sosin [†][1], D. Baillard[1], P. Biedrawa[2], A. Gothe[3], L. Gentini[1],
W. Jasonek[2], François-Xavier Nuiry[1], V. Rude[1], P. Sarvade [1], R. Seidenbinder[1], K. Widuch[1]

[1]CERN, Geneva, Switzerland

[2]AGH, University of Science and Technology, Krakow, Poland

[3]Aarhus University, Faculty of Technical Sciences, Denmark

Abstract

In order to optimize alignment activities in a highly radioactive environment, the Geodetic Metrology Group at CERN has developed a standardized featuring 6 degree of freedom (DoF) Universal Adjustment Platform (UAP). After a first prototyping phase in 2021 with a manual UAP, the design has been consolidated and is now compatible with the installation of motorized actuators to form a remotely adjustable 5-6 DoF platform able to perform positioning with micrometre resolution. This paper presents the UAP and related motorized actuator development, elaborated in the frame of the High-Luminosity Large Hadron Collider project. The mechanical integration approach, design solutions, and test results are discussed.

INTRODUCTION

The CERN Large Hadron Collider (LHC) accelerator will soon be upgraded to operate at five times higher nominal luminosity to increase its potential for discoveries after 2029. In the frame of this project, named High-Luminosity-LHC (HL-LHC), nearly 1.2 km of beam components will be replaced [1, 2]. One of the key parameters to increase the integrated luminosity is the precise alignment of the accelerator components of the two high luminosity experiments in the Long Straight Sections (LSS). For the first time, a Full Remote Alignment System (FRAS), composed of a set of micrometre sensors and actuators, will be implemented on the HL-LHC components to determine continuously the position of the components and re-adjust them remotely if needed [3].

In the frame of this project, a Universal Alignment Platform (UAP), able to adjust lightweight accelerator components (up to 2000 kg) within 6 Degrees Of Freedom (DoF), has been developed by the Geodetic Metrology Group at CERN. This platform is an adaptive framework that will be used for several accelerator components such as collimators. It is based on in-house designed components, that can be scaled to the accelerator component according to its supporting points, available volume, etc. The concept of such a platform has been already presented in [4]. This paper focuses on the platform components characterization and details the proposed motorisation solution to perform remote adjustments in the frame of FRAS.

---

* michel.noir@cern.ch

† mateusz.sosin@cern.ch

6 DOF PLATFORM CONCEPT

The UAP platform is composed of the following elements (Figure 1):

- A lower interface plate (Blue) that is considered as fixed.
- A set of 6 micrometre actuators (Red) to perform adjustments in all DoF. The radial actuation is carried out by radial jigs while the vertical and longitudinal adjustments are performed by vertical jigs.
- Backlash-free joints (grey), with tailored length to remove any hyperstatism.
- A set of actuating shafts and supports (Orange), gathered at the front part of the platform for an easy access during the actuation of each jig.
- An upper plate (green) on which the accelerator component can be installed.
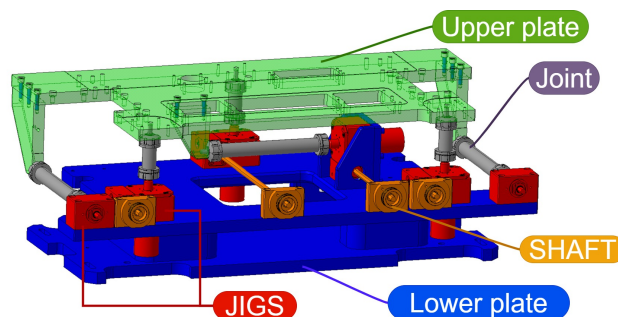
Figure 1: UAP Platform Composition.

Jigs, Joints and actuation shaft designs are now internally available at CERN and each user adapts the upper and lower plate to his needs. All these components are proposed for two models: a Light platform version (Safe Working Load - SWL- up to 300 kg) and a Heavy one (SWL up to 2000 kg). The application of this framework guarantees a common alignment procedure for all lightweight elements regardless the specificity of the supported component design. The first application has been developed in collaboration with the collimator team at CERN to validate the concept via 2 prototyping phases and obtain a robust design before serial production.

Based on this manual design, the paper presents the different steps of design and tests phases towards a motorized version compatible with the FRAS project.

DESIGN AND ANALYSIS OF CSNS-II PRIMARY STRIPPER FOIL

J. X. Chen[1], L. Kang[1], J. B. Yu[1], G. Y. Wang[1], L. Liu[1], Y. J. Yu[1], J. S. Zhang[1], J. Y. Zhang[1]

Institute of High Energy Physics, Chinese Academy of Sciences, Beijing, China

[1] also at Spallation Neutron Source Science Center, Dongguan, China

Abstract

Stripper foil is a key equipment for converting negative hydrogen ions into protons in the RCS injection zone of CSNS. The structure of the CSNS primary stripper foil adopts a rotating steel strip structure, and the maintenance time is long, requiring operators to carry out maintenance work in close proximity for a long time. The energy of CSNS-II injection beam has significantly increased from 80 MeV to 300 MeV, and the radiation dose in the injection area will also increase, making it impossible to maintain the equipment in close proximity for a long time. Therefore, it is necessary to redesign the primary stripper foil. This article will analyze the stripper efficiency and beam injection thermodynamics of CSNS-II stripper foil, carry out automatic foil store replacement structure design, motion analysis, and prototype testing, and envision remote maintenance solutions to achieve maintenance and repair of the stripper foil with minimal human intervention.

INTRODUCTION

Stripper foil is a key equipment for converting negative hydrogen ions into protons in a Spallation Neutron Source device. The CSNS stripper foil includes the primary stripper foil and the secondary stripper foil. The primary stripper foil adopts 100 μg/cm² diamond-like carbon film with a capacity of 22 pieces and a theoretical stripping efficiency of 99.7% [1-3]. The proton beam after being peeled off by the primary stripper foil enters the RCS for acceleration. The secondary stripper has a foil storage capacity of 1 piece with a 200 μg/cm² diamond-like carbon foil. A negative hydrogen ion absorption block is designed on the secondary stripper foil to absorb negative hydrogen ions that have not been stripped off through the primary stripper foil. The H_0 particles, after stripping one electron through the secondary stripper foil, are change into protons and extracted to the beam dump [4, 5]. The structure of the primary stripper foil of CSNS adopts a rotating steel strip structure, and the foils are uniformly distributed on the rotating steel strip. Each foil needs to be installed separately. At the same time, according to the radiation protection requirements of CSNS, the stripper foil does not consider radiation shielding and does not reserve installation space for radiation shielding. During the operation of the CSNS accelerator, the service life of the primary stripper foil is less than 1 month per piece, and the residual dose on the surface of the foil rack after operation can reach up to 2000 μSv/h, in addition, the operator needs to carry out maintenance work in close proximity for a long time. The secondary stripper foil structure is similar to the primary stripper foil structure,

but there is no rotating steel strip structure. According to physical requirements, the CSNS-II stripper foil still adopts two sets of stripper foil devices, including one primary stripper foil and one secondary stripper foil, which have the same function as the CSNS stripper foil. However, due to the increase in radiation dose, it is impossible to maintain the equipment in close proximity. Therefore, a new overall foil store quick replacement mechanism must be adopted and a new maintenance plan must be redesigned.

ANALYSIS OF THE FOIL DURING BEAM INJECTION

According to the physical design scheme of the CSNS-II RCS injection zone, as shown in Fig. 1, the RCS injection beam energy is increased from 80 MeV to 300 MeV. After the injection energy of CSNS-II is increased to 300 MeV, according to the relationship between foil thickness and stripping efficiency shown in Fig. 2, in order to maintain a stripping efficiency of 99.7%, the thickness of the primary stripper foil needs to be increased to 260 μg/cm², and according to the size of the beam spot, the transverse size of the foil is required to be no less than 20 mm * 60 mm [4], and the material is HBC.

According to the analysis of beam injection into the stripper foil, when the injection energy is 300 MeV and the film thickness is 260 μg/cm², the number of repeated beam passes is 15, and the half axis size of the elliptical beam spot is 3 * 1.5 mm. Assuming that the beam spot is uniformly distributed within the central range, the rest is Gaussian distribution. The mathematical model of a Gaussian heat source is shown in formula (1).

$$D(x, y) = \frac{E_{\text{total}}}{2\pi\sigma_x\sigma_y} \exp\left(-\frac{x^2}{2\sigma_x^2}\right) \exp\left(-\frac{y^2}{2\sigma_y^2}\right) \quad (1)$$

Among them, E_{total} is the total energy deposited on the foil, and σ_x, σ_y are the radius of the major and minor axes of the elliptical Gaussian heat source. It is known that the injection point is 7 mm away from the edge of the foil. Therefore, the mathematical model of the Gaussian heat source is shown in formula (2).

$$D(x, y) = \frac{E_{\text{total}}}{2\pi\sigma_x\sigma_y} \exp\left(-\frac{(x-0.007)^2}{2\sigma_x^2}\right) \exp\left(-\frac{(y-0.007)^2}{2\sigma_y^2}\right)$$

$$(2)$$

TECHNOLOGIES CONCERNING METAL SEALS OF THE UHV SYSTEM FOR ACCELERATORS

H. Y. He, L. Liu, P. C. Wang, Y. S. Ma, B. Tan, Institute of High Energy Physics, Beijing, China

Abstract

Reviewed the domestic research on structural design and sealing function principle of the metal seals, wildly used in the Ultra High Vacuum (UHV) system for accelerators. Analysed and summarized the key technologies concerning the material, contact forms, machining process and test methods of sealing performance. The study will become the basis of designing, machining and quality measuring for the ultra-vacuum metal seals. It provided the foundation for generating seals standards to promote the development of vacuum technology application.

Introduction

V The metal sealing ring is a key sealing component of the accelerator ultra-high vacuum system, achieving a detachable metal to metal end face seal. Ultra-high vacuum systems such as the Beijing Positron and Negative Electron Storage Ring, Spallation Neutron Source, and High Energy Synchrotron Radiation Light Source in China have sealing rings that provide high-temperature degassing and baking at 300 °C, long-term radiation corrosion protection, and almost no penetration of small molecule gases during use. Traditional sealing rings cannot perform well under these harsh working conditions [1]. Metal sealing rings have been widely used in the field of ultra-high vacuum systems, and products with cross-sectional shapes such as O-shaped sealing rings, C-shaped sealing rings, and Δ knife edge sealing rings have reached the practical stage. The C-shaped sealing ring optimized from the basic O-ring, with the C-shaped opening facing towards atmospheric pressure, forms excellent self-sealing; At the same time, the Δ knife edge sealing ring utilizes the advantage of good plastic flow of soft metal to help compensate for the concave and convex gaps and scratches on the surface of the sealing end face, and prevent leakage [2]. At present, stable and reliable ultra-high vacuum metal sealing rings are mainly provided by foreign companies in fields such as accelerators, nuclear power, aerospace, and shipbuilding in China, such as GARLOCK in France and VAT in Switzerland. Due to technological lockdowns, domestic researchers can only obtain partial performance information about metal sealing rings through product manuals. The lack of systematic sealing theory and product standards has hindered the development of ultra-high vacuum metal sealing ring technology in China.

By analysing the research status of ultra-high vacuum metal sealing rings in China in recent decades, this paper summarizes the sealing contact forms, metal materials, and sealing leakage rate measurement methods, explores key issues of structural design optimization and material simulation, forming and processing methods, and sealing performance measurement technology, laying a foundation for establishing a theoretical system of ultra-high vacuum metal sealing rings and promoting engineering applications.

Classification of Metal Static Sealing Materials and Structures

Seals can be divided into two categories: static seals and dynamic seals. The main application of ultra-high vacuum metal sealing is the static sealing of detachable flange connected circular vacuum pipelines. Under external loads, the metal material undergoes plastic deformation and flow to compensate for the gap between the joint surfaces, making it smaller than the diameter of the gas molecules, forming an interface blockage and achieving effective sealing.

The materials and structures of metal sealing rings complement each other, and the research and optimization of materials and the development of finite element simulation analysis have driven the design and development of sealing ring structures. The working performance of metal sealing rings varies with changes in material, geometric shape, and wall thickness.

According to the sealing principle, the material of metal sealing rings is generally required to have certain compression deformation ability, strength, rigidity, rebound ability, and creep resistance. The earliest Baker Hughes Z seal, Caledyne CMTM seal, and Owen X-PAN seal designs used stainless steel, copper, and aluminum sealing rings, which generate radial rebound and expansion through cross-sectional compression. The sealing technology is widely used in industries such as motivation and petroleum. In recent years, with the increasing demand for scientific research and vacuum technology, sealing technology for covering soft metals with high compressive strength and tensile rate metals such as Inconel nickel alloy and Nimonic alloy has become one of the research hotspots. High strength and stiffness represent greater resistance to deformation, allowing for a more stable and reliable vacuum seal with the same sealing force. In addition, the basic requirements for ultra-high vacuum metal sealing rings are the gas release rate and permeability of the metal material. Choose materials with low adsorption, diffusion, and permeability to prevent interface cracks and isolated voids, which are more suitable for obtaining and cleaning extreme vacuum. In addition, the flange and flange locking chain in the accelerator ultra-high vacuum system are made of carbon steel materials such as stainless steel 316L with low magnetic permeability. Therefore, the working pressure of the metal sealing ring should be less than 98 MPa for high-pressure sealing [3].

MECHANICAL SYSTEM OF THE U26 UNDULATOR PROTOTYPE FOR SHINE

S. W. Xiang, T. T. Zhen†, S. D. Zhou, Y. Y. Lei, J. Yang, W. Zhang, Z. Q. Jiang,
R. B. Deng, H. X. Deng
Shanghai Advanced Research Institute, Chinese Academy of Sciences, Shanghai, China

Abstract

The Shanghai High repetition rate XFEL and Extreme light facility (SHINE) is under construction and aims at generating X-rays between 0.4 and 25 keV with three FEL beamlines at repetition rates of up to 1 MHz. The three undulator lines of the SHINE are referred to as the FEL-I, FEL-II, and FEL-III. Shanghai Synchrotron Radiation Facility (SSRF) will manufacture a total of 42 undulators (U26) with a period length of 26 mm for FEL-I and 22 undulators (U55) with a period length of 55 mm for FEL-II. Both the U26 and U55 are 4 m long and use a common mechanical system. By using the specially designed double lever compensation springs can eliminate different magnetic force on the drive units. A U26 prototype has been developed and tested at SSRF. This paper describes the mechanical system design, simulation and testing results of the U26 prototype, as well as its compatibility with U55.

INTRODUCTION

SHINE has three undulator lines [1-3], with FEL-I and FEL-II arranged side by side in the same tunnel, as shown in Fig. 1. Due to space limitations, the vacuum chamber needs to be installed and aligned on the undulator frame outside the tunnel. The width of the undulator is 1.1 m, and the transportation access space is 1.5 m to ensure that the undulator can be transported normally.
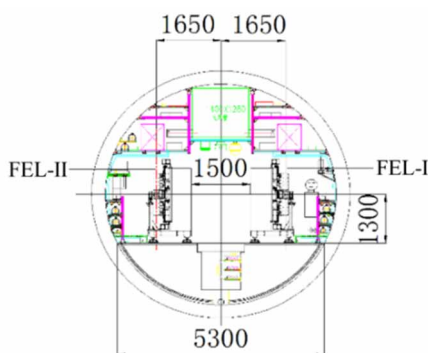
Figure 1: Cross section of the SHINE undulator tunnel.

MECHANICAL SYSTEM DESIGN

Considering that both U26 and U55 are 4 meters long, the mechanical system will be the same, but the magnetic structures will be different. The mechanical system is composed of a L-shape steel frame, girders, drive units, compensation springs, and alignment jacks, as illustrated in

Figure 2: SHINE U26 prototype mechanical system.

Fig. 2. The function of the mechanical system is to support and drive the upper and lower girders with magnet structures to move symmetrically relative to the magnetic center. Mechanical tolerances are determined by FEL physics, and the main parameters of the mechanical system are listed in Table 1.

Table 1: Main Parameters of the Mechanical System

Parameter	Value	Unit
Maximum gap range	7-200	mm
Nominal gap range	7-14@U26	mm
	7-30@U55	
Maximum magnetic force	26@U26	kN
	65@U55	
Gap variation under maximum magnetic force	≤10@U26	µm
	≤20@U55	
Gap drive repeatability	±1	µm
Taper range	±0.2	mm
Moving range of the magnetic center	±0.4	mm

The frame is a welded steel structure supported by a set of six jacks for leveling and alignment. The drive units adopt four motors to adjust the gap and the taper, and consists of motors, gearboxes, lead screws, linear guides, limit switches, hard stops, and encoders. In order to improve the rigidity of the girder, hardened and tempered 42CrMo forging are selected. The double lever compensation springs (DLCS) is composed of two sets of disc springs with different stiffness, as shown in Fig. 3. It is installed between the upper and lower support plates, which can eliminate the magnetic force on the drive units.

PROTOTYPE OF HIGH STABILITY MECHANICAL SUPPORT FOR SHINE PROJECT*

Rongbing Deng[†], Fei Gao, Zhidi Lei, Xuefang Huang, Tingting Zhen, Haixiao Deng,
Shanghai Advanced Research Institute, Chinese Academy of Sciences, Shanghai, China

Abstract

Quadrupole stability of undulator segment is key to the beam performance in SHINE project. Vibration stability requirement of quadrupole is not larger than 200 nm displacement RMS between 1 and 100 Hz, but the field test of SHINE tunnel shows that the tunnel vibration during the day time is greater than 200 nm. In this paper, a mechanical support including a marble base and an active vibration reduction platform is sophisticated designed. Vibration stability of the key quadrupole fixed on this support is expected to be improved and the performances of the quadrupole meet the demands.

INTRODUCTION

Shanghai HIgh repetition rate XFEL aNd Extreme light facility (SHINE) is under construction. In undulator segment, the position of quadrupole is key to the beam performance. The position accuracy and stability of quadrupole are both nms. Quadrupole is supported by girder and girder is fixed to the ground. The high stability of mechanical support for quadrupole is important to assure the quality of the beam therefore. In SPring-8 [1], it is the cordierite ceramic support because ceramic has a low thermal expansion rate. In addition, sand is filled in the support to increase heat capacity to insure good stability. Support in SLAC [2] is a Mild Steel girder, which has sand inside and thermal insulation outside to ensure stability. In SHINE, the technical requirements of quadrupole are shown in Table 1.

Table 1: Technical Requirements of Quadrupole

Item	Value	Unit
Adjustment range of quadrupole center (H/V)	$\geq \pm 0.5$	mm
Adjustment step of quadrupole (H/V)	≤ 0.05	µm
Positioning accuracy of quadrupole (H/V)	$\leq \pm 0.1$	µm
Stability of Magnetic Center Vibration of Quadrupole (H/V, RMS, > 1 Hz)	≤ 0.20	µm

Acceptance requires that over 80 % of the total vibration measurement data (all day) meet the above stability requirement.

STRUCTURAL DESIGN

The overall mechanical support, as shown in Fig. 1, includes two parts: a marble base and an upper support. The marble base is fixed to the ground by grouting with steel plate. The thickness of grouting is not less than 40 mm and a raised plate below the marble used for adjusting the height displacement changes in the initial and later stages. The upper girder directly supports the beam equipment. The active vibration reduction platform plays an important role in dynamic vibration reduction and precise positioning. Adjustment range of the base is ± 10 mm both in vertical and horizontal direction. Adjustment range of the upper support is ± 10 mm in vertical direction and ± 5 mm in horizontal direction.

The active vibration reduction platform is fixed to the quadrupole base plate, and the seismometers are fixed on top of the marble to monitor the background vibration. Based on the vibration signal of seismometers, the piezoelectric motors in the active vibration reduction platform feedback adverse displacements to attenuate the vibration transmitted from the surrounding environment of the support platform to the quadrupole. The control cabinet is placed on the near undulator frame, as shown in the following figure.
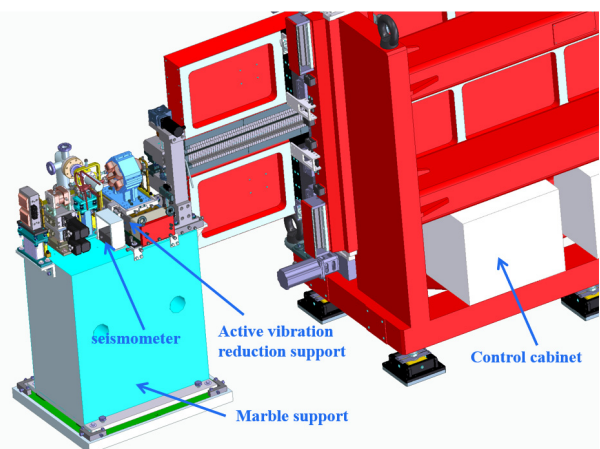
Figure 1: Mechanical support model.

The active vibration reduction platform is driven by piezoelectric motors, including 4 sets of vertical motors and 1 set of horizontal motors. A spring compensator is used to counteract gravity. A grating ruler is installed on the outer side to locate closed-loop feedback and facilitate the installation of lead plates for radiation protection. Considering a movement range of ± 0.5 mm, vertical and horizontal mechanical limits are designed internally, and vertical and

A MICRO-VIBRATION ACTIVE CONTROL METHOD BASED ON PIEZOELECTRIC CERAMIC ACTUATOR*

Z. Lei, R. Deng†, H. Deng

Shanghai Advanced Research Institute-Chinese Academy of Sciences, Shanghai, China

Abstract

In linear accelerator, ground vibration is transmitted to beam element (quadrupole magnet, etc.) through support, and then reflected to the influence of beam orbit or effective emittance. In order to reduce the influence of ground vibration on beam orbit stability, an active vibration isolation platform can be used. In this paper, an active vibration isolation system is proposed, which realizes the inverse dynamic process based on a nano-positioning platform and combines with a proportional controller to reduce the transmission of ground-based excitation to the beam element. The absolute vibration velocity signal obtained from the sensor is input to the controller as feedforward signal. The controller processes the input signal and then the output signal drives the piezoelectric ceramic actuator to generate displacement, realizing the active vibration control. The test results of the prototype show that the active vibration isolation system can achieve 50 % displacement attenuation, which indicates that the vibration control strategy has certain engineering application value in the construction of large accelerators.

INTRODUCTION

Shanghai High Repetition rate XFEL (X-ray Free Electron Laser) and Extreme light facility (SHINE) currently under construction is one of the most efficient and advanced free electron laser user installations in the world [1, 2]. It consists of a superconducting linac with an energy of 8GeV, three unshaker lines, three optical beam lines, and the first 10 experimental stations. The superconducting linear accelerator is composed of superconducting acceleration modules, each 1.3 GHz module is about 12 meters long, and mainly includes 8 TESLA type 9-cell superconducting cavities [3], couplers, tuners, BPM and superconducting quadrupole iron at one end. In order to achieve the submicron beam stability requirements of the superconducting linac and to suppress the cavity frequency deviation caused by mechanical vibration, the position jitter tolerance is generally not more than 10 % of the beam size [4]. In particular, engineering requires that the amplitude of some quadrupole magnet be less than 0.15 µm (1 Hz-100 Hz) perpendicular to the beam direction. SHINE facility is close to the Shanghai Synchrotron Radiation Facility (SSRF). The German Electron Synchrotron Institute has

compared and analyzed the ground vibration of major light sources around the world, and the results show that the ground vibration level of the SSRF campus is significantly higher than that of other light sources [5]. Therefore, it is of practical significance for engineering construction to develop an active vibration isolation platform suitable for large accelerators.

DESIGN OF THE ACTIVE VIBRATION CONTROL STRATEGY

In order to reduce the influence of foundation vibration on quadrupole magnet, an active vibration isolation platform is used to reduce the transfer rate of displacement from foundation to magnet. In this paper, an active vibration isolation system is proposed, which realizes the inverse dynamic process based on a nano-positioning platform and combines with a proportional controller to reduce the transmission of ground-based excitation to the beam elements. The absolute vibration velocity signal obtained from the sensor is input to the controller as a feedforward signal. The controller processes the input signal and then the output signal drives the piezoelectric ceramic actuator to generate displacement to realize active vibration control.

EXPERIMENTAL RESULTS

For the evaluation of the proposed control strategy, the test bench shown in Fig. 1 is used. Ground broadband vibration act as excitation, and four piezoelectric actuator implements the described isolating strategy in the direction of gravity for damping the vibration in the upper mass M (260 kg).
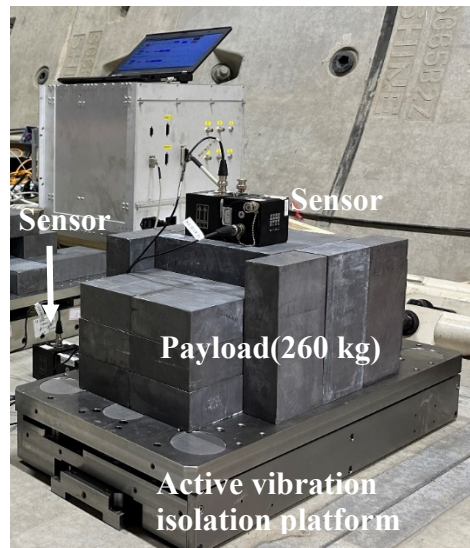
Figure 1: Test bench.

GIRDERS FOR SOLEIL-II STORAGE RING

J. Da Silva Castro†, K. Tavakoli, S. Ducourtieux, Z. Fan, F. Lepage, A. Nadji
Synchrotron SOLEIL, Saint-Aubin, France

Abstract

After two decades since its establishment, the SOLEIL Synchrotron facility needs to adapt to follow new scientific fields that have emerged since. After the Conceptual Design Report (CDR) phase for the facility Upgrade, the SOLEIL teams have been working for several months on the Technical Design Report (TDR). The "SOLEIL Upgrade" project is called "SOLEIL II" and is divided into several sub-projects. Among these sub-projects, one concerns storage ring Girders that will support all magnets of the new Lattice. These 86 Girders, each one supported by 2 plinths, must ensure an excellent degree of vibration stability. Before obtaining a final design for these Girders, a significant amount of study work has already been carried out (design, finite elements simulations, sub-assembly prototyping, dynamic measurements, tests, etc.). To validate the concepts, a fully equipped prototype girder was launched into manufacturing. In this contribution the preliminary studies and the ongoing investigations on SOLEIL II girder design will be presented.

INTRODUCTION

SOLEIL [1] teams have been working for several months on its Technical Design Report of "SOLEIL II" project that aims to study and install an accelerator with new performances. One sub-project concerns girders of storage ring that will support the magnets of the new Lattice. These girders must make it possible to achieve an excellent degree of vibration and thermal stability, including adjustment precision, with acceptable manufacturing costs. The difficulty is to find the best compromise between the level of specifications and the costs to achieve them. Figure 1 shows the previous magnets supports and the current philosophy. That will constitute a substantial budget saving.
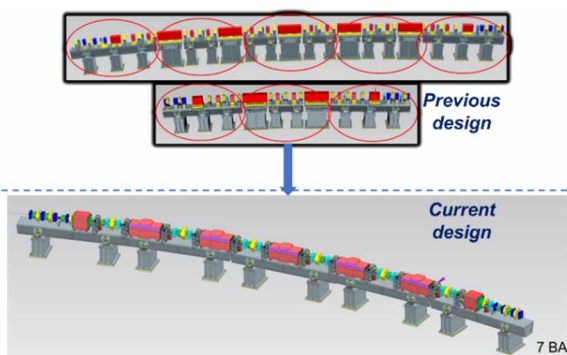
Figure 1: Previous and current magnets support situation (magnets in 7BA cell and 4BA cell of SOLEIL-II lattice.

---

† jose.dasilvacastro@synchrotron-soleil.fr

Previously girders were supported by 3 plinths. Currently girders are supported by 2 plinths. Now the target defined by accelerator physicists for the 1st modal frequency is ≈ 40 Hz. After few iterations, we came up on four girder length families, with two assembling configurations, single or double dipole [2]. The high density of multipoles is a real challenge in terms of components integrating on girders [3].

Table 1 allows to compare previous and current magnets supporting philosophies. At the cost of a reduction of the 1st modal frequency target, the number of supports and plinths has been drastically reduced.

Table 1: Previous and Current Supporting Situations

	Previous	**Current**
Girders Nb.	98	86
Long dipole plinths Nb.	76	0
Standard plinths Nb.	236	172
First modal frequency Hz.	70	40

GIRDERS AND PLINTHS INTERFACE

Figure 2 shows the design of girder and plinth interface that allows to adjust and lock girder position. Adjustment principle consists in, a preload first applied by spring washers. Then the girder is aligned with adjusting elements using Nivell wedge and Push and pull screws. Finally, girder is locked by the spring washers, loaded at 45000 N.
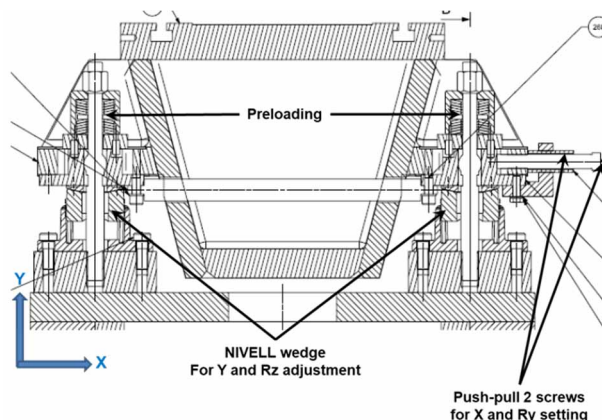
Figure 2: Girders positioning and locking system.

MODAL ANALYSIS

Current specification for the 1st modal frequency is 40 Hz minimum. FE simulations on both pessimistic configurations, regarding supported loads were carried out. In both case the 1st modal frequency is a transversal (X) bending mode of the plinths. Girder dynamic bending occurs from the 4th modal frequency at 105 Hz for single dipole

THE GIRDER SYSTEM PROTOTYPE FOR ALBA II STORAGE RING

L. Ribó [†], J. Boyer, N. Gonzalez, C. Colldelram, L. Nikitina, F. Perez
ALBA Synchrotron Light Source, Cerdanyola del Valles, Spain

Abstract

The main goal of the upgrade of ALBA Synchrotron Light Facility into ALBA II is the transformation of the current accelerator into a diffraction limited storage ring, which implies the reduction of the emittance by at least a factor of twenty. The upgrade will be executed before the end of the decade and will be profiting at maximum all existing ALBA infrastructures, in particular the building. The whole magnet layout of the lattice has to be supported with a sequence of girders for their positioning with respect to another located in an adjacent girder with an accuracy of 50 µm to ensure the functionality of the accelerator. Besides the girders must enable the remote repositioning the magnets against the overall deformation of the site while ensuring the vibrational stability of the components on top. Easiness of assembling and installation of the different subsystems of the machine on top of the girder has to be considered also as a design requirement, in order to minimize the installation time. Two prototypes are planned to be built next year in order to check its full functionality.

FROM ALBA TO ALBA II

ALBA current storage ring is composed by 264 magnets, which are distributed in 16 cells in an array of 2 girders of 6 meters for each cell. ALBA II proposed layout is composed by 592 magnets, in the same arc length as current ALBA storage ring [1], meaning that the compactness ratio has increased by a factor of 2 in the new projected storage ring with respect to the old one. In Fig. 1 is represented an overall distribution of one sector for the current and new storage ring, where the reduction of free space can be appreciated.
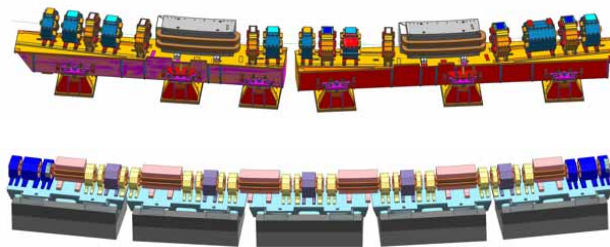
Figure 1: Current magnetic distribution of ALBA (top) and ALBA II cell layout (bottom).

As it can be seen on Table 1, the tolerances for positioning the girder will thus need to be tighter corresponding to a low emittance new machine, where the emmitance is reduced by a factor of 20 [2].

Table 1: Sizes Comparison

Dimension	ALBA	ALBA II
Compactness grade	49 %	80 %
Vacuum chamber size	28×56 mm	18 mm
Dynamic aperture	50 mm	6 mm
Beam Size	60 µm	5 µm

A NEW GIRDER DESIGN

In order to support the magnetic arrays, a new girder design is required. Taking into consideration the deformation of ALBA slab in the last 12 years, motorization for vertical positioning may be considered as a demand to be able to automatically compensate the small incremental vertical deformations and maintain electron beam stable in dynamic aperture.

The chosen strategy for conditioning the vacuum cell, will lead to a determinate vacuum section design, but according to the actual design status there are two possible layouts, which differ on the number and length of girders. That's why it is foreseen to prototype a girder design that will be fabricated in two different lengths, considering the ALBA II cell nowadays possible configurations. Apart from that, the girder design has to be modular enough in order to facilitate a full assembly outside the tunnel, together with the magnets and interfaces to minimize the installation time. In Table 2 the specifications for the girders prototype are summarized, in Fig. 2 the architecture and the main axes of movements are represented.
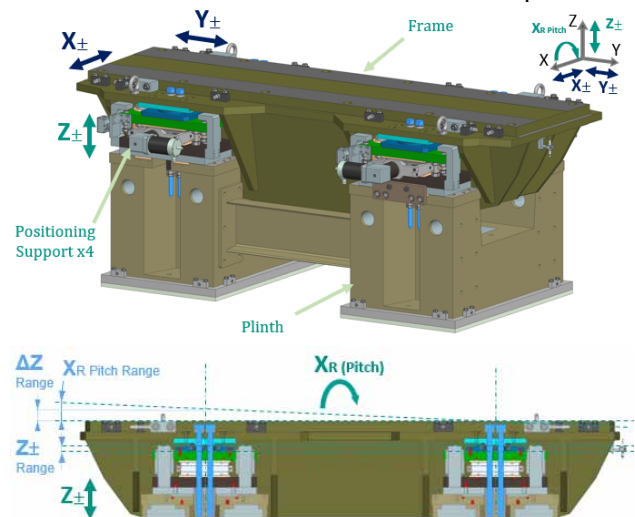
Figure 2: Motion axes and architecture.

---

† lribo@cells.es

MECHANICAL DESIGN AND MANUFACTURE OF ELECTROMAGNETS IN HEPS STORAGE RING

L. Wu[†], C. H. Li, S. Y. Chen, S. Yang, Y. D. Xu, Institute of High Energy Physics, Beijing, China

Abstract

The HEPS storage ring comprises 48 7BA (seven-bend achromat) cells. There are 37 independent magnets in every cell, of which 5 dipoles are permanent magnets and the rest of magnets are all electromagnets including quadrupoles, D-Q (dipole-quadrupole) combined magnets, sextupoles, octupoles and corrector magnets. These electromagnets with small aperture and high magnetic field gradient should achieve high machining and assembly precision. In October 2023, all storage ring electromagnets manufacturing have been completed. This paper mainly introduces the mechanical design, processing and assembly, and the manufacturing issues in the machining period.

INTRODUCTION

High Energy Photon Source (HEPS) is the first high-energy diffraction-limited storage ring light source in China which will be put into operation at the end of 2025. The electron beam energy of the storage ring accelerator is 6 GeV, which can provide 300 keV high-energy X-rays. HEPS storage ring comprises 48 7BA cells that are grouped in 24 super-periods, with a circumference of 1360.4 m and the natural emmitance of 34.2 pm rad. Each 7BA cell has 37 independent magnets of various types and 22 sets of correction coils for generating correction fields. Table 1 shows the types and quantities of the magnets in one cell [1-2].

Table 1: Magnet Types and Quantities of One Cell

Magnet Type	Quantity per Cell	Quantity in Total
Longitudinal gradient dipole	5	240
D-Q combined magnet	6	288
Quadrupole	14	672
Sextupole	6	288
Octupole	2	96
Corrector	4	192
Independent magnet in total	37	1776

The longitudinal gradient dipoles adopt permanent magnet scheme, and the other magnets in HEPS storage ring are electromagnet. These electromagnets are characterized by high gradient, small aperture, high precision requirements and compact layout. The decrease of magnet aperture makes it difficult to manufacture and obtain high magnetic field precision. Compared with the usual medium or big aperture magnets, the high-order component of the ma-

gnetic field of the small-aperture magnet, especially the non-systematic magnetic field, is more sensitive to the machining and assembly accuracy of the pole. Starting from September 2019, on the basis of the research of HEPS-TF (Test Facility) magnet prototypes, the design, bidding and production of various types of magnets were officially launched, and by October 2023, all electromagnets were completed and delivered.

MECHANICAL DESIGN AND ASSEMBLY

Quadrupole and D-Q Combined Magnet

There are 20 quadrupoles and D-Q combined magnets per cell in the storage ring, for a total of 15 kinds. D-Q combined magnets are also quadrupoles in structure with their beam center deviates from the magnetic center at a certain distance during installation. In order to facilitate the installation of the magnet coil, they are designed as four part segmented poles.

According to the length and structure of the magnet, all quadrupoles are divided into three categories, including: Type I, type I+ (with correction coil), type II. And there are also three types of D-Q combined magnets: ABF1/4, ABF2/3 and BD1/2. The structures and main dimensions with the unit of millimeter are shown in Figure 1.

Type I:510×510×(180\201\245\260\327)

Type I+:540×540×(180\192\374)

Type II: 510×510×(180\201\260)

ABF1/4: 336×336×180

ABF2/3: 480×480×580

BD1/2: : 640×640×1040
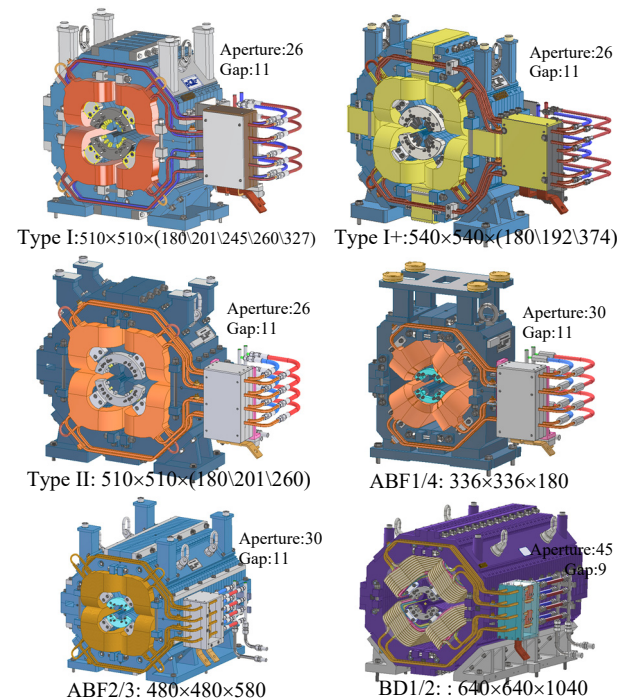
Figure 1: Structure of quadrupole, D-Q combined magnet.

† wulei@ihep.ac.cn

NEG FILM DEVELOPMENT AND
MASSIVE COATING PRODUCTION FOR HEPS*

Y. S. Ma[†], F. Sun, T. Huang, Y. C. Yang, D. Z. Guo, H. Y. Dong, P. He
Institute of High Energy Physics, Beijing, China

Abstract

Massive production facilities of NEG coated vacuum chambers have been developed for HEPS in Huairou, Beijing, which based on the NEG coating prototypes of HEPS-TF. The facilities can achieve simultaneous coating of 16~20 vacuum chambers of HEPS including irregular shaped vacuum chambers. The pumping performance of the NEG coated vacuum chambers has been measured by test facilities. After heating at 200 °C for 24 hours, the highest pumping speed of H_2 is about 0.65 l/s·cm², and the highest capacity of CO is about 1.89×10^{-5} mbar·L/cm². The lifetime is more than 20 cycles of air exposure and re-activation. The pumping performance meets the design requirements of HEPS. Currently the NEG coated vacuum chambers are applied to the storage ring of HEPS.

Introduction

HEPS (High Energy Photon Source) was designed to be a fourth-generation synchrotron radiation light sources with the lowest emissivity and highest brightness in the world. One crucial technology is to coat non-evaporable getter (NEG) films on the inner wall of vacuum chambers of small aperture in order to meet ultra-high vacuum requirements.

The NEG coating is a deposition of a titanium, zirconium, vanadium alloy on the inner surface of the chamber, typically achieved through DC magnetron sputtering. The utilization of NEG coatings has been widespread in the fourth generation of light sources to meet the stringent vacuum requirements, primarily due to the low conductance of the vacuum chambers, like MAX-IV [1] and Sirius [2]. NEG coating have been massively empoyed in the straight sections of the LHC [3], approximately 6 km of vacuum chambers were coated with NEG film.

NEG Coating Development

A DC magnetron sputtering facility has been established at IHEP for the investigation of NEG coating since 2016, as depicted in Fig. 1 [4].

For achieving a uniform thickness distribution, the NEG coating chamber is equipped with a cathode made of twisted wires of high-purity (99.95 %) titanium (Ti), zirconium (Zr), and vanadium (V), each having a diameter of 1 mm. To maintain the proximity of the cathode wires to the chamber's axis, several ceramic spacers are strategically placed along the chamber's length, along with two adapters at the ends.

To create the necessary magnetic field, a solenoid with dimensions of 1500 mm in length and 280 mm in diameter

is externally mounted on DT4. The ion pump is utilized to attain ultra-high vacuum (UHV), and the NEG bulk pump is employed to evacuate residual gases such as CO and H_2O to achieve UHV conditions.

The chambers are initially evacuated using a turbomolecular pump group, reaching a range of 10^{-9} mbar. They are then subjected to a 48-hour bake-out process at a temperature of 200℃, followed by a helium leak test to ensure their integrity before the coating process. A Residual Gas Analyzer (RGA) is utilized for monitoring residual gases during the coating process.

Prior to the coating process, thorough cleaning of the NEG-coated chamber with etching 50 µm and passivion is conducted to prevent any significant contamination or surface defects that may adversely affect the quality of the film.

During the coating process, krypton gas of high-purity (99.999 %) is used as the working gas, set at approximately 0.01 mbar. The chamber temperature is maintained at around 120 °C to facilitate the sputtering process.

Figure 1: Prototype of NEG coating facility.

Massive Coating Production for HEPS

Previously, high-quality NEG coating has been achieved by NEG coating prototypes. However, the circumference of the HEPS storage ring is approximately 1360.4 m, including about 1000 vacuum chambers to be coated. Therefore, massive production facilities has been developed to meet engineering requirements (see Fig. 2).

Except for the dipole-magnet vacuum chambers, which were made of 316L stainless steel, the other vacuum chambers in the storage ring were made of Cr-Zr-Cu alloy copper (C18150). To reduce the impedance of the stainless steel vacuum chambers, a 20 µm copper film has been coated on the inside. All of the Cr-Zr-Cu vacuum chambers, including those with a diameter of 22 mm, ante-chamber, and racetrack shape, with NEG coating is ongoing.

ACCELERATORS

Storage rings

REALIZATION OF A COMPACT APPLE X UNDULATOR*

L. Roslund[†], K. Åhnberg, M. Al-Najdawi[1], L. Balbin, S. Benedictsson M. Ebbeni, M. Holz,
H. Tarawneh, MaxIV Laboratory, Lund, Sweden
[1]also at SESAME, Allan, Jordan

Abstract

The APPLE X is a compact, elliptically polarizing undulator with a small round magnetic gap that provides full polarization control of synchrotron radiation at a lower cost and in less built-in space than comparable devices (Fig. 1). The APPLE X will be the source for MAX IV's potential future Soft X-ray Laser (SXL) Free Electron Laser (FEL). The mechanical design, finite element analysis optimization, assembly process, magnetic measurements, and shimming of a full-scale 2 m, 40 mm-period Samarium-Cobalt (SmCo) permanent magnet undulator are presented.
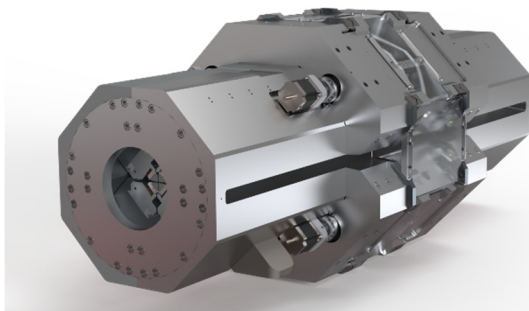
Figure 1: MAX IV APPLEX X prototype.

INTRODUCTION

A Soft X-ray Laser (SXL) beamline utilizing MAX IV Linear accelerator and the FEL technology is being designed at the MAX IV Laboratory and in collaboration between several Swedish Universities [1]. The baseline goal of the SXL beamline is to generate intense and short pulses in the range of 250 eV-1000 eV, and the conceptual design was reported in [2]. The set of features the undulator needs to fulfil includes being compact and light-weight, provide for independent gap- and phase adjustment, enable full polarization control, and K-value tuning via a radial gap operation. As a byproduct of the design, the undulator has the ability to create transverse field gradients as well as to neutralize its transverse field in a fixed-gap operation. An additional requirement is the ability to shim every individual magnet in the fully assembled undulator for magnetic fine-tuning. After a design review, in particular the shortening of the undulator length from 3 m to 2 m due to optimizations in the FEL design, prototyping of the APPLE X undulator is ongoing since late 2021 and has recently entered the assembly phase. The most recent key

figures of the APPLE X undulator as it is being build are summarized in Table 1.

Table 1: Key Figures

Magnet Type	SmCo (B_r = 1.12 T)
Period Length	40 mm
Photon Energy	0.25-1 keV
Magnetic Gap Range	8.0-17.3 mm
Effective K range	3.9-1.51
Max. gap / min. eff. K	28 mm / 0.55
Undulator Magnetic Length	2 m
Weight	2800 kg

DESIGN

The main concept of the design is to handle the magnetic forces with an as tight and short mechanical circuit as possible. The reason being to reduce the lever arms and thus also the forces experienced by the structure of the device. Focus in the detailed design has therefore been to keep the size down on each step from magnet to keeper, shimming wedge, girder, motion wedge and strongback (Fig. 2).
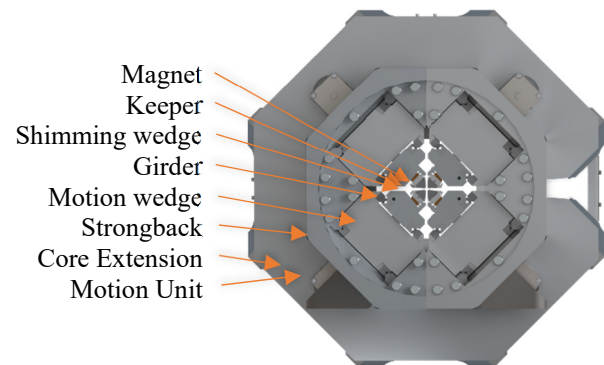
Figure 2: Outline of component stack

Nestled in through this is then the motion units (Fig. 3) one for each girder controlling radial motion and longitudinal motion on each individual girder. At first the design was a closed strongback in two half-moon parts forming a full circle around the inner parts, but due to a limitation in current magnetic measurement techniques the device is required to have a lateral opening on one side for access of a Hall-probe mounted on an arm moving along the device measuring the magnetic field. Initially the design was aiming at measurements being performed with a pulsed-wire system but will in the prototype accommodate a lateral opening for hall probe measurements and gives us the opportunity to commission a pulsed-wire system for magnetic measurements [3]. When successful, this new set-up will allow us to remove

OVERVIEW OF THE UNIFIED UNDULATOR SOLUTION FOR THE PolFEL PROJECT

J. Wiechecki[†], National Synchrotron Radiation Centre SOLARIS, Kraków, Poland
P. Krawczyk, R. Nietubyć, National Centre for Nuclear Research, Otwock-Świerk, Poland
P. Romanowicz, D. Ziemiański, Cracow University of Technology, Kraków, Poland

Abstract

The PolFEL project, consisting of building a free electron laser, will be the first in Poland and one of the several sources in the world of coherent, tuneable electromagnetic radiation within the wide spectrum range from THz to VUV, emitted in pulses from femtoseconds to picoseconds, with high impulse power or high average power. The research infrastructure will include a free electron laser (FEL), a photocathode testing laboratory, end-stations, and laboratories necessary for the operation of the apparatus, and laboratories for users from the beamlines. The main FEL accelerator will consist of three independent branches, which will include chains of undulators adjusted to three different energy ranges: VUV, IR and THz. The main challenge was the unification of the final undulator solution, so that it could be applied to all three branches. The main goal of this approach was to save time, costs, human and material resources. The overview of issues and solutions related to the construction of undulators for the PolFEL project, and the challenges that had to be fulfilled to reach the final design, is presented in this publication.

PROJECT OVERVIEW

The PolFEL facility will be built at the National Centre for Nuclear Research in Otwock – Poland. The main goal of this infrastructure is to design, develop and build a free electron laser facility located in this part of Europe [1]. All activities will be supported by the largest research centres in Europe. This device will provide a wide wavelength range of electromagnetic radiation from 0.6 mm down to 60 nm. This will be possible since the linac will be split into three independent branches for different ranges: VUV, IR and THz.

Due to significant differences in the requirements towards the electron beam, which leads to the differences in geometry of the applied magnets, it is not possible to design a common solution for all three branches. However, to simplify the undulator design, increase safety, and reduce manufacturing and design costs it was assumed that the main frame for all undulators and drive systems would be unified.

BOUNDARY CONDITIONS

The PolFEL project requires three independent types of undulators with three different magnet configurations and quantities, as described in Table 1. This directly impacts the operating range of the undulators' girders and the forces acting on the i-beams. Each magnet must be settled on the

girder within a certain position not exceeding the defined range of tolerances in the vertical direction and rotation.

On the other hand, each solution must be mechanically rigid, stable, and portable. The repeatability of the girder's movement and its position is the most critical factor that must be fulfilled to guarantee the stability of the electron beam. Furthermore, each undulator must have an opportunity to be aligned not only with the geological survey network but also to align its girders with the electron beam in real-time mode when the accelerator is fully operational.

Due to the huge amount of undulators that must be manufactured, each design must be reliable, simple, and cost-effective.

Table 1: Assumptions

Feature	VUV	THz	IR
Quantity	6	1	3
Period length [mm]	22	160	60
No. of effective periods per segment	73	8	25
Girder length [mm]	1644.5	1560	1605
Magnet material		$Nd_2Fe_{14}B$ $N_{45}UH$	
Magnet dimensions [mm] (W x H x L)	50/20 /5.5	100/100 /40	100/60 /15
Magnetic force acting on the beam in V direction [N]	300	4000	19000
Min / Max operational gap	8.5 / 13	100 / 200	22 / 60
Full open gap in [mm] where B=0 T	100	600	250
Vertical adjustment of the magnetic blocks [µm]	±100	±750	±450
Girders parallelism tolerance in z-axis (roll) [rad]	<1.5·10⁻³	<1·10⁻²	<3.5·10⁻³
Girders parallelism tolerance in x-axis (pitch) [rad]	±5·10⁻⁶	±30·10⁻⁶	±15·10⁻⁶
Girders parallelism tolerance in y-axis (yaw) [rad]	±0.25·10⁻³	±0.5·10⁻³	±0.35·10⁻³

CONSTRUCTION DETAILS

The high requirements put on each type of undulator forced an in-depth analysis. Many solutions have been taken into consideration [2-6], however, the most convenient and optimized idea was to unify the design of the undulators for all branches. This way, a common construction for all three devices has been designed, which

_____
† jaroslaw.wiechecki@uj.edu.pl

DESIGN AND DEVELOPMENT OF COATED CHAMBER
FOR IN-AIR INSERTION DEVICES

P.C. Wang[*,1], Y. Wang, University of Science and Technology of China,

National Synchrotron Radiation Laboratory, Hefei, China

L. Zhang[†], J.M. Liu, X.Y. Sun, B.L. Zhu,

Y.S. Ma, S.M. Liu, B. Tan, Y.G. Wang, H.Y. Dong

Institute of High Energy Physics, Beijing, China

[1] also at Institute of High Energy Physics, Beijing, China

Abstract

The insertion devices (ID) is an important guarantee for further improving the performance of the light source and meeting the needs of different users. For in-air ID (undulator, wiggler, etc.), the magnetic structure is in the air, and there is a vacuum chamber in the middle of the magnetic structure to ensure the normal movement of the beam. In order to increase the magnetic field strength, the magnetic gap is generally relatively small. Factors such as small space, high precision, and low conductance all pose challenges to the design and processing of vacuum chamber. This paper introduces the development process of the vacuum chamber prototype of the coating type ID. Taking the application of the prototype in the HEPS project as an example, the simultaneous analysis and vacuum pressure distribution calculation are carried out, and the NEG coating scheme is proposed as an more economical means to obtain ultra-high vacuum. And the prototype NEG coating progress is introduced.

INTRODUCTION

The HEPS is a 6 GeV, green field light source, with the aim of generating X-ray synchrotron radiations with brightness of higher than 1×10^{22} ph/(s·mm^2·mrad^2·‰BW) and photon energy of up to 300 keV at the designed beam current of 200 mA [1–5]. The ID is one of the important light-emitting components of the synchrotron radiations light source and meeting the application needs of different users [6, 7]. The main types of ID include in-air undulators/wiggler, in-vacuum undulators/wiggler, and polarization adjustable undulators. In-air IDs are usually used in applications where the photon energy is relatively low and the peak field strength is required for a line station that is not particularly high. The vacuum chamber is an important part of the ID, and its successful development is crucial. In order to obtain a vacuum chamber that meets the engineering needs, we carried out the vacuum chamber design, prototype development, NEG coating.

COATED CHAMBER FOR IN-AIR ID

Design Requirements and Layout

According to the layout of the linear section in the HEPS storage ring, specific requirements are proposed for the dimensions of the vacuum chamber along the Z-axis. This includes a distance of 5754 mm between BPMs at odd-numbered ends, which encompasses: 2 gate valves, 2 RF bellows, 2 transition vacuum chambers, and 2 front feeder coils with ID and their respective vacuum chambers. The experimental line stations necessitate a magnetic structure length of 5 m for these ID. Considering welding, installation space, and flange thickness requirements for the vacuum chambers, it is imperative that their Z-direction length exceeds 5 m. The layout of the 5 m in-air undulator (IAU) linear section is shown in Fig. 1.
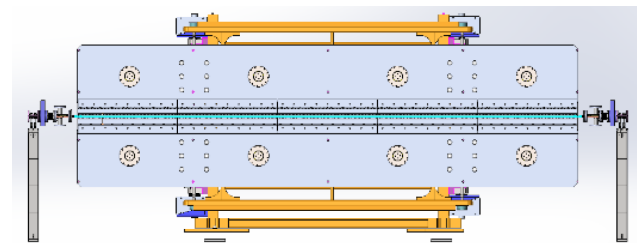
Figure 1: Layout of IAU.

According to the needs of the IAU, the parameters of the vacuum chamber can be proposed, as shown in Table 1.

Table 1: Parameters Vacuum Chamber

Parameter	Value
ID minimum gap in Y direction	11.0 mm
Straightness of vacuum chamber	±0.2 mm
Roughness of the inner surface	<Ra 0.8 μm
Thickness of vacuum chamber	9.3(±0.2) mm
Beam channel aperture size in Y direction	7.3(+0.05/-0.3) mm
Flatness of vacuum chamber	0.2 mm
Length of flange to flange	5376 mm
Cooling water velocity	<3 m/s
Static vacuum pressure	6.65×10^{-8} Pa
Dynamic vacuum pressure	1.33×10^{-7} Pa

Material Selection

Due to the characteristics of the undulator magnets, a vacuum chamber with narrow cross section (7.3 mm × 22 mm) and 5376 mm length is proposed. To achieve the necessary cross section geometry, mechanical strength, and vacuum

* wangpc@ihep.ac.cn

† zhanglei87@ihep.ac.cn

CLSI LINAC UPGRADE PROJECT

L. Lin, J. Campbell, S. Carriere, F. Le Pimpec, K. Wyatt

Canadian Light Source Inc., Saskatoon, Canada

Abstract

The Canadian Light Source Inc. (CLSI) is undertaking a significant Linear Accelerator (LINAC) injector Upgrade Project to enhance both the mechanical reliability and operational stability of Canada's primary research synchrotron facility. In late 2018, a critical gun failure led to a seven-month facility downtime. . This incident raised concerns that the original LINAC from 1980 continued to be a high risk to daily facility operations. Furthermore, several other mechanical systems within the facility, including cooling/heating water, HVAC, and certain aspects of the LINAC vacuum systems, have also aged, resulting in decreased reliability. The upgrade to the LINAC and its associated mechanical systems presents an opportunity to significantly improve the operational reliability of the entire facility.

INTRODUCTION

The CLSI's existing LINAC complex is based on a 1960s-era 2856 MHz RF, normal-conducting 250 MeV electron linear accelerator, capable of producing a 40 mA beam current. This accelerator is followed by an Energy Compression System (ECS) and a transfer line, which injects the beam into a Booster Ring, raising its energy to 2.9 GeV before the beam is injected into the Storage Ring. The LINAC operates in a multi-bunch mode at a rate of 1 Hz and can also work in a top-up mode, injecting a bunch train every few minutes. The existing LINAC is powered by a 220 kV DC thermionic electron source with bunching sections that achieve 13 MeV before injection into S-band traveling wave accelerating structures [1].

CLSI now requires a reliable, stable, and serviceable Injector, consisting of an electron source and a LINAC capable of generating a 250 MeV electron beam. This Injector should support a variable repetition rate ranging from 1 to 10 Hz. CLSI has acquired a "turnkey" Injector from Research Instrument GmbH (RI). This Injector will encompass various components, including the electron source, bunching sections, accelerator sections, RF plant, compression system, distribution system, vacuum systems, transport optics, diagnostics, control systems, and associated cooling/heating systems. The new Injector components are currently in the fabrication process, with a planned delivery date at CLSI in March 2024. User operations will resume after a 6-month downtime for installation and commissioning.

REQUIREMENTS

The new Injector, as shown in Fig. 1 [2], must meet the performance parameters outlined in Table 1 [1]. One of the key Injector characteristics is the requirement to remain operational even if one of the modulators feeding the RF structures fails. This feature will ensure continuous operation until the next maintenance period. The maximum repetition rate of the modulators and klystrons is set at 10 Hz.

Figure 1: The new injector.

Table 1: Injector Performance Parameters

Parameters	Values	Units
Accelerator Particles	electrons	n/a
Nominal Beam Energy	250	MeV
Minimum Beam Energy in any RF failure mode	180	MeV
Single Bunch Mode Beam charge in 500 MHz Bunch	1.5	nC
Single Bunch Mode Bunch Length 1 σ	1	ns
Multi Bunch Mode Beam charge per 500 MHz Bunch (adjustable)	>0.08	nC
Multi Bunch Mode Train Length, 5 to 70 bunches at 500 MHz (2 ns RF buckets)	10 to 140	ns
Center energy stability (pulse to pulse)	≤0.1	% (RMS)
Energy Spread	≤0.5	% (RMS)
Normalized Emittance (1s) (X or Y)	≤50	π mm·mrad
Injector Frequency adjustable to	3000.24 ± 0.030	MHz
Booster Synchrotron RF Frequency	500.04 ± 0.005	MHz
Injector Nominal Repetition rate	1	Hz
Modulators and Klystrons Repetition Rate	1 to 10	Hz
Pulse to pulse beam position variation (RMS)	0.2	mm
Pulse to pulse beam angle variation (RMS)	0.05	mrad

SCOPE

Research Instrument GmbH (RI) will provide a complete "turnkey" Injector. The Injector system will interface with several CLSI systems for which CLSI will be responsible, as illustrated in Fig. 2 [1].

As depicted in Fig. 2, there is a shared responsibility between RI and CLSI for both design and procurement. The hands-on installation and commissioning will be carried out by CLSI personnel under the guidance of RI's technical specialists.

PROJECT PLANNING

Project planning has been underway since late 2021. Through detailed schedule development, the project team, in coordination with RI, has established the "Dark Period" duration, set at six and a half months. The "Dark Period" has been divided into four major phases: dismantling of the existing injector, service integrations, installation, and

DESIGN AND TESTING OF HEPS STORAGE RING MAGNET SUPPORT SYSTEM

Zihao Wang, Chunhua Li, Shu Yang, Lei Wu, Siyu Chen, Yuandi Xu, Shang Lu, Xiaoyang Liu,
Minxian Li, Ningchuang Zhou, Haijing Wang
Institute of High Energy Physics, Chinese Academy of Sciences, Beijing, China

Abstract

Very low emittance of High Energy Photon Source (HEPS) demands high stability and adjusting performance of the magnet support. The alignment error between girders should be less than 50 µm. Based on that, the adjusting resolution of the girder are required to be less than 5 µm in both transverse and vertical directions. Besides, the natural frequency of magnet support system should be higher than 54 Hz to avoid the amplification of ground vibrations. To fulfill the requirements, during the development of the prototype, the structure was designed through topology optimization, static analysis, grouting experiments, dynamic stiffness test and modal analysis, and the rationality of the structure was verified through prototype experiments. During the tunnel installation, the performance of the magnet support system was again verified to be better than the design requirements through test work after installation.

INTRODUCTION

HEPS storage ring consists of 48 modified hybrid 7BA achromats. The circumference is 1360.4 m and each arc section is about 28 m. HEPS is designed with very low emittance of less than 60 pm·rad to provide much brighter synchrotron light. Precise positioning and stable supports of the magnets are required.

The alignment error between magnets on a girder should be less than 30 µm in horizontal and vertical direction, and that between girders should be less than 50 µm. Also, natural frequency of magnet support system should be higher than 54 Hz to decrease amplification of ground vibrations, which is very challenging. The requirements are listed in Tables 1 and 2 [1].

Table 1: Alignment Tolerance

Tolerances	Magnet to Magnet	Girder to Girder
Transverse	±0.03 mm	±0.05 mm
Vertical	±0.03 mm	±0.05 mm
Longitudinal	±0.15 mm	±0.2 mm
Pitch/yaw/roll	0.2 mrad	0.1 mrad

Table 2: Requirements for Support System

Parameter		Value
Resolution	Transverse	⩽ 5 µm
	Vertical	⩽ 5 µm
	Longitudinal	⩽ 15 µm
Natural frequency		⩾ 54 Hz

According to the layout of the magnets, there are 6 support units for the multipoles in each arc section, including 2 FODO modules, 2 MULTIPLET modules and 2 QDOUNLET modules, as shown in Fig. 1. The adjacent multipoles share one girder and are seated on the plinths through adjustable wedge mechanisms, while the 5 longitudinal dipoles are bridged between the plinths.
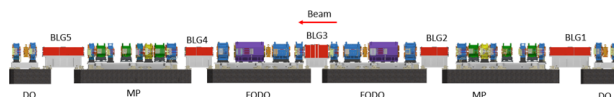
Figure 1: One arc section(1/48).

Stringent alignment accuracy requests high adjusting resolution of the girders. Table 2 shows the requirements. The resolution should be better than 5 µm in transverse and vertical directions and 15 µm in longitudinal direction.

DESIGN OF THE SUPPORT SYSTEM

The support system is designed as Fig. 2 shows. The girder should be capable of moving in 6 dimensions and the adjusting mechanisms are designed with 6 sets in vertical direction, 2 sets in transverse and 1 set in longitudinal direction. Each magnet is supported by a special adjusting mechanism to realize the three-direction adjustment, in which the sextupole is supported by the mover, which is able to realize the online adjustment.
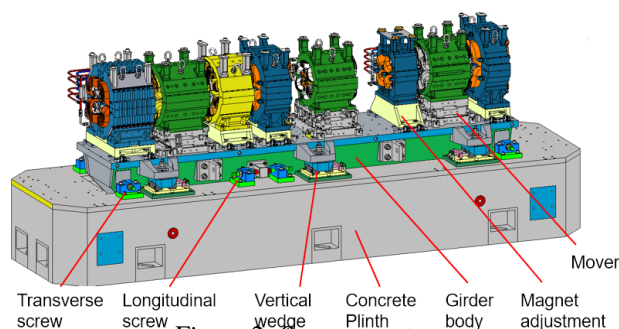
Figure 2: Support system.

Girder Body

After pre-simulation optimization [2], the effects of different structural parameters of the girder body on its deformation and natural frequency are analyzed, and the optimal stiffness is obtained by optimizing the shape of the cross-section and the distribution of the stiffeners. The structure of

VACUUM SYSTEM OF SPS-II: CHALLENGES OF CONVENTIONAL TECHNOLOGY IN THAILAND NEW GENERATION SYNCHROTRON LIGHT SOURCE*

T. Phimsen[†], S. Boonsuya, S. Chitthaisong, P. Sunwong, S. Prawanta, S. Chaichuay, K. Sittisard,
T. Pulampong, S. Srichan, N. Juntong, P. Sudmuang, P. Klysubun
Synchrotron Light Research Institute, Nakhon Ratchasima, Thailand

Abstract

Siam Photon Source II (SPS-II) is Thailand's first 4th generation synchrotron light source. It not only provides high-energy and high-brightness synchrotron radiation for both academic and industrial research after its completion, but it also strategically aims to strengthen the Thai industrial community during the design and construction period. The vacuum system is expected to play a crucial role in enhancing the country's manufacturing capability. Most of the main components in the system are planned to be domestically fabricated through technology transfer. Instead of using NEG coating technology, the vacuum system design of the SPS-II storage ring is based on conventional technology, leveraging the potential and expertise of the Thai industry. This paper reviews the challenges and adaptations made in the traditional design of the dense DTBA magnet lattice, considering magnet aperture limitations. The vacuum chambers and bending magnets have been modified to accommodate IR beamlines, which are included in the second-phase plan. The pressure profile of the vacuum system in the storage ring is evaluated, and the progress of the overall vacuum system of SPS-II is described.

INTRODUCTION

Siam Photon Source II (SPS-II) is Thailand's first 4th generation synchrotron light source, currently under design and prototype development [1]. One of the key systems of SPS-II is the vacuum system, which is responsible for maintaining the high-vacuum environment required for the operation of the particle accelerators and beamlines. Most of the main components in the system are planned to be domestically fabricated through technology transfer. This domestic production of the SPS-II vacuum system presents a significant opportunity to enhance local manufacturing capabilities. It is worth noting that, in 2022, the manufacturing sector accounted for more than 27 % of Thailand's GDP, according to data from the World Bank [2].

Compact lattice designs, similar to MBA lattices found worldwide, present limited space for vacuum components. The small gap between magnet poles limits chamber conductance and makes it difficult to evacuate outgassing, primarily from photon stimulated desorption (PSD). Non-Evaporable Getter (NEG) coating technology has been adopted by many light sources to overcome this

limitation [3-5]. However, there are a few challenges associated with this technology that should be considered.

One issue to consider is the complexity of evenly and uniformly applying NEG coatings to intricate vacuum chambers. Complex geometries can make this application process challenging. Additionally, there is concern about the cost and complexity of replacing NEG coatings if they become contaminated or damaged, and the coatings' lifetimes.

Instead of relying on NEG coating technology, the vacuum system design for the SPS-II storage ring is based on conventional technology, harnessing the potential and expertise of the Thai industry. This strategic decision aims to strengthen the Thai industrial community during the design and construction phases.

After conducting parallel studies and development of prototypes for both SUS (stainless steel) and aluminum chambers, the decision to proceed with aluminum was made based on advice from RIKEN and NSRRC experts, as well as the constraints of a short research and development (R&D) period. The advantages of aluminum, including its lightweight nature, high strength-to-weight ratio, corrosion resistance, thermal conductivity, machinability, and cost-effectiveness, were key factors in selecting it as the material for further development.

VACUUM CHAMBER DESIGN

The lattice of the storage ring is the Double-Triple Bend Achromat (DTBA), which comprises 4 normal dipole magnets (BM), 2 combined-functions dipole magnets (DQ), 16 quadrupole magnets (QD, QF), 8 sextupole magnets, and 2 octupole magnets per cell as displayed in Fig. 1. The storage ring consists of 14 DTBA cells (23.393 m/cell), resulting in a total ring circumference of 327.502 m.
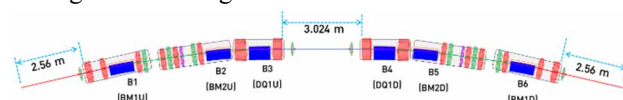
Figure 1: Schematic diagram of DTBA unit cell.

Each cell of the vacuum chamber can be divided into various sections: standard straight sections, middle straight sections, upstream arc section (including bending chambers PVCB-1 and PVCB-2), and downstream arc section (including bending chambers PVCB-3 and PVCB-4), as depicted in Fig. 2. The system has been designed to accommodate the use of three synchrotron radiation sources: two insertion devices (ID) located in the standard and middle straight sections, and the 5th bending magnet located in the downstream side of the cell.

STABILITY AND VIBRATION CONTROL FOR HIGH ENERGY PHOTON SOURCE IN CHINA

Fang Yan[†], Guopin Lin, Gang Xu, Zhe Duan, Xiyang Huang, Daheng Ji, Yi Jiao, Yuanyuan Wei,
Zihao Wang, Yunin Yang[1], Xiangyu Tan, Ping He, Weimin Pan

Key Laboratory of Particle Acceleration Physics and Technology, Institute of High Energy Physics,
Chinese Academy of Sciences, Beijing, China

[1] also at China Agricultural university, Beijing, China

Abstract

The High Energy Photon Source (HEPS) is the first high-energy diffraction-limited storage ring (DLSR) light source to be built in China with natural emittance of few tens of picometer radian. Beam stability is critical for such an ultralow-emittance facility. Controlling and minimizing the vibration sources and their transmissions internally and externally of HEPS is an important issue for achieving the stability needed to operate the high brightest beams. In this presentation, we report the ground motion analytical model related with frequency, the designed site vibration specifications together with the careful consideration and basis. Also, the stable design concepts, passive and active ways to minimize effects on the stability of the photon beam and critical accelerator and beamline components caused by ambient ground motion sources and the actual control effect will be introduced in detail.

INTRODUCTION

The High Energy Photon Source (HEPS), is a fourth-generation photon source with designed natural emittance of 0.0342 nm.rad at 6 GeV, 200 mA beam current and a circumference of 1360.4 m [1]. The design sketch is shown in Fig. 1. HEPS storage ring consists of 48 modified hybrid 7 BAs with brilliance specification of 10^{22} photons/s/mm^2/mrad^2/0.1%BW [2]. With such an ultralow emittance design, HEPS has a very challenging beam stability requirement. The tolerance on the floor motion is required to keep beam fluctuation smaller than 10% of the RMS beam size and 10% of the beam divergence in the meanwhile with FOFB. According to the designed lattice, the RMS beam position and angular spread has to be smaller than 1 µm/0.2 µrad horizontal and 0.3 µm/0.1 µrad vertical respectively [3]. To fulfil such rigorous restrictions, special cares are mandatory in developing site vibration specifications, stable building design concepts, and passive and active ways to minimize effects on the stability of the photon beam and critical accelerator and beamline components caused by ambient ground motion sources.

This contribution presents the novel analytical ground motion model developed, the challenges faced, the effects obtained for the stability and vibration controlling of HEPS in China. The first section is a brief introduction of the project backgrounds. The second section presents the beam dynamics model developed. The detailed specifications

Figure 1: The design sketch of HEPS infrastructure in Beijing China.

established for controlling the vibrations together with the supporting reasons are introduced in the third section. The construction of all the infrastructure has been completed now. The actual stability status is presented in the fourth section. The last section is a summary.

BEAM DYNAMICS MODEL

Frequency Unrelated Model

The baseline lattice of the HEPS storage ring consists of 48 modified hybrid 7BAs, the schematic figure of each cell is shown in Fig. 2 [4]. Vibrations sources are usually difficult to be traced, whether it is microtremors or culture noises. Normally, vibrations are simulated as random noises (uncorrelated and unrelated with frequencies). Random vibrations are introduced into 14 quadrupoles and 6 dipole-quadrupole combination components (with corrector inside) of each cell. The components painted in blue are quadrupoles while the dipole-quadrupole combinations are painted partly in purple and partly in blue as shown in Fig. 2. Vibrations with displacement RMS integral of 25 nm (bare ground vibration level) with frequency of 1-100 Hz are introduced in. The vibration induced close orbit is recorded and the RMS orbit fluctuation and angular dispersion for each position are obtained. Then RMS orbit fluctuation and angular dispersion over RMS beam size and divergence at ID position with and without FOFB (Fast Orbit FeedBack) are plotted as shown in Fig. 3 and Fig. 4 respectively. From the simulations, we can see that, if 25 nm vibrations introduced in the lattice, the orbit and dispersion fluctuation can fulfil the 10% requirement with FOFB correction but not without FOFB.